NORTHWESTERN UNIVERSITY

Assessing the Human Cochlea Using Stimulus Frequency Otoacoustic Emissions

A DISSERTATION

SUBMITTED TO THE GRADUATE SCHOOL
IN PARTIAL FULFILLMENT OF THE REQUIREMENTS

for the degree

DOCTOR OF PHILOSOPHY

Field of Communication Sciences & Disorders

By

Uzma Shaheen Akhtar

EVANSTON, ILLINOIS

June 2022

ABSTRACT

Assessing the Human Cochlea Using Stimulus Frequency Otoacoustic Emissions

Uzma Shaheen Akhtar

Otoacoustic emissions are currently used for various clinical purposes; however, stimulus frequency otoacoustic emissions (SFOAEs) evoked using a single tone are not utilized clinically due to uncertainties regarding their generation mechanism, their spatial source(s) in the cochlea, and their susceptibility to various cochlear insults, particularly in humans. Over the years, various models have been proposed relating SFOAE levels to cochlear mechanical irregularities and SFOAE phase gradient delays to cochlear tuning properties. However, these models have not been systematically evaluated across a wide frequency range and in ears with cochlear aging. The current work addresses these gaps in knowledge towards assessing the clinical utility of SFOAEs. First, the relationship between SFOAEs and behavioral thresholds and tuning were examined up to 14 kHz. Second, various metrics of SFOAEs were compared across different age groups in the first five decades of life.

The findings revealed a good correlation between behavioral and SFOAE based estimates of threshold and tuning, suggesting that SFOAE levels and delays, as predicted by the most current models of SFOAE generation, arise from roughly similar cochlear regions that determine behavioral thresholds and tuning.

Furthermore, SFOAE levels and bandwidth declined with each decade of life, suggesting that SFOAEs are sensitive to early auditory aging. The current findings may be useful in designing future studies in ears with known pathologies towards further evaluating the sensitivity and specificity of SFOAEs and their full clinical potential.

ACKNOWLEDGMENTS

This dissertation could not have been possible without the intellectual guidance, generous support, and creative feedback from my PhD mentor, Dr. Sumitrajit (Sumit) Dhar. Sumit helped me develop into the scientist that I am today, patiently guiding me through every analysis and re-analysis, meticulously reading through every manuscript draft written and revised, and brilliantly reimagining every data point plotted and replotted. From day 1, Sumit has been a teacher, a mentor, an ally of women in science, and a constant through unpredictable times. Over the last seven years, I have witnessed so many colleagues and trainees be inspired by his passion and optimism for science and the field of Audiology, all while making science look easy and providing plenty of dad jokes so that we never forget that good science can also be fun. I feel a lifetime of gratitude towards him for all his scientific teachings, his relentless professional guidance and valuable life lessons he imparted upon me. Thank you, Sumit.

My PhD committee, Drs. Jonathan Siegel, Ryan McCreery and Jason Sanchez have provided constant support and helpful feedback through many discussions over the last few years. I am very grateful for their guidance, their time, and their contributions to this dissertation.

The research experiments within this dissertation were performed using software programs and analysis codes from colleagues who generously shared resources and provided their expertise.

I owe the successful completion of my experiments to Dr. Shawn Goodman, who generously provided his ARLas software and hours and hours of training and troubleshooting to get the software up and running.

I am also grateful to Dr. Simon Henin for his help with programming the interface for the research hardware. Dr. Karolina Charaziak generously shared the program for measuring psychophysical tuning curves. Chun Chan helped develop the software program for measuring behavioral thresholds.

I am also grateful to all the participants who completed my studies.

Many others contributed in various ways which I am thankful for. Members of the Auditory Research Lab at Northwestern University, past and present, were always there for helpful discussions and constructive feedback including Dr. Sriram Boothalingam, Dr. Samantha Stiepan, Dr. James Dewey, Dr. Niall Klyn, Dr. Courtney Coburn Glavin, Dr. Mary Meskan, Dr. Alexandra Brockner, and Dr. Jasleen Singh.

Members of the Cochlea Journal Club at Northwestern University, past and present, also need recognition for allowing me to share my research and for providing helpful feedback. Thank you, Dr. Mary Ann Cheatham, Dr. Jonathan Siegel, Dr. Mario Ruggero, Dr. Beverly Wright, Dr. Sumit Dhar, Dr. Jason Sanchez, Dr. Tina Greico-Calub, Dr. Pam Souza, and Dr. Elizabeth Norton.

I thank my mentors Dr. Arturo Moleti and Dr. Renata Sisto for their helpful guidance over the years and for generously sharing their time-frequency analysis code with me.

I thank my family, friends, and life coach for their constant support and encouragement, and for grounding me through challenging times.

Lastly, I thank my husband Michael Yu for his relentless support. He believed in me, encouraged me, and made me laugh every day. I could not have succeeded without his love, friendship, and many, many acts of kindness.

LIST OF ABBREVIATIONS

ANF – auditory nerve fiber

ANSI – American National Standards Institute

ARHL – age related hearing loss

BM – basilar membrane

CAP – compound action potential

CEOAE – click-evoked otoacoustic emissions

CF – characteristic frequency

CM – cochlear microphonic

CP – characteristic place

CWT – continuous wavelet transform

DPOAE – distortion product otoacoustic emissions

EPL – emitted pressure level

FFT – fast Fourier transform

FPL – forward pressure level

HL – hearing level

I/O – input-output

IFFT – inverse fast Fourier transform

IHC – inner hair cell

LL – long-latency

LSF – least-squares fit

ML – multiple-latency

OAE – otoacoustic emission

OHC – outer hair cell

PCA – principal component analysis

PTC – psychophysical tuning curve

RL – reticular lamina

SFOAE – stimulus frequency otoacoustic emissions

SIN – speech in noise

SL – sensation level

SL – short-latency

SNR – signal to noise ratio

SOAE – spontaneous otoacoustic emissions

SPL – sound pressure level

TEOAE – transient evoked otoacoustic emissions

TM – tectorial membrane

To Ruby and Lucas

TABLE OF CONTENTS

LIST OF FIGURES

LIST OF TABLES

CHAPTER 1

Introduction

1.1. Overview

Otoacoustic emissions (OAEs), sounds emitted from the cochlea and measurable in the ear canal, provide an objective and indirect window into the biomechanical processes of the cochlea[1]. Specifically, OAEs are linked to the normal function of sensory outer hair cells (OHCs) within the cochlea, a normal electrochemical environment within the cochlear ducts, and normal transmission through the middle ear[2]. Hence, OAEs can be used as objective measures of OHC function in clinical settings[3].

Absence, damage or dysfunction of OHCs, due to genetic conditions or environmental factors, are a major cause of hearing loss[4,5], that negatively affects communication, social, and vocational functioning in adults and significantly impacts speech, language and academic development in children[6]. The discovery of OAEs has revolutionized the process for screening newborn hearing loss at birth in two ways. For one, OAE screeners do not require a voluntary response and thus can be measured in any population, including newborns. Second, the cost-effectiveness and efficiency of OAE screeners allows newborns to be screened by any tester with minimal training, a major boon for their ubiquitous use across the globe[7].

Despite their initial and most impactful clinical application, OAEs are not used to their full potential for assessing human cochlear function in routine

audiological practice. In adult audiology clinics today, OAEs are most commonly used for monitoring patients who are receiving ototoxic medications [8] or for confirming inorganic hearing loss [9]. OAEs have also been studied for differential diagnosis of hearing loss due to tinnitus[10], endolympathic hydrops[11] or acoustic neuroma[12]. Recent studies of different types of OAEs suggest that differential diagnosis of hearing loss may be possible through examining the joint profile of OAEs[13,14].

However, attempts to use OAEs to their full capabilities in clinical practice have been thwarted by a lack of understanding of different types of OAEs, their generation mechanisms, their cochlear site(s) of origin, and the connection of OAEs to various pathologies. All of these factors contribute to the widespread lack of clinical utilization of OAEs. Furthermore, OAEs are often not recordable with a mild or worse hearing loss using current clinical paradigms[15]. For the vast majority of adult patients who seek audiological care once significant hearing impairment has already begun, this begs the question: what are OAEs useful for in routine clinical practice?

The answer to this question is *early detection and routine monitoring of cochlear changes* – whether in response to an injurious event or due to gradual decline related to natural aging. The focus of this dissertation is the latter – detecting early onset cochlear changes due to aging using OAEs. Hence, the goals of this chapter are: 1) to highlight the importance of early detection and monitoring of age-related hearing loss, 2) to describe the anatomical and physiological

mechanisms of auditory aging, 3) to discuss the current clinical standards (or lack thereof) for detecting early onset age-related hearing loss, 4) to establish the need for more accurate and sensitive tools for detecting age-related dysfunction, 5) and to review the various OAE types for detecting age-related cochlear dysfunction.

1.2. Age-Related Hearing Loss

The hearing sense is critical for everyday human communication. Humans, like other animals, use hearing to communicate for basic survival and safety, but also use hearing, speech, and language together to connect with each other on a social and emotional level, and even use hearing to coordinate movement with music in the form of dance for pure enjoyment. When the hearing sense is critically altered, human communication inevitably suffers in many contexts that include social interaction, academic learning, or workplace functioning.

Although hearing loss has many different causes, including some genetic and some idiopathic, only some types of hearing loss may be preventable or modifiable. At one extreme, hearing loss due to recreational or occupational noise, may be completely preventable, if appropriate workplace modifications and/or hearing protective measures are implemented[16]. On the other hand, hearing loss due to genetic conditions or as a side effect of chemotherapies, potent antibiotics or other lifesaving therapeutics may not always be avoidable[17], as those treatments are usually life preserving.

Somewhere between these two extremes lies age-related hearing loss (ARHL), i.e., hearing loss that occurs as a result of the natural aging process in the auditory system. ARHL is highly prevalent, and hearing loss is expected to affect over 900 million people across the world by the year 2050[18]. In the U.S., 1 in 6 adults (age 18+), i.e. 37.5 million Americans, reported some trouble hearing based on findings from the 2012 National Health Interview Survey[19].

The Beaver-Dam epidemiological study of hearing loss in older adults demonstrated that the prevalence of hearing loss was extreme among the elderly (90.0% among 80-92 year-olds [y.o.]); however, even in 48-59 y.o., the prevalence was quite high (20.6%)[20]. In fact, findings of a longitudinal study of age-related hearing loss showed that hearing starts declining in one's fourth decade of life[21]. Several cross-sectional studies since have confirmed these early suggestions that hearing loss occurs much sooner in life than initially realized[22,23].

More recent estimates of prevalence, obtained using audiometric data from the National Health and Nutrition Examination Survey from 2001-2010, show that 38.17 million Americans have a hearing loss in both ears[24], which is projected to affect 73.5 million Americans by the year 2060[25]. With these staggering numbers, ARHL is considered a major public health issue and requires a multi-faceted approach towards understanding causes, innovating treatments, and employing policies and measures for preventing or reducing ARHL.

1.2.1. Importance of early detection and monitoring of age-related hearing loss

ARHL severely impacts the auditory processing abilities of an individual with hearing loss. In particular, ARHL is associated with poorer speech perception ability, both in quiet and in noise[26,27] and increased listening effort[28]. Gieseler et al., (2017) measured unaided speech-in-noise performance among 438 individuals with hearing loss and found that performance in speech perception ability was largely explained by pure-tone average (proportion of variance explained was 58.48%)[27]. Although studies of hearing loss in the elderly[27] are helpful in explaining the degree of the speech and cognitive deficits due to hearing loss that coincides with old age, another subset of studies are needed to identify the relationship between speech perception in noise and hearing loss due to normal aging (i.e. without significant contributions from exacerbating environmental toxins).

Aiming to answer this question, Stiepan et al., (2020) reported on a variety of auditory tests in 921 audiometrically normal individuals, ages 10-68 years, who did not report a history of environmental toxins[23]. They found that age was not correlated with QuickSIN SNR loss in these audiometrically normal individuals[23]. These findings may suggest that preventing age-related hearing loss from worsening could mitigate the adverse consequences on speech perception and further reinforce the importance of early detection and intervention for ARHL.

1.2.1.1. Effects of ARHL on Communication Partners. ARHL not only affects speech understanding and cognitive load but has also been shown to affect social and psychological factors[29], both for the individual with hearing loss as well as their communication partners[30]. Using patient and partner reports from 78 studies, Vas

et al., (2017) created two separate frameworks for classifying the impact of hearing loss for patients (Domains of Hearing Loss- Persons with Hearing Loss – DoHL-P) and their communication partners (Domains of Hearing Loss- Communication Partners – DoHL-CP)[30]. Complaints, examples and quotes from patients and their communication partners were used to further classify the impact into three supra-domains: auditory, social, and self[30].

Within each domain, the patient's impact exceeds their partner's, with some shared impacts across subdomains. In the auditory domain, the subdomains of hearing, listening, communicating and speaking may be affected for both the patient and their partner. On the other hand, the social domain highlights the negative impacts on the social life, isolation, occupational, and relationship subdomains on both individuals. Lastly, the self domain includes the increased role of the communication partner in daily functioning as well as the emotions, identity, stigma, and effort of both the communication partner and the individual with hearing loss[30].

1.2.1.2. ARHL and Cognitive Costs. Although decades of research have established that ARHL is associated with poorer physical, mental, cognitive, and psychosocial health of an individual[29,31,32], the significant pervasiveness of ARHL in broader domains of human health are now being realized. Treatment of ARHL using conventional tools such as hearing aids and hearing assistive devices can be helpful for improving communication and reducing listening effort for patients[33,34] and their communication partners[35]. Despite these potential benefits, individuals

with hearing loss wait an average of 8.9 years before pursuing treatment for various reasons including not enough perceived hearing handicap[36]. However, this gap between diagnosis and uptake of hearing aid may soon change as today there is even greater impetus for early identification and treatment of ARHL in order to preserve cognitive functioning[37].

Maharani et al., (2018) repeatedly tested the cognitive outcomes of 2,040 adults, aged 50+, in the Health and Retirement Study before and after the individuals started using hearing aids. They found that the trajectory of cognitive decline as measured using episodic memory scores was less steep following the start of hearing aid use compared to before[37]. These findings suggested that timely intervention of ARHL with hearing aids may alter the progression of cognitive decline. Considering that the number of Americans with hearing loss is estimated to be 73.5 million by the year 2060[25], slowing cognitive decline in any capacity could avoid a national dementia epidemic.

1.2.1.3. ARHL and Other Costs. In addition to preserving cognitive function and mitigating a national dementia epidemic, early and timely detection and intervention of age-related hearing loss may also mitigate severe individual and societal consequences[38]. Reed et al., (2019) retrospectively followed 4,728 participants over a 10-year period to examine medical costs, hospitalizations, emergency department visits, and various other measures in order to determine the healthcare costs of untreated hearing loss. They found that compared to adults

without hearing loss, untreated hearing loss was associated with higher medical costs and more inpatient hospital stays[38].

Based on these findings, the authors hypothesized that the observed relationship between untreated hearing loss and higher healthcare costs may be in part due to poor patient-provider communication[39] and mediated by poorer cognitive, physical, and psychosocial health[29,31,32]. Because of these major downstream effects, ARHL is a target of many multi-pronged research investigations aimed at early detection, treatment, and prevention of ARHL as well as understanding the genetic and environmental causes of ARHL and the interplay between nature and nurture.

1.2.1.4. Causes of ARHL. ARHL is thought to be a multigenic condition that interacts with environmental factors[40,41]. Environmental exposures can also lead to epigenetic regulation of genes related to hearing[42]. Gates, Couropmitree & Myers (1999) studied siblings and parent-child dyads to determine the heritability of ARHL and found a familial association of hearing thresholds in relatives compared to spouses, an effect that was stronger in women and differentiated by the type of hearing loss (sensory presbycusis was more heritable than strial presbycusis)[43]. A Danish twin study of over 5,000 participants reported a 40% genetic heritability of self-reported hearing difficulty and a higher rate of concordance in monozygotic compared to dizygotic twin pairs[40].

ARHL is exacerbated by the lifetime accumulation of exposure to ototoxic compounds and loud noise[44], a side effect of modern industrialization. Studies of

ARHL in pre-industrial societies have shown that hearing function is sustained later in life in the absence of environmental toxins[45,46]. This suggests that although ARHL may not be preventable, early identification and preventative measures may delay the onset of significant ARHL and associated consequences for communication and overall well-being.

1.2.1.5. Current approach to treatment of ARHL. The identification and intervention of ARHL in clinical practice today can be described as wait-and-see, as it relies on the patient to experience significant communication difficulty before a rehabilitative treatment is pursued. Although this reactive approach is in part due to the limited treatment options available for hearing loss currently, the need for a more proactive approach to diagnosis and treatment of ARHL is becoming more apparent with the increasing feasibility of regenerative or molecular medicine for treating ARHL[47] and otoprotectants for preventing or reducing ARHL[48]. When these treatments become common practice in clinics, sensitive and precise clinical tests of auditory function will be needed, in order to detect ARHL at its earliest onset and to differentiate the various sites of dysfunction that may contribute to ARHL.

1.2.2. Current clinical standards (or lack thereof) for detecting early-onset ARHL

ARHL is an insidious condition that manifests within the fourth decade of life[21]. In fact, ARHL is now considered a major modifiable factor during middle age for preventing dementia later in life[49]. Historically, ARHL has only been treated when there is a measurable hearing loss or self-perceived hearing handicap[36];

however, new evidence suggests that even subclinical hearing loss can be detrimental to cognitive and mental health[50]. In order to prevent ARHL from contributing to or exacerbating cognitive decline, there needs to be early identification of ARHL. Yet, there is no universal screening program in the U.S. to detect ARHL in adults – efforts both domestically and globally are currently underway[51-53].

ARHL is typically only identified once a patient seeks out consultation from a medical physician or hearing professional. ARHL is then diagnosed based on a combination of 1) patient complaints about their hearing (perceived difficulty by the individual or a communication partner), 2) the patient's case history (positive family history of hearing loss and negative history of exposure to environmental toxins such as ototoxic compounds and loud noises) and 3) the results of behavioral pure-tone audiometry at frequencies 0.25-8 kHz (gradually sloping high-frequency sensorineural hearing loss).

For some patients, even if there is significant self-report of hearing difficulty, the measured loss is not considered significant for conventional treatments (i.e. hearing aids and hearing assistive devices)[54]. Kochkin's 2007 MarkeTrak VII survey showed that 19-34% of adults who visited a medical doctor or hearing professional for a hearing related complaint were told to wait and retest hearing[55]. This may be due to the loss being not considered significant enough to warrant treatment with hearing aids or the results of their behavioral pure-tone audiometry tests being normal[54].

Tremblay et al., (2015) found that the prevalence of individuals with normal hearing (< 20 dB HL at 0.5-8 kHz) who report hearing difficulty was 12.0%[56], which is estimated to be approximately 25.3 million adults in the U.S.[57]. This is a significant number of individuals who are experiencing hearing difficulty, yet the findings of behavioral audiometry are deemed to be clinically normal. Although the underlying reasons for this discrepancy between subjective reports and clinical test results may vary[54,58], the discordance points to the insufficiency of current clinical tests in detecting early-onset ARHL.

Modification of clinical assessment protocols would improve the diagnosis for patients who may experience perceptual deficits in their communication due to their early onset ARHL. However, there is also a need to identify individuals with early-onset ARHL who are asymptomatic – i.e., do not yet experience subjective difficulty – through universal adult hearing screening programs. In 2020, the United States Preventive Services Task Force (USPSTF) conducted a systematic review of studies of adults aged 50 years or older who are asymptomatic of hearing loss in order to assess whether screening for ARHL in primary care settings would improve long-term health outcomes.

The report determined that there is insufficient evidence to assess the efficacy of adult hearing screening programs[59]. A response statement by the American Academy of Audiology on the initial draft of the report acknowledged the USPSTF report, pushing for additional research on adult hearing screenings and

the potential benefits of adult hearing screening programs in mitigating more severe health outcomes such as cognitive decline and dementia[60].

Before these efforts can be properly implemented in a large-scale screening program and the appropriate tools for screening are identified, the limitations of current clinical tests must be thoroughly examined. Current clinical tests for detecting ARHL that only rely on behavioral pure-tone audiometry are insufficient in the following ways:

1.2.2.1. Standard pure-tone audiometry is band-limited. Only a limited range of frequencies (0.25-8 kHz) are tested[61], even though early onset ARHL starts at frequencies much higher (> 8 kHz)[22,62,63]. Historically it was believed that ultra-high frequency (> 8 kHz) did not contribute significantly to speech perception ability; however, recent work has challenged this notion[64]. Hearing at the ultra-high frequencies contributes to not only enhanced quality of speech and music[65], but also sound localization, and speech intelligibility[63,66].

Moore & Tan (2003) showed that decreasing the high frequency cut-offs of filtered speech (~10 kHz) and music (~16 kHz) negatively affected the perceived quality of the signals[65]. Best et al., (2005) showed that individuals poorly localized speech stimuli that were low-pass filtered at 8 kHz compared to broadband unfiltered speech[66]. Vitela et al., (2015) tested speech intelligibility of vowels and consonants that were band-pass filtered to only contain spectral energy between 5.7 and 20 kHz[67]. They found that performance on these band-limited speech tokens,

that included both vowels and consonant, was above chance, suggesting a significant role of high frequency hearing in speech perception[67].

A separate line of research suggests that ultra-high frequency hearing may also contribute to speech articulation[68,69]. Berlin (1982) reported that 76 individuals with hearing loss had exceptional speech detection and articulation, despite having profound hearing loss at frequencies below 8 kHz[68]. When thresholds above 8 kHz were measured, these profoundly-deaf individuals were found to have good residual hearing above 8 kHz[68]. These early reports of profound hearing loss below 8 kHz with good residual hearing above 8 kHz and the revived interest in the ecological value of ultra-high frequency hearing in everyday listening together reinforce the idea that current clinical tests that only evaluate a limited range of frequencies are insufficient[64].

1.2.2.2. Pure-tone audiometry only assesses threshold sensitivity. In addition to being frequency limited, behavioral pure-tone audiometry only assesses the sensitivity of an individual to a set of sinusoidal tones. However, human communication and listening abilities extend beyond just detecting soft pure-tones. In other words, signals such as speech and music have a broad spectral bandwidth, large amplitude fluctuations, and wide dynamic range. Not surprisingly, 99% of individuals with any degree of hearing loss report difficulty hearing in noise, despite use of a hearing aid to amplify soft sounds[70]. In clinical practice today, hearing aid gain is prescribed based on pure-tone thresholds, with little to no parameter optimization of other aspects of sound processing, in order to remediate

the effects of abnormal temporal processing, reduced dynamic range[71], and broadened auditory filters[72] that typically accompany hearing loss.

Although these deficits i.e. degraded temporal resolution, abnormal growth of loudness, and poor frequency resolution, are known to affect individuals with significant sensorineural hearing loss[73], there is also evidence that these deficits may also be present in individuals who have audiometrically normal hearing[74-76]. Badri, Siegel & Wright (2011) measured auditory filter shapes in normal-hearing individuals with self-reported difficulty understanding speech in the presence of background noise and controls who did not report this difficulty[76]. They found that auditory filter bandwidths at 2 kHz, (a frequency where thresholds were normal in both groups), were broader in the speech-in-noise group compared to the control group[76]. Furthermore, the speech-in-noise group displayed poorer hearing sensitivity at ultra-high frequencies of 10, 12.5 and 14 kHz compared to controls[76].

Harris & Dubno (2017) examined temporal processing abilities using neural phase synchrony in the electroencephalography (EEG) in young and older adults with normal hearing (≤ 25 dB HL from 0.25-4 kHz) and found that the phase locking value of the EEG was lower in the older group than the younger group, suggesting an age-related deficit in temporal processing[77]. Although, the two groups fell within the normal definition of hearing, there were significant differences in hearing sensitivity of the two groups even at 2-4 kHz[77].

The authors concluded that the age-related deficits may be a consequence of peripheral changes not detectable by the current clinical definition of pure-tone

audiometry[77]. A recent report by Gatlin & Dhar (2021) describes the arbitrary development of the now widely accepted clinical definition of normal-hearing[78]. All of these reports together highlight the need for more advanced clinical protocols that provide a comprehensive, accurate and precise diagnosis of ARHL and extend beyond defining normal hearing based on behavioral measures of hearing sensitivity alone.

1.2.2.3. Pure-tone audiometry is not sensitive to specific cellular damage. Another line of research, highlighting the shortcomings of current clinical tests of ARHL, suggests that behavioral measures of hearing sensitivity are not able to accurately diagnose the site of dysfunction in ARHL[79-81]. Landegger, Psaltis & Stankovic (2016) examined 131 human temporal bones in order to correlate the audiometric thresholds to histological assays of cellular damage in the cochlea and found that similar audiometric profiles could yield many different combinations of cellular damage (e.g. combined loss of the two types of sensory cells, loss of specific sensory cells, loss of auditory neurons, or atrophy of the vasculature)[79]. They concluded that behavioral audiometric tests are not sensitive enough for defining candidacy for novel therapeutics that target specific cellular structures or physiological mechanisms[79].

Perhaps these findings are not surprising as behavioral measures assess the entire auditory pathway from the periphery to the cortex and thus cannot pinpoint the decrements exclusive to the peripheral hearing mechanism, a primary site for age-related degradation. Accordingly, for decades, clinicians have used the

crosscheck principle to confirm behavioral findings with other measures for an accurate diagnosis of auditory dysfunction[82]. Although historically the crosscheck principle has been mainly applied to pediatric assessments[82], there are advantages to utilizing objective measures in addition to behavioral audiometry to more accurately characterize the nature of auditory dysfunction due to aging.

The anatomical and physiological bases of peripheral auditory aging are reviewed in the next section. However, it should be noted that various compensatory mechanisms in the central auditory system, specifically the cingulo-opercular network and the premotor cortex, may also work to counteract the perceptual consequences of peripheral age-related hearing loss, particularly in speech perception[32]. Additionally, animal studies of induced peripheral damage have shown declines in electrophysiological measures but not in behavioral measures, due to central gain enhancement[83].

1.2.3. Anatomical bases and physiological mechanisms of auditory aging in the periphery

ARHL is thought to be primarily due to peripheral loss or degradation of various sensory and supporting structures within the cochlea as well as the neurons that relay sensory information to the central auditory system[84]. According to Gates & Mills (2005), peripheral auditory aging is likely more common in human ARHL[85], although there is evidence of age-related changes in the central auditory system (specifically gray and white matter atrophy and changes in the composition of

metabolites in the brain)[86]. In some cases, the peripheral ARHL may be the primary cause that leads to secondary degeneration of the central auditory system[85].

Currently there is no clinically utilized differential diagnosis for peripheral and central ARHL, and the rehabilitative treatment for both types of ARHL is the same. However, in a future where advanced therapeutics and protective compounds will be available to target peripheral and central ARHL separately, it would be advantageous to differentially diagnose peripheral from central ARHL. Currently, distinguishing peripheral vs central ARHL in humans may be difficult without histological, physiological, and epidemiological studies of all auditory structures from the periphery to the cortex. Given that central auditory aging is much more complex, the current work continues the tradition of more classical studies of ARHL, which have focused on the peripheral aging of the cochlea. The historical path leading to the current understanding of ARHL is reviewed in the next section.

1.2.3.1. Histological studies of ARHL. In 1955, Schuknecht used pre-mortem audiological findings and post-mortem histological findings from human temporal bones together to propose four different subtypes for ARHL: sensory, neural, metabolic, and mechanical (metabolic and mechanical are also referred to as strial and cochlear conductive, respectively[87-89]). Later, Schuknecht added two additional categories: indeterminate and mixed[89], with the latter still being used today as the catch-all diagnosis referred to as sensorineural hearing loss. While all of these studies initially established the heterogeneity seen in human auditory aging, the

precise mechanisms and sites of age-related hearing loss have remained a topic of debate.

Findings from the work of Schuknecht and colleagues are still being actively refined. For example, Schuknecht & Gacek (1993) found that approximately 25% of all ARHL cases were indeterminate, i.e. the pathological changes observed via microscopy did not explain the hearing losses[89]. In all these cases, the outer hair cell survival, strial health, and cochlear neuronal counts did not exceed the criteria established by Schuknecht & Gacek correlating cytocochleograms to their distinct audiometric profiles[89]. Furthermore, the audiometric configurations and severity in these cases were highly variable[89]. Lastly, the audiogram profiles and corresponding cytocochlear phenotypes were often, but not always correlated, which gave rise to the mixed etiology of ARHL[89]. It should also be noted that isolated pathologies of the sensory cells, neuronal cells, and stria vascularis were less common than the mixed and indeterminate ARHL[89].

From these findings, the following questions on the physiological sites and mechanisms of ARHL have emerged. Specifically, does human ARHL indeed manifest more commonly as a mixture of damage to various cytological structures[79]? If so, what factors contribute to the susceptibility of each of the structures to aging? Alternatively, does damage to different structures manifest as isolated pathologies, each with its own time course and additive effect on physiological and behavioral measures of auditory function? More specifically, is strial damage due to aging a primary cause of ARHL[90]? How does neuronal loss, synaptic dysfunction, and de-

afferentation contribute to the functional deficits seen in speech perception ability in normal and aging humans[91,92]? Lastly, how does loss of or damage to OHCs contribute to ARHL with and without the harmful contributions of noise exposure[80,93]?

Following Schuknecht's seminal phenotypic classifications, many human and animal studies have focused on correlating the patterns of the audiogram to specific structures and physiological mechanisms. Mills et al., (1990) observed that the audiometric configuration of thresholds, estimated using electrical potentials, in quiet-raised gerbils resembled the profile of human strial loss[94], as defined by a relatively flat configuration, with elevated thresholds at low frequencies and gradually sloping thresholds at high frequencies[88]. Later, Schmiedt et al., (2002) showed that aged gerbils had strikingly similar patterns of compound action potential thresholds to gerbils treated with furosemide to disrupt strial function[95]. In addition, the two groups had similar the endocochlear potentials measured at the round window[95]. These findings together established the gerbil as the model for studying human strial ARHL[95].

Animal models of sensory loss, induced by exposure to loud noise or ototoxic compounds, produce a distinct sensory profile, defined by a steep slope of high-frequency thresholds[4,5,96]. Ryan & Dallos (1975) injected chinchillas with kanamycin to selectively ablate OHCs and obtained behavioral thresholds before performing post-mortem histological counts of surviving outer hair cells[4]. They found that the patterns of OHC loss and behavioral threshold shift were quite similar in that both

showed a steep high-frequency loss[4]. The similarity of the two patterns was evident by an excellent agreement (r = 0.86) between the highest frequency at which thresholds were normal and the first location of the cochlea from the apex at which OHC loss was 50%[4].

Burton et al., (2020) recently examined the histopathological and perceptual correlates of noise exposure in macaques and found that OHC survival in response to intense noise exposure was related to poorer audiometric thresholds and broader auditory filters, although interactions between OHC, IHC, and synaptic survival may explain the variability seen in histological and perceptual observations[97]. Although these animal models of ARHL have been extensively useful in isolating the specific contributions of various cellular structures and mechanisms, human ARHL is widely accepted to be a complex combination of various loss types and mechanisms, including loss of auditory nerve synaptic connections to hair cells[46]. Not surprisingly, the audiogram is not used clinically for differential diagnosis of pathologies of different cell types, and accordingly, attempts by researchers to isolate or differentially diagnose pathologies solely on the basis of the audiogram have seen variable success[90,96].

Dubno et al., (2013) used a machine learning classification system based on animal models of sensory, metabolic, and metabolic+sensory pathologies to predict audiometric profiles of 1,728 human audiograms[90]. They found that 338 exemplars of the various audiometric phenotypes (older-normal, metabolic, sensory, and metabolic+sensory) were correctly identified (accuracy range 82.4-100%) by three

different classifier methods[90]. Furthermore, the threshold, demographic, and noise exposure history of individuals with non-exemplar audiograms (n = 1,390) were quite similar to those of the exemplars, suggesting cross-validation of the automatic classification method[90]. However, the classification of non-exemplars displayed lower confidence than those of exemplar cases, suggesting some cases did not meet the proposed audiometric phenotypes[90].

Since Schuknecht's early studies, advances in microscopy have made histological analysis of human cochleae more precise. Specifically, Wu et al., (2020a) used differential interference contrast microscopy, as opposed to the bright-field microscopy used by early studies, and an improved method for determining hair cell survival that uses the hair bundles and cuticular plates, as opposed to the nuclei of the hair cells used in previous studies[81]. Furthermore, Wu et al., (2020a) have been able to utilize through-section analysis, which improves the hair cell survival count as it accounts for the increase in total number of hair cells as the slide section plane moves from the center of the modiolus, tangentially to the edge of the cochlea[81].

Using these improved histopathological assays, Wu et al., (2020b) showed that patterns of hair cell and auditory nerve fiber survival better mirrored the audiometric patterns than strial survival[80]. These findings challenge the distinct classical audiometric phenotypes proposed by Schuknecht and further emphasize the mixed nature of peripheral cellular decrements that accompany age-related hearing loss in humans[80]. Additionally, Wu et al., (2020b) found that temporal

bones of individuals with a positive history of noise exposure had significantly poorer hair cell survival in the cochlear base than non-noise exposed individuals[80].

Although hearing levels also separated the two noise groups, OHC loss was more prominent and spanned across a wider range of the cochlea in the noise exposed group[80]. These new insights about the susceptibility of OHCs to aging and noise exposure further support the rationale for using objective measures of OHC function in assessing peripheral auditory dysfunction due to aging. Furthermore, the ability of various objective measures of OHC function in the differential diagnosis of different structures affected in ARHL needs to be thoroughly investigated.

1.2.3.2. Physiological Studies of ARHL. In addition to the anatomical changes observed in histological studies, many physiological and molecular changes in ARHL have also been investigated and reported[84]. In the central system, the physiological changes are associated with altered composition of brain neurochemicals and altered brain morphometrics[86,98-100]. In the peripheral system, physiological effects of aging can be seen in the endocochlear potentials (EP)[101], auditory nerve function[102-104], as well as in the molecular pathways associated with cell survival and cell death[42,84]. A brief review of the literature relevant to these topics is presented below.

A. Effects of ARHL on brain neurotransmitters in animals. Caspary et al., (1995) reported on a series of studies investigating age-related changes in the inhibitory neurotransmitter GABA of the rat inferior colliculus[105]. The findings from

these studies suggested that loss of GABA function with aging could alter the balance of excitatory and inhibitory auditory processing[105]. Chen et al., (2013) found age-related changes in GABA levels of human frontal and parietal regions[106]. Aging is also related to reduced levels of the neurotransmitter glycine in the cochlear nucleus, which is thought to be important for intensity and temporal coding[100].

Although the extent of these neurochemical changes on perceptual abilities is yet to be determined, some evidence suggests that age-related changes in temporal coding abilities, without a concomitant relationship with audiometric hearing thresholds, may be partly due to changes in central physiology[86]. In one animal study, increasing GABA levels in the brains of aging mice using Vigabatrin reversed the effects of aging as evidenced by improved thresholds in the treated mice compared to control mice[107]. Whether restoring neurotransmitter deficiencies can also ameliorate the age-related decline of human perceptual abilities is unknown and may not be as easily addressable given the complex etiologies of human ARHL.

B. Effects of ARHL on brain morphology in humans. In neuroimaging studies of the human auditory cortex, ARHL has been associated with reduced total brain volume[108], reduced gray matter[109] and cortical thinning[110]. In 2,908 participants, Rigters et al., (2017) found that hearing loss was associated with decreased total brain volume, independently of age[108]. Towards understanding the effects of aging and hearing loss on brain morphometrics, Lin et al., (2014) followed 126 participants (ages 56-86 years at baseline) across 6.4 years on average and found that individuals with hearing loss had greater declines in whole brain and right

temporal lobe gray matter volume over time than those with normal hearing (pure-tone average at 0.5, 1, 2, and 4 kHz better than or equal to 25 dB HL)[109].

In a similar design, Eckert et al., (2019) followed thirty older adults longitudinally across 2.62 years on average and found that although pure-tone thresholds were significantly associated with lower cortical gray matter volume, the aging effects were not clearly distinguishable across individuals[98]. In yet another study, Profant et al., (2014) compared age-related changes in the gray matter of the auditory cortex in young controls and two groups of elderly with mild to moderate and moderate to severe presbycusis[111]. They found that young controls showed higher volumes and greater thickness of gray matter than the two elderly groups, but the two elderly groups did not differ from each other, suggesting smaller differences in brain morphometrics due to hearing loss may not be easily detectable[111].

C. Cochlear microphonics and the endocochlear potential. In animal models of aging, direct measurements of the endocochlear potentials and ionic concentrations have been performed. Schmiedt (1996) measured the endocochlear potential at the round window in young and aged gerbils and found the average round-window EP was significantly lower in the aged group, but endolymphatic potassium on average was similar between the two groups[101]. In another study, Gratton et al., (1996) showed that lower EP was associated with poor strial capillary health in aged gerbils[112].

Because direct EP measurements cannot be made in humans, the cochlear microphonic has been proposed as a potentially useful, non-invasive measure of the electrochemical environment of the cochlea; however, many uncertainties about the origins of the CM[113], its susceptibility to various toxins[114], and its clinical effectiveness in detecting various pathologies still exist[115]. These topics will be reviewed in section 1.2.4.1. Briefly, although simultaneous measurements of the endocochlear potential and auditory nerve tuning curves in cats have shown a 1 dB elevation of threshold for every millivolt decrease in the EP after furosemide injection[116], CM has not shown a similar decrease in response to cochlear manipulations[113].

D. Auditory nerve function in humans. Investigating the pure effects of aging in auditory nerve function has been difficult in humans in which contributions from other ototoxic insults cannot be easily parsed out. With this caveat, studies of various samples of human ARHL have been conducted. Konrad-Martin et al., (2012) measured the auditory brainstem response (ABR) in 131 veterans aged 26-71 years of age and found that wave I amplitudes decreased as a function of age, even after adjusting for hearing loss[102]. Bramhall et al., (2018) reported a similar effect of aging in a non-veteran population with varying degrees of hearing loss[103].

McClaskey et al., (2018) compared the amplitudes of click-evoked compound action potentials (CAP) as a measure of human auditory nerve activity in young (18-30 years) and old (55-85 years) individuals with clinically normal audiograms up to 3 kHz[104]. They also found that older participants had smaller CAP amplitudes

compared to younger participants, despite clinically normal hearing up to 3 kHz[104]. All of these studies suggest that aging is associated with a decline in electrophysiological markers of auditory nerve function that may be a result of or coincide with other structural or functional peripheral changes.

E. Molecular changes in the cochlea. There is evidence that various molecular anti-aging and pro-aging pathways in the cochlea contribute to the vast heterogeneity seen in age-related hearing loss[84]. Intracellular mechanisms such as free radical accumulation, disruption of calcium homeostasis, MAPK signaling pathways, apoptosis, and immune response are some examples that lead to cell death[84]. On the other hand, protective or survival signaling through the ROS-opposing mechanisms, PI3K/PKC/AKT signaling, anti-apoptotic pathways, and purinergic pathways help with cell survival[84]. Together, the precise combination of these mechanisms at play determines an individual's susceptibility to ARHL.

A recent review by Wang & Puel (2020) describes the intrinsic and extrinsic factors involved in determining one's susceptibility to ARHL[42]. Intrinsic factors such as genetic predisposition, epigenetics, and biological aging may not be as readily modifiable, in contrast to extrinsic factors such as exposure to harmful noise or ototoxic compounds and smoking, which are potentially modifiable on an individual or societal level[42]. Towards addressing the societal impact of environmental toxins in exacerbating ARHL, epidemiological studies of ARHL have been useful in identifying populations at risk.

1.2.3.3. Epidemiological Studies of ARHL. The epidemiology of ARHL in the U.S. has been long studied using population-based cohorts from the Framingham Heart Study[117,118], Baltimore Longitudinal Study of Aging[31,119,120]; the Beaver Dam Epidemiology of Hearing Loss Study[20,121,122], the National Health and Nutrition Examination Survey[123]; and the Blue Mountains Eye Study[124]. From these studies, several comorbidities associated with ARHL have been identified.

For example, Agrawal et al., (2008) found that in 3,853 US adults aged 20-69, hearing loss prevalence increased at an earlier age in participants with a history of occupational noise exposure as well as cardiovascular risks such as smoking, hypertension, and diabetes mellitus[123]. Similarly, in a longitudinal study, Cruickshanks et al., (2015) reported that smoking, adiposity as measured by waist circumference, and unmanaged diabetes mellitus were all associated with a greater risk of hearing loss in 1,925 participants aged 43-84[121].

More recently, Reed et al., (2019) used data from the Atherosclerosis Risk in Communities study to report an association between elevated systolic blood pressure measured at baseline with poorer hearing thresholds measured 25 years later[125]. Joo et al., (2020) reported that the use of ototoxic medications (specifically, loop diuretics and nonsteroidal anti-inflammatory drugs) was associated with progressive hearing loss in participants followed over a 10-year period in the Epidemiology of Hearing Loss study[126].

From these studies, it is clear that myriad risk factors for ARHL exist; however, from these population-based studies, predicting individual susceptibility is

still a challenge. Although ARHL manifests similarly across individuals in both clinical metrics and functional deficits, the numerous and highly individualized mechanisms involved in ARHL warrant the need for more accurate and sensitive tools for detecting, preventing, and treating age-related cochlear dysfunction. The ideal tools for this precise approach to ARHL will be reviewed in the next section.

1.2.4. Need for more accurate and sensitive tools for detecting age-related cochlear dysfunction

Until recently, ARHL could only be treated using traditional interventions such as wearable or implantable devices[47], hearing assistive technologies[44], and communication skills training including auditory training[127]. Clinical trials of novel treatments to reverse ARHL using regenerative hair cell technology are currently underway and have shown promising results[128]; however, this initial study of hair-cell regeneration in humans has brought to question the usefulness of behavioral and functional tests of hearing in this context and has highlighted the need for more sensitive and accurate tools for quantifying ARHL, differentiating between various etiologies of ARHL, and monitoring the functional status of target structures.

In a preliminary sample of 24 adults with sensorineural hearing loss, in a randomized, double-blind, placebo-controlled trial, McLean et al., (2021) demonstrated that although the regenerative compounds (FX-322) were safe and well-tolerated, the hearing related assessments did not show a drastic or consistent improvement with treatment compared to placebo group[128]. Specifically, none of the

treated ears showed a statistically significant improvement in pure-tone thresholds from baseline to 90 days post-treatment, although four out of 15 in the treatment group showed a 10 dB improvement in thresholds at 8 kHz only[128]. Similarly, four out of 15 in the treatment group showed a clinically significant improvement in speech intelligibility in quiet from baseline to 90 days post-treatment[128]. Two of the four also showed a clinically significant improvement in speech perception ability in noise (an improvement of more than 3 dB signal-to-noise ratio needed for 50% correct) [128].

McLean et al., (2021) highlight some limitations of their study and conclude that perhaps they did not detect significant and consistent improvements in pure-tone thresholds because frequencies > 8 kHz were not tested in their protocol[128]. Furthermore, the degree of hearing loss may have contributed to the ceiling effect in speech intelligibility scores of mild hearing loss individuals, making speech perception measures insensitive to monitoring subtle changes in function due to treatment[128]. In addition to the limitations presented by McLean et al., (2021), another major limitation of this study is that it largely focused on behavioral outcome measures, including pure-tone thresholds and speech intelligibility scores in quiet and in noise.

Using behavioral measures of hearing that assess the entire auditory pathway, not individual structures along the pathway, may not be ideal in this context, especially because the target of the regenerative treatment is cochlear hair cells (Note: the exact proportion of outer vs inner hair cell regenerated is yet to be

fully investigated[129]). Additionally, speech perception tasks may not be ideal for monitoring treatment effects because of the redundancies available in speech perception which arise from parallel processing streams[130] and the contributions of factors such as linguistic experience, musical ability, and cognitive ability[131]. Furthermore, because the participants in the trial were diagnosed with sensorineural hearing loss associated with a history of noise exposure or idiopathic sudden sensorineural hearing loss, the degree to which each of these etiologies differentially affects outer hair cells cannot be determined in this population using behavioral measures of hearing.

Although the protocol used by McLean et al., (2021) mirrored clinical protocols used in audiology clinics today, the findings strongly elucidate the idea that before sensitive and accurate diagnosis, treatment, and monitoring of ARHL can be achieved, current clinical protocols will need to be significantly altered in the following ways: 1) objective measures of the cochlea will need to be included; 2) the bandwidth of frequencies assessed will need to be expanded; 3) profiles of dysfunction due to various etiologies will need to be established.

1.2.4.1. Objective measures of cochlear function. The use of objective measures of outer hair cell function, such as the cochlear microphonic (CM)[113,114,132] and otoacoustic emissions (OAEs)[1,133], may be important for establishing clinical candidacy and monitoring benefit from novel treatments such as regenerative compounds[128] and gene therapy[134] that specifically target outer hair cells. Attempts to assay cochlear function using serological biomarkers (i.e. serum prestin levels)

are ongoing but are not yet validated for clinical use[135]. The CM is a field potential recordable from the round window of the cochlea and is thought to represent the alternating transducer currents in response to mechanical stimulation of OHCs[113], whereas OAEs are acoustic signals which are recorded in the ear canal as by-product energy from mechanical processes related to cochlear amplification and tuning[136].

Although both OAEs and the CM offer a window into the live human cochlea, which cannot be accessed otherwise, each is measured away from their respective site(s) of generation, thereby limiting their specificity for identifying the cochlear place of dysfunction. In order to understand the spatial localization of the CM, Cheatham et al., (2011) examined the CM in wild-type and prestin knock-out mice. In wild-type, the CM masking functions matched the compound action potential (CAP) masking functions at 32 kHz, but at lower probe frequencies, the tips of the CM masked functions were always higher in frequency than the probe, suggesting that CM measured at the round window primarily reflects the status of the summed spatial activity of basal OHCs and not those within the peak region of amplification[113].

Because both CAP and CM masking functions were remote measures of the cochlea, the discordance between the two measures at lower probe frequencies can be interpreted as evidence of basal contributions. Furthermore, there was little difference between the CM masking functions of wild-type and prestin knock-out mice[113], suggesting that the CM, particularly at low frequencies, is a passive

response that does not represent active cochlear amplification or tuning of the apical cochlea related prestin-based electromotility. Using a different approach, Charaziak, Siegel & Shera (2017) later showed that in chinchilla with noise induced damage, the residual CM measured using a saturating tone, can be more sensitive to the site of the noise induced damage than the raw CM. However, how well the CM can be used in humans for this purpose is currently unknown[132].

Several groups have investigated, in different animal models, the use of various acoustic suppressors and acoustic trauma[114,132,137-139] towards spatially localizing the response of the CM. However, the CM is still to be used in clinical assessment of outer hair cell function for several reasons. In addition to the basal sources contributing to the CM, an inherent limitation of CM measurements is that the recording electrode is away from the source and typically placed at the round window in animals[114,132] and in the ear canal[140] or at the ear drum in humans[141]. Therefore, as the source of the potential moves further apically, as in low frequency stimulation, there is poor signal to noise ratio at the recording electrode.

Furthermore, some evidence suggests that the CM at low frequencies may be influenced by neural components[114,142]. All of these caveats limit the use of low frequency CM for clinical diagnosis. At higher frequencies (> 2 kHz), although the recording electrode is closer to the source of the potential, the amplitudes of tone-burst evoked CMs are smaller and their morphology is poorer compared to CMs in response to low frequency tone-bursts[143]. Therefore, using the CM to assess the

function of the high-frequency encoding cochlear base clinically remains a challenge.

Compared to CM measurements, OAE measurements are less invasive, recordable at frequencies up to 20 kHz[144,145], and are thought to be spatially localized, at least for the basal half[146,147]. Although recent imaging studies have shown broader vibrations of the reticular lamina compared to basilar membrane[148], subsequent suppression experiments have shown that for both near CF and below CF probes, only near CF and below CF suppressors are effective, not above CF suppressors, suggesting that amplification and tuning at CF is not likely to have significant contributions from locations basal to CF[149]. How these broad reticular lamina vibrations contribute to OAEs is not yet fully understood. However, when OAEs are compared across species, human OAEs appear to be less affected by the presence of 1/3 octave basal suppressors compared to other laboratory animals[147], suggesting that the spatial source of human OAEs may be different from other animals.

Some have argued that OAEs are a better indicator of OHC function than the raw CM[150] as measured clinically, because OAEs are more sensitive to changes in OHC function than the raw CM. Indeed, in mice lacking prestin, Liberman et al., (2004) showed that DPOAE thresholds were elevated, whereas the raw CM, particularly at low-levels, was not significantly different from wild-type mice[151]. These findings suggest that the raw CM alone cannot provide an accurate assessment of OHC function and must be supplemented with OAEs.

1.2.4.2. Extended bandwidth recording of OAEs. OAEs are currently being used clinically for screening, differential diagnosis of specific pathologies such as auditory neuropathy[152], and ototoxicity monitoring[153,154]. However, clinical protocols for OAE measurements are limited to frequencies 8 kHz or lower, even though frequencies above 8 kHz may be more informative. Reavis et al., (2008) measured DPOAEs and behavioral thresholds for monitoring ototoxic damage in 53 individuals undergoing treatment with cisplatin, carboplatin and ototoxic antibiotics[155]. They found that DPOAEs at frequencies higher than 2.5 kHz were the best predictors of change in cochlear status due to ototoxicity but the sensitivity of DPOAEs at frequencies above 8 kHz could not be determined because the majority of the participants in this study had non-recordable DPOAEs at baseline[155].

In a more comprehensive study with a stricter inclusion criteria for measurable DPOAEs at baseline, Poling et al., (2019) measured behavioral thresholds and DPOAEs at multiple stimulus levels and ratios in patients receiving ototoxic medications[153]. They found that the sensitivity of DPOAEs for detecting ototoxicity-induced change in cochlear function was highest, when baseline DPOAEs were present at frequencies > 8 kHz[153]. Additionally, the highest frequency at which DPOAEs were measurable at baseline generally decreased with increasing age in these participants[153]. Although DPOAE levels may decline as a function of age at higher frequencies, other properties of DPOAEs could also be informative[153]. In an earlier study, Poling et al., (2014) had previously shown that

the fine structure frequency spacing of DPOAEs > 8 kHz became wider across five age groups, suggesting frequency spacing may be an important metric for quantifying age-related cochlear decline[145].

1.2.4.3. Profiles of cochlear dysfunction. In addition to revising the clinical protocols and establishing new metrics of change, before OAEs can be used for precision diagnostics and monitoring, OAE profiles linking phenotypes to various etiologies will need to be thoroughly investigated. Several groups have used OAEs combined with other measures of auditory function to differentially diagnose the site of dysfunction by means of inducing acoustic damage or treatment with ototoxic compounds in animal models[96], or investigating known genetic conditions such as auditory neuropathy in humans[156].

Mills (2006) examined the effects of furosemide and noise on auditory brainstem response (ABR) thresholds and DPOAE input-output functions in gerbils, aiming to differentially diagnose hearing loss due to strial vs OHC loss[96]. The findings of Mills (2006) showed that DPOAE thresholds increased and DPOAE amplitudes decreased with strial damage; however, the thresholds were shifted by only ~30 dB[96]. On the other hand, with acoustic damage, DPOAE thresholds were shifted by as much as 60 dB and DPOAE levels were much more reduced compared to strial damage[96]. Furthermore, the configuration and frequency range affected by each condition was dramatically different compared to normal gerbils who were not exposed to furosemide treatment or acoustic trauma[96].

In the case of acoustic trauma, both the ABR thresholds and DPOAE levels were normal at low frequencies and displayed a sloping loss at high frequencies, whereas with strial damage, the entire frequency range was affected[96]. Combining all of these metrics, Mills (2006) proposed a model that could be used to differentially diagnose OHC loss, strial loss and neural/IHC loss[96]. Although some efforts have been made towards applying this model to understand human aging and its effects on DPOAEs[157], this model is yet to be validated in humans, in whom ototoxic or acoustic damage cannot be induced in a controlled manner due to ethical concerns and histology phenotyping can only be performed after post-mortem cochlear resection.

Another source of empirical evidence for the need to establish profiles of dysfunction comes from observational studies of different OAE types to various noise-induced or age-related pathologies[13,14,158]. In a longitudinal study of noise-exposed and non-noise-exposed individuals, Lapsley-Miller et al., (2004) measured DPOAEs, TEOAEs, and behavioral hearing thresholds across four years and found that behavioral thresholds as measured clinically using a 5 dB step size were the least sensitive to change across years and with noise exposure, whereas TEOAEs were the most sensitive[158]. A subset of individuals with temporary and permanent threshold shifts were also studied and the findings showed that DPOAEs were not as affected by temporary or permanent threshold shift as TEOAEs, suggesting a different sensitivity of each emission type to different degrees of noise exposure[158].

Towards understanding the use of both types of OAEs for differential diagnosis, Abdala & Kalluri (2017) measured DPOAEs and SFOAEs in individuals with normal-hearing and slight to moderate sensorineural hearing loss[13]. They found that compared to normal-hearing individuals, the OAE metrics of hearing-impaired individuals were quite variable such that individuals with similar audiograms had different joint OAE profiles in which one or both OAEs were affected[13]. These findings not only confirm the insensitivity of the audiogram to different pathologies of the inner ear, but also highlight the possibly distinct sensitivities of the two OAE types.

Abdala, Ortmann & Shera (2018) later investigated the different sensitivities of DPOAEs and SFOAEs for detecting age-related changes[14]. They found that both DPOAEs and SFOAEs declined across age groups[14]. However, as age increased, the difference between the two OAE levels became smaller, suggesting different chronologies of the two OAE types for aging, with SFOAEs declining earlier than DPOAEs[14]. Whether this differential timeline is due to slow degradation of different anatomical structures or functions is unknown.

An approach that has been used to connect OAE data to specific anatomical structures involves genetic mutations of proteins found in the OHC soma (prestin) and the stereocilia bundle (stereocilin). Liberman et al., (2004) measured DPOAEs and CM in mutant mice that lacked prestin and found that DPOAEs were in the noise floor across all stimulus levels in the homozygous mutants compared to wildtype[151]. However, DPOAEs were measurable in some mice with better CAP

thresholds at high stimulus levels only[151]. Based on the absence of DPOAEs at low levels and presence at high levels, it was suggested that prestin-based electromotility is not necessary for DPOAE generation at high levels[151].

Liberman et al., (2004) further suggested that the presence of DPOAEs at high levels in prestin-deficient mice may be related to stereociliary nonlinearity[151]. In a study aimed to understand the role of stereociliary nonlinearity and generation of DPOAEs, Verpy et al., (2008) measured DPOAEs in mutant mice lacking stereocilin, a protein found in the stereocilia hair bundle that is responsible for linking individual stereocilium together in an organized bundle[159]. They found that homozygous stereocilin mutant mice lacked DPOAEs even at very high levels[159], further confirming the hypothesis proposed by Liberman et al., (2004) that stereociliary nonlinearity is necessary for DPOAE generation.

Cheatham et al., (2011) showed that in mice with a prestin knock-in mutation, OHCs are structurally similar to wild-type mice[160], but the prestin mutants have reduced nonlinear capacitance and electromotility[161]. Furthermore, SFOAE input-output functions in the mutant mice were shifted to ~30 dB higher probe levels compared to wild-type mice[160]. These findings suggest that in mice, SFOAEs are at least somewhat dependent on normal somatic electromotility. Whether mutations of the stereocilia bundle proteins also lead to altered SFOAEs is unknown. Studies of tectorial membrane mutations and their relationship to SFOAEs will be reviewed in later sections.

Evidence from animal models with punctate lesions or specific mutations offer insights regarding the generation site, mechanism, and sensitivity of different OAEs to cochlear dysfunction. However, human cochlear dysfunction is likely complex and modifying clinical protocols for more sensitive and accurate diagnosis of cochlear dysfunction will first require a thorough examination of various OAEs in known genetic conditions or environmentally vulnerable populations. Here, the focus will be to investigate emissions evoked using a single tone, or stimulus frequency otoacoustic emissions (SFOAEs). Before delving into SFOAEs, cochlear anatomy and physiology will be reviewed in the next section.

1.3. Cochlea - The Hearing Organ

Before the brain forms the percept of hearing, auditory signals are processed peripherally[162]. The peripheral hearing mechanism refers to all structures that receive, transform, and process auditory signals before sending them centrally to be perceived[162]. After sound travels through the ear canal, it passes through the middle ear as mechanical energy[162]. The mechanical motion of the stapes footplate in and out of the oval window initiates pressure waves that propagate along the cochlear partition, converting the mechanical energy into hydrodynamic pressure[162]. Because of the incompressibility of the fluid within the cochlea and the push-pull displacements of the oval and round windows, the pressures in scala vestibuli and scala tympani are inversely related[162]. This pressure differential between scala

tympani and scale vestibuli results in the displacement of the basilar membrane at its resonant place[163].

The vibrations of the basilar membrane at the resonant place results in the deflection of the tallest stereocilia of the stereociliary bundle of the sensory cells within the envelope of the incident wave[162]. The magnitude of basilar membrane displacement determines whether the stereocilia of just outer hair cell or both outer hair cell and inner hair cell are deflected[162]. The deflection of the tallest stereocilia results in stimulation of the other stereocilia of the bundle that are physically tethered together via tiplinks[162]. The transduction of ions through the mechanically gated channels of the stereocilia of the sensory cells then causes voltage changes within the cell that are responsible for the somatic electromotility of the outer hair cells and responsible for initiating the signaling sequence for vesicle formation and release in the inner hair cells that will ultimately stimulate the auditory nerve[162].

While OHCs are thought to be involved in the active amplification of mammalian cochlear mechanical responses, the inner hair cells (IHCs) are known to transduce cochlear mechanical response into electrical signals to the auditory nerve[164]. Albeit the entire transduction and signaling sequence is highly complex, the peripheral processing of sound that allows for the various perceptual hearing abilities is dependent on the structural and mechanical properties of the cochlea, which will be briefly reviewed hereafter.

1.3.1. Cochlear Structural Properties

The osseous cochlea contains three fluid-filled compartments: 1) scala vestibuli; 2) scala tympani; and 3) scala media, also known as the cochlear duct[162]. Scala vestibuli and scala tympani are filled with perilymph that is continuous with the vestibule and semicircular canals that make up the vestibular system; whereas scala media is filled with endolymph which is specialized for establishing the electrochemical gradients responsible for hearing[162]. The scala media is separated from scala vestibuli via the Reissner's membrane along its top boundary and is separated from scala tympani via the basilar membrane along its bottom boundary[162]. The basilar membrane and the osseous spiral lamina together make up the cochlear partition that coils from the base of the cochlea towards the apex, where it terminates at the helicotrema, a screw shaped bony segment where the fluids of the scala vestibuli mixes with the fluid of the scale tympani[162].

The structural properties of the basilar membrane vary from the base to the apex, such that the basilar membrane is thick, narrow, and stiff near the stapes footplate getting thinner, wider, and floppier further away from the stapes footplate[162]. Békésy (1947) was the first to measure this stiffness gradient in human cadaver ears and concluded that the stiffness gradient is important for establishing cochlear tonotopicity, i.e. the frequency and place mapping of the cochlea, such that high frequency stimulation resonates towards the base of the cochlea whereas low frequency stimulation resonates towards the cochlear apex[165]. Furthermore, this stiffness gradient establishes gross frequency filtering of auditory signals[165].

Atop the cochlear partition that coils within the cochlear duct of the osseous cochlear labyrinth sits an epithelial structure called the organ of Corti that houses the primary sensory cells of the auditory system[162]. The organ of Corti consists of the outer hair cells (OHCs), inner hair cells (IHCs), various supporting cells and the tectorial membrane (TM)[162]. The TM is a large strip of extracellular matrix that is attached to the spiral limbus on the medial side, and on the lateral side, the TM overlies the inner and outer hair cells, attaching to the tips of the tallest cilium of the OHC hair bundles[166].

Until recently, it was thought that the tallest of the stereocilia was attached to the TM in only OHCs and not IHCs; however, new evidence challenges the classic view of the TM attachment to IHCs[167]. Hakizimana & Fridberger (2021) used confocal microscopy in guinea pig to show that, similar to the OHC-TM connection, the tips of the tallest cilium of the IHCs are also embedded in the TM[167]. In addition to having stereociliary bundles, the mammalian OHCs express a transmembrane protein called prestin, which has a special area for binding Cl^-, throughout their somas[164].

The three, sometimes four, rows of OHCs are laterally located on top of Deiter's cells, whereas a single row of IHCs are surrounded by other supporting cells medially[168]. The two types of sensory cells are separated by the inner and outer pillar cells, separated at the bottom, adjoining at the top and creating a tunnel underneath, known as the tunnel of Corti, which is filled with cortilymph[168]. The cuticular plate of the OHCs, IHCs, and the tops of the various supporting cells

together form the reticular lamina[168]. The reticular lamina separates the cortilymph that bathes the bodies of the OHCs and IHCs, from the endolymph that bathes the stereociliary bundles of OHCs and IHCs[168]. Together the gross structural architecture of the cochlea sets up the passive mechanical response, which is further enhanced by active processes.

1.3.2. Cochlear Mechanical Properties

When sound energy arrives at the stapes, piston-like stapes motion is initiated[169]. The motion of the stapes in and out of the oval window generates differential pressure between the scala vestibuli and scala tympani which initiates a traveling waves that propagate along the cochlea partition, resulting in mechanical vibration of the basilar membrane[170]. Because of the mass and stiffness gradient of the basilar membrane, each location along the length of the basilar membrane maximally vibrates in response to a particular frequency[165]. This property has led to the popular labeling of specific longitudinal sections of the cochlear partition by their characteristic frequency.

Von Békésy (1947) measured the amplitude and phase of different tones at a fixed location on the basilar membrane relative to the stapes movement[165]. Although his experiments were performed in human cadaver ears using very high stimulus levels, von Békésy found that the amplitudes of basilar membrane displacement in response to different tones were greatest at their resonant (or characteristic frequency) places along the cochlea[165]. Furthermore, the phase difference between the stapes and the measurement location increases as the

frequency of stimulation approaches the resonant frequency, suggesting that the displacement waves were not just simple resonances but traveling waves instead[165].

Johnstone & Boyle (1967) later showed that mechanical tuning curves in live guinea pig cochleae were sharper than von Békésy's cadaver ears[171]. Rhode (1973) also showed that compared to pre-mortem, there was a ten-fold decline in the amplitude of basilar membrane vibrations within 10 minutes of the death of the animal, which was a hundred-fold after 1 hour of death[172]. Later, Sellick et al., (1982) compared pre- and post-mortem basilar membrane motion measurements in guinea pig cochleae and found that input-output functions became linear and tuning curves became broader with the death of the animal[173]. These findings together were support for the idea of an active process in the living cochlea that provides the amplification at low stimulus levels, frequency tuning, and compression at high stimulus levels.

Towards identifying the role of the outer hair cells in the active mechanical process, Ruggero & Rich (1991) treated chinchilla cochleae with furosemide (a loop diuretic that reduces the endocochlear potential) to block outer hair cell transduction and observed the basilar membrane vibrations before and after treatment[174]. The findings showed a decrease in frequency tuning, particularly at low stimulus levels as well as a reduction in basilar membrane velocity with furosemide treatment[174]. Although these findings confirmed that hair cell transduction is important for active amplification, tuning, and compression of the

mammalian cochlea, the mechanisms by which OHCs accomplish these functions are still being investigated.

The current view is that active cochlear processes are a result of two OHC mechanisms: prestin-based somatic electromotility and calcium-dependent hair bundle motility[161,175]. In response to the basilar membrane motion, the kinocilium of the hair bundle embedded in the tectorial membrane shear, opening the mechanically gated transducer channels of the stereocilia and allowing the influx of potassium ions[176]. When the potassium flows in, it depolarizes the cell, which forces chloride to dissociate from the prestin molecules, changing their conformation from long state to short state[176]. Because the potassium influx happens on a cycle-by-cycle basis, the conformational change in prestin follows this cycle-by-cycle change, and the outer hair cell goes through elongation and shortening of the soma depending on the frequency of the stimulus[176]. Although recent in vivo recordings in mice have shown that the tops and bottoms of OHCs have opposite displacements at frequencies up to 20 kHz, suggesting a cycle-by-cycle amplification at these very high frequencies, the exact mechanism of amplification at ultra-high frequencies remains a topic of controversy and active investigation[177].

Although this prestin-based mechanism is thought to be sufficient for the cochlear frequency range of most mammals, in species with ultrasonic hearing, hair bundle motility may supplant prestin-based electromotility to achieve cochlear amplification and tuning at frequencies up to 100 kHz[176]. More recently, the role of the reticular lamina (RL) and the tectorial membrane (TM) in cochlear

amplification and tuning is also being investigated[149]. High resolution imaging of live organ of Corti mechanics using low-coherence interferometry[178] and optical coherence tomography[148,149] showed that vibrations of the RL and TM were larger and more compressive than those of the basilar membrane and were similarly affected by the death of the animal.

Although these findings initially implicated the role of the RL and TM in the active cochlear process, subsequent experiments in mice have shown that despite the broad and large mechanical motions of the RL and TM, suppression responses of the BM and RL support the hypothesis that longitudinal coupling of OHCs is strongest near the peak of the traveling wave, despite broad amplification of below CF response of the RL[149]. The complex interactions between BM, TM, and RL that result in the stimulation of OHCs are yet to be fully characterized.

Nonetheless, through their active mechanical process, OHCs enhance the vibrations of the organ of Corti, particularly at low input levels[179]. These enhancements of mechanical vibrations are thought to generate backwards propagation of energy through fluid compression in the cochlear duct[180]. This energy acts upon the stapes and conducts mechanical vibrations that travel back towards the ear canal, where the transformed mechanical energy is measured with a sensitive microphone as acoustic energy[180]. These packets of acoustic energy emitted by the cochlea are referred to as otoacoustic emissions (OAEs)[1,181]. Decades of research has shown that OAEs can provide a quick and objective measure of cochlear status and will be reviewed in the next section.

1.4. Otoacoustic Emissions – Derivates of Cochlear Processes

In 1978, Professor David T. Kemp first reported on an acoustic phenomenon in human ears[1]. By placing a microphone and speaker probe assembly into the ear canal, Kemp (1978) recorded the ear's physiological response to transient clicks and tones of different frequencies[1]. Kemp's recordings, fittingly referred to as "echoes", had several key characteristics: 1) the echoes were absent in a non-human hard cavity as well as deaf human ears; 2) they were highly personalized to an individual ear across normal-hearing adults; 3) they displayed frequency-specific delays consistent with the tonotopic organization of the cochlea; and 4) they were level-dependent in their response and sometimes recordable at levels below an individual's subjective hearing threshold[1].

Probst et al., (1986) found repeatable characteristics of click- and tone burst-evoked OAEs in normal hearing adults but also found a correlation between OAEs evoked with stimulus and spontaneous OAEs evoked without stimulus, suggesting a common generation mechanism across spontaneous, transient-evoked, and tone-burst evoked OAEs[182]. Although OAE generation mechanisms are still a topic of debate among investigators, it is well established that OAEs arise from within the cochlea. Hubbard and Mountain (1983) first showed that electrical current delivery intracochlearly resulted in otoacoustic emissions in the ear canal[183]. Nuttall & Ren (1995) later measured the guinea pig basilar membrane motion in response to electrical stimulation of the cochlea and found that the basilar membrane motion

was correlated with electrical energy measurable at the round window and acoustic energy measurable in the ear canal[184].

1.4.1. Sensitivity of OAEs to Various Cochlear Manipulations

The sensitivity of OAEs to chemical or environmental insults, pathophysiological processes, and genetic manipulations are also well documented. For example, DPOAEs are reduced in animals exposed to acoustic trauma[2,185], furosemide[96], and ototoxic drugs[186,187]. In humans, Helleman et al., (2018) reported that a history of long-term noise exposure is linked to a deterioration in OAEs over time albeit great variability in OAEs was observed likely due to the heterogeneity of the studies included in the systematic literature review[188].

Systemic diseases (e.g., diabetes) and homeostatic shifts (e.g., postural changes) can also alter OAEs. In two mice models of diabetes mellitus, DPOAEs were found to be reduced from baseline to 6 months, particularly at high frequencies, compared to control mice who did not show any changes[189]. Voss et al., (2010) measured DPOAEs before and after inducing postural changes in 12 normal-hearing adults and found that DPOAE levels and phase angles were consistently lower in the upright position compared to the tilted position, presumably due to the posture-induced change in intracranial and intracochlear pressure[190]. Furthermore, genetic mutations of prestin, stereocilin, or tectorial membrane alter ear canal OAEs in different ways[151,159,191]. All of these areas of research support the clinical use of OAEs for a non-invasive, objective, and quick assessment of cochlear function.

1.4.2. Clinical Use of OAEs

Indeed, since their discovery, OAEs have been used widely for many screening purposes from newborns to school screenings to hearing conservation purposes. Beyond screenings, OAEs have also been used for more advanced purposes, such as monitoring for changes in auditory status due to ototoxic medications or noise exposure, for differential diagnosis of cochlear vs retrocochlear type of hearing loss, and to cross-check behavioral findings when reliability of behavioral tests is questionable. Despite these various uses, clinical application and utilization of OAEs have not yet reached their full potential[192].

One of the reasons for this underutilization is that advanced measurements of OAEs (i.e., using extended high frequency stimuli, multiple levels, or multiple types of OAEs) do not change the course of treatment for most types of hearing loss, as treatments are often devices that amplify signals coming to the ear and not therapies that restore cochlear structures or functions. However, novel therapies and treatments for prevention and correction of hearing loss will necessitate major revisions to current diagnostic testing protocols that include advanced measurements of OAEs for differentiating outer hair cell loss, strial dysfunction, synaptic or neural loss[16,92,193] and earlier detection of signs of cochlear dysfunction due to environmental toxins or pathophysiological processes.

Clinical use of advanced OAE measurements is also hindered by the lack of understanding about where and how OAEs are generated in the cochlea. Although OAEs were first described over 40 years ago[1], the where and how of OAE generation

is still a relevant and timely topic of many scientific investigations[146,147,194]. A better understanding of the spatial extent of OAE generation would allow for more accurate diagnosis of the regions of cochlear dysfunction, whereas understanding the mechanisms by which OAEs are generated may improve the accurate identification of cellular and molecular targets for novel treatments.

1.4.3. OAE Generation Sources & Mechanisms

Towards determining the extent of OAE generation region, Charaziak & Siegel (2015) measured suppression tuning curves using stimulus frequency otoacoustic emissions (SFOAE) and compound action potentials (CAP) in chinchilla before and after inducing acoustic trauma at far basal locations and found that although CAP tuning was not affected by the acoustic trauma away from the 1 kHz characteristic place, SFOAE tuning curves became broader, concluding that SFOAEs are not indicative of cochlear function in a place-specific manner[146]. Findings were similar when a high-frequency interference (suppressor) tone was used to temporarily suppress the basal contributors instead of using acoustic trauma to permanently ablate basal contributors[146]. Although Charaziak & Siegel's findings indicate low-frequency SFOAEs may not be place-specific, the generation extent of high-frequency SFOAEs is yet to be fully determined, particularly in humans in whom intracochlear measurements are not possible.

When human OAEs are compared to other animals, evidence suggests that OAE generation may be more localized in humans. Martin et al., (2011) compared

distortion product otoacoustic emissions (DPOAEs) across humans, rabbits, chinchillas, and rats using the interference tone paradigm[147]. Although Martin et al., (2011) aimed to understand the influence of interference tones (IT) on the different components of DPOAEs, their findings showed that DPOAEs measured with and without a 1/3-octave IT were quite similar in level across rabbits, chinchillas, and rats; however, in humans, the DPOAEs measured with IT were lower in level compared to DPOAEs measured without IT, particularly at higher frequencies (> 2 kHz), suggesting less contribution from regions basal of the peak response in humans compared to other animals[147]. These findings could be interpreted as evidence for a more localized DPOAE generation in humans compared to other laboratory species.

OAE generation sources (where) and mechanisms (how) are theorized to vary with the emission type. Shera & Guinan (1999) have described at least two classes of emissions – reflection emissions and distortion emissions[195]. Reflection emissions, such as spontaneous (S), transient-evoked (TE) or stimulus frequency (SF) OAEs, are hypothesized to be net intracochlear wavelets reflected from the heterogenous anatomical and mechanical irregularities along the cochlea, similarly to light wavelets reflecting within an optical glass prism[195]. Distortion emissions, such as distortion-product (DP) OAEs, are different from reflection emissions in that their hypothesized primary generation results from the nonlinearity of the stereocilia bundle, and a secondary reflection mechanism is also involved[195].

1.4.4. OAE Types & Applications

Understanding where and how various types of OAEs are originated in the cochlea would allow for more precise diagnostics; however, as it is, TEOAEs are used as a global measure of cochlear function for purposes such as screening for hearing loss, whereas DPOAEs are used for more frequency-specific applications such as cochlear monitoring. Studies have shown that TEOAEs are more sensitive than DPOAEs in detecting hearing loss, such that ears with even a mild hearing loss will show absent TEOAEs[15] whereas DPOAEs may be recordable even when hearing loss is moderate[196].

Although TEOAEs are easily recordable in clinical settings, they are not used to draw place-specific conclusions regarding the cochlea. SFOAEs on the other hand are evoked using a single tone and as such, SFOAEs are thought to be more frequency-specific, and presumably more place-specific, than other types of OAEs. Recent evidence suggests that DPOAEs are recordable at much higher frequencies than SFOAEs even in young, normal-hearing adults[197]. Furthermore, SFOAEs and DPOAEs may be differentially affected by aging[13,14]. These findings suggest that SFOAEs may be more sensitive to cochlear status. However, many questions about SFOAE generation, SFOAE relationship to other measures of hearing (Chapter 3) and SFOAE sensitivity to aging (Chapter 4) remain unanswered and will be addressed hereafter.

1.5. Stimulus Frequency Otoacoustic Emissions

Stimulus frequency otoacoustic emissions (SFOAEs) are sounds emitted from the cochlea in response to a single tone. SFOAEs are thought to arise from the summed reflections of the forward going traveling wave and the impedance irregularities encountered by the incident wave[1]. When SFOAE levels are plotted as a function of frequency, there is a periodicity of the SFOAE peaks and dips, referred to as microstructure – a characteristic that was initially thought to be a result of periodically spaced irregularities in the anatomical array of hair cells along the cochlear spiral[198].

The anatomical irregularities would allow for increased scattering at certain positions along the cochlear spiral thus leading to increased emission amplitudes at certain frequencies. However, early anatomical studies did not find evidence for the periodic points of increased scattering, but instead a "generalized irregularity" and "cellular disorganization"[199]. Even when some irregularity was found in the appearance and disappearance of the fourth row of outer hair cells, the frequency spacing of OHC fourth row and SFOAE maxima were not identical (albeit the spacing of both did change proportionally with frequency region)[199]. Lonsbury-Martin et al., (1988) concluded that the frequency spacing of SFOAEs reflects normal variation/anomalies of the organ of Corti and is not sensitive to signs of cochlear injury[199].

Because spontaneous otoacoustic emissions (SOAEs) and SFOAEs are both thought to be reflection type emissions, characteristics of SOAEs have also been

investigated towards understanding the generation mechanism of reflection emissions. Some evidence in support of the local irregularities hypothesis of reflection emission generation comes from the presence of spontaneous OAEs in a case-study dog with a sharp transition in ABR thresholds around the frequency of the SOAE[200], and intentionally noise-damaged chinchilla[201] with spontaneous otoacoustic emissions around histologically confirmed total dead regions.

1.5.1. Reflection Emissions & Relationship to Behavioral Microstructure

Another approach for understanding OAE generation has been to compare OAEs to perceptual hearing abilities. Commonalities in OAEs and behavioral responses have been long observed. For example, microstructure is not unique to OAEs, as it is also found in psychophysical measures of hearing thresholds and loudness[202,203]. Kemp (1979) first posited that microstructure of thresholds and microstructure of emissions is inversely related, such that threshold dips (also referred to as minima) occur around the same frequency as emission peaks (also referred to as maxima)[203]. Similar to OAEs, spectral oscillation in threshold microstructure was also thought to be related to the regular periodicity of cochlear micromechanical irregularities[203]. If this were true, the forward and backward traveling waves measured at the stapes should also show spectral periodicity[203].

Shera & Zweig (1993) refer to this as cochlear reflectance, defined as the complex, frequency-dependent ratio between the backward wave pressure and the forward wave pressure measured at the stapes[204]. Empirically derived cochlear

reflectance was observed to vary slowly in amplitude and linearly in phase as a function of frequency[204]. This linear phase rotation as a function of frequency of cochlear reflectance suggests OAE spectral oscillations do not arise from inherent regularly spaced cochlear inhomogeneities, and instead, they must arise from constructive and destructive interference between the incident and reflected cochlear waves due to variations in their respective phases[204].

The microstructure phenomenon is also related to standing wave resonances in the cochlea[203,205]. The theoretical framework explaining the maxima and minima in both thresholds and OAEs – referred to as the intracochlear reflections framework[203] – posits that the origin of microstructure is the constructive and destructive interactions between primary reflections, originating initially in response to a stimulus, and non-primary reflections that are re-introduced in the cochlea from the impedances encountered at the middle ear boundary[203].

When the standing waves combine constructively with the primary and/or non-primary reflections, the interaction enhances the OAE amplitude and improves behavioral threshold[203]. On the other hand, when the primary and/or non-primary reflections interact with the standing waves destructively, their interaction reduces OAE amplitude and worsens behavioral thresholds[203]. The intracochlear reflections framework predicts maxima in OAEs and corresponding minima in thresholds will be separated at predictable frequencies[203].

Several studies have measured the microstructure of OAEs and behavioral thresholds towards understanding their respective origins and their shared

association. Long & Tubis (1988) showed that threshold microstructure and OAE levels were both sensitive to aspirin toxicity[206]. With increasing dosage of aspirin, which is known to cause temporary and reversible OHC toxicity, threshold microstructure disappeared and levels of both spontaneous and evoked OAEs declined[206]. Dewey & Dhar (2017a) measured microstructure of behavioral thresholds and SFOAEs for frequencies between 2-5 kHz and found that SFOAEs, measured at very low levels, have peaks that correspond with minima of behavioral threshold microstructure[207].

Furthermore, the frequency spacing of SFOAE maxima and number of cycles of SFOAE phase accumulated across adjacent maxima was close to one cycle[207]. Baiduc, Lee & Dhar (2014) later showed that SOAEs and behavioral microstructure were related at ultra-high frequencies as well[208]. All of these findings provide additional evidence for the intracochlear reflections model. Perhaps more importantly, these studies suggest that low-level reflection emissions, at least in normal-hearing ears, correspond to the region that determines behavioral thresholds. Additional studies examining the generation region and mechanism of SFOAEs are discussed below.

1.5.2. Anatomical Correlates of SFOAEs

The conflicting reports of anatomical observations and otoacoustic emissions have been puzzling - large interspecies morphological differences across vertebrates exist, yet SFOAE generation shares a common mechanism across vertebrates with

just a tectorial membrane (frog), both a TM and a flexible basilar membrane (lizard); TM, BM, and a traveling wave (chicken); and TM, BM, traveling wave, and hair cell somatic electromotility (humans)[209]. Even within the lizard suborder, both species with a TM and without a TM exist and offer insights into OAE generation mechanisms.

Bergevin et al., (2011) compared SFOAE phase gradient delays in nine different species of lizard and found that the species that lacked a TM had shorter delays compared to those with a TM[210]. These findings suggested a role of the TM in the observed SFOAE phase gradient delays. However, whether these associations in lizard ear are also representative of the mammalian cochlea remains unknown. Since the comparative reports of Bergevin et al., (2008; 2011), some helpful insights from genetically modified mice have emerged.

Cheatham et al., (2014) showed that, in mice with *CEACAM16* mutation that prevents the formation of the striated-sheet matrix of the TM, SOAEs were numerous compared to wild-type mice, SFOAE and TEOAE levels were higher than wild-type mice, but DPOAEs and auditory brainstem response (ABR) were normal[191]. Goodyear et al., (2019) recently showed that the cochleae of *CEACAM16* mutant mice age faster than wild-type mice and thus can serve as a model for late-onset human hereditary hearing loss[211].

Cheatham et al., (2016) later showed that another TM mutation in mice lacking otoancorin, which results in a detached tectorial membrane phenotype, also produced increased SOAEs compared to wildtype mice[212]. Cheatham et al., (2018)

further reported that compared to wild-type mice, *TECTA* gene mutant mice have a higher incidence of spontaneous OAEs[213]. Like Ceacam16, alpha-tectorin (TECTA) and beta-tectorin (TECTB) are noncollagenous proteins that make up the striated-sheet matrix of the tectorial membrane[213]. Like otoancorin, a homozygous *TECTA* mutation results in a detached tectorial membrane and hearing loss; whereas a heterozygous *TECTA* mutation causes a semidominant phenotype such that the Kimura's membrane separates from the TM but still makes contact with the OHC stereocilia[213].

The numerous TM mutations studied, each with its own phenotypic reflection emission signature, coupled with the interspecies data together suggest that myriad anatomical and mechanical configurations could independently create the internal physical dynamics necessary for the generation of reflection emissions. Perhaps this fundamental hypothesis could explain the large amount of individual variability seen in the presence, number, and frequency of SOAEs and the levels of SFOAEs even among normal-hearing adult humans[182,197,214] and neonates with presumably pristine cochleae[215,216].

Anatomical studies of hair cell distributions in human cochleae show that, although the number of inner hair cells and outer hair cells vary across age groups and across individuals within the same age group, there is heterogeneity of hair cell counts[93] even among fetal human cochleae[217]. How this heterogeneity contributes to the large inter-subject variability of reflection emissions is yet to be determined.

1.6. Rationale

Despite the large inter-subject variability of reflection emissions, several key findings suggest that reflection emissions are clinically viable tools for assessing cochlear dysfunction. First, reflection emissions are more sensitive than distortion emissions to cochlear manipulations and various pathologies. For example, in studies of human DPOAEs, the reflection component is more affected by salicylates than distortion component[218], by efferent activation[219], and by aging[220]. Second, reflection emissions have been shown to be repeatable over time. A 33-year-long monitoring of SOAEs of one individual ear showed that SOAE levels are stable from year to year within an individual, suggesting that reflection emissions are an excellent monitoring tool; however, SOAE levels and frequencies do shift slightly as a function of age, suggesting some sensitivity to age-related changes in cochlear status[221].

SFOAE levels and phases have also been shown to be repeatable over time within an animal[222] and within individual human ears[223,224]; however, most human studies have examined SFOAEs for frequencies at or below 8 kHz even though cochlear aging begins at ultra-high frequencies (above 8 kHz). Historically, SFOAEs have been difficult to measure because of the methodological manipulations (compression/suppression) necessary to extract the emission from the stimulus, both occurring at the same frequency[222]. However, advances in SFOAE measurement using faster, swept-tone stimuli have seen some success, making SFOAE recordings easier.

Despite advances in SFOAE recording and analysis techniques, a comprehensive examination of human SFOAEs is lacking, specifically evaluating their sensitivity and specificity – a necessary step towards incorporating SFOAEs within a clinical setting. Before the sensitivity and specificity of SFOAEs can be investigated, many questions must be addressed about their generation mechanism and source, their relationship to other measures of hearing sensitivity and tuning, and their performance in detecting age-related cochlear dysfunction.

The purpose of this dissertation is to address the question on the clinical viability of SFOAEs as a sensitive and accurate tool for assessing cochlear dysfunction. Towards answering this question, first, the relationship between SFOAEs and behavioral measures of threshold and tuning was examined across a wide frequency range (0.5-14 kHz). One of the reasons SFOAEs are not utilized clinically is because it is not fully understood how SFOAEs are related to psychophysical measures of auditory sensitivity and tuning[225]. Specifically, can SFOAEs predict hearing thresholds? Does SFOAE phase slope relate to psychophysical tuning? Towards answering the first question, the purpose of the first study (Chapter 3) is to investigate the relationship between SFOAE levels at different stimulus levels and behavioral hearing thresholds up to 14 kHz. The purpose of the second study (Chapter 4) is to examine tuning estimates from the phase gradient of SFOAEs as compared to psychophysical tuning up to 14 kHz.

Another reason SFOAEs are not utilized clinically is because sensitivity of SFOAEs to early age-related changes in cochlear function has not been fully

characterized, especially for the high frequency encoding cochlear base. Specifically, how are SFOAEs affected in early auditory aging? Do SFOAEs decline before thresholds are affected due to age-related cochlear changes? The purpose of the last study (Chapter 5) is to characterize SFOAE levels, phase, and bandwidth across four age groups. The sensitivity of various properties of SFOAEs to aging were examined and the findings will be reported in Chapter 5. Lastly, the implications of the findings from the three studies will be discussed in Chapter 6.

CHAPTER 2

General Methods

2.1. Overview

The study was performed at the Auditory Research Laboratory at Northwestern University in Evanston, Illinois over the course of 1.5 years from November 2019 – March 2021. Participants were recruited from Northwestern University campus and the greater Chicago metropolitan area via flyers and word-of-mouth or through the Communication Research Registry (STU00070769 [PI – Molly Losh]). The child participants were also recruited through the Child Studies Group registry (STU0020141 [PI – Tina Grieco-Calub]). Adult participants provided informed consent to participate in the study procedures. Minor assent and parent permissions were obtained from child participants and their parent/guardian. Participants were compensated monetarily for their participation in the study. All study procedures were approved by the Institutional Review Board at Northwestern University (STU00000295).

2.2. Inclusion/Exclusion Criteria

Participants were required to meet the following inclusion criteria: 1) normal otoscopic examination as evidenced by the absence of active outer or middle ear infection, excessive cerumen, or foreign body in the ear canal; 2) normal middle ear function as characterized by a Type A tympanogram with peak compliance within

0.3-1.4 mmhos for adults (age 19.5-61.5 years) and 0.2-0.9 mmhos for pediatrics (age 2.8-5.8 years)[226]; 3) normal-hearing as defined by pure-tone thresholds of ≤ 20 dB HL across standard audiometric frequencies of 0.25, 0.5, 1, 2, 3, 4, 6, 8 kHz[61] in at least one ear.

2.3. Equipment

Experiments were performed in a double-walled, audiometric booth with the participant comfortably seated in a reclining chair. All experimental, behavioral and otoacoustic emission measurements were done using the Etymotic Research ER-10X Extended Bandwidth Research Probe System (Etymotic Research, Elk Village, IL). Digital-to-analog and analog-to-digital conversion were performed using an RME Fireface 400 audio device (Audio AG, Germany) at a sampling rate of 96 kHz and 24-bit resolution. Signals were generated and recorded via custom written software in MATLAB (2015B) running on a Macintosh computer (Mac OS 10.12).

Stimulus level verification was done by first using a known sound source (Bruel & Kjaer 4231 tone generator producing 1 kHz 94 dB SPL tone) coupled to an ear simulator (Bruel & Kjaer type 4157) and then using the ER10x speakers to generate and measure stimulus levels produced using our custom stimulus generation script. Stimulus levels measured using known source and ER10x speakers with custom generated signals were found to be within 1 dB of each other for 1 kHz pure-tone.

ER10x microphone sensitivity was checked every 3 months using a known sound source (Bruel & Kjaer 4231 tone generator producing 1 kHz 94 dB SPL tone) and Fluke 117 voltmeter. The measured sensitivity of the microphone was found to be stable (within 3 dB), and therefore, default manufacturer specified sensitivity of 0.05 V/Pa was always used in computing the pressure recorded at the microphone.

Signals were routed through ER-10X sound drivers (Etymotic Research, IL) and presented into the participant's ear canal coupled by a silicone ear tip (Sanibel Supply, MN). Microphone voltages were amplified at +20 dB programmable gain and high-pass filtered at 350 Hz. Recorded OAE responses were corrected to emitted pressure level (EPL) to account for the standing wave related influences in the pressure recorded at the microphone. The recorded pressures were not corrected for the microphone frequency response due to its relatively flat output up to 16 kHz.

2.4. Thévénin Source Calibration

Forward pressure level (FPL) calibration methods based on the Thévénin-equivalent source properties of the ER-10X probe were used to calibrate in the ear canal by first isolating the forward-going and reflected components of the stimulus pressure wave in the ear canal and then correcting for the stimulus reaching the eardrum. Calibration program was provided by Dr. Shawn Goodman, University of Iowa, with custom-written MATLAB software ARLas (version date November 7, 2017). The in-situ calibration procedure provided a frequency by frequency

maximum output level in dB forward pressure level, from which all outgoing digital stimuli were scaled accordingly.

2.4.1. Source calibration.

The Thévénin-equivalent source impedance characteristics of the ER10x probe system were obtained in a set of cavities with known lengths of 2.9, 3.6, 4.15, 5.2, and 6.9 cm. Calibration stimulus was a logarithmic chirp (0.2-20 kHz). The frequency response of the ER-10x drivers as provided by the manufacturer was used to correct the outgoing calibration stimulus. Calibration level was set at 15 dB below the maximum output to ensure adequate signal to noise ratio and appropriate loudness comfort of the chirp in the ear canal. Temperature of the probe and calibration cavity was set and maintained at body temperature (37 degrees Celsius). Cavity diameter was estimated at 0.8 cm. 48 chirps were played and recordings were averaged before frequency domain analysis using fast- Fourier transform (FFT). The following variables were computed: 1) measured load pressure relative to stimulus (PL_{ER10x}); 2) load impedance (ZL_{ER10x}); 3) measured source pressure (PS_{ER10x}); and 4) measured load impedance (ZS_{ER10x}).

2.4.2. Load calibration.

Calibration chirps from source calibration done on the same day were presented to the ear canal. Load impedance of the ear canal (ZL_{ec}) was estimated using measured load pressure (PL_{ec}) and Thévénin-equivalent source characteristics

of the ER10x probe system as such: $ZL_{ec} = (ZS_{ER10x}.* PL_{ec}) / (PS_{ER10x} - PL_{ec})$. From $ZL_{ec,}$ the following variables were computed: 1) complex forward pressure level (FPL), where $FPL = (PL_{ec}/2) * (1 + z0 / ZL_{ec})$ and z0 is the surge impedance of the ear canal; 2) complex reflected pressure level (RPL) where $RPL = (PL_{ec}/2) * (1 - z0 / ZL_{ec})$; 3) complex pressure reflectance (PR), where PR = RPL / FPL; and 4) power reflectance (PPR), where $abs(RPL)^2 / abs (FPL)^2$. A calibration was determined as successful if the absorbance was less than or equal to 0.2 at 100-200 Hz[227], and power reflectance was less than or equal to 1 between 250 -10,000 Hz[228].

2.5. Screening Procedures

Following the consent process, otoscopy was performed to rule out any outer or middle ear infections or debris, cerumen or foreign bodies in the ear canal. Only ear canals without debris and evidence of infection were enrolled in the study. Tympanometry was performed in both ears using an MAICO MI26 immittance bridge (MAICO Diagnostics GmbH, Berlin, Germany). If tympanometric findings were within normal, screening audiometry was performed in both ears with a tablet-based audiometer (SHOEBOX, Ottawa, Ontario, Canada) using a yes/no procedure for 0.25, 0.5, 1, 2, 3, 4, 6, 8 kHz. The game feature of the SHOEBOX audiometer was used with child participants. After instructing the participant using the SHOEBOX instruction video, calibrated EARTone 3A earphones connected to the iPad and coupled to foam ear tips were inserted into the ear canal. Only ears with thresholds ≤ 20 dB HL at all frequencies were included in the study.

2.6. Screening OAEs

2.6.1. Distortion product otoacoustic emissions (DPOAE) screener

DPOAEs for f_2 = 1-20 kHz were recorded using L_1/L_2 = 65/55 dB FPL and f_2/f_1 = 1.22 at the beginning of each test session. The stimuli were 3 concurrently swept frequency segments with a rate of 1 octave/second. Each concurrent sweep was created with three different starting phases (0, 0.33, and 0.66 radians), which were then concatenated so that the time-domain averaging process would cancel the stimulus tones leaving just the emission pressure. 16 sets of measurements (runs) were recorded and processed as described in the signal processing section 2.6.3. Pilot data showed near equivalence of the emission levels obtained using discrete tones, single sweeps, and concurrent sweeps when measured at these levels and absence of emissions in a hard, emission-less cavity.

The purpose of the DPOAE screener was to a) check for presence of OAEs at moderate levels, b) ensure a low biological noise floor, and c) to ensure cochlear status did not change between sessions for repeated measurements. DPOAEs were determined to be robust and reliable if the average signal to noise ratio (SNR) between 1 and 4 kHz was greater than or equal to 10 dB SNR and the noise floor below 1 kHz was less than or equal to 0 dB EPL. If average noise floor exceeded 0 dB EPL, the participant was determined to be too noisy for subsequent measurements and further data collection was terminated. For measurements across multiple sessions, repeatability of baseline DPOAEs was assessed. DPOAEs

were found to be repeatable if the average absolute difference between measurements from different days were within 3 dB of each other. If the average was more than 3 dB, participant was rescheduled for testing on another day.

2.6.2. Spontaneous otoacoustic emissions (SOAE) recordings

Ear canal pressure without acoustic stimulation was recorded for three minutes to detect SOAEs. Offline processing was then performed to characterize the number, frequency, and level of SOAEs in each ear. Briefly, the time domain signal was first high-pass filtered at 0.25 kHz and overlapping Hanning windows of 4 seconds or 0.25 Hz resolution were created. Root-mean-square amplitudes and FFT of each window were computed. Only data with the lowest 25% of RMS levels were kept and FFT estimates of magnitude and phase were averaged. An automatic algorithm employing noise rejection, peak-picking, and Lorentzian modeling of candidate SOAEs was implemented according to Abdala, Luo & Shera (2017) with a few modifications[229].

2.7. Signal Processing

All OAE measurements were high-pass filtered (cutoff frequency = 350 Hz) to remove any low frequency components from biological and environmental noises. Following filtering, additional transient movement-related noises were removed by performing a three-step artifact rejection procedure. First, if the raw pressures contained large transients that were 10 times larger than the maximum

stimulus pressure, that run, i.e., individual stream of recording, was removed. Second, root-mean-square (RMS) values of each run were computed and any runs with RMS values outside of the interquartile range of all RMS values were removed. Third, buffers were rejected if more than 50% of the frequency domain signal estimates of individual runs were outside the 25^{th} or 75^{th} percentile of signal estimates of all runs.

Once runs were combed for clean data, recordings of similar conditions were split into an odd and even buffer and added together to give a time-domain average of the signal and subtracted to give a time-domain average of the noise. The averaged time-domain waveforms of the signal and noise were then sent through a frequency domain analysis using a method of least squares fit (LSF) which used time-windowing and custom frequency-phase functions to estimate magnitude and phase of signals based on frequencies provided in the model[230].

CHAPTER 3

Investigating Auditory Sensitivity and Stimulus Frequency Otoacoustic Emissions

3.1. Introduction

Successful everyday hearing abilities such as detection, discrimination, and localization are a culmination of acute auditory sensitivity, expansive dynamic range, and fine frequency selectivity. Acute auditory sensitivity (detection of soft sounds), expansive dynamic range (ability to comfortably hear sounds over a large range of input levels), and fine frequency selectivity (distinguishing between the spectral components of sounds) are attributed to the active mechanical processes within the sensory apparatus of the cochlea [231]. The mechanical vibrations as a result of sensory outer hair cell (OHCs) activity yield acoustical byproducts recordable in the ear canal, which are referred to as otoacoustic emissions (OAEs). OAEs are of great clinical interest for screening, diagnosis, and monitoring of cochlear dysfunction due to their objective and non-invasive nature. Here, psychoacoustic measures of sensitivity were investigated in relation to acoustic byproducts of cochlear activity in response to a single tone, i.e., stimulus frequency otoacoustic emissions (SFOAEs).

Psychoacoustic responses to sounds and otoacoustic emissions are thought to originate from the same underlying cochlear mechanical properties. The earliest comparisons of OAEs and auditory sensitivity by Kemp (1979) revealed that the two share a phenomenon called microstructure, a term used to describe peaks and

valleys in both measures when either the threshold of audibility or OAE level is plotted as a function of frequency[203]. Later, Zwicker & Schloth (1984) showed that the two microstructures are inversely related such that the frequencies of behavioral microstructure minima (valleys) coincide with the maxima frequencies (peaks) in the emissions spectra[232]. There have been decades of clinical interest in using OAEs to determine hearing status[233-235], to predict behavioral thresholds[236,237], and even to assess the tuning properties of the auditory system[220,224,238]. Although behavioral thresholds are measured in response to single tones, most previous studies have examined OAEs evoked using two tones, i.e., distortion product otoacoustic emissions[236,239]. OAEs that are methodologically similar to behavioral paradigms (i.e., SFOAEs evoked in response to a single tone) have been least studied[197,207,240,241].

In efforts to predict behavioral thresholds from SFOAEs, several groups have evaluated input-output (I/O) functions, which are thought to mimic mechanical measurements of the basilar membrane or reticular lamina for characterizing the gain and compressive non-linearity of the cochlea[231]. Avan et al., (1991) examined estimated thresholds from SFOAE I/O functions in normal and impaired ears, albeit at a limited low frequency range (0.7-2 kHz)[240]. Ellison & Keefe (2005) evaluated levels and signal-to-noise ratios (SNRs) of SFOAEs at a higher frequency range (0.5 – 8 kHz) in order to determine how well overall SFOAE levels and SNRs predicted behavioral thresholds[241].

Using two different methods, both Avan et al., (1991) and Ellison & Keefe (2005) reported a moderate correlation between SFOAE levels and behavioral thresholds, albeit at low frequencies (1-2 kHz). In another approach, Dewey & Dhar (2017a) measured behavioral thresholds and SFOAEs in 1/100-octave steps from 2-5 kHz and found a moderate, but statistically significant, correlation between auditory sensitivity, SFOAE levels and microstructure depths at near threshold stimulus levels[207].

Although these studies established the connection between SFOAEs and behavioral thresholds at low and mid frequencies, understanding the relationship between SFOAEs and behavioral thresholds may be particularly important at frequencies above 8 kHz, because these cochlear regions are first affected by dysfunction due to aging and ototoxicity[145,193]. Only one study has examined the relationship between behavioral thresholds and high-frequency OAEs using clicks[242]. Click-evoked otoacoustic emission (CEOAEs) are thought to arise via the same generation mechanism as SFOAEs[195]. Goodman et al., (2009) found that behavioral thresholds accounted for 28% of the variance in CEOAE levels at 8 kHz and 43% of the variance at 10.1 kHz and did not find any significant correlations between CEOAE levels and behavioral thresholds at 12.7 or 16 kHz[242].

In an investigation of high frequency SFOAEs in young, normal-hearing adults, Dewey & Dhar (2017b) showed that the frequency at which SFOAE levels declined dramatically was closely related to the frequency at which behavioral thresholds crossed the 18 dB FPL intercept, suggesting that SFOAEs may be tightly

related to behavioral thresholds[197]. They also reported that DPOAE levels were correlated with SFOAE levels when DPOAE levels were matched to SFOAE levels at $2f_1$-f_2 rather than at f_2. Nonetheless, there was considerable variability of SFOAE levels across individuals when measured at a fixed stimulus level as used by Dewey & Dhar (2017b).

Although the clinical utility of SFOAEs in predicting audiometric thresholds has been questioned due to the large variation in SFOAE levels *across* individuals, there is still a need to understand how well SFOAEs relate to behavioral thresholds *within* an individual. The earliest studies of SFOAE and behavioral thresholds equalized the stimulus levels within an individual[232] in terms of sensation level relative to behavioral thresholds. The current study extends these threshold-based measurement of SFOAEs up to 14 kHz.

SFOAEs recorded in the ear canal are thought to be a mixture of short-latency and long-latency components[243,244]. Long-latency (LL) components of the SFOAE are thought to reflect the activity from the tonotopic cochlear place as determined by their phase gradient delays, without contributions from components that arise via reflections from non-characteristic places[215]. Using advanced filtering techniques, the LL components coming from the characteristic place, or the peak region of the traveling wave can be disentangled from short-latency components coming from more basal regions[242,243] to the extent that latency of SFOAEs can be directly tied to region of origin within the cochlea. Furthermore, zero-latency

components which may be associated with an imperfect probe cancellation can also be mitigated[244].

The current study is the first to examine human SFOAEs across a wide range of frequencies (0.75 – 14 kHz) using a time-frequency analysis technique based on continuous wavelet transform and the characteristic delay-frequency relation described by Moleti et al., (2012). In contrast to previous studies which have mostly examined the total SFOAE recorded in the ear canal, time-frequency analysis was used to separate different latency components of the total ear canal SFOAE[23,146,197,207,224,240,241,243,245-247]. Time-frequency analysis can improve the detection of SFOAEs above the noise floor and filter the total ear canal SFOAEs into long and short latency components[244].

The purpose of this study is to investigate the relationship between SFOAE levels and behavioral measures of auditory sensitivity up to 14 kHz. It was hypothesized that, because SFOAEs and behavioral threshold measurements are methodologically similar, they are both determined by activity across similar cochlear regions. Hence, the two measures are predicted to be correlated, given that SFOAEs are filtered to isolate long-latency components presumably corresponding to the characteristic place for a given frequency. In order to test this hypothesis, SFOAE levels at 10, 20, and 30 dB sensation levels were measured at eight center frequencies (0.75, 1, 2, 4, 8, 10, 12.5 and 14 kHz), and an estimated threshold from the SFOAE input-output function was computed at each frequency, which was then compared to the behavioral threshold at that frequency.

3.2. Methods

Normal-hearing participants between the ages of 6-45 years were recruited from the greater Chicago metropolitan area. Data were collected from a randomly chosen ear of 28 individuals (19 females, 9 males), aged 12-43 years (M = 27.55, SD = 6.89). Participant demographics are shown in Figure 3.1. All participants were required to have normal otoscopic, tympanometric, and audiometric screenings as described in Screening Procedures below. Participants were excluded from being enrolled in the study if they had excessive cerumen in the ear canal. Participants who could not complete the behavioral procedures in a timely fashion were also excluded from the study. Finally, whose who displayed excessive noise or recording artifacts due to physical movement or swallowing during OAE measurements were excluded.

3.2.1. Screening Procedures

A combination of several standardized tests and procedures was employed to screen participants for eligibility. Otoscopy was performed to rule out any outer ear abnormalities or debris, cerumen, or foreign bodies in the ear canal. Only clear ear canals were enrolled in the study. Tympanometry was performed in both ears using a Maico MI 26 Tympanometer. If tympanometric findings were within normal, screening audiometry was performed in both ears with a tablet-based audiometer (SHOEBOX, Ottawa, Canada) using a yes/no procedure for 0.25, 0.5, 1, 2, 3, 4, 6, and 8 kHz. The game feature of the SHOEBOX audiometer was used with

participants younger than 18 years of age. After instructing the participant using the SHOEBOX demo video, calibrated EARTone 3A insert earphones connected to the iPad and coupled to foam ear tips were inserted into the ear canal. Only ears with thresholds ≤ 20 dB HL at all frequencies were included in the study.

3.2.2. General Procedures

Measurements were made across two test sessions, each lasting about two hours. Psychophysical tuning curves (PTCs) were also measured during each session, the data for which are presented in Chapter 4. The center frequencies of interests were 0.75, 1, 2, 4, 8, 10, 12.5 and 14 kHz. Four of the eight frequencies were tested during the first test session and the remaining four frequencies were tested during the second session, within four weeks of the initial session. For each participant, a pseudo-frequency randomization order was created such that the first test frequency on each day was either 2 or 4 kHz as the PTC procedure is easier at these frequencies for most participants compared to other frequencies of interest.

Thresholds for each frequency were always obtained first. Following threshold measurement, the participant was asked to either complete the PTC task or sit quietly for SFOAE measurements for that frequency. If the participant could not complete threshold testing or the practice PTC, the session was terminated, and the participant was compensated for their participation before dismissal from the study. The order of measure (SFOAE vs PTC) was counterbalanced across participants. The frequency randomization and measurement order were followed

across both sessions until all thresholds, PTCs, and SFOAE measurements for all 8 center frequencies were completed. An in-situ calibration was done prior to initiating measurements at each test frequency.

3.2.3. In-situ Calibration

Before data collection began, participants were seated in a reclining chair in the audiometric booth. The ER10x (Etymotic Research, Elk Grove Village) probe assembly was placed in a randomly selected ear, as long as hearing was symmetrical and within normal range in both ears, otherwise the normal/better ear was selected. The cable of the ER10x probe was draped over the back of the recliner so that the cable did not come in contact with the participant's shoulders or torso. The cable was then taped to the chair to prevent slippage of the probe out of the ear canal. The participant was instructed to keep their head still and avoid talking, coughing, or excessive swallowing. The participant was given the option to read a book quietly or watch a silent captioned television show or movie.

Once the participant was seated comfortably and the probe was in the ear canal, chirps were played, and the forward-pressure level calculation was performed so that stimuli could be calibrated within each individual ear canal based on the impedance of the ear canal compared to previously measured source pressure and impedance. Calibration was performed at the start of each session and repeated throughout the session, every 20 minutes or sooner if probe slippage or movement

was detected via visual inspection or reported by the participant. Successful calibration criteria as described in General Methods were used.

3.2.4. Behavioral Thresholds

Hearing thresholds were estimated using a modified Békésy tracking procedure following Levitt (1971) and described fully in Lee et al., (2012)[22,248]. In brief, stimuli were FPL-calibrated sinusoidal pure-tones that were 250 ms in duration and pulsed on and off using an inter stimulus interval of 250 ms. Participants were instructed to hold down a mouse key as long as the pulsed tone was audible.

The initial presentation level of the tone was 60 dB FPL, and the initial step size was 6 dB, which decreased to a step size of 2 dB following a training period. First, reversal was determined as the first time the button press was released, and the second reversal was determined as the first time the button was pressed after the first reversal. Following the first two reversals, which were considered a training period, subsequent reversals were used to compute a midpoint for each ascending run (increasing stimulus level), and a running mean and standard error for such midpoints.

The threshold was determined as the mean of the midpoints after at least seven midpoints were obtained and the standard error was less than 1. If a threshold could not be found within the first 200 trials or a threshold was unreliable

at 200 trials, (standard error > 3), the frequency was skipped and threshold not computed for that frequency.

3.2.5. Stimulus Frequency Otoacoustic Emissions (SFOAEs)

3.2.5.1. SFOAE Recording. SFOAEs were recorded for probe levels corresponding to 10, 20 and 30 dB sensation level (SL) relative to the behavioral hearing threshold for each frequency sweep with center frequencies (f_c) of 0.75, 1, 2, 4, 8, 10, 12.5 and 14 kHz. Probe frequencies (f_p) were swept in 1/4 octave segments spanning 0.5*f_c to ~1.5*f_c for f_c up to 8 kHz and from 0.7*f_c to 1.3*f_c for f_c above 8 kHz. Suppressor frequency (f_s) was always 47 Hz lower than f_p and at least 15 dB above the level of the probe frequency (L_p) for stimulus levels greater than 55 dB FPL, or 70 dB FPL for stimulus levels less than 55 dB FPL. The sampling rate was 96,000 samples/second.

Sixteen sets of ear canal pressure recordings were made, where each set contained four interleaved blocks of stimuli: probe alone (p), probe with suppressor (ps+), probe alone (p), and probe with suppressor inverted in phase (ps-). First, recordings were split into odd and even buffers and summed together to get an average pressure recording and subtracted to get the noise floor. All probe only (p) blocks were averaged together and all probe plus suppressor (ps) blocks were averaged together. The SFOAE residual was computed as the difference between the two blocks.

Models of probe and suppressor were created separately in a least-square-fit (LSF) based analysis using custom phase functions created during stimulus generation. The analysis window (t_{win}) was fixed at 3000 samples or 0.0313 s. Magnitude and phase were determined by identifying the model that minimized the RMS error within each analysis window.

3.2.5.2. SFOAE Wavelet Analysis. After the magnitude and phase of SFOAEs were obtained, time-frequency analysis of the SFOAEs was performed using the continuous wavelet transform technique described by Moleti et al., (2012)[244]. The technique builds on previous time-frequency analyses[205,249] by continuously varying the filtering parameters along a quasi-hyperbolic delay curve.

Briefly, a family of wavelet basis functions with a sampling frequency of 40,960 Hz were created (Equation 5 of Moleti et al., [2012]) [244]. The frequency resolution of the wavelet basis functions was 10 Hz for 0.75 and 1 kHz, 20 Hz for 2 and 4 kHz, 40 Hz for 8 kHz, and 80 Hz for 10, 12.5 and 14 kHz. SFOAE spectra were interpolated to match the frequency resolution of the wavelets. For each center frequency, the complex SFOAE spectra were then convolved with the wavelet basis functions in the frequency domain (Equation 6 of Moleti et al., [2012]) [244], from which wavelet coefficients in the time-frequency domain were obtained after an inverse FFT (Equations 1 and 7 of Moleti et al., [2012])[244].

The wavelet coefficients were filtered separately using three different delay cutoff values that varied with frequency (Equations 2 and 3 of Moleti et al., [2012]) [244]. For frequencies < 8 kHz, the first delay cut-off parameter was set at -0.5 to 0.5,

which created the hyperbolic function used to constrain the zero-latency component. The second delay cut-off parameter was between 0.5 and 1.5 for the long-latency component, also referred to as the first-reflection component. The third delay cut-off was between 1.5 and 3, which allowed the separation of the second-reflection component. For frequencies ≥ 8 kHz, the first cut-off was set at -0.5 to 0.25, whereas the second cut-off was set between 0.25 and 1.5, and the third cut-off was set between 1.5 and 3.

The filtered components were then convolved again with the wavelet basis functions and an integral was performed (Equation 8 of Moleti et al., (2012)[244]) to give the filtered time domain functions. The reconstructed time-domain functions were then converted back to frequency domain after an FFT. Latency estimates for each component were computed from the weighted average of the filtered wavelet coefficients. To ensure the quality of the recordings included in the wavelet analysis, only spectra with noise floors below 0 dB EPL and signal-to-noise ratio of 3 dB were analyzed.

3.2.5.3. SFOAE I/O Threshold Estimation. SFOAE levels from a given sweep for each center frequency and each level were averaged together in 1/3 octave bins to yield estimates of the mean SFOAE level around the center frequency with 3 dB SNR criteria applied. Thresholds from the SFOAE I/O functions were estimated using two methods.

In the first method, mean 1/3-octave band averaged SFOAE levels for each center frequency were converted to linear units, and a linear regression was

performed similar to Boege & Janssen (2002)[250]. In order to maximize the number of points included in threshold estimation while ensuring only clean data were included, only octave band averages computed after applying a 3 dB SNR were kept. The x-intercept of the linear fit representing the level of the probe needed to produce a 0 μPa emission level was considered the emission threshold derived from the I/O function. A cubic[251] or two-line fit[252,253] was not performed due to the sparsity of the I/O functions only containing three levels (10, 20 & 30 dB SL). The I/O functions at these levels displayed monotonic growth for the most part with a few exceptions. Slopes from these functions were computed as the difference in OAE levels at 10 and 30 dB SL, divided by the dB-difference between these two stimulus levels (i.e., 20).

In order to avoid fitting the saturated portions of the I/O function, only functions with probe levels ≤ 55 dB FPL were included in the analysis. Although SFOAE level growth can become compressive around 40 dB SPL[13], the functions reach saturation above ~ 50 dB SPL[14]. Data points were excluded from the fitting analysis, if all three data points did not meet 3-dB SNR criteria.

In the second method, 1/3-octave band averaged SFOAE and noise floor levels were converted to linear pressure units. Two separate linear regression lines were fit to SFOAE and noise floor pressures and predicted values for six points along the input output function were computed before converting the pressure values back to sound pressure level. The signal to noise ratio of each point was computed and the lowest probe level at which SNR was 6 dB was assigned as the emission threshold.

Gong, Liu & Peng (2020) used a similar SNR-based method to predict threshold, with two exceptions: 1) they used a 9 dB SNR or better as the criterion for threshold; and 2) they required at least one level above lowest probe level to also have SNR of 6 dB or more[254].

SNR-based threshold estimation was not very successful as only a few ears met the SNR criteria for fitting the I/O function. Musiek & Baran (1997) reported that predicting thresholds from SNR criteria-based estimates of DPOAE thresholds can be inaccurate[255]; therefore, only thresholds estimated using the linear regression 0 μPa extrapolation method were used in subsequent analyses.

3.2.6. Statistical Analysis

In order to examine the relationship between SFOAE levels and behavioral thresholds, repeated measures correlational analyses were performed using the {rmcorr} package in RStudio (version 1.2.5033) which uses analysis of covariance (ANCOVA). As described in Bakdash & Marusich (2017), repeated measures correlation accounts for the non-independence of observations from a repeated measures dataset and attempts to adjust for inter-subject variability while avoiding the assumptions of traditional correlational analyses regarding the independence of observations[256]. Linear regression models were fit, and analysis of variance was performed using the {stats} package. Significance levels were set at $p < 0.05$.

3.3. Results

Here the relationship between SFOAE levels and behavioral thresholds was examined for 0.75 – 14 kHz using time-frequency analysis that isolated the long-latency (LL) component of the SFOAEs. Participant demographics (n = 28) are shown in Figure 3.1, which showed that most of the participants were 18-35 years of age, mostly females, and mostly white/non-Hispanic.

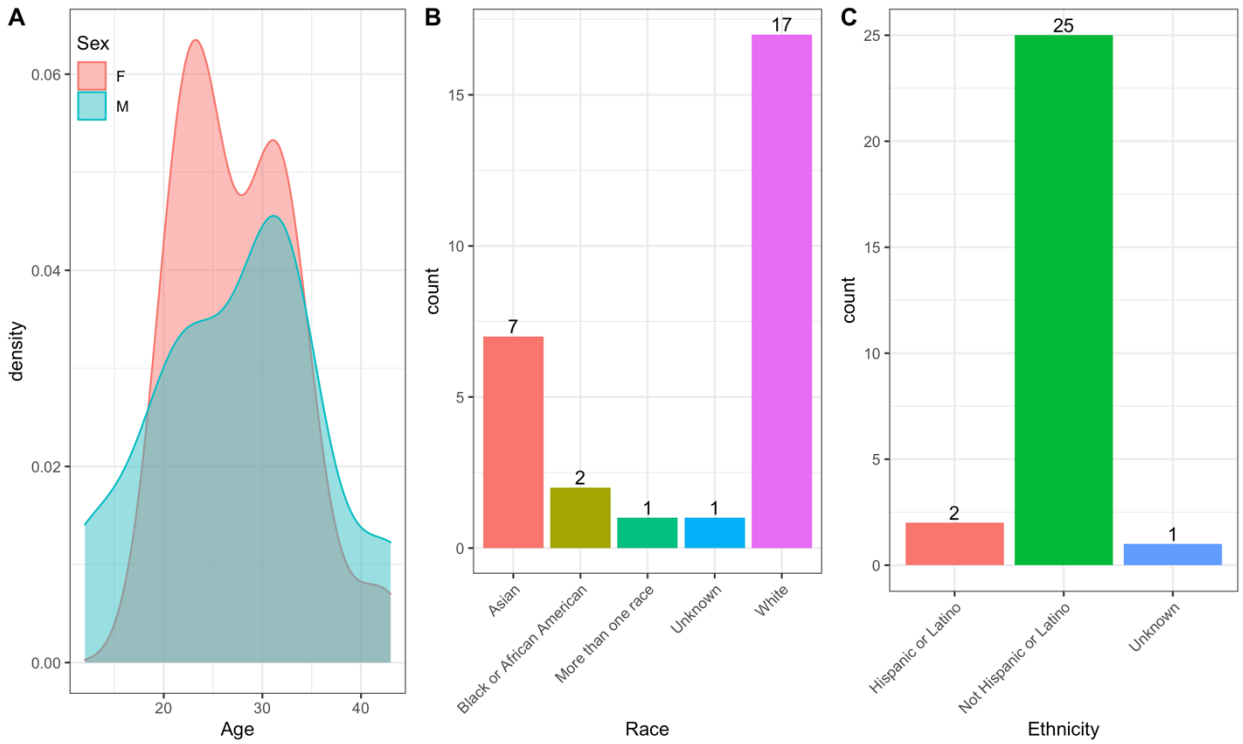

Figure 3.1. Participant Demographics including age, sex, race, and ethnicity. Panel A plots the sex distribution by age. Panel B shows the counts for each response choice for the race question, whereas Panel C shows the counts for each response choice for ethnicity. As shown in Panel A, most participants were female between the ages of 20 and 30 years. Panel B shows that most participants reported their race as White followed by Asian. Lastly, Panel C shows that all but 3 participants reported non-Hispanic or Latino ethnicity.

3.3.1. Behavioral Thresholds

In this sample of normal-hearing individuals (as defined by the clinical criteria of 20 dB HL or better thresholds at 0.5-8 kHz), median thresholds across frequencies were within ±10 dB FPL in the 0.75-10 kHz frequencies, with median thresholds becoming worse and the range of thresholds becoming more variable at 12.5 and 14 kHz (see Figure 3.2). Because of this increase in threshold variability at 12.5 and 14 kHz, the possibility of an aging effect on thresholds was examined, which showed that mean thresholds were within 2 dB across all frequencies for the two comparison groups (18-25- and 30-35-year-old) (see Table 3.1). There were not enough data from individuals younger than 18 years (n = 1) and older than 35 (n = 2) for comparison. Aside from the threshold variability at 12.5 and 14 kHz, there was also a large range of thresholds across participants at all other test frequencies. Specifically, the range of thresholds across individuals was as high as 24 dB at 10 kHz and below.

Table 3.1. Mean Behavioral Thresholds (dB FPL) (top row) and Standard Deviations (bottom row) by Frequency (kHz) Across Two Age Groups

Age group	N	0.75	1	2	4	8	10	12.5	14
18-25 years	13	11.46	10.51	17.05	12.10	17.41	18.35	28.36	36.60
		7.17	4.01	4.50	3.89	3.20	4.22	12.32	17.70
30-35 years	12	8.79	8.13	13.99	10.74	18.22	18.88	27.47	37.58
		3.53	4.46	4.23	5.67	4.61	6.22	9.04	11.05

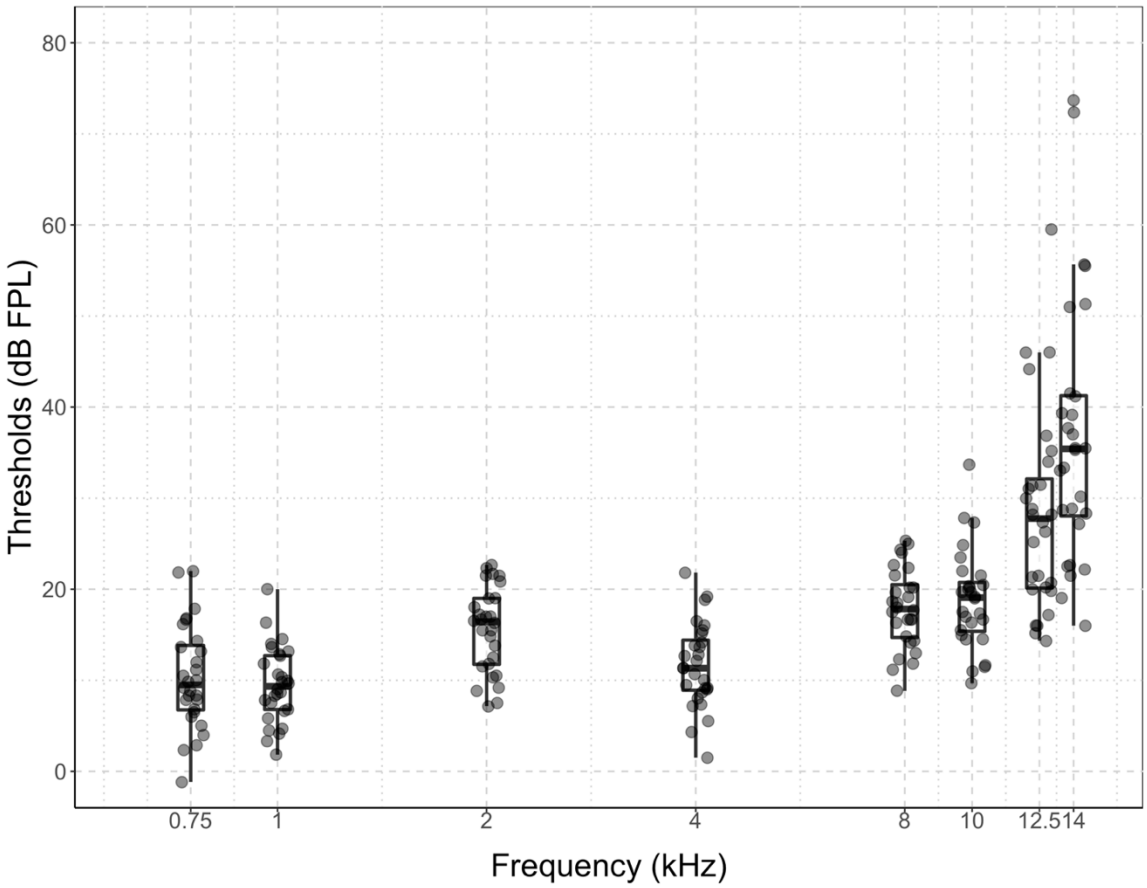

Figure 3.2. Boxplots of behavioral thresholds measured using a modified-Békésy tracking procedure for pure-tones calibrated in terms of forward pressure level (FPL). Individual participants are represented by individual symbols. In general, thresholds were relatively similar across frequency (median thresholds < 20 dB FPL) up to 10 kHz; however, starting at 12.5 kHz, thresholds worsened dramatically, even in this relatively young, normal-hearing sample.

3.3.2. Total and Filtered SFOAE Levels as a Function of Probe Level

The total SFOAE recorded in the ear canal is likely a mixture of 1) the LL component with the expected delay from the peak region in response to the incident traveling wave: 2) the SL component whose latency is consistent with energy coming from basal sources in response to the initial stimulus waves and, 3) the

multiple reflections whose latency is much longer than expected from the peak region and thus is consistent with delays of multiply reflected intracochlear waves. Separating out the LL component from the total SFOAE required filtering the SFOAEs based on their characteristic delay as a function of frequency. This relationship between SFOAE delay and frequency and the level dependence of this relationship can be visualized in Figure 3.3.

As can be gleaned from the time-frequency contour plots in Figure 3.3, the continuous wavelet transform filtering technique filters the total SFOAE into short-latency, long-latency, and multiple reflection components as constrained by each component's delay curve. Comparing the panels in Figure 3.3, it can be observed that SFOAE latencies decrease as a function of increasing probe levels and increasing frequency. In addition, the intensity and localization of the signal increases as stimulus levels increase. In other words, the signal becomes less dispersed at 30 dB SL compared to 10 dB SL for each ear and frequency. Furthermore, at low probe levels and low frequencies, it appears that multiple reflections are more pronounced than at high probe levels and high frequencies. Although the frequency- and level-dependence of the delays shown in Figure 3.3 are representative of the dataset, these time-frequency contours are highly individualized across ears and across frequencies, such that the frequency at which the contour plots showed the highest intensity signal was not always correlated with the center frequency.

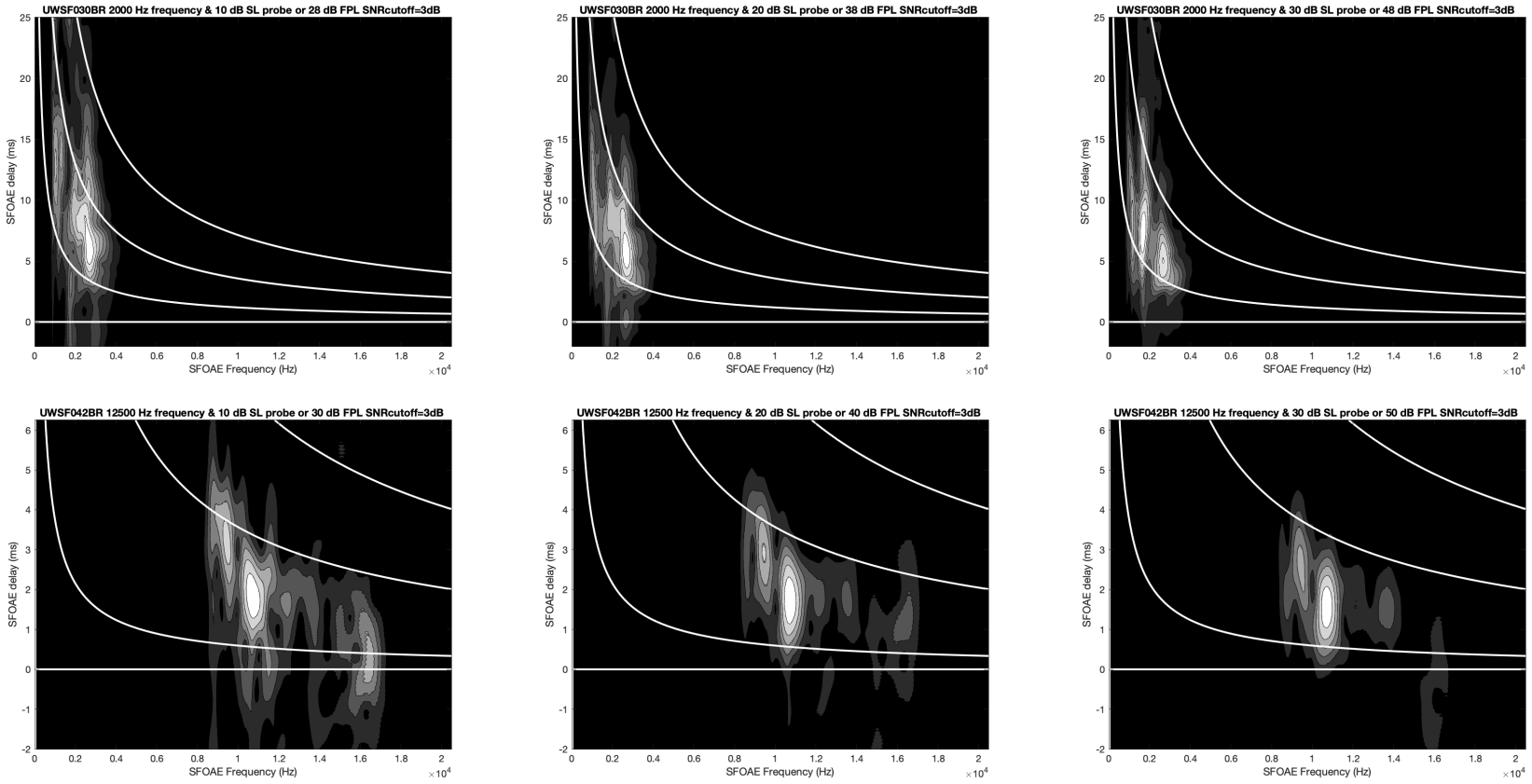

Figure 3.3. Examples of time-frequency contour plots at two frequencies and all three probe levels. Each panel represents an individual time-frequency representation of SFOAE components for a given ear, frequency, and probe level in dB SL and its equivalent dB FPL as indicated by panel headings. Data for 2 kHz (top) and 12.5 kHz (bottom) center frequencies are shown for 10, 20, and 30 dB SL (left, middle, and right, respectively). Solid white curves represent the quasi-hyperbolic delay curves for each component's latency cut-off. The brightness of the signal represents higher level of the component normalized to the background signal in each plot.

Figure 3.4 shows the 1/3-octave average of levels and noise floors for unfiltered and filtered SFOAEs. Comparing the two panels in Figure 3.4 revealed that the levels of filtered LL SFOAEs were generally lower than the unfiltered total SFOAE. Across participants, the filtered LL SFOAE levels were more variable than the total SFOAE level. Furthermore, the noise floors of the filtered data (normalized to the time window for each component) were much lower than the unfiltered noise floors, which improved the SNR drastically, particularly at frequencies at and above 8 kHz.

Figure 3.4 also shows the probe level dependence of the total and LL SFOAE levels, such that higher stimulus levels yielded larger emissions levels on average across all frequencies and for both unfiltered and filtered SFOAEs. Additionally, there was a slight trend for lower levels of LL SFOAEs compared to total SFOAEs as a function of frequency at and above 8 kHz. The noise floors were slightly higher for the 30 dB SL compared to the other probe levels; however, this effect was not observed in most individual data across ears and frequencies (see Figure 3.5).

A few observations can be made from the individual panels of filtered SFOAE data in Figure 3.5. First, the 1/3-octave band averages of filtered LL SFOAEs appeared to be highly individualized to an ear. Second, the LL SFOAEs were robust up to 4 kHz in most participants and started to decline in level at 8 kHz and above. Third, the noise floors were relatively low between 2 and 16 kHz in most participants, while in others, the noise floors were elevated for the low (0.75-1 kHz)

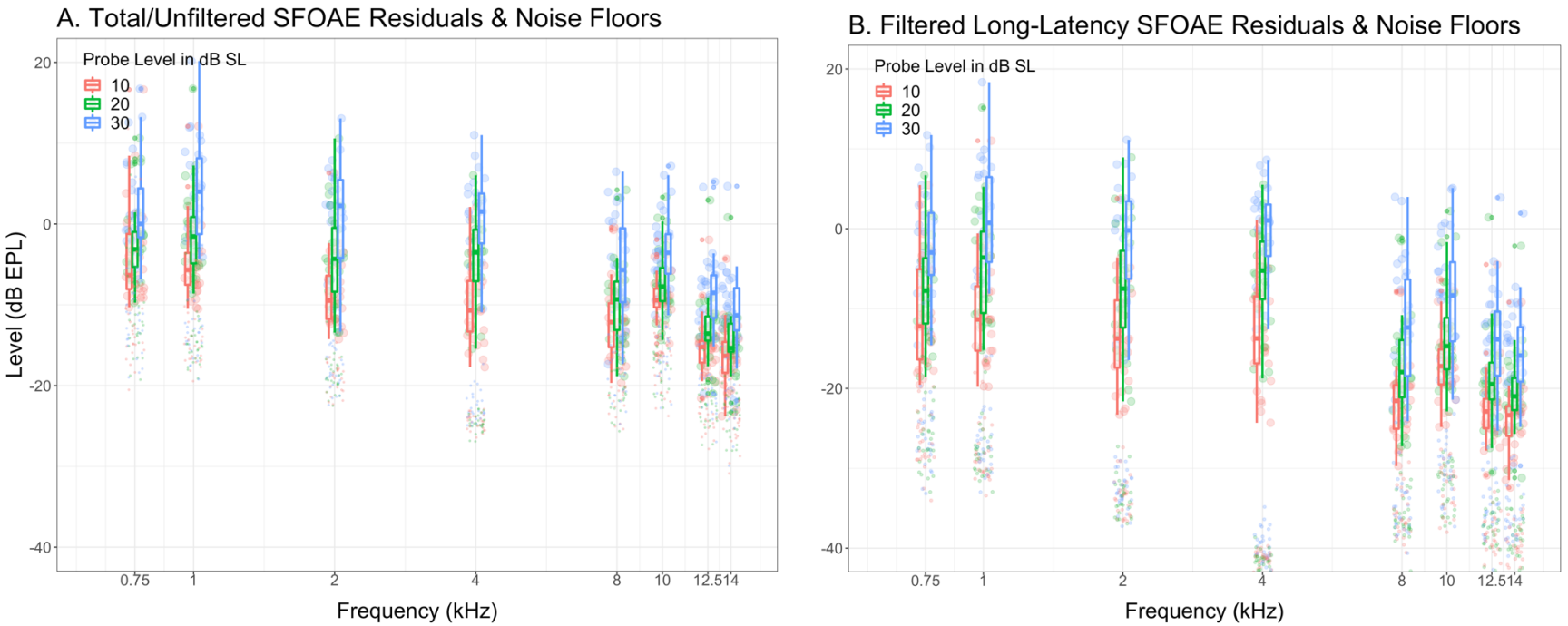

Figure 3.4. Boxplots of total/unfiltered and filtered long-latency SFOAE levels plotted as a function of frequency for all three probe levels for all participants. Larger circles represent SFOAE levels and smaller circles represent noise floors averaged across 1/3 octave bands for each participant.

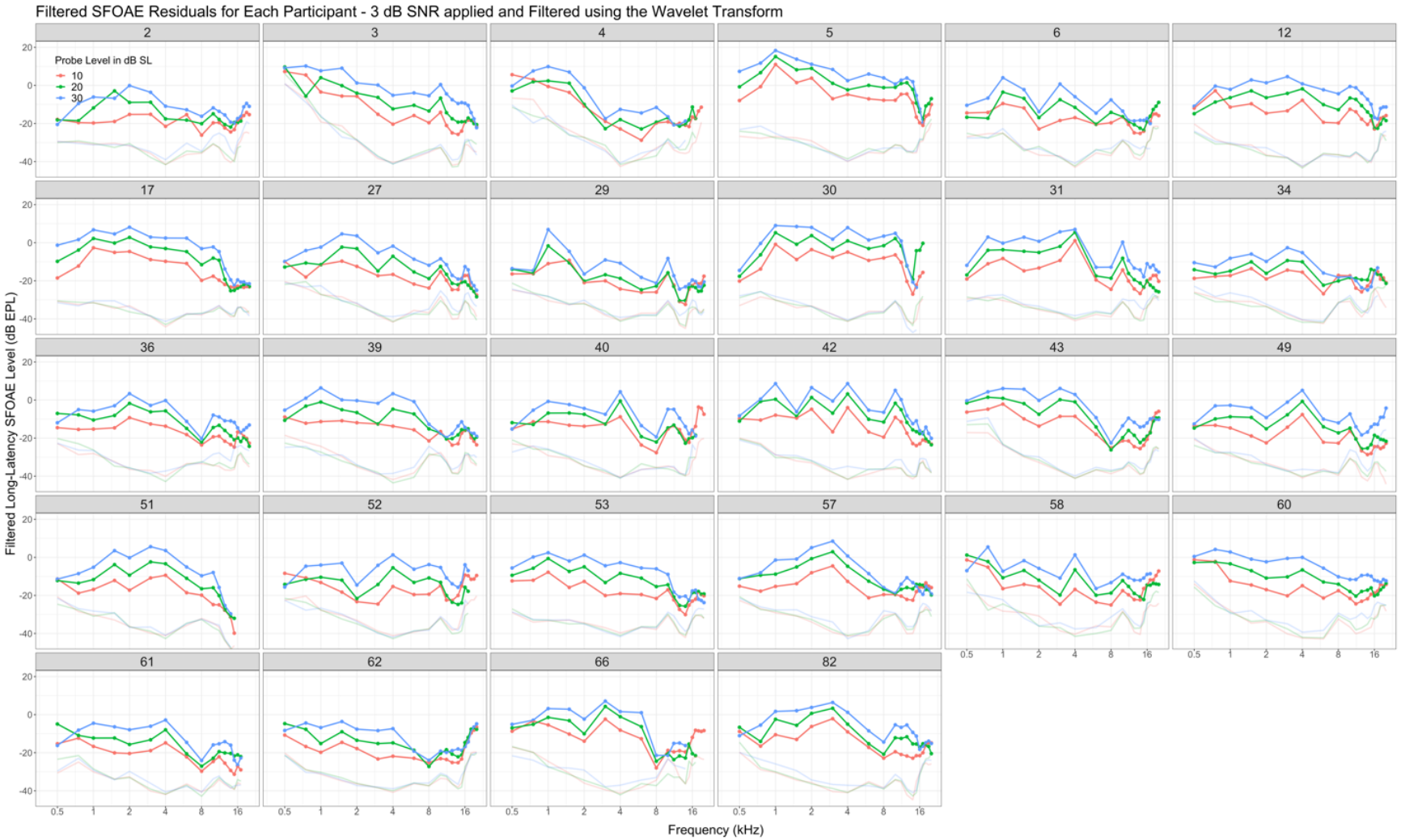

Figure 3.5. Filtered LL SFOAE levels in dB EPL plotted as a function of frequency for all three sensation levels for each participant. Each panel represents data from one participant indicated in panel headings. Darker symbols/lines represent the SFOAE level whereas the lighter lines represent the noise floors for each probe level.

and/or ultra-high (>16 kHz) frequencies. The levels of LL SFOAEs in these individuals did not consistently show the level dependence, an indication of emission growth as it relates to cochlear activity.

3.3.3. Characteristics of SFOAE I/O Functions Measured using Sensation Level (SL)

Towards examining the relationship between SFOAEs and behavioral thresholds at each frequency, particularly within an individual, the SFOAE input-output functions were extrapolated to obtain an I/O estimated threshold. The I/O functions were fit with a linear regression after both the SFOAE and the probe levels were converted into linear pressure units, hence the linear fit. As seen in Figure 3.6, the I/O functions generally demonstrated a compressive yet monotonic growth, with a few exceptions. For 12.5 and 14 kHz, some I/O functions had missing observations due to poor signal to noise ratio at those frequencies. The noise floors were generally similar across probe levels, except at some frequencies in some ears which showed a slightly increased noise floor at the highest stimulus level.

Non-monotonic I/O functions were observed at some frequencies in some participants. Because of this non-monotonic behavior, the linear fit to the I/O function sometimes yielded an erroneous threshold estimate. Threshold values that were artificially high (greater than 55 dB FPL [n=8]) or artificially low (less than -20 dB FPL [n=6]) were removed from further analysis. Given that only 14 out of 195 (6.83%) of the estimated thresholds were considered erroneous, the success rate of

the I/O fitting procedure was satisfactory (~93%). Figure 3.7 shows the fitting quality of the I/O functions with examples of successful and unsuccessful fittings,

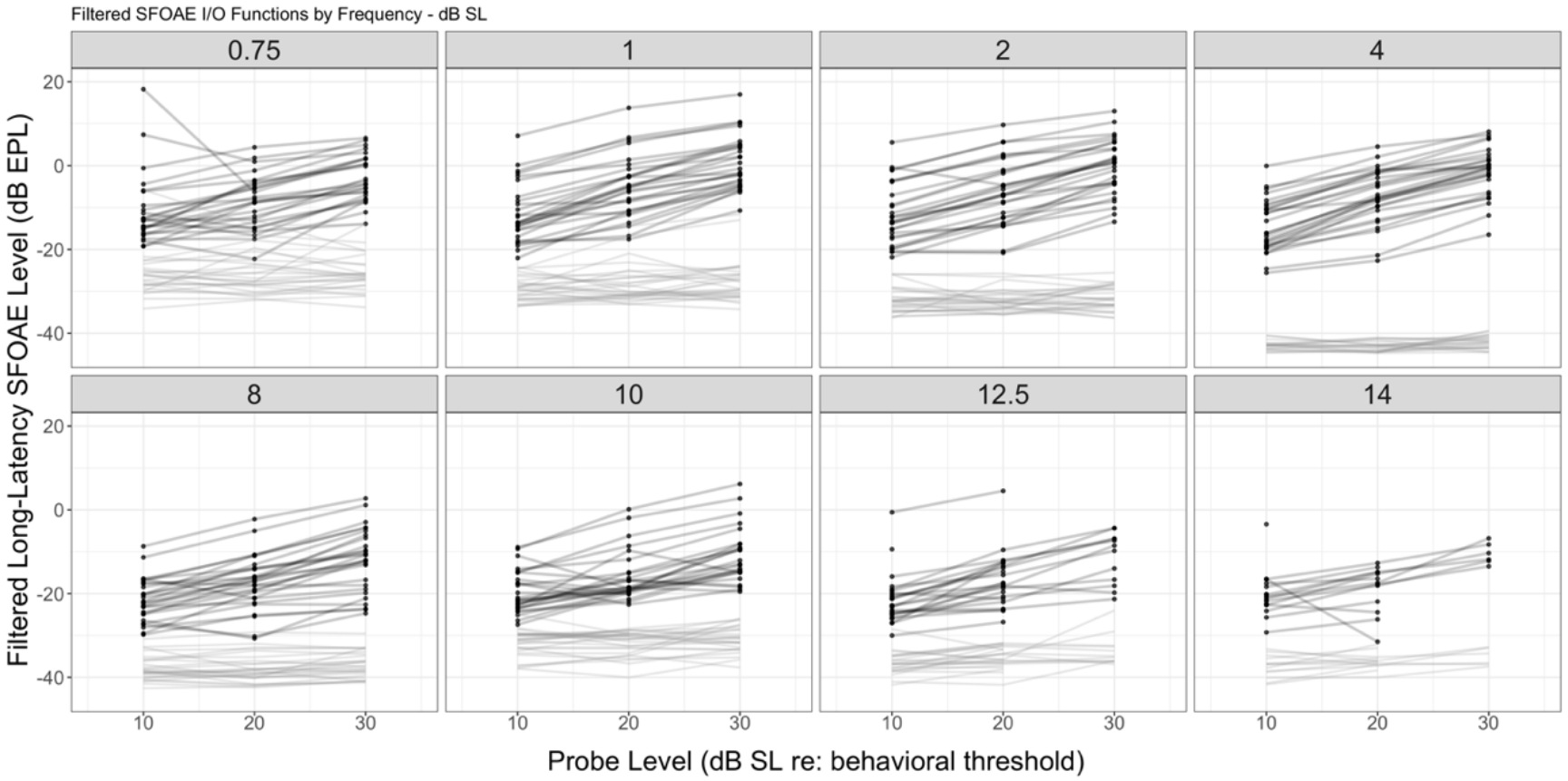

Figure 3.6. Filtered SFOAE levels plotted as a function of probe level in dB SL for all participants. Center frequencies (kHz) are shown in panel headings. Dark symbols and lines indicate the LL SFOAE levels, whereas lighter lines represent the noise floors.

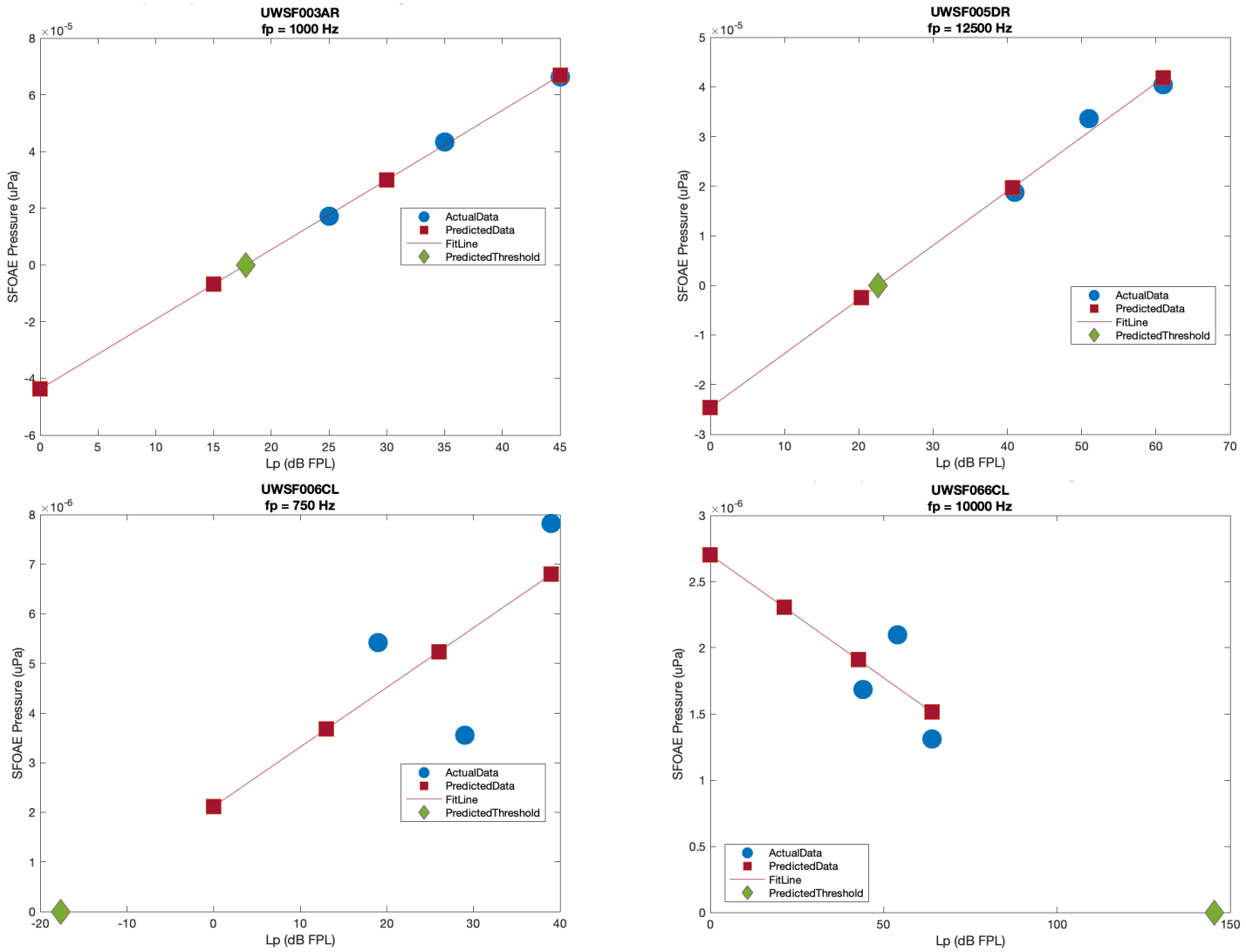

Figure 3.7. Four individual fits to the input-output functions. Top row shows examples of I/O fits that were successful as actual (blue circles) and predicted data (red squares) fall on the fit line. Bottom row shows examples of unsuccessful fits with actual and predicted data deviating (left) or non-monotonic growth of the emission with increasing stimulus levels (right). Predicted thresholds are represented by green diamonds.

the latter of which occurred when the emission growth at all three probe levels was non-monotonic. Note that the x-axis was plotted in dB units for easy interpretation of the probe levels, even though both SFOAE and probe levels were converted into linear units before the data were fit. The mean slopes from these I/O plots are shown in Table 3.2, which showed that slopes were between 0.44 to 0.60 dB/dB but not consistently varying with frequency.

Table 3.2. Mean Slopes and Standard Deviations of SFOAE I/O Functions by Frequency (kHz)

Frequency (kHz)	N	Mean slope (dB/dB)	Standard deviation
0.75	23	0.44	0.23
1	28	0.49	0.19
2	27	0.46	0.21
4	28	0.54	0.24
8	26	0.50	0.21
10	23	0.47	0.21
12.5	22	0.55	0.22
14	18	0.60	0.12

3.3.4. Correlation between SFOAE and Behavioral Thresholds

When SFOAE I/O estimated thresholds for all 28 subjects were pooled across eight frequencies, and behavioral thresholds were regressed on I/O estimated thresholds, as shown in Figure 3.8, the repeated measures correlational analysis showed a high correlation between behavioral thresholds and SFOAE I/O estimated thresholds ($r\,(177) = 0.863$, $p < 0.001$). Although the two measures were strongly correlated, the fit line was below the unity line, i.e., SFOAEs generally

underestimated thresholds, albeit within ~5 dB of behavioral thresholds (*MAE* = 5.340 dB). 18 observations detected as outliers using Cook's distance were removed from the correlational analysis but can be seen in Figure 3.8 as red symbols. To determine if the outliers were significantly influencing the data, linear regression models with and without suspected outliers were created, which showed an adjusted R-squared value of 0.415 with the outliers, which improved to an adjusted R-squared value of 0.738 after removing the 18 outliers.

Separating the long-latency component from the total SFOAE levels only slightly improved the correlation between SFOAE I/O estimated thresholds and behavioral thresholds ($r[177] = 0.86$, $p < 0.001$ for LL SFOAE vs. $r[160] = 0.80$, $p < 0.001$ for total SFOAE); however, I/O functions that used LL SFOAE resulted in fewer erroneous thresholds (i.e. I/O thresholds lower than - 20 dB or higher than 55 dB FPL) compared to the total SFOAE (14 for LL and 35 for total). In order to determine the utility of using I/O thresholds computed using just the highest two probe levels, the correlational analysis was repeated, which showed that although more observations were retained using two points on the I/O function, the repeated measures correlation was weaker ($r[177] = 0.76$, $p < 0.001$).

Frequency by frequency correlational analyses also showed statistically significant correlations between LL SFOAEs and behavioral thresholds (Figure 3.9); however, the strength of the relationships varied from strong to weak, likely due to the small number of observations and restricted range of values. These correlational analyses were based on Pearson's product moment correlation which should be

interpreted with caution due to the non-independence of the observations in this repeated-measures design. A linear mixed effects model using frequency and behavioral threshold as fixed variables, controlling for repeated frequencies, and participant as random variable, resulted in a beta coefficient (equivalent to Pearson's r) of 0.843. A model without frequency as a fixed effect resulted in a beta coefficient of 0.939, whereas a model without behavioral threshold resulted in beta of 0.0001.

An analysis of variance of the models with and without frequency as a fixed variable showed that the two models were not significantly different (X^2 (2, N = 177) = 2.101, p = 0.350). On the other hand, models with and without behavioral thresholds were significantly different (X^2 (2, N = 177) = 144.14, p < 0.001). From the scatterplots of data subset by frequency, it can be noted that the number of observations decreased as frequency increased, with nearly half of the participants not included at 14 kHz for likely a combination of reasons, including not meeting SNR criteria at all three levels or an estimated threshold that was outside the -20 to 55 dB FPL range.

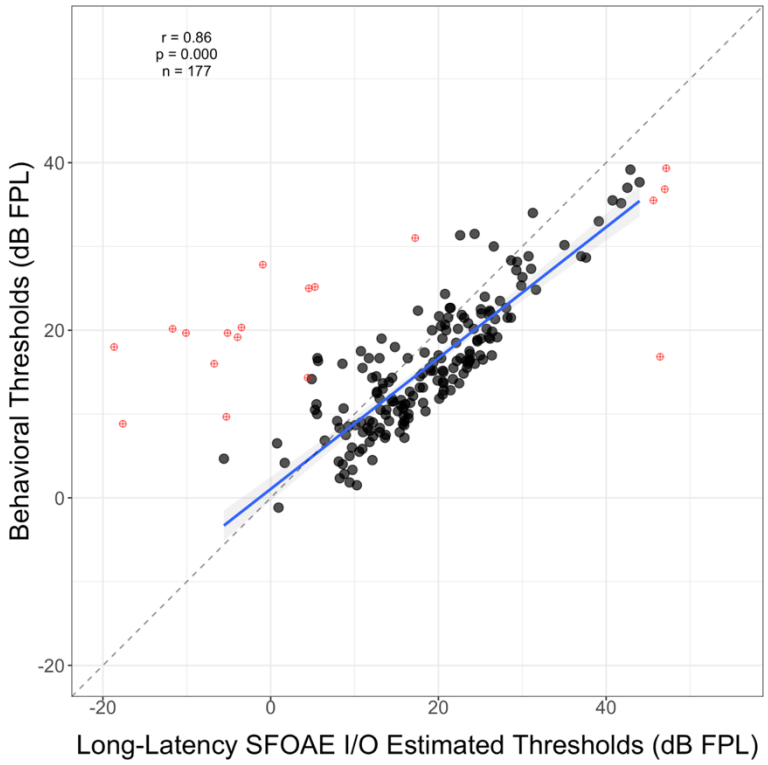

Figure 3.8. Scatterplot of behavioral thresholds (dB FPL) plotted against LL SFOAE I/O estimated thresholds (dB FPL) for across all frequencies. Circles indicate data from each frequency and ear. Solid line indicates the linear fit to the data, whereas dashed line represents unity or hypothetical perfect correlation. Outliers detected using Cook's distance, excluded from the linear regression, are indicated by red symbols.

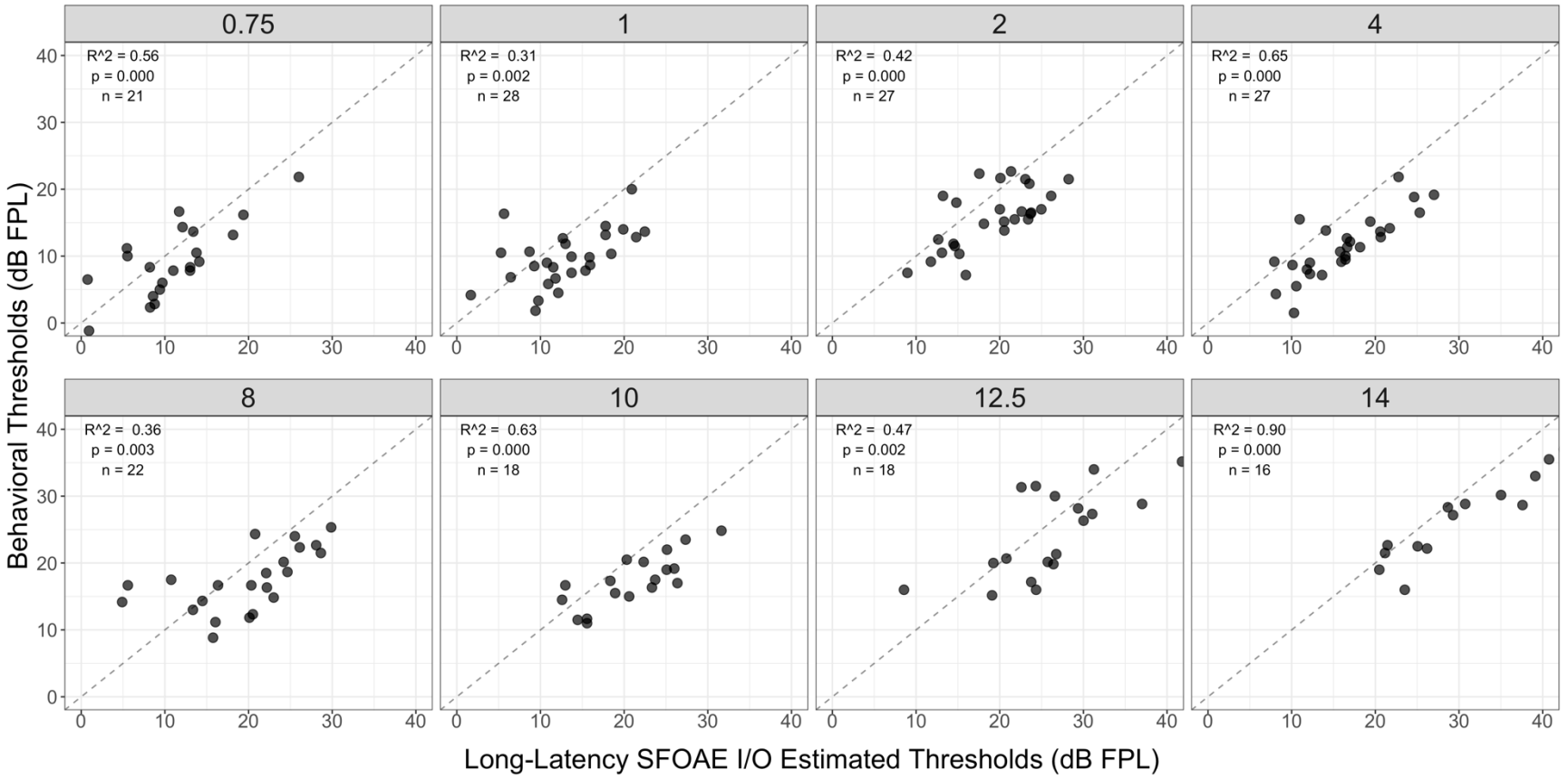

Figure 3.9. Scatterplots of behavioral thresholds (dB FPL) and LL SFOAE I/O estimated thresholds (dB FPL) by frequency (kHz) as indicated by panel headings. Circles indicate data from each individual ear, and the dashed line indicates hypothetical perfect correlation between the two measures.

3.4. Discussion

The purpose of this study was to examine whether behavioral measures of threshold were related to SFOAE I/O estimated thresholds, when SFOAE probe levels were set individually based on the hearing threshold for each frequency and SFOAE levels were filtered based on the modeled latency for each frequency. SFOAEs, recorded from 28 ears of normal-hearing individuals for center frequencies 0.75, 1, 2, 4, 8, 10, 12.5 and 14 kHz, were found to be correlated with behavioral thresholds across all frequencies and within a given frequency. The findings suggest that behavioral measures and SFOAEs share a common generation source within an individual, such that when measurement methods are designed to be approximately equivalent, SFOAEs can predict behavioral thresholds within 5.340 dB on average. However, measurement error related to the quality of SFOAE recordings, particularly at high frequencies, weakens the relationships observed between the two measures and will be discussed in further detail hereafter. Nonetheless, the current study has implications for the clinical use of SFOAEs for assessment and monitoring of cochlear sensitivity across a wide cochlear frequency range.

3.4.1. Theoretical Basis for Using Sensation Level for SFOAE I/O Functions

In a previous investigation of the relationship between SFOAEs and behavioral thresholds, Dewey & Dhar (2017a) evaluated the microstructure of behavioral thresholds and SFOAEs for frequencies between 2-5 kHz[207]. In short,

SFOAEs and behavioral thresholds were measured in 12 subjects at 47 frequencies over 0.46 octave span around a carefully selected region of good SNR to give very fine resolution measurements at 1/100-octave intervals[207]. Using these very precise and brute-force measurements, they found that low-level SFOAEs have peaks that coincide with minima of behavioral threshold microstructure[207]. Furthermore, when the behavioral thresholds were converted to a sensitivity measure by inverting the sign, the sensitivity microstructure magnitude (overall strength) and depth (peak to peak response) were significantly correlated with SFOAE microstructure magnitude ($r = 0.74$) and depth ($r = 0.78$) [207].

The findings from Dewey & Dhar (2017a) suggested that low-level SFOAE and behavioral microstructure are tightly coupled within an individual. In a different study, Dewey & Dhar (2017b) showed that the average DPOAE corner frequency were also similar to behavioral corner frequency; however, low-level DPOAE microstructure and threshold microstructure were not compared in their study[197]. Using a different approach based on extrapolating threshold from SFOAE I/O functions, a similar result was found in the current study on the relationship between behavioral thresholds and SFOAEs ($r = 0.85$), perhaps unsurprisingly, since SFOAE and behavioral threshold measurements both represent cochlear responses to a single tone. The current study extends the findings of Dewey & Dhar (2017a), who measured SFOAEs between 2 and 5 kHz, to a much wider frequency range (0.75 – 14 kHz).

Although the probe levels in the current study (9 – 69 dB FPL) were higher than the fixed levels used by Dewey & Dhar (2017a) (0, 6, 12, and 18 dB FPL), the higher probe levels were useful in measuring high-frequency SFOAEs. At frequencies above 8 kHz where hearing thresholds vary drastically across individuals (see Figure 3.2) [257], using fixed stimulus levels across individuals may yield any SFOAEs that are below or above threshold. This would contribute to the variability of SFOAE derived estimates of cochlear function and how they relate to behavioral measures. The current study used sensation level to equalize the stimulus levels across frequencies within an individual. SFOAE I/O functions have been shown to grow monotonically at least up to 30 dB SL[204,232] or 40 dB SPL [13]; therefore, linearly extrapolating to 0 μPa and estimating its corresponding 0 dB SL in this study has provided a reasonable agreement between SFOAE I/O and behavioral thresholds.

3.4.2. Comparison to Previous Studies

In an original study, Ellison & Keefe (2005) measured SFOAEs and behavioral thresholds in 85 ears and showed that SFOAE SNR explained up to 51% of the variance in behavioral thresholds in ears with normal hearing and varying degrees of hearing loss[241]. However, SFOAE levels were not found to be a significant predictor of hearing status in the Ellison & Keefe (2005) study[241]. Unfortunately, individual correlations were not reported for SFOAE levels and audiometric

thresholds; therefore, the findings from the two studies cannot be directly compared.

In a similar approach, Gong, Liu & Peng (2020) recently reported on SFOAE I/O derived thresholds for 0.5-8 kHz in 230 normal hearing ears and 737 ears with sensorineural hearing loss[254]. Based on a similar linear regression method used in the current study, Gong, Liu & Peng (2020) reported stronger correlations between SFOAE I/O thresholds and audiometric thresholds than the current study (see Figure 7 of reference) at 1 and 2 kHz, likely due to the wide range of hearing loss in their study[254]. However, their correlations at 4 and 8 kHz were weaker than the current study[254]. Despite the stronger correlations at 1 and 2 kHz reported by Gong, Liu & Peng (2020), there was significant variability between participants at each frequency tested, even among participants with normal hearing (thresholds below 20 dB HL) [254]. In the current study, this variability was not seen, perhaps due to the individually determined stimulus levels for each participant and frequency, the use of time-frequency analysis based on the frequency-delay model of SFOAEs, and/or the quality of the stimulus and emission calibrations.

Goodman et al., (2009) also used advanced calibration methods and component filtering to examine the relationship between behavioral thresholds and otoacoustic emissions for 1 to 16 kHz[242]. Although Goodman et al., (2009) used click-evoked otoacoustic emissions (CEOAEs) and not SFOAEs, they reported a significant correlation between CEOAE levels and behavioral thresholds at 8 and 10.1 kHz but not at 12.7 and 16 kHz[242]. The percentage of variance explained in

CEOAE levels by behavioral thresholds as reported by Goodman et al., (2009) was 28% at 8 kHz and 43% at 10 kHz, compared to 36% and 63% at 8 and 10 kHz, as interpreted from the R-squared values of individual regressions in the current study[242].

Goodman et al., (2009) did not find any significant correlations between CEOAE levels and behavioral thresholds at 12.7 and 16 kHz, likely due to the poor signal to noise ratio at those frequencies in their data, even at the highest click levels of 73 dB peSPL[242]. In contrast, a significant correlation at 12.5 kHz was found in the current study. This difference between the two studies could be due to the different outcome variables used, i.e., CEOAE levels used by Goodman et al., (2009) and SFOAE I/O derived thresholds used in the current study.

Similar to the current study, Charaziak et al., (2013) measured SFOAEs at 10, 20, and 30 dB SL for two probe frequencies, albeit for the purpose of comparing SFOAE suppression tuning curves to psychophysical tuning curves. The average SFOAE levels reported by Charaziak et al., (2013) were -0.9, 6.0 and 10.5 dB SPL at 1 kHz and -2.4, 4.2, and 8.3 dB SPL at 4 kHz for 10, 20, and 30 dB SL respectively[258]. At those same probe frequencies, our median levels were much lower (see Figure 2), likely because we isolated the long-latency component from the total SFOAE, whereas the total SFOAE levels reported by Charaziak et al., (2013) could be elevated due to contributions from multiple internal reflections[259] and /or other sources basal to the peak of the traveling wave[146].

Another difference between our study and Charaziak et al., (2013) is that in the representation of SFOAE levels based on emission pressure level (EPL) rather than sound pressure level (SPL)[258]. Because OAEs are measured in an enclosed space with the probe assembly on one end and the tympanic membrane I on the other end, standing waves resulting from reflections within the enclosed ear canal space can affect the emission pressure in a constructive or destructive manner. According to Charaziak & Shera (2017), by compensating for ear canal acoustics and representing OAE levels in dB emission pressure level (dB EPL), the emission recorded in the ear canal should represent the initial outgoing OAE wave at the TM that is free from reflections within the enclosed ear canal cavity[260]. As shown by Charaziak & Shera (2017), OAE levels in dB EPL can be as much as 10 dB lower than OAE levels in dB SPL (see Figure 5B from reference). Therefore, it is possible that the combination of these two methodological differences between the current study and Charaziak et al., (2013) could explain the discrepancy between SFOAE levels at the comparison frequencies.

In the current study, SFOAEs increased in level as a function of stimulus level and the rate of growth was compressive (0.44 to 0.6 dB/dB). The current study is most similar to Charaziak et al., (2013) using 10, 20, and 30 dB SL for SFOAE measurements[258]. Although Charaziak et al., (2013) did not report the slope of their growth curves at 1 and 4 kHz, these values can be computed from Table 2 of the reference, which provides the mean total SFOAE levels for all three probe levels and both probe frequencies. Using the same method of slope calculation as the

current study, the slope estimates from Charaziak et al., (2013) are 0.57 dB/dB at 1 kHz and 0.54 dB/dB at 4 kHz, which are quite similar to the current slopes of 0.49 dB/dB at 1 kHz and 0.54 dB/dB at 4 kHz. In another study of SFOAE I/O functions, albeit not measured in dB SL, Schairer et al., (2003) showed that at moderate to high stimulus levels, SFOAE levels grew at a rate of 0.44 and 0.61 dB/dB for 2 and 4 kHz[253].

Animal studies of basilar membrane input-output functions in response to a single tone have shown different compressive growths at moderate levels in the base (0.2 – 0.3 dB/dB) and in the apex (0.5 – 0.8 dB/dB)[231]. Using higher resolution motion measurements of the basilar membrane (BM) and OHC/Deiter Cell (DC) junction, Dewey et al., (2021) have recently shown that BM displacement I/O functions in mice are quite similar to displacements measured at OHC-DC at CF for low stimulus levels (~30 dB SPL or lower) with slopes of ~1 dB/dB[177]. However, at the compression knee-point of ~ 30 dB SPL, the two I/O functions start to differ[177]. Because the OHC-DC displacements saturated at lower levels (~55 dB SPL) than BM displacements which did not saturate until ~75 dB SPL, the slope of compression was quite different between the two[177]. Furthermore, the OHC-DC displacements were more compressive at higher stimulus levels, even at non-CF frequencies where BM responses were linear[177].

Then, why are SFOAE I/O functions from humans less compressive than BM and OHC-DC I/O functions? One simple explanation could be a difference in cochlear mechanics and SFOAE generation between mice and humans. Although

this explanation is parsimonious, it does not account for the relatively frequency-independent slopes in the current study. The compression slopes across all frequencies in the current study were similar to those from the apex in animals (0.5 – 0.8 dB/dB)[231]. Could this just be an inherent limitation of OAEs that represent the spatial integration of the activity across the entire cochlear activation pattern and not as pinpoint displacement of the CF as in measurements of the BM, OHC, and various associated structures?

Accounting for this spatial integration of OAEs over its generation region and contributions from non-CF places, filtering SFOAE and TEOAE components into short-latency and long-latency components showed a more compressive growth of the long-latency component than the short-latency components[261]. This provides further support for the extended generation of reflection emissions that could be mitigated with advanced computational approaches to assess the cochlear regions of interest. Utilizing these techniques, the long-latency component of SFOAEs were correlated with behavioral thresholds across all frequencies, further validating their clinical potential.

In the current study, the noise floors generally did not grow with increasing stimulus levels, which indicates that the current measurements were not significantly influenced by system distortion[253]. In a few instances, the noise floor increased at 16 kHz and above, which may be related to poor signal to noise ratio at those frequencies, probe jitter which could result in an incomplete cancellation of

probe across measurement blocks[262], or the sensitivity of the microphone above 16 kHz[197,242].

3.4.3. Filtering the long-latency SFOAE component

Previous studies examining the clinical utility of SFOAEs for predicting thresholds or identifying hearing loss[241] reported on the total SFOAE residual recorded. The current study demonstrates that filtering the total SFOAE based on the frequency-delay relationship provided higher agreement between LL SFOAE and behavioral thresholds compared to the total SFOAE. These findings suggest the relationship between total SFOAE recorded in the ear canal and behavioral thresholds may be complicated by the presence and contributions of multiple intracochlear reflections[253] and multiple components arising from regions in the cochlea other than the characteristic place[242,261].

Although the exact relationship between OAE I/O growth and physiological responses (i.e., basilar membrane [BM] and reticular lamina [RL]) can only be modeled in humans[261], animal studies have found both linear and nonlinear growth of physiological responses for different stimulus parameters. In chinchilla, basilar membrane velocity in response to characteristic frequency (CF) tones has been shown to be non-linearly compressive at moderate stimulus levels[263]. However, BM and RL responses to non-CF tones are also highly linear (panel 3H and 3I of reference)[149]. At very low stimulus levels and at very high stimulus levels, the responses are linear[263,264]. These animal studies suggest that I/O growth functions

of SFOAEs are also likely to be influenced by stimulus parameters such as the probe level and potential contributions from regions other than the characteristic place.

Using time-frequency filtering, Sisto et al., (2013) measured the I/O growth rate of different latency components of TEOAEs and SFOAEs in three participants[261]. They found linear growth of the short-latency component, which presumably arise from regions basal to the characteristic place, and compressive growth of long-latency components, similar to the findings of Goodman et al., (2009). In the current study, LL SFOAE I/O functions also showed compressive behavior at the three probe levels tested (see Figure 3.6). Therefore, the non-linear and compressive growth of LL SFOAE I/O functions supports the hypothesis that LL SFOAEs reflect the activity of the active region of the cochlea, where BM and RL responses are also non-linearly compressive.

3.4.4. Relationship between SFOAEs & Behavioral Thresholds

A strong correlation between SFOAE I/O estimated thresholds and behavioral thresholds was found in the current study for 0.75 to 14 kHz center frequencies. The strengths of the correlations in the present study were much stronger than previous reports[197,240,241]. There are several possible explanations to help interpret our findings. First, previous studies that did not find correlations between SFOAE levels and behavioral threshold measurements did not equalize the stimulus levels between the two measures. In a recent study, Dewey & Dhar (2017b) measured

behavioral thresholds and SFOAEs at 0.5 to 20 kHz at a single, fixed level of 36 dB FPL in 23 normal-hearing females. They found that although the group averages of the two measures (SFOAEs and behavioral thresholds normalized to 1 kHz) looked similar, there were large discrepancies between individual SFOAE spectra and behavioral hearing sensitivity across individuals[197]. Dewey & Dhar (2017b) found that levels of SFOAEs measured at a fixed level were largely uncorrelated with behavioral thresholds at 8-16 kHz[197]. This is not surprising as there is a large range of thresholds measurable across individuals, whereas SFOAE levels were only recorded for a fixed level of 36 dB FPL; therefore, any differences in the stimulus arriving in the cochlea would contribute to greater mismatch between SFOAEs and behavioral thresholds because of the significant dependence of SFOAEs on middle ear status for forward and reverse transmission.

The association between SFOAEs and behavioral thresholds at high frequencies (>8 kHz) remained largely unexplored until the current investigation[23,197]. Although SFOAE I/O estimated and behavioral thresholds were correlated up to the highest measurable frequency, high-frequency SFOAEs showed a dramatic decline at a lower frequency than behavioral thresholds. This finding could be interpreted in several different ways. One hypothesis is that SFOAE levels are more sensitive than behavioral thresholds for detecting changes in cochlear status. Because SFOAE generation is hypothesized to be the coherent summation of wavelets arising from within the peak amplification region[149], changes in generators

due to dysfunction could reduce the total number of wavelets contributing to the summed response that is measured in the ear canal.

An alternative hypothesis of SFOAE generation suggests that a dysfunctional cochlea creates impedance irregularities which serve as inflection points for the incident wave generated from the peak amplification region. In this case, the overall number of generators contributing to the SFOAE is expected to increase. This hypothesis has been proposed in light of evidence of measurable SFOAEs in ears with some degree of hearing loss[13,265]. In the current study, individuals with hearing loss at the 0.5-8 kHz frequencies were not included as evaluated by Abdala & Kalluri (2017); therefore, the hypothesis of increased irregularities due to cochlear dysfunction was not testable; however, evidence for the two divergent hypotheses of SFOAE generation within the same age group comes from another study by Dewey & Dhar.

Dewey & Dhar (2017b) identified various different landmark frequencies from the audiometric data and compared them to landmark frequencies of SFOAE spectra, similar to Lee et al., (2012). They found a significant correlation between two of these measures: 1) the corner frequency of the SFOAE spectra ($f_{sf\text{-}C}$), defined as the highest frequency at which SFOAE amplitudes declined at a rate of -4 dB/octave; 2) the 18-dB FPL threshold intercept frequency ($f_{t\text{-}18}$) i.e., the behavioral frequency where thresholds were equal to 18 dB FPL[197]. Based on this comparison, Dewey & Dhar (2017b) observed two different patterns across their participants: A) $f_{sf\text{-}C}$ was very close to $f_{t\text{-}18}$ and SFOAEs were not measurable above this frequency, or

B) $f_{sf\text{-}C}$ was lower than $f_{t\text{-}18}$ but SFOAEs re-emerged as a single low-level peak or multiple low-level peaks above $f_{t\text{-}18}$[197] Both of these patterns support the two different mechanisms by which SFOAEs may be generated – one that is sensitive to hypofunction and corresponds to behavioral thresholds and the other that is an indication of hyperfunction due to damage and diverges from behavioral thresholds.

Another possible explanation of the mismatch between behavioral thresholds and the high frequency decline of SFOAEs is that high frequency SFOAEs are limited by the reverse transmission characteristics of the middle ear[242]. Although studies of middle ear mechanics have shown a reduction in stapes velocity at high frequencies (>4 kHz)[169], others have suggested that stapes velocity is likely not a good indicator of reverse transmission, as the pressures measured in the scala vestibuli and scala tympani in forward and reverse transmission are very different due to the different impedances of the oval and round windows[266,267].

It remains to be determined whether a combination of these occur with aging and will be tested in a subsequent study using young, pristine hearing ears as a reference for aged ears. If there is a mismatch between SFOAEs and behavioral thresholds in the youngest age group, the reverse transmission hypothesis may be supported, whereas if there is not a mismatch between SFOAEs and behavioral thresholds at high frequencies in the youngest age group, it supports the sensitivity of SFOAEs to cochlear damage hypothesis. A combination of the two could be manifested as a persistent difference between the high-frequency SFOAEs and behavioral hearing thresholds, a difference that becomes more pronounced as a

function of age and could be evidenced as a change in slope of the high-frequency SFOAE decline with age. Perhaps the true impact of cochlear damage due to aging in humans may only be testable using longitudinal studies of behavioral thresholds and SFOAEs.

3.4.5. Limitations

Because the goal of the current study was to examine SFOAEs and behavior in clinically normal ears, the generalizability of the current findings to clinical practice remains to be investigated in impaired ears. A main limitation of the current study is that only three stimulus levels were used which may have impacted the degree of the observed correlations. However, given the dearth of SFOAE data using stimulus levels in dB SL, the current study adds to the current knowledge, particularly at frequencies > 8 kHz. I/O functions at center frequencies up to 14 kHz were collected; however, only half of the I/O functions met the quality controls that resulted in an estimated threshold. This is a major limitation in ears in which significant cochlear damage is suspected and SFOAE I/O functions are essentially futile. The silver lining may be in the differential diagnosis of retrocochlear vs cochlear or soma vs stereociliary OHC dysfunction, which will require extensive further investigation.

3.5. Conclusions

The present study aimed to understand the relationship between the long latency component of SFOAEs and behavioral estimates of auditory sensitivity across a wide range of frequencies in clinically normal-hearing individuals. The findings showed that SFOAE LL levels were correlated with behavioral thresholds when stimulus levels across individuals are considered carefully and only cochlear contributions from the CF place are isolated based on their delays. The current study has implications for advancing the use of SFOAEs as clinical tool for the objective and non-invasive assessment of cochlear status, particularly at the highest measurable frequencies where cochlear dysfunction is most evident.

CHAPTER 4

Tuning Estimates from the Delays of Stimulus Frequency Otoacoustic Emissions

4.1. Introduction

Auditory frequency selectivity, i.e., the ability to distinguish between sounds of different spectral content, is thought to contribute to various perceptual abilities including speech perception in noise[268]. One method for assessing frequency selectivity is to measure psychophysical tuning curves (PTCs) [268]. Psychophysical tuning curves (PTCs) are iso-response curves that are constructed when a listener responds to a tone in the presence of a masker that varies in level and frequency[269]. Since the earliest PTC measurements in humans [270-272], PTCs have been used for diagnosing dead regions (Moore, 2001) and assessing frequency selectivity[273]. Although PTC measurement paradigms have improved over the years, making them more efficient and easier to implement[274,275] even in children [276,277], the task remains too challenging and time-consuming to be implemented in clinical protocols.

Frequency selectivity, as measured at the level of the auditory nerve, has been related to the mechanical tuning of the cochlea[179]. As such, objectively assaying cochlear tuning using otoacoustic emissions (OAEs) has been proposed as a faster alternative to PTCs[224,245,246]. Not only are OAEs fast and easy to measure, requiring no input from the listener, OAEs are byproducts of active cochlear processes, making them an appropriate tool for assessing cochlear tuning. However,

the relationship between OAEs and PTCs, particularly at high frequencies (>8 kHz), is not well characterized. In the current study, PTCs were examined for frequencies up to 14 kHz and related to the delays of OAEs evoked using a single tone, i.e., stimulus frequency otoacoustic emissions (SFOAEs), in an effort to non-invasively assess cochlear tuning.

The passive tuning profile of the cochlea is based on the mechanical mass and stiffness gradient of the basilar membrane, which allows the incident traveling wave to maximally vibrate at its resonant place along the cochlear partition[165]. The cochlea actively filters the incident traveling wave based on the tuning profile established by the passive mechanical stiffness gradient[231,278]. Furthermore, because the traveling wave is locally amplified, the cochlea is actively dispersive[279] such that the waves travel at different rates as they approach their characteristic place [280]. As an active and non-linear system, the cochlea introduces delays in the incident traveling wave as it reaches its resonant place.

This phenomenon is empirically observed in the phase lag of the basilar membrane vibrations relative to the vibrations at the stapes footplate[231]. Because cochlear place can be mapped to frequency, when the basilar membrane phase is plotted as a function of frequency, the slope of the basilar membrane phase vs. frequency can be interpreted as the forward-going delay related to cochlear tuning and filtering[231]. Similarly, the phase of SFOAEs varies as a function of frequency, and as such, the phase gradient has been related to the round-trip cochlear delay associated with cochlear tuning and spectral filtering[246].

Several groups have examined how the phase gradient of SFOAEs relates to behavioral or neural tuning in animals[222,243,245-247]. Sumner et al., (2018) measured SFOAEs, PTCs, and auditory nerve fiber (ANF) tuning in ferrets and found that tuning estimates from all three measures were similar[247]. However, few studies have characterized this proposed relationship between behavioral tuning and SFOAE-based tuning within the same human ears[224,246,247].

Wilson et al., (2020) examined this relationship at two probe frequencies in 24 normal-hearing, young adults and found a correlation between behavioral tuning and SFOAE delay-based tuning at 4 kHz but not at 1 kHz[224]. The discrepancy at 1 kHz may be in part due to differences in cochlear mechanics and OAE generation at the apex[224]. However, further characterization of the phase gradient of SFOAEs across a wide range of frequencies and levels is needed to fully evaluate the utility of SFOAEs in clinical protocols for assessing tuning.

The purpose of this study is to investigate the relationship between SFOAE phase gradient to behavioral measures of auditory tuning up to 14 kHz. The hypothesis tested was whether the phase gradient of SFOAEs reflects the delay associated with cochlear filtering that ultimately contributes to behavioral tuning for a given frequency region. Sharpness of tuning derived from SFOAE phase gradient delays were compared to behavioral tuning estimates at equivalent stimulus levels of 10 dB sensation level at eight center frequencies (0.75, 1, 2, 4, 8, 10, 12.5 and 14 kHz). SFOAE delay-based tuning estimates at 10, 20, and 30 dB SL were also compared. Tuning is non-linearly level-dependent, such that tuning

curves are sharpest at low levels and become broad at high stimulus levels[281]; therefore, it was predicted that tuning estimates from SFOAE delays will also demonstrate the level-dependence of tuning estimates seen in other behavioral and physiological data[149,179,273,278].

4.2. Methods

Participants were 28 individuals (19 females, 9 males), aged 12-43 years (M = 27.55, SD = 6.89). The inclusion criteria, screening and general procedures were the same as described in sections 3.2.1. and 3.2.2. of Chapter 3. Furthermore, details of the in-situ calibration, behavioral thresholds and SFOAE measurements common to both studies are presented in the sections 3.2.3., 3.2.4., and 3.2.5. of Chapter 3.

4.2.1. Psychophysical Tuning Curves (PTCs)

Behavioral tuning estimates were obtained using a fast-swept PTC method described by Sęk and Moore (2011)[275]. Signals were FPL-calibrated pulsed pure-tones with a total duration of 500-ms and an interstimulus interval of 200 ms presented at 10-dB sensation level. The masker was a narrowband noise of 320 Hz bandwidth that was logarithmically swept in frequency over 240 seconds. The noise sweep ranged from 0.5 to 1.5 * probe frequency for frequencies < 10 kHz[275,282] and from 0.7 to 1.3 * probe frequency for frequencies at or above 10 kHz[283].

Because thresholds at high frequencies are typically poorer, the starting frequency of the swept noise was lower than probe frequency at or above 10 kHz

and higher than the probe frequency below 10 kHz. Participants were asked to listen for the pulsing probe tone while ignoring the noise masker. At the start of each measurement, the pulsing probe tone alone was played without the masker for approximately 1 minute so that the participant became familiar with the tone they were listening for.

The participants were instructed to listen for the probe tone, ignoring the masker and indicate if the tone was audible by pressing the space bar on a keyboard. When the space bar was pressed or released, the masker level increased or decreased, respectively, at the rate of 2 dB/s in 0.5-dB steps[258,275,282] until the entire PTC was obtained.

The raw PTC tracings were smoothed using a loess fit (MATLAB) using three different smoothing parameters (low, medium, and strong, i.e., 25%, 40%, and 60% smoothing span). However, in order to compare to previous literature[146], only low smoothed PTCs were included in final analysis. Estimates of tuning sharpness for PTCs (Q_{erb}) were computed based on the height and area of the tuning curve. Using the *findpeaks* function (MATLAB), the tip of the smoothed PTC i.e., f_{tip} was identified. The height and area of the function were calculated using the *trapz* function (MATLAB), and the equivalent rectangular bandwidth was computed as the area divided by the height. Q_{erb} was computed as f_{tip} divided by the equivalent rectangular bandwidth.

Values were excluded from analysis if the tuning curves did not meet the following quality criteria: 1) the shapes of the tuning curves were irregular

(inverted); 2) the tip of the tuning curve was lower in level than the behavioral hearing threshold for that frequency; and 3) the hearing threshold or the tip of the tuning curve for a given frequency exceeded 50 dB FPL (see Figure 4.1).

4.2.2. SFOAE Tuning Estimation from Phase-Gradient Delays

For each ear, frequency, and level, the average latency (τ) of the first reflection component was computed from the filtered wavelet coefficients [284]. τ (s) was multiplied by frequency (Hz) to compute N_{sfoae} (delay in equivalent number of cycles) and two separate tuning estimates from the Shera & Guinan model[285] and the Moleti & Sisto model[284] were computed according to Wilson et al., (2020)[224].

4.2.3. Statistical Analysis

All data were analyzed in RStudio using packages {psych}, {stats}, {rmcorr}, {dplyr}, {plyr}, {readr}, {tidyr}, {ggplot2}, {ggridges} and {ggpubr}. SFOAE and PTC tuning estimates were analyzed using repeated measures correlational analyses in the {rmcorr} package in RStudio (version 1.2.5033). Effects of frequency and level were tested by first generating linear mixed effects model with all variables and interactions included in the full model, reducing models by removing variables, and then comparing model performance using analysis of variance. Significance levels were set at $p < 0.05$.

4.3. Results

SFOAEs at 10, 20, and 30 dB SL and PTCs at 10 dB SL re: behavioral thresholds at 0.75 – 14 kHz were collected from ears of 28 normal-hearing individuals. Demographic descriptive data are presented in Figure 3.1, which shows that participants were between the age of 12 and 43 years, mostly female, white, and non-Hispanic or Latino. The current study extends the findings of Wilson et al., (2020)[224] to multiple levels and frequencies up to 14 kHz using the long-latency component of SFOAEs combined with behavioral measures of tuning.

4.3.1. Behavioral Thresholds and Psychophysical Tuning Curves (PTCs)

Behavioral thresholds were measured using a modified Bekesy tracking procedure, whereas PTCs, measured using a fixed-probe, swept-masker paradigm, were obtained at 10 dB above the behavioral threshold for each probe frequency. Behavioral thresholds and smoothed PTCs are shown in Figure 4.1. In general, tuning curves were sharp with sensitive tips up to the highest probe frequency (14 kHz) so long as thresholds were similar across all test frequencies (e.g., Participants 3, 12, 39, 43). Tips of tuning curves shifted upwards if there was some degree of threshold shift at frequencies > 8 kHz compared to thresholds at or below 8 kHz (e.g., Participant 2, 6, 31, 34). On the other hand, PTCs became inverted when thresholds exceeded 50 dB FPL above 8 kHz (e.g., Participant 4, 40, 51, 52, 66).

Although PTCs were obtained at all eight probe frequencies from all 28 participants, a few quality criteria were established to select data for full analysis

and comparison. First, tuning estimates (Q_{erb}) could not be computed from some of the irregularly shaped or flat PTCs (n = 10 out of 224). Another 8 observations were removed from the group analysis, if the behavioral thresholds for a frequency exceeded 50 dB FPL. Lastly, if the smoothing procedure yielded a tip level of the PTC that was lower than the behavioral threshold for that frequency, those observations (n = 28) were also excluded from further analysis.

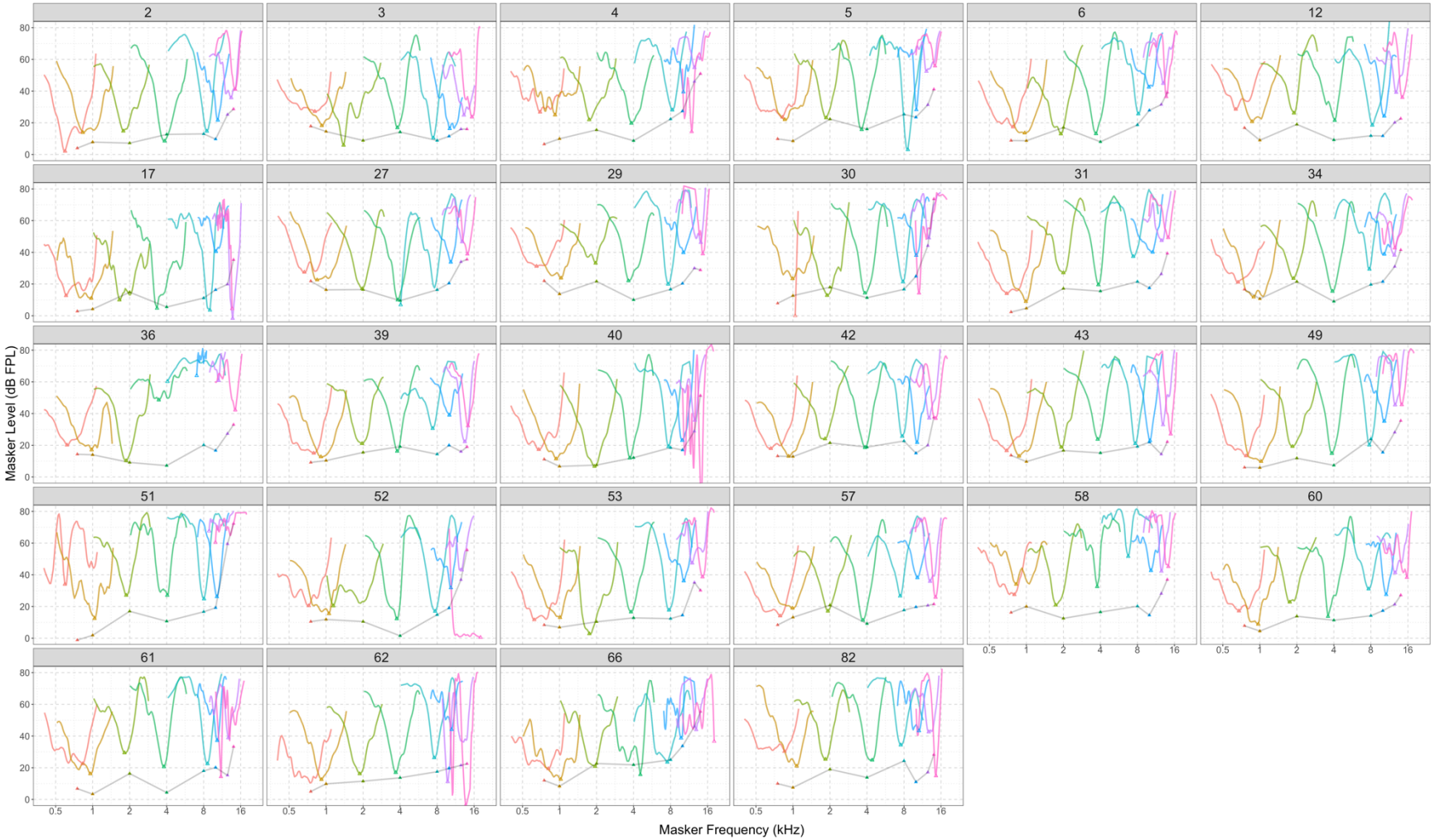

Figure 4.1. Behavioral thresholds and smoothed psychophysical tuning curves for all participants. Individual participants are plotted in each panel. Within each panel, thresholds for each frequency (depicted by color) are indicated by unfilled triangles and connected by solid gray line, whereas tips of tuning curves are indicated by filled triangles.

Despite these quality controls, the behavioral tuning estimates displayed outliers with much larger or much smaller values compared to other participants. Figure 4.2 shows boxplots of behavioral tuning estimates as a function of frequency for all participants. A clear frequency dependence can be observed in the sharpening of tuning (higher Q_{erb}) as a function of increasing frequency up to 8 kHz, above which the median Q_{erb} plateaus around a value of 15. The variability of the tuning estimates also increased at ~10 kHz.

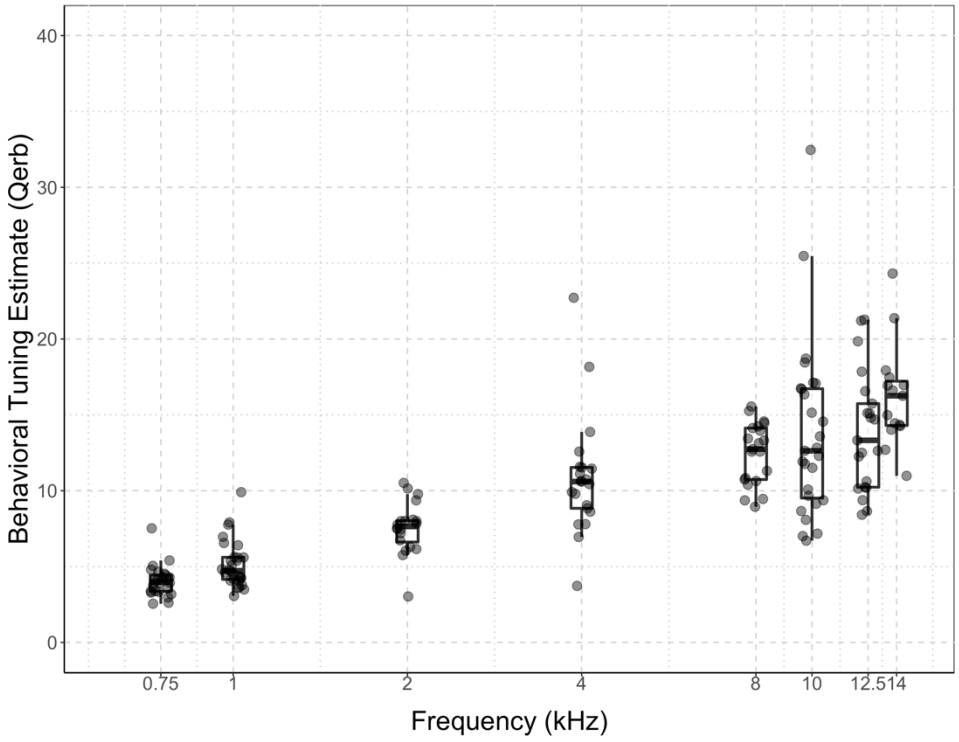

Figure 4.2. Boxplots of behavioral tuning estimates plotted as a function of frequency for all participants. Individual participants are represented by individual circles.

4.3.2. SFOAE Phase as a Function of Frequency

In order to compute tuning estimates from SFOAE delays, phase was measured around each center frequency. Phase data from the unfiltered SFOAEs are shown in Figures 4.3 and 4.4 for probe levels in dB SL and dB FPL, respectively. The individual data show that phase accumulation varied across participants, across levels, and across frequencies. For some individuals, phase accumulation increased with increasing probe level (e.g., Participant 2, 3, 6, 31, 36, 39, 40, 49), whereas in others, phase accumulation decreased with increasing probe level (e.g., Participant 5, 30). In most cases, there was no consistent change in phase with level, either for stimulus represented in dB SL (Figure 4.3) or in dB FPL (Figure 4.4).

In a few instances, there seems to be acausal phase, i.e., phase leading instead of lagging (e.g., Participant 40, 62) which likely indicates the measurement may have been infiltrated with artifactual recordings. In other cases, the phase starts accumulating but flattens out when in a region of poor SFOAE SNR. The most notable pattern that emerges is the flattening of phase above 8 kHz for most participants. The flattening phase appears to coincide with the decline of SFOAE levels and reduced SNR at and above 8 kHz as demonstrated in Figure 4.5.

The variable patterns of phase accumulation may be indicative of interference from multiple components of the evoked emissions, particularly at high levels and low frequencies, or stimulus artifact, the influence of which may be reduced if not eliminated by time-frequency filtering using the continuous wavelet

transform. Consistent with this hypothesis, at very high frequencies and high probe levels (> 55 dB FPL), noise floors increased compared to stimulus levels of 55 dB FPL or lower. Although data from probe levels > 55 dB FPL were not included in the tuning analysis, phase data from all probe levels were used in the continuous wavelet transform filtering for computing the phase delay estimates.

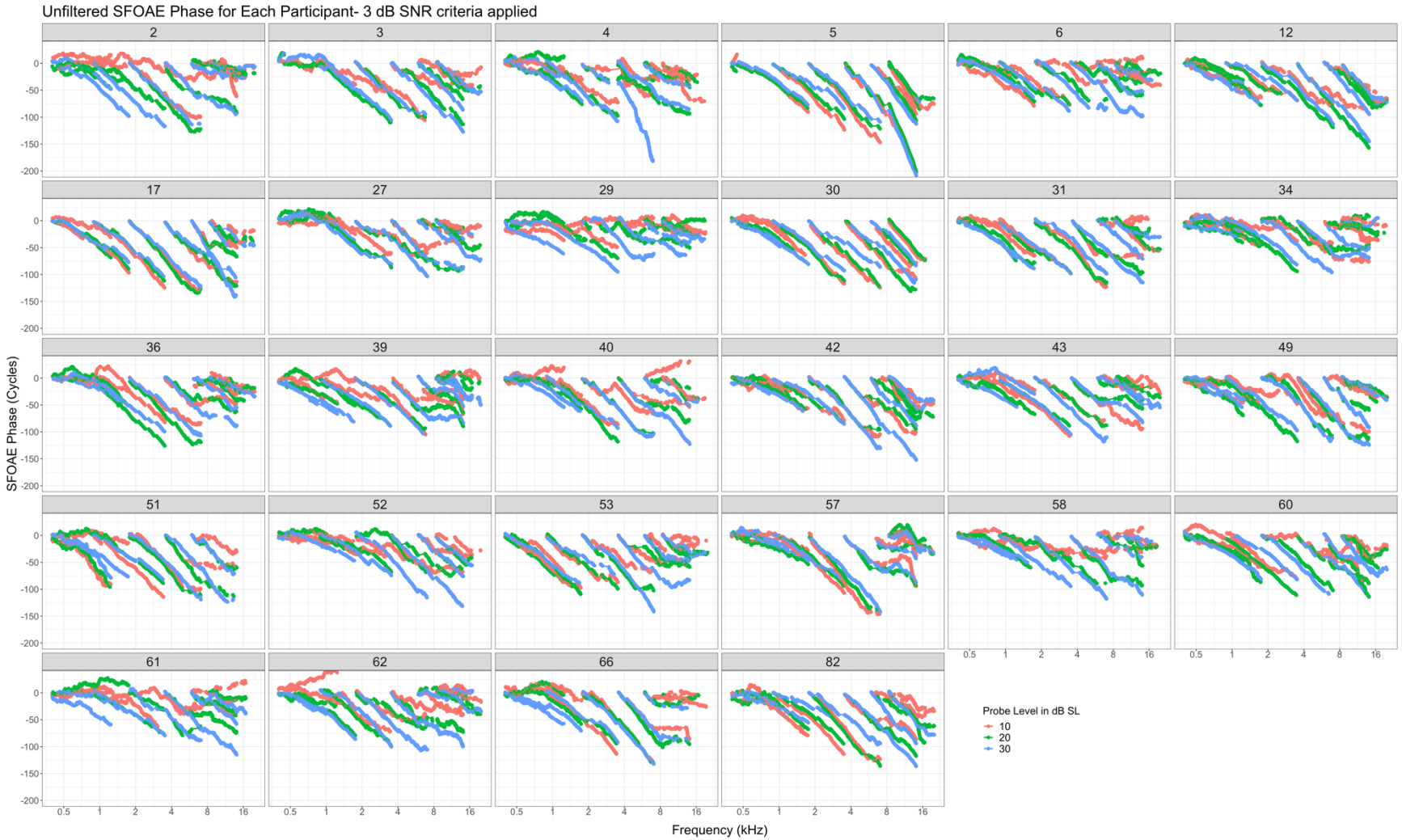

Figure 4.3. SFOAE phase as a function of frequency for all three sensation levels and all participants. SFOAE phase in cycles is plotted as a function of frequency for all three probe levels represented by different colors. SFOAE phase was estimated from the least-squares fitting algorithm and referenced to the lowest frequency measured for each of eight center frequencies. Panel headings indicate participant for which data are plotted in each panel. Only phase data for which the SFOAE levels passed a 3 dB SNR criterion are plotted.

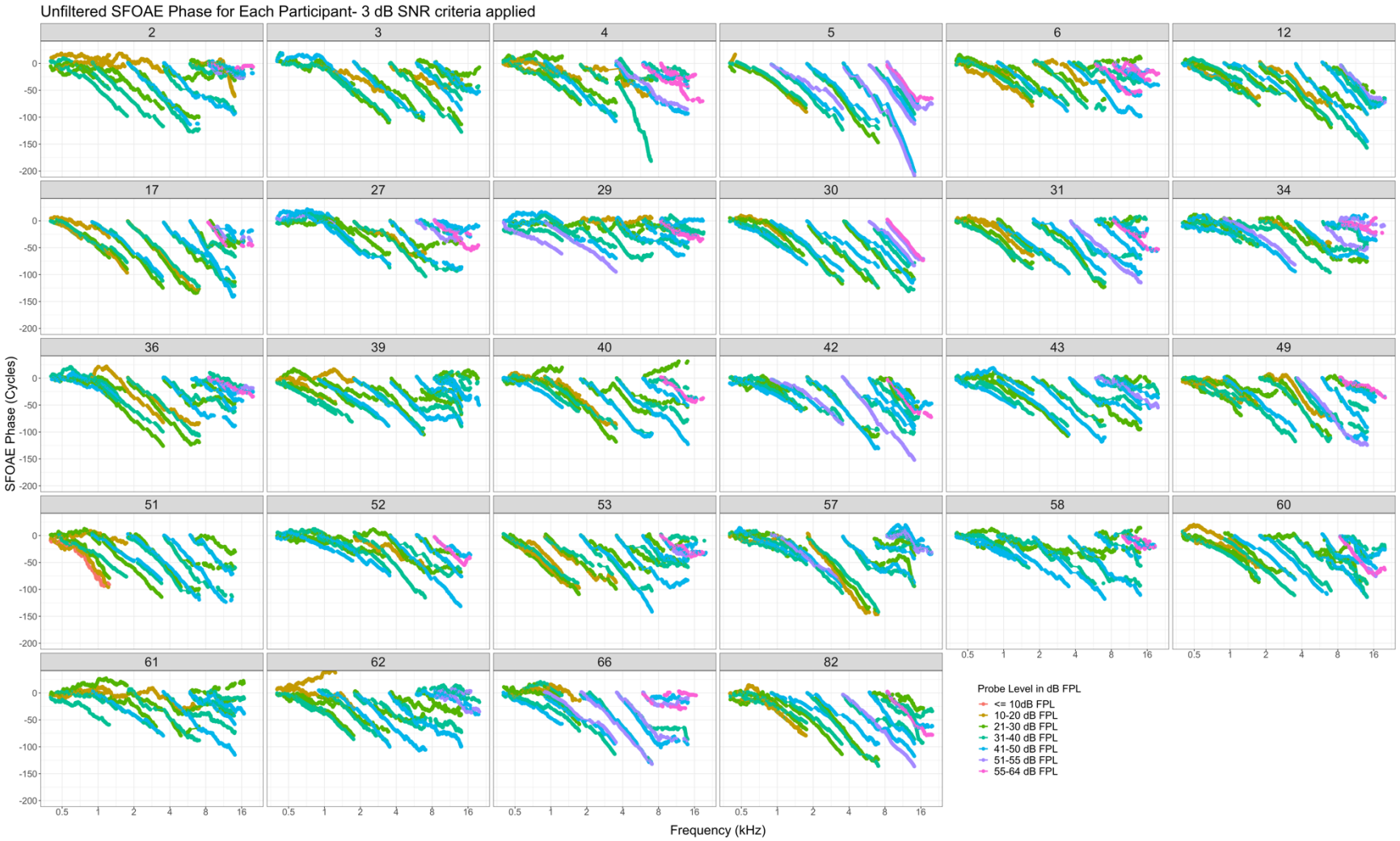

Figure 4.4. SFOAE phase as a function of frequency for all participants plotted by stimulus levels in dB FPL. Color represents the probe level in dB FPL. Only phase data for which the SFOAE levels passed a 3 dB SNR criterion are plotted.

Figure 4.5. Filtered long-latency SFOAE levels as a function of frequency for all participants plotted by stimulus levels in dB FPL. Darker lines connected by symbols represent the SFOAE levels, whereas lighter colored lines represent the noise floors. Color represents the probe level in dB FPL as described in figure legend. Multiple data points at each frequency are present because data were collected for overlapping frequencies around each center frequency.

4.3.3. Phase-Gradient Delays as a Function of Frequency and Probe Level

After filtering the total SFOAE based on the delay cut-offs of individual SFOAE components, the filtered SFOAE components were processed with an inverse FFT to estimate delays. The delay estimates from the filtered long-latency component of the SFOAEs are shown in Figure 4.6. The loess fit to the data showed that SFOAE delay estimates are level dependent, albeit at 2 kHz and below. This level dependence of the long-latency SFOAE delays is better visualized, when probe levels are represented in dB FPL rather than dB SL (Figure 4.7). A break in the delays around ~1.5 kHz is notable in both delay-frequency plots. When delays are expressed in dimensionless units, a clear dependence of delays across the entire frequency range can be observed, along with breaks in the frequency-delay functions.

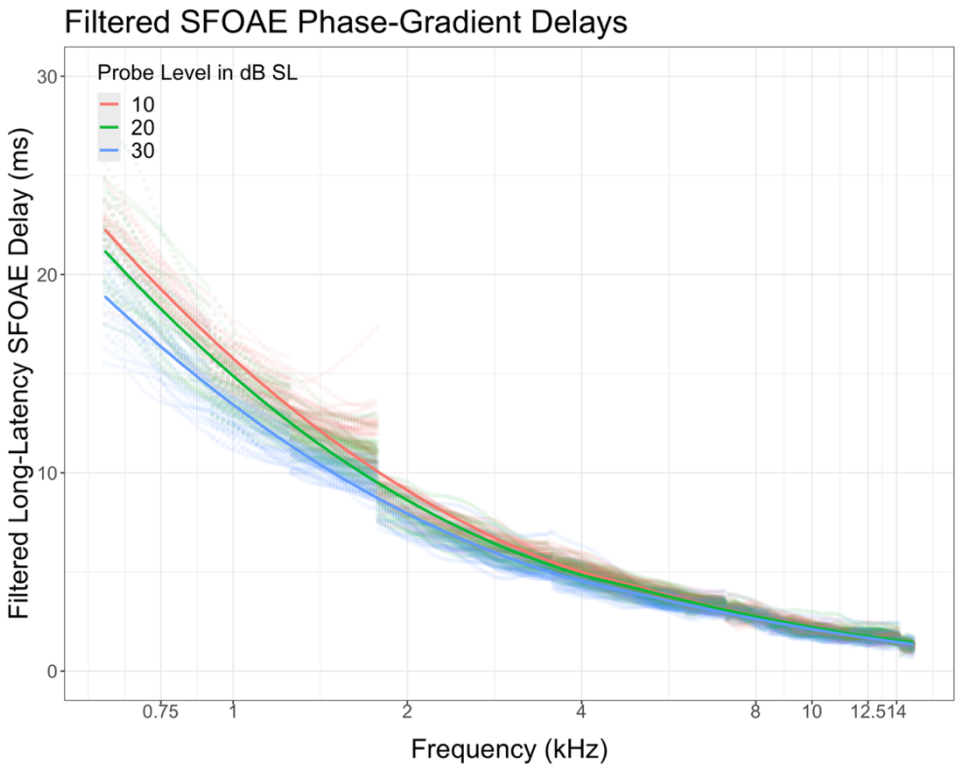

Figure 4.6. Long-latency SFOAE delays as a function of frequency for all three probe levels in dB SL. Delays (ms) were computed using CWT filtering. Individual delays across participants are represented by the circles, whereas the loess fit across participants are shown by solid lines for each stimulus level.

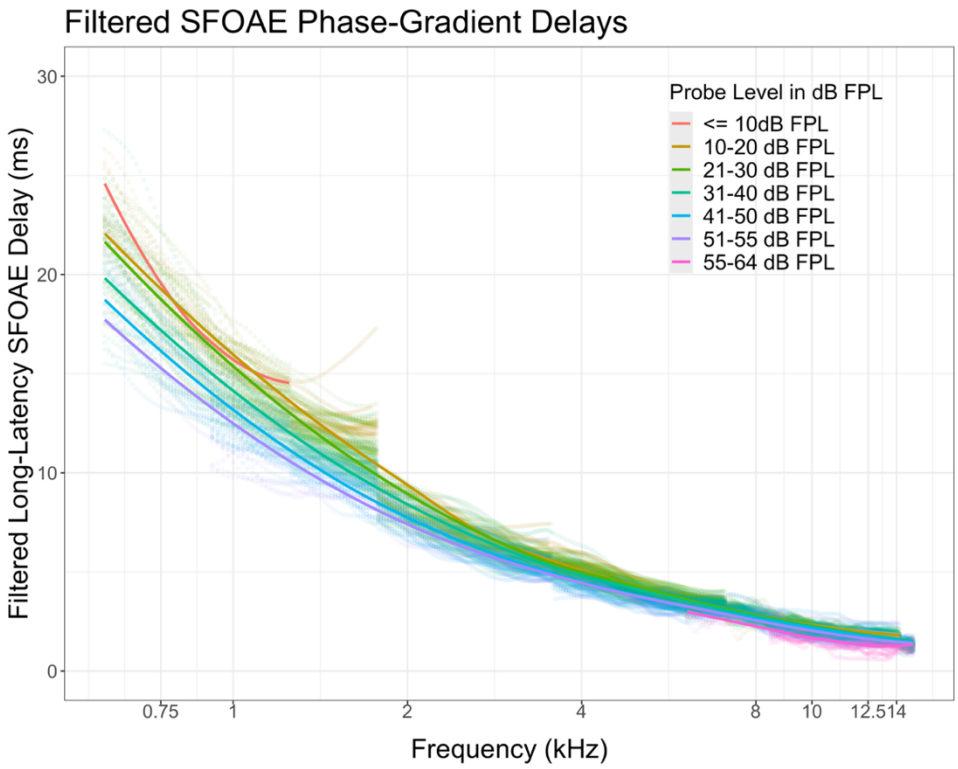

Figure 4.7. Long-latency SFOAE delays as a function of frequency for probe levels in dB FPL. Delays (ms) for the long-latency component are plotted as a function of frequency for probe levels in dB FPL as indicated by different colors (key in figure legend). Individual delay values across participants are represented by the circles, whereas the loess fit across participants are shown by solid lines for each stimulus level in dB FPL. Because stimulus levels were set according to behavioral thresholds for each of the eight center frequencies, not all participants have data at all seven stimulus levels for each center frequency.

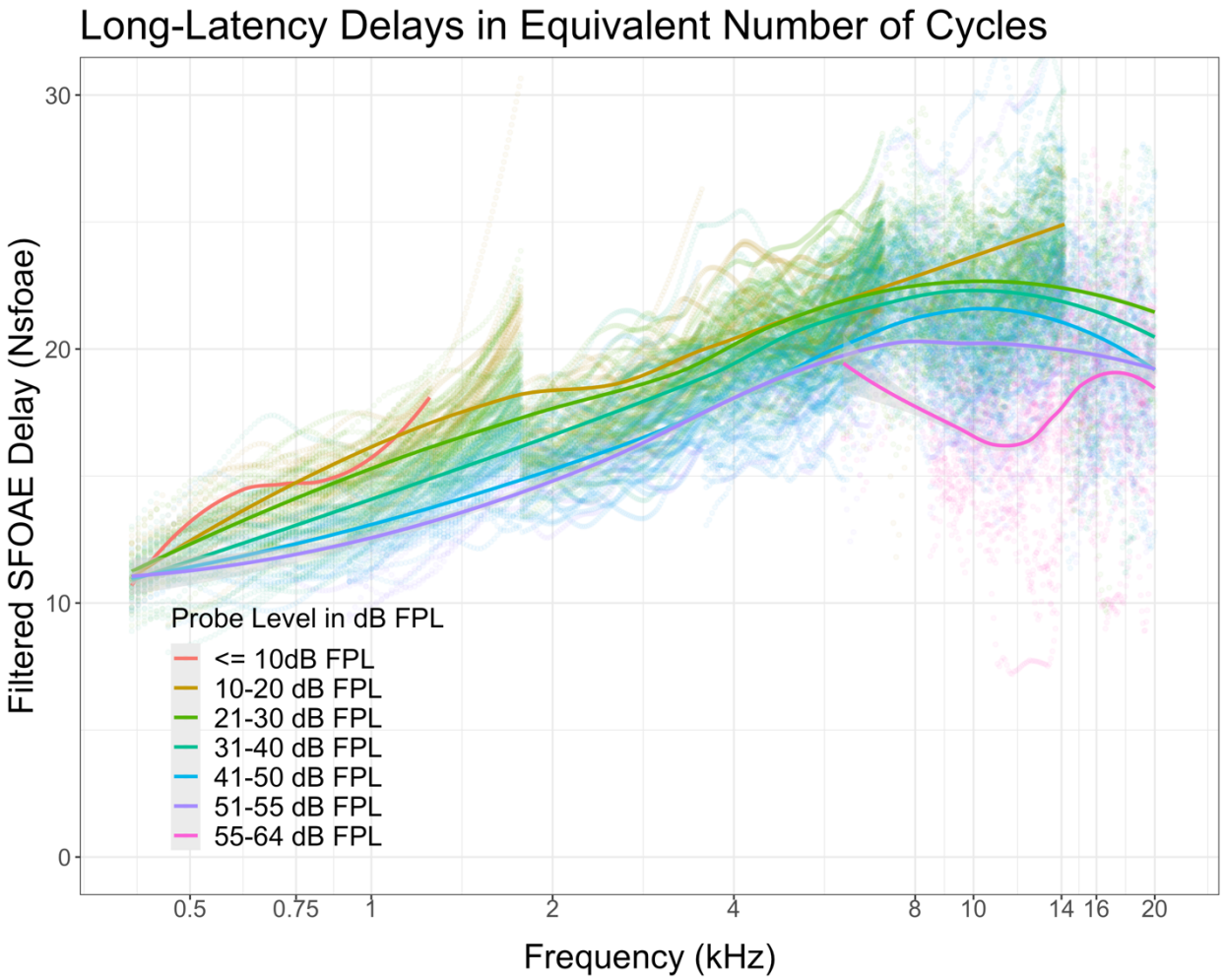

Figure 4.8. Dimensionless SFOAE delays as a function of frequency for probe levels in dB FPL. Dimensionless delays (equivalent number of cycles [Nsfoae]) for the long-latency component are plotted as a function of frequency for probe levels in dB FPL as indicated by different colors (key in figure legend). Individual delay values across participants are represented by the circles, whereas the loess fit across participants are shown by solid lines for each stimulus level in dB FPL.

4.3.4. Tuning Estimates from SFOAE Delays

Tuning estimates calculated from the phase-gradient of the long-latency SFOAE delays are shown in Figure 4.9. Similar to behavioral tuning, the SFOAE delay-based tuning demonstrated a clear frequency dependent sharpening of tuning up to 8 kHz. Above 8 kHz, tuning estimates decreased and became more variable. A slight level dependence in the tuning estimates can also be observed, such that tuning values tend to be higher for the lowest probe levels compared to the highest probe levels, in contrast to the raw phase data from Figure 4.3 and 4.4, which did not show a consistent level dependence.

The effects of frequency and level on SFOAE-based tuning were tested statistically using multilevel mixed effect modeling. In the full model, probe level in dB SL and probe frequency in kHz, their interaction, and the intercept were used as fixed effects variables and participants as the random effects variable. When intercept was removed in the second model, the analysis of variance showed a significant effect of the intercept (X^2 (1, N = 585) = 99.309, $p < 0.001$). Next, probe level was removed and compared to the full model, which revealed a significant effect of signal level (X^2 (1, N = 585) = 16.631, $p < 0.001$). In the fourth model, probe frequency was removed and again this model was compared to the full model, which revealed a significant effect of frequency (X^2 (1, N = 585) = 56.471, $p < 0.001$). Lastly, the interaction term was removed in the fifth model and compared to the full model, which showed a significant interaction between level and frequency for SFOAE-based tuning (X^2 (3, N = 585) = 72.413, $p < 0.001$).

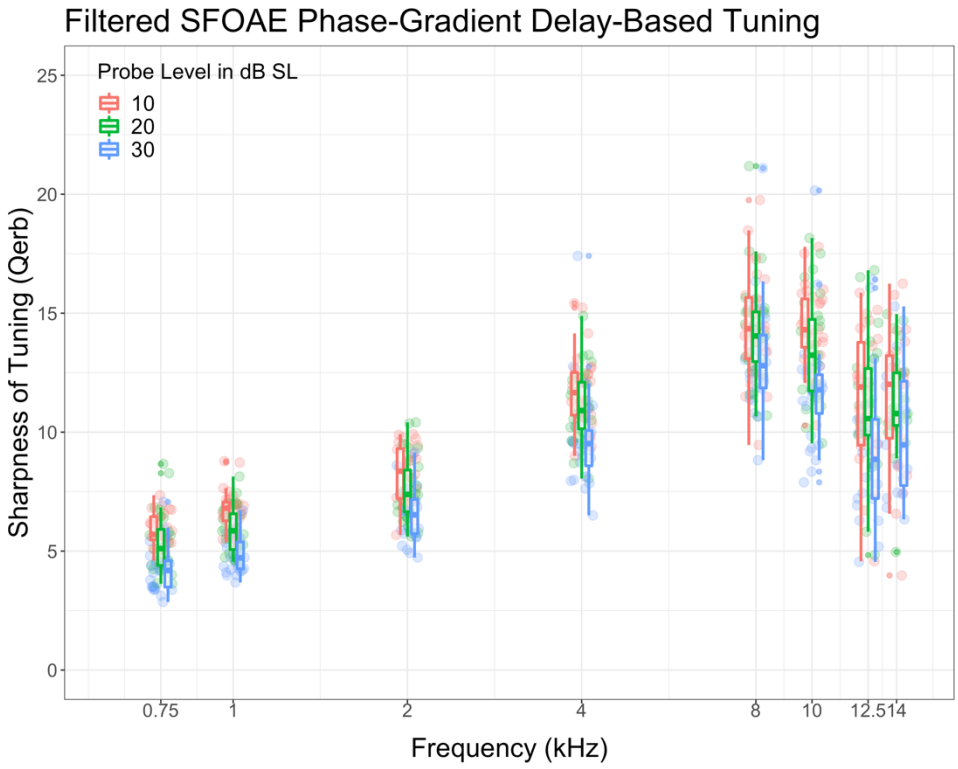

Figure 4.9. Boxplots of filtered long-latency SFOAE delay-based tuning estimates for all three probe levels and all participants. Circles represent data from each individual ear where color represents the probe level in dB SL (sensation level).

4.3.5. Correlation between Behavioral and SFOAE Delay-Based Tuning

Because there was a statistically significant effect of level on SFOAE delay-based tuning estimates, only estimates for 10 dB SL probe levels were used for comparison to behavioral data. When behavioral and SFOAE delay-based tuning were compared using repeated measures correlation analysis, the two tuning measures were found to be strongly correlated ($r(176) = 0.71$, $p < 0.001$). Figure 4.10 shows the correlation between the two measures with all frequencies pooled

together. The regression line was very close to the unity line, suggesting that SFOAEs predicted behavioral tuning quite well; the mean absolute error between the two measures was 2.057.

This correlation was also statistically significant when SFOAE tuning estimates were computed using the Shera & Guinan model ($r(176) = 0.73$, $p < 0.001$), although the SFOAE tuning estimates were much sharper than behavioral tuning. Frequency-by-frequency analyses, however, did not show any correlations as measured by Pearson's product moment correlation coefficients (Figure 4.11). Furthermore, the number of observations were reduced by almost half at 14 kHz, suggesting a limited use of SFOAE based tuning estimates at frequencies where SNR is poor, similar to the findings of I/O data from the previous study (Chapter 3). In contrast to the previous study, which did not have many missing observations from 2 – 8 kHz, the current study had missing data from up to 8 participants. Interestingly, the frequencies with the most data for this study were 1 and 10 kHz, perhaps establishing this study's equivalent of the Goldilocks frequencies for assessing tuning.

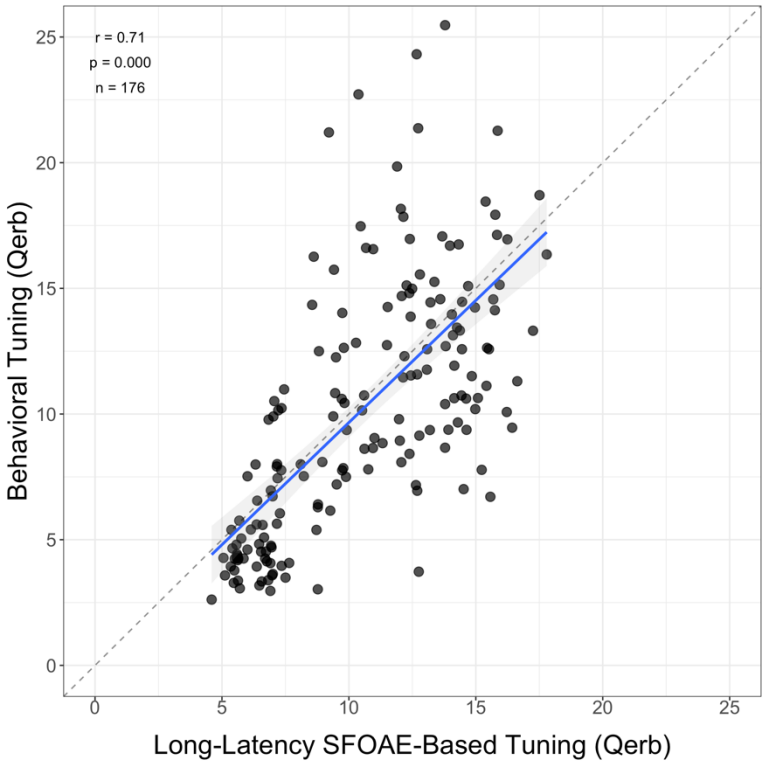

Figure 4.10. Scatterplot of behavioral tuning (Qerb) plotted against SFOAE delay-based tuning (Qerb) pooled across all frequencies. Circles indicate data from each frequency and ear. Solid line indicates the linear fit to the data, whereas dashed line represents unity or hypothetical perfect correlation. r represents the repeated measures correlation coefficient.

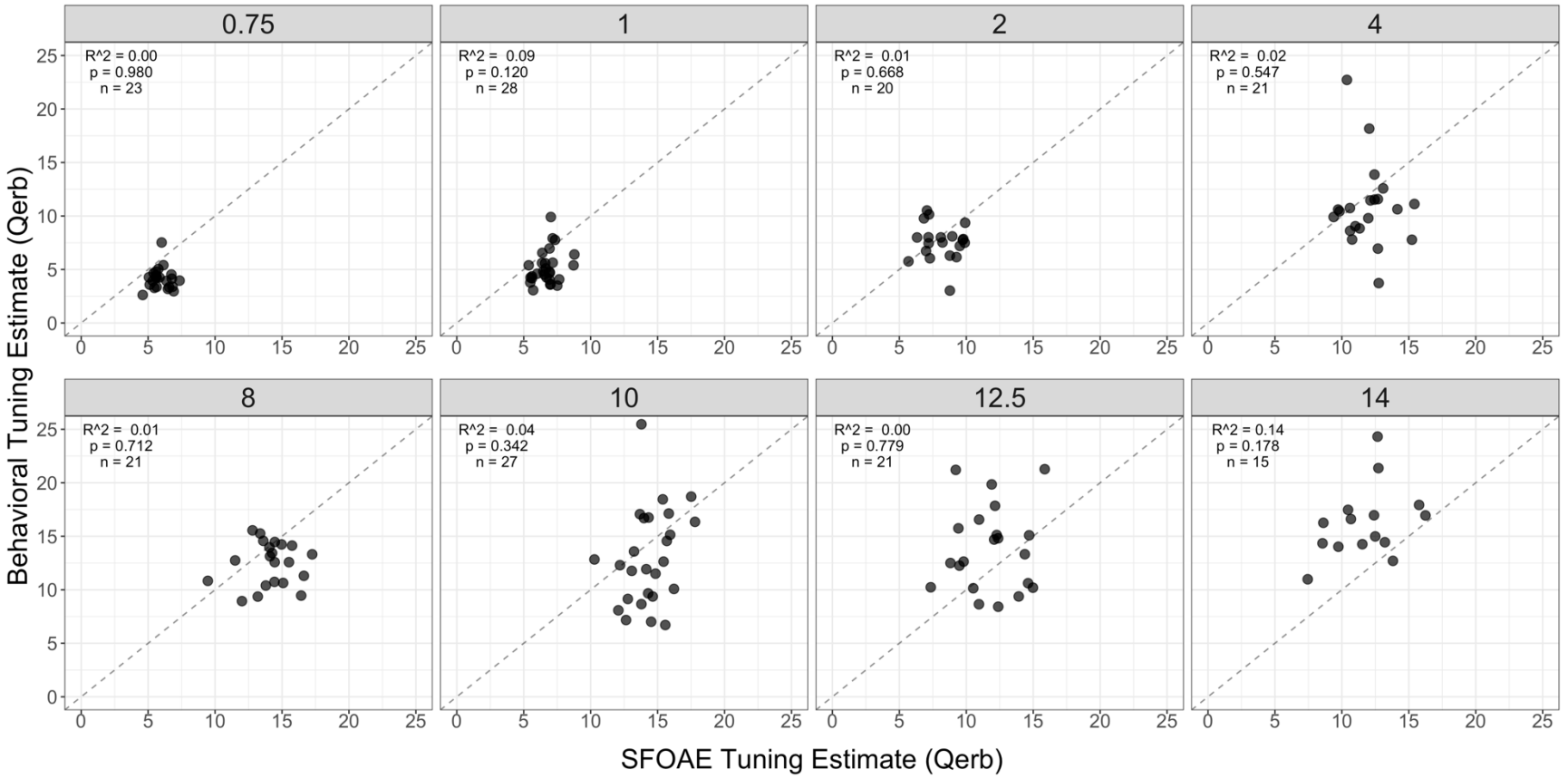

Figure 4.11. Scatterplots of behavioral tuning and SFOAE delay-based tuning for each test frequency. Panel headings indicate the frequency of interest (kHz). Circles indicate data from each individual ear, and the dashed line indicates hypothetical perfect correlation between the two measures. R^2 represents the Pearson's product moment correlation coefficient for each frequency

4.4. Discussion

The purpose of this study was to examine whether SFOAE-based tuning estimates were related to behavioral measures of tuning as a first step towards investigating the clinical utility of SFOAEs for assessing cochlear tuning. Behavioral thresholds, psychophysical tuning curves, and SFOAEs were recorded from 28 ears of normal-hearing adults for center frequencies 0.75, 1, 2, 4, 8, 10, 12.5 and 14 kHz. Both behavioral and SFOAE delay-based estimates showed frequency dependent tuning up to 8 kHz and a plateau above 8 kHz. Furthermore, behavioral estimates of tuning were found to be correlated with the SFOAE delay-based estimates of tuning, albeit only when data across frequencies were pooled together, i.e., individual frequency correlations were not significant. The potential explanations for the current findings, comparisons to previous literature, and implications for phase-based delay measure as a tool for clinical assessment of tuning will be discussed hereafter.

4.4.1. Variability of High-Frequency Psychophysical Tuning Curves

In our sample of normal-hearing individuals, a worsening of behavioral thresholds and tuning as a function of frequency was observed. The variability of high-frequency thresholds among normal-hearing individuals has been previously noted in the literature[257]. On the other hand, studies of high-frequency tuning curves (> 8 kHz) in normal-hearing adults are scarce and limited to a small sample.

Furthermore, to our knowledge, no study has examined the objective correlates of high-frequency tuning curves (> 8 kHz).

Buus et al., (1985) measured psychophysical tuning curves at 13 kHz and above for eight participants (ages 19-34 years) and found a high degree of variability across participants[283]. They attributed the variability in tuning curve sharpness and morphology to reduced audibility for the high frequency probes as well as possible influence of the difficulty in signal calibration at high frequencies[283]. In the current study, the probe tones were calibrated in terms of forward pressure level at the eardrum, in an attempt to mitigate the influence of ear canal acoustics for high-frequency threshold and tuning measurements.

More recently, Yasin & Plack (2005) measured four normal-hearing adults (ages 20-36 years) for 12-17.5 kHz using forward-masking paradigm[286]. Although a forward-masking paradigm was not used in the current study, both Yasin & Plack (2005) and Buus et al., (1985) as well as the current study show a variety of abnormal tuning patterns across individuals[283,286]. The following patterns emerged in this study: 1) sharp tuning curves with slightly elevated tips and slightly elevated thresholds (20-40 dB FPL); 2) sharp tuning curves with significantly elevated tips and elevated thresholds (40-50 dB FPL); 3) irregular, inverted or flat tuning curves with significantly elevated thresholds (exceeding 50 dB FPL). In cases of exceptionally good hearing across the entire frequency range (< 20 dB FPL up to 14 kHz), tuning curves were sharp with sensitive tips up to the highest tested frequency.

A classic study of auditory nerve threshold tuning curves in response to noise- and kanamycin-induced cochlear pathology in cats showed that tuning curve abnormalities were related to the health of both outer hair cells and inner hair cells[287]. Specifically, Liberman & Dodds (1984) examined auditory nerve tuning curves in response to noise-induced damage which affected the stereocilia of both OHCs and IHCs, as well as kanamycin-induced damage which only affected the OHCs presumably leaving the IHC stereocilia intact[287]. They found that total loss of OHCs due to noise damage elevated tuning curve tips, without affecting the tails[287].

This suggested that in addition to providing sensitivity at the characteristic place, OHCs act to decrease sensitivity at frequencies away from the characteristic place[288]. One explanation of this phenomenon is that damage or loss of OHCs could in turn decrease the stiffness of the cochlear partition and increase the mechanical response at frequencies away from the characteristic place[287]. This phenomenon is also correlated with an increase in maximum discharge rate of the auditory nerve fibers of cats in response to acoustic trauma[289]. Studies of noise-trauma in macaque monkeys on the other hand have seen a mixture of OHC, IHC, and/or synaptic loss, resulting in both threshold elevation and broadening of tuning[97].

In the instances where PTCs became inverted or irregularly shaped combined with thresholds exceeding 50 dB FPL, it is unclear whether IHC dysfunction/loss, OHC dysfunction/loss, or a combination of both is present. Although the behavioral tuning paradigms in this study were consistent with patterns of damage seen in animal studies, behavioral paradigms are not able to disentangle OHC loss from

IHC loss, nor make their relative contributions apparent, making them insufficient for differential diagnosis of cochlear pathology in clinical settings.

Additionally, successfully completing the procedure to yield a behavioral tuning curve at high frequencies can be a difficult task, as not all participants were able to complete the task successfully. Furthermore, because of reduced audibility at high frequency regions of the cochlea, behavioral tuning paradigms can result in inverted or irregularly shaped tuning curves as the probe and masker move in and out of regions of good hearing to poor hearing, making it difficult to quantify the tuning at those frequencies. Given the strong correlation between behavioral and SFOAE delay-based tuning, clinical assessment of cochlear tuning for improving diagnostic accuracy and differentiating between sites of dysfunction seems feasible using SFOAE delays.

4.4.2. Variability of SFOAE Phase & Delay Estimates

The phase of SFOAEs and associated delays have long been studied for understanding cochlear mechanics and generation of SFOAEs[222]. The original theory of SFOAE generation via coherent reflections[204] predicts a frequency dependence of the phase-gradient delay, which represents the difference in relative phases between the incident and reflected waves. The relative phases of incident, reflected, and then multiply reflected waves can have a significant effect on the magnitude and phase of the emissions recorded in the ear canal, resulting in fine structure[205,290].

Similar to previous studies, random fluctuations and jumps, sometimes quite large, were observed across ears, across frequencies, and across levels in the current study. The random jumps and fluctuations in phase have been previously shown to be both intrinsic to the emission itself and extrinsic as in its efferent modulation. Siegel et al., (2005) showed that large phase jumps corresponded with deep notches in the level spectra of SFOAEs[222]. Later, Zhao et al., (2015) showed that efferent activation using contralateral broadband noise in humans resulted in frequency shifts in the peaks of SFOAEs, which corresponded with a jump in SFOAE phase[291].

Because of these irregularities in phase obtaining reliable phase-gradient delay based tuning estimates has been a challenge[292]. Some of the fluctuations in phase are a result of poor signal to noise ratio, but the majority of the error is inherent to the OAE itself, presumably due to the contribution from delayed OAE components[292]. Shera & Bergevin, 2012 argue that the "emission itself is intrinsically irregular" consistent with the models of reflection emissions which relate OAE generation to micromechanical irregularities[292]. Nonetheless, the irregularities in phase must be reconciled and have been previously mitigated using several processing strategies including SNR exclusion[285], SNR-weighting[293], and smoothing[223,294].

Shera & Bergevin (2012) compared several different techniques in simulated SFOAEs, first only using post-hoc signal processing strategies on the magnitudes and phase of the SFOAEs, and later using time frequency analyses (including CWT) to examine the phase inaccuracies related to intracochlear reflections[292]. They

concluded that the effect of multiple intracochlear reflections on phase and associated delays are not likely to significantly influence species level comparisons of delays and tuning but are more likely to influence estimates of delays within an ear, particularly in ears with spontaneous emissions[292]. In the current study, effects of multiple intracochlear reflections and contributions from short latency components were reduced by filtering out the main emission component using CWT and deriving the delay estimates that correspond to the frequency-delay function from the cochlear tonotopic place.

Employing the CWT in the current study did not show a significant difference in the physical latencies of SFOAE with increasing stimulus levels, except at frequencies at or below 2 kHz. A distinct break was observed in the individual delays around ~1.5 kHz which has been previously observed in DPOAE phase[249] and SFOAE delays[295]. However, when latencies were expressed in a dimensionless unit Nsfoae (equivalent number of cycles) by multiplying the delay in seconds by the probe frequency, a clear level dependence was seen. That is, lower stimulus levels resulted in longer latencies in cycles than higher stimulus levels.

Modeling the level-dependence of SFOAE phase, Talmadge et al., (2000) showed a flattening of phase with increasing probe levels from 20 to 40 dB SPL and proposed a nonlinear generation mechanism of SFOAEs at high stimulus levels[290]. Goodman et al., (2003) later showed a similar finding of shallower phase with increasing stimulus levels in guinea pig, albeit at much higher stimulus levels of 62 to 86 dB SPL[296]. At the lowest two levels (62 and 68 dB SPL), the phase was quite

similar and varied with frequency as predicted by the linear reflection theory of SFOAE generation[296]. Later, Choi et al., (2008) showed that latencies of human SFOAEs were similar at low stimulus levels of 32, 42, and 52 dB SPL and were lower at 62 dB SPL, suggesting contributions from short-latency components at higher stimulus levels[297]. Perhaps these differences are due to the varying contributions of multiple internal reflections and/or non-CF sources between species.

The level dependence of the dimensionless delay function (delay in number of equivalent cycles [Nsfoae]) has been previously shown by Moleti, Pistilli & Sisto (2017) for 15, 25, 35, and 45 dB SPL for 0.5-5 kHz[295]. The current results extend these findings to a wider stimulus level range (10 - 55 dB FPL) and frequency range (0.5-20 kHz). Taken together, the level and frequency dependence of the dimensionless delays further provide evidence of the extended generation region of the long-latency component as a function of increasing level and the scaling invariance of this component as a function of frequency. However, how these data directly relate to BM and RL responses remains colored with complexity.

4.4.3. Theoretical Relationship between SFOAE Delays & Tuning

At low stimulus levels, SFOAEs are thought to be generated as summed energy from linear coherent reflections arising from or near the peak of the traveling wave[146,198]. Because the cochlea is tonotopically organized and the length of the cochlea for a given species is known, the travel time between stimulus onset

and resonant cochlear response can be computed as the physical delay[298]. In empirical measurements of cochlear vibrations[179,180] and fluid pressure[299], the travel time of the stimulus to its characteristic place is referenced to the stapes vibration[300].

However, since the physical delay cannot be measured in humans, it is instead inferred from the frequency-place map of the cochlea, which predicts shorter delays for high frequency stimuli resonating in the base of the cochlea and longer delays for low frequency stimuli[246]. Furthermore, since the stiffness gradient of the basilar membrane sets up the gross tuning profile of the cochlea and the active and nonlinear cochlear processes help to sharpen this tuning, the non-invasively measured delays as a function of frequency can be related to cochlear tuning[246].

In order to understand this relationship between SFOAE delays and tuning, it is also important to relate the spatial origin of SFOAEs in the cochlea to physiological measurements of the basilar membrane[222,301] or auditory nerve tuning[245,247]. Studies that have examined the spatial extent of SFOAE generation have reported a broader generation region than previously predicted[146,222,285], with multiple reflections as an additional mode of emission generation that could significantly contribute to the measured emission in the ear canal[244].

The updated model of SFOAE generation posits that the spatial extent of SFOAE generation extends slightly basal to the peak region, thereby predicting that the SFOAE recorded in the ear canal will have multiple delays[242,244,284]. Indeed, these multiple delay structures can be observed in the time-frequency analysis of

SFOAEs and TEOAEs[244]. When individual components of the SFOAE are constrained by their characteristic delay cut-offs, the latency derived from the long-latency component yields an estimate of tuning that is reflective of the characteristic region with little influence of additional sources and nonlinear mechanism of generation. The current study leverages the advanced time-frequency analysis techniques described by Moleti et al., (2012) to estimate long-latency SFOAE delays and uses the parameters predicted by the transmission line long-wave model to compute tuning estimates[224,261,302,303].

Since the theoretical relationship between SFOAE delays and tuning has been proposed, two major questions have remained unanswered: 1) what does the delay of SFOAEs indicate regarding the tuning properties of the cochlea? and 2) is this non-invasive estimate of tuning predictive of cochlear status within individual ears, beyond the macro chasm of species-level differences only[245]? The current study aimed to address these gaps by comparing SFOAE delay-based estimates of tuning to psychophysical tuning across a wide frequency range within the same human ears. In this study, there was a strong relationship between the two measures when data across all frequencies were pooled, suggesting that the delays of SFOAEs do in fact relate to the gross profile of tuning across the cochlear length. As for predicting cochlear status within an ear, the current findings certainly add to the current knowledge; however, further investigation in ears with known etiologies of cochlear dysfunction (e.g., in individuals with ototoxicity, noise toxicity or auditory neuropathy) may be warranted.

4.4.4. Comparison to Previous Studies of SFOAE Delay & Tuning

SFOAE delays estimated using the average latency of the long-latency component were only slightly level dependent as seen in Figures 4.6 and 4.7. Moleti & Sisto (2016a) reported on the level dependence of SFOAE delays for 0.5-5.5 kHz in four normal-hearing ears using 15, 25, 35, and 45 dB SPL probe levels and a 55 dB SPL suppressor (see Table 4.1)[284]. The delay estimates, which were obtained using the same time-frequency filtering technique as Moleti & Sisto (2016a), are compared to the delays reported by Moleti & Sisto (2016a) in Table 4.2[284]. In both studies, a level and frequency dependence of delays can be observed, such that delays became longer as frequency and level decreased; however, the delay estimates from the current study (Table 4.2) were generally longer than the estimates from Moleti & Sisto (2016a) (Table 4.1).

Table 4.1. Average delay (ms) of SFOAEs as a function of frequency for four stimulus levels, reproduced from Table 1 of Moleti & Sisto (2016a).

Probe Level	Frequency (Hz)								
(dB SPL)	750	1250	1750	2250	2750	3250	3750	4250	4750
15	15.9	11.1	8.3	7.0	6.1	5.4	5.0	4.7	4.1
25	15.2	10.9	8.1	6.4	5.7	5.2	5.0	4.7	4.0
35	14.6	9.8	7.3	5.8	5.2	4.8	4.7	4.4	4.0
45	13.8	8.9	6.8	5.3	4.7	4.4	4.1	3.8	3.6

Table 4.2. Average delay (ms) of SFOAEs from current study at levels equivalent to Moleti & Sisto (2016a).

Probe Level (dB FPL)	Frequency (Hz)								
	750	1250	1750	2250	2750	3250	3750	4250	4750
12	20.4	14.4	-	-	-	-	-	-	-
22	18.5	13.7	11.2	7.6	6.7	6.1	5.3	4.8	4.2
32	18.3	12.6	10.1	7.9	6.8	5.9	5.2	4.8	4.2
42	16.9	11.1	9.3	7.9	6.4	5.7	5.1	4.6	4.1

Several methodological differences could account for this difference between the two studies. First, the probe levels in the current study were calibrated in forward pressure level and adjusted across individuals based on the participants' hearing thresholds. Second, the recorded SFOAE in the ear canal in dB EPL were also corrected for individual differences in ear canal acoustics. Third, although these stimulus and emission correction methods likely had little influence on the delay estimates, the hearing sensitivity of the individuals from the Moleti & Sisto (2016a) study could potentially greatly influence the delay estimates[284]. Sisto & Moleti (2002) previously showed that TEOAE latencies of individuals with hearing loss were longer than those with normal hearing[304], although this result is not easily interpretable as longer latencies typically indicate sharper tuning. It is possible that the estimates reported by Moleti & Sisto (2016a) are based on exceptionally good hearing of four individual, whereas the current estimates are from a wider range of hearing abilities from 28 participants.

Lastly, the suppressor level used in the current study was higher (70 dB FPL) than Moleti & Sisto (2016a) who used a 55 dB SPL suppressor[284]. Studies of SFOAE suppression have shown that the level of suppressor needed to fully suppress the SFOAE can vary with probe level and suppressor frequency[258,305]. Based on the suppression data, it is expected that a 70 dB FPL suppressor would have achieved complete suppression for the probe levels of up to 55 dB FPL used in the current study.

In the case of a 55 dB SPL suppressor used by Moleti & Sisto (2016a), it is possible that complete suppression was not achieved at their highest probe level of 45 dB SPL, particularly at frequencies above 1 kHz[284]. In the absence of full suppression (either due to suppressor frequency being too far away from the probe or the suppressor level being too low), the source of the SFOAE residual is predicted to shift slightly basal to the characteristic place, thereby reducing the SFOAE latency[306]. Generalizing the conclusions of Moleti & Sisto (2016b)[306] to suppressor level, the higher suppressor level in the current study was likely a more effective suppressor than the 55 dB SPL used by Moleti & Sisto (2016a)[284].

An additional difference between the two studies is the varying frequency resolution of the current study with increasing frequency, whereas Moleti & Sisto (2016a) used a fixed 20 Hz frequency resolution across the entire 0.5-5.5 kHz frequency range[284]. Despite these differences between the current study and Moleti & Sisto (2016a)[284], both studies reported a level and frequency dependence of SFOAE delay-based tuning, consistent with cochlear tuning.

Tuning estimates from SFOAE delays as a function of frequency have previously been related to behavioral tuning in humans, albeit at a limited frequency range[224]. Wilson et al., (2020) compared SFOAE delay-based tuning estimates to simultaneously-masked PTCs at 1 and 4 kHz and found a significant correlation between SFOAE and behavioral tuning at 4 kHz but not at 1 kHz[224]. In the current study, there was a strong correlation between SFOAE-based tuning and behavioral tuning when data across all frequencies were pooled together, suggesting that the two measures can globally assess tuning across the entire cochlear length. However, no significant correlations were found at any individual frequencies, likely due to the restricted range of tuning values at 0.75-8 kHz, frequencies at which thresholds did not vary across participants by more than 20 dB FPL.

The lack of frequency-specific correlations suggests that the relationship between behavioral tuning and objective estimates of tuning at specific frequencies may be complicated for different reasons. At frequencies below 4 kHz, the data clustered together suggesting a lack of heterogeneity in cochlear function and relatively normal hearing and behavioral tuning at those frequencies across participants. At 4 and 8 kHz, although thresholds on average stayed within the normal range, there was greater variability of the behavioral tuning curves compared to lower frequencies and compared to SFOAEs, perhaps due to subtle changes in cochlear function.

At 10 kHz and above, threshold and tuning variability both increased dramatically, extending the range over which the correlations could be explored and

signifying a greater degree and heterogeneity of cochlear dysfunction across ears. Consistent with this hypothesis, a greater number of observations were lost at 12.5 and 14 kHz, due to the lack of measurable SFOAEs, difficulty in task performance for PTCs at high frequencies, and/or incomputable tuning estimates from abnormal PTCs.

In the current study, the mean behavioral Q_{erb} values of 5.16 and 10.85 at 1 and 4 kHz, respectively, which were similar to values reported previously by Wilson et al., (2020) (7.31 and 9.67 at 1 and 4 kHz, respectively)[224]. However, SFOAE Q_{erb} values cannot be directly compared to the Wilson et al., (2020) study, due to the methodological differences in probe levels, stimulus calibration, and higher mean age of the participants in the current study (27.55 years vs 22.4 years)[224].

Although SFOAE-delay based tuning estimates above 8 kHz have not been previously investigated in humans, Wilson et al., (2021) reported highly variable tuning estimates above 8 kHz using the level ratio functions of distortion product otoacoustic emissions[307]. It was speculated that the higher variability of the DPOAE level ratio functions at high frequencies, also observed in rhesus monkeys[308] and primates[309], could be related to cochlear outer hair cell dysfunction. The current study validates the Wilson et al., (2021) findings and provides evidence for their hypothesis regarding poorer cochlear function in the base, as seen by poorer hearing thresholds at 10, 12.5, and 14 kHz in the current study.

Despite poorer hearing thresholds at frequencies above 8 kHz, behavioral tuning estimates continued to increase up to 14 kHz (Figure 4.2), perhaps because

estimates from tuning curves whose shapes were irregular or inverted could not be computed and therefore, excluded from group analysis. In other words, since these observations were excluded, the means continued to increase, rather than decreasing again above 8 kHz. These findings suggest that behavioral tuning metrics may not be affected unless there is significant hearing loss.

For example, tuning curves are significantly altered for dead regions, i.e., regions of complete cochlear hair cell loss[281,310], but slight damage or dysfunction of hair cells can sustain sharp frequency tuning with some loss of sensitivity[287]. On the other hand, SFOAE delay-based tuning estimates declined at 10 kHz and above, suggesting that while behavioral tuning may not be sensitive to slight yet diffuse damage, SFOAEs may in fact be more sensitive at those frequencies. The gold standard for assessing frequency tuning at ultra-high frequencies remains elusive.

4.4.5. Comparison to Other OAE-Based Tuning Measures

Previously, one approach for assessing cochlear tuning using SFOAEs has been to measure the suppression tuning curves (STCs) in an iso-response paradigm. In this method, the suppressor level needed to sustain a criterion level of SFOAE residual is plotted as a function of suppressor frequency. Studies of SFOAE STCs have shown variable effects of probe frequency and level[305], likely due to the difficulty in measuring STCs, particularly at high frequencies. Despite these difficulties, Keefe et al., (2008) reported that SFOAE STCs were similar to behavioral tuning estimates of simultaneously masking paradigms[305,311].

In another study, Charaziak, Souza & Siegel (2015) reported that behavioral tuning curves were normal for participants with slight to mild and mild to moderate hearing loss at the probe frequencies of 1 and 4 kHz, but their SFOAE suppression tuning curves (STC) could not be measured[225]. Based on this observation and the large inter- and intra-subject variability they observed in the SFOAE-STCs in their earlier study[258], the authors concluded SFOAE-STCs may not be a clinically useful tool for assessing tuning.

Another measure of tuning using distortion products in response to two tones has been previously investigated. Wilson et al., (2021) recently investigated the iso-input tuning of DPOAE levels plotted as a function of f_2/f_1 ratio at f_2 = 0.75 to 16 kHz and found that mean Q values doubled from 1 to 8 kHz with means increasing from ~5 to ~10, for the lower probe levels of 52/37 dB FPL[307]. Slightly higher values of Q were seen in the current study, likely due to the single tone SFOAEs compared to the two tones in the Wilson et al., (2021) study. However, in both studies, the Q nearly doubles from 1 to 8 kHz[307].

Although Wilson et al., (2021) separated the distortion component from the total DPOAE in the ear canal to estimate the cochlear tuning of the f_2 region with little contributions from the $2f_1$-f_2 place, there was a moderate correlation between DPOAE based tuning and behavioral tuning[307]. In contrast, the current findings showed a strong correlation between SFOAE delay-based and behavioral tuning, likely due to similar equivalent intracochlear levels between the two measures in the current study compared to the Wilson et al., (2021) study[307].

Here the phase-gradient delay of SFOAEs to estimate cochlear tuning was utilized rather than SFOAE STCs and DPOAE level ratio functions. Unlike previously investigated OAE-based measures of tuning, phase-gradient delay estimates have properties that could be clinically useful, e.g., they are easy to measure, are highly repeatable across and within individuals with normal hearing [224], are not influenced by the effects of two-tone suppression[312], and are sensitive to cochlear status as indirectly assayed by OAEs (as seen by flat phase at frequencies with poor signal to noise ratio). However, how this measure can be utilized in the context of a clinical test battery remains to be investigated.

4.4.6. Clinical Implications for Assessing Tuning using SFOAE Delay

The current behavioral findings demonstrate that individual ears exhibited a variety of tuning patterns at high frequencies depending on the amount of hearing loss present and the presumed underlying cause of the hearing loss. This finding on its own calls for a revised protocol for assessing cochlear status of individuals with perceptual speech perception deficits but have clinically normal hearing. However, the clinical protocols used currently for diagnostic assessment of auditory function do not include a measure of auditory tuning.

The findings of the current study suggest that SFOAE delay based tuning measures may be an easy and objective alternative to psychophysical tuning curves that require up to 2 hours for one frequency in a traditional laboratory paradigm[274]. Because the current study was limited to understanding the relationship between

SFOAE and behavioral tuning in normal hearing individuals, it remains to be investigated how SFOAE delay-based tuning measures may be affected in individuals with different etiologies of hearing loss. If selective inner hair cell loss or dysfunction can be differentiated from outer hair cell or dysfunction using SFOAE-based measures of tuning, either independently or in combination with other objective measures, future diagnosis and monitoring of hearing loss may be ameliorated.

The current study was motivated by the discrepancies between audiometric testing and perceptual difficulties reported by individuals who have difficulty understanding speech in noise. Although the current study further supports the need for precise diagnostics, additional research is needed to understand the specific contributions of cochlear function to everyday listening abilities, particularly at high frequencies.

4.5. Conclusions

The current study aimed to understand the relationship between SFOAEs and behavioral estimates of frequency tuning across a wide range of frequencies in clinically normal-hearing adults. Building upon previous findings, the frequency- and level-dependence of SFOAE based tuning estimates was consistent with the tuning properties of the cochlea and further related to the frequency-dependent behavioral tuning. The findings warrant additional investigation of the type and

degree of dysfunction affecting cochlear tuning particularly in the high-frequency base of the cochlea and the associated costs for everyday perceptual abilities.

CHAPTER 5

Stimulus Frequency Otoacoustic Emissions in Early Auditory Aging

5.1. Introduction

Age-related hearing loss (ARHL) affects 1 in 3 adults over the age of 65 years[20,117], making it a common chronic health condition among older adults. The most recent hearing report from the World Health Organization estimates that by 2050, a staggering 900 million people worldwide will suffer from a disabling hearing loss[18]. Over the years, ARHL has been regarded as an inevitable and unpreventable condition that can only be treated once it is functionally manifested, as listening difficulty in an individual's everyday life, and clinically manifested, as a measurable hearing loss in audiometric assessments[44].

Although ARHL has been historically known to be a condition affecting older adults over the age of 65, evidence suggests that ARHL may be present as early as the fourth decade of life, when compared to pristine ears (age 10-21 years) [21-23,145]. New evidence linking ARHL and cognitive decline[31,120] has sparked a drive to prevent, detect, and treat ARHL sooner. Furthermore, new molecular therapeutic options for restoring hearing loss would require that ARHL is a) differentially diagnosed from other types of hearing loss so that therapeutics are targeted to the appropriate cellular structures and/or pathways, and b) detected sooner so that protective therapeutics can be administered as early as possible[42,47,48,134]. Because ARHL typically originates in the cochlea[80], the earliest signs of ARHL may be

detected using sensitive measures of cochlear function, such as otoacoustic emissions (OAEs). OAEs are byproducts of the nonlinear cochlear processes related to the activity of the outer hair cells (OHCs).

Because of their direct relationship to OHCs, OAEs are a sensitive tool for detecting OHC changes due to various cochlear insults and for differentially diagnosing ARHL[8,158,188,313,314]. Several lines of investigation suggest that different types of OAEs are better suited for different clinical purposes. For example, Lapsley-Miller et al., (2004) showed that in individuals with temporary and permanent threshold shifts, distortion product otoacoustic emissions (DPOAEs) are not as affected as transient evoked otoacoustic emissions (TEOAEs)[158], perhaps due to contributions from synchronized SOAEs. Furthermore, TEOAEs are thought to be more sensitive to mild hearing loss compared to DPOAEs[233,315]. More recently, patterns of TEOAE SNRs have even been related to audiometric patterns of ARHL due to various pathologies[316].

Much less is known about the relationship between ARHL and OAEs evoked using low level pure-tones, i.e., stimulus frequency otoacoustic emissions (SFOAEs). Although TEOAEs are thought to arise via the same reflection mechanism as SFOAEs[317], TEOAEs are evoked using broadband stimuli which stimulate broad regions of the cochlea[318]. SFOAEs are thought to be more frequency-specific than TEOAEs[319] and generated via a single mechanism compared to the dual-mechanisms of DPOAEs[320].

Over the years, SFOAEs have been studied extensively in normal-hearing and hearing-impaired individuals[13,197,203,223,224,241,244,253,321,322]; however, the sensitivity of SFOAEs to early age-related changes in cochlear function has not been fully characterized[14,23].

Abdala, Ortmann & Shera (2018) measured DPOAEs and SFOAEs in 77 humans (ages 18-76 years) for frequencies up to 8 kHz and reported that SFOAEs were not as sensitive to aging as DPOAEs[14]. While DPOAE levels were dramatically reduced across all frequencies in middle-aged and older-adult groups compared to young-adults, SFOAE levels were only reduced in the highest frequencies (2-8 kHz) [14], suggesting DPOAEs are a better diagnostic tool for detecting hearing loss. When hearing loss was removed as a variable and only subjects with normal-hearing were considered (see Figure 9 of reference), a clear aging effect can be seen for both types of emissions, albeit the slope of DPOAE decline with age is much steeper[14]. Nonetheless, the notable variability of both DPOAE and SFOAE levels in normal-hearing participants ages 42 years or younger warrants further investigation.

In another investigation, Abdala, Luo & Guardia (2019) measured SFOAEs in newborns and found that SFOAE levels and apical/basal transition frequencies were similar[215], but SFOAE phase gradient was much steeper in newborns compared to adults from a previous investigation[216]. A steeper phase gradient is associated with longer SFOAE delays, where the phase-gradient delay is theoretically related to cochlear tuning[224,285,323]. Therefore, the finding of sharper cochlear tuning in newborns compared to adults, despite similar levels requires

further investigation regarding the relationship between SFOAE phase-gradient delays and tuning.

In addition to SFOAE levels and delays, the high-frequency extent, or bandwidth, of SFOAEs as a function of age have not been previously studied. High frequency SFOAEs (>8 kHz), corresponding to regions first affected by cochlear aging, largely remain uninvestigated in adults[23,197] as well as in children[215,324]. Stiepan et al., (2020) recently reported on SFOAE levels from 0.75 – 18 kHz in participants as young as 10 years and as old as 68 years of age}[23]. They found that mean SFOAE levels decreased with each increasing age group for frequencies up to 6 kHz}[23]. At 8 kHz and above, all age groups showed similar SFOAE levels that mirrored the rising noise floors for those frequencies}[23]. In light of these findings, it remains to be determined whether high-frequency SFOAE measurements without artifact are feasible and more importantly, whether they can be useful in identifying age-related dysfunction in the cochlear base.

Therefore, the purpose of this study is to investigate how SFOAEs change with age across the first five decades of life in a cross-sectional examination of 9-45 year olds up to the highest frequency of human hearing. Because SFOAEs arise from cochlear activity, the sensitivity of SFOAE levels, tuning estimates, and bandwidths to cochlear aging was tested.

5.2. Methods

The study was performed at the Auditory Research Laboratory at Northwestern University in Evanston, Illinois over the course of 1.5 years from November 2019 – March 2021. Participants were recruited from Northwestern University campus and the greater Chicago metropolitan area via flyers and word-of-mouth or through the Communication Research Registry (STU00070769 [PI – Molly Losh]). Participants younger than 18 years of age were also recruited through the Child Studies Group registry (STU0020141 [PI – Tina Grieco-Calub]).

Adult participants provided informed consent to participate in the study procedures. Minor assent and parent permissions were obtained from participants younger than 18 years old and their parent/guardian. Participants were compensated monetarily for their participation in the study. All study procedures were approved by the Institutional Review Board at Northwestern University (STU00000295).

Note: Data collection was paused from March 2020 to August 2020 due to university closure in response to the COVID-19 global pandemic and did not resume until it was deemed safe for human research by the Institutional Review Board at Northwestern University. All participants recruited after March 2020 were screened for COVID-19 symptoms before they were allowed to participate in the study.

5.2.1. Participants

Participants were 68 normal-hearing individuals (48 females, 20 males) between the age of 9 and 45 years (M = 29.79, SD = 9.62). Participants were required to meet the following inclusion criteria: 1) normal otoscopic examination consistent with a healthy ear canal and an absence of any ear abnormalities, excessive cerumen, or foreign body in the ear canal; 2) normal middle ear function as characterized by a Type A tympanogram with peak compliance within 0.3-1.4 mmhos for adults and 0.2-0.9 mmhos for pediatrics[226]; 3) normal-hearing as defined by pure-tone thresholds of ≤ 20 dB HL across standard audiometric frequencies of 0.25, 0.5, 1, 2, 3, 4, 6, 8 kHz[61] in at least one ear. Participants were excluded from the study if they had excessive cerumen in the ear canal, abnormal middle ear function, or failed the pure-tone screening in both ears.

5.2.2. General Procedures

Each participant was screened using otoscopy, tympanometry, and pure-tone audiometry to determine if they met the inclusion criteria. Following screening, participants were comfortably seated in a reclining chair in a sound-treated booth that met the ANSI standard for ambient noise levels[325]. Behavioral thresholds were obtained using a modified Békésy tracking method at 21 frequencies from 0.125-20 kHz[22] and at additional frequencies in 1/18-octave steps chosen individually for each participant, typically above 8 kHz (additional description of these measurements is included in section 5.2.3.). At frequencies for which the participants did not respond

at even the maximum limit of our equipment, an artificial threshold of 105 dB FPL was used.

SFOAEs were collected in short sweeps spanning 0.375-20 kHz using two probe levels of 30 and 36 dB FPL and a suppressor level of 70 dB FPL. In order to avoid any practice or learning effects, frequencies were split into four sets of behavioral frequencies and corresponding frequency sweeps for SFOAE measurements. Frequency sets were randomized using a random sequence generator, and the order of measurements (SFOAEs vs behavioral) was counterbalanced across participants.

5.2.3. High-Resolution Corner Frequency Threshold Measurements

After obtaining a complete tracking threshold audiogram at standard frequencies, thresholds around the corner of the audiogram were measured in 1/18 octave steps. These will be referred to as the high-resolution frequencies. First, the start frequency, i.e., the lower end of these high-resolution frequencies, was determined as the lowest of three consecutive frequencies where thresholds do not change by more than 5 dB. Second, the stop frequency, i.e., the higher end of the high-resolution frequencies, was determined as the frequency at which threshold exceeds 60 dB FPL. Thresholds were measured in 1/18 octave steps between the start and stop frequencies. Finally, the behavioral corner frequency was manually picked by multiple raters using a custom written MATLAB program.

The raters were blinded to the age of the participants. An intra-class correlation showed excellent repeatability of raters across participants (ICC3k (67, 134) = 0.92, $p < 0.001$ for behavioral thresholds). In short, the analysis program gathered all the behavioral thresholds for both standard audiometric frequencies as well as high-resolution frequencies. If multiple thresholds were obtained at a single frequency (to assess reliability of measures), the thresholds were averaged. Next, the thresholds were interpolated in 100 Hz steps between 6 and 20 kHz to obtain a smoothed threshold curve using a MATLAB spline smoothing method. The smoothed threshold curve was useful as raters picked the corner frequency of the thresholds. The raters were instructed to pick the corner frequency for each participant as the lowest frequency where thresholds increased precipitously, and the threshold slope was steep. The corner frequencies from multiple raters were averaged.

Additional metrics from the interpolated behavioral thresholds were obtained automatically. These included the frequency at which behavioral thresholds intercepted 30 dB FPL (the lower SFOAE probe level), 36 dB FPL (the higher SFOAE probe level), 18 dB FPL, and 60 dB FPL (the end frequency of the audiogram). Two additional metrics were calculated from the corner and end frequencies and their corresponding thresholds to yield the slope of the audiometric decline in dB/Hz and dB/octave.

5.2.4. Stimulus Frequency Otoacoustic Emissions (SFOAEs)

SFOAEs were recorded for probe levels of 30 and 36 dB forward pressure level (FPL), where probe frequencies (f_p) were swept in 1/4 octave segments spanning 0.375-20 kHz. Suppressor frequency (f_s) was always 47 Hz lower in frequency than f_p and 70 dB FPL. The sampling rate was 96,000 samples/second. For each frequency sweep, 16 sets of ear canal pressure recordings were made, where each set consisted of four stimulus blocks: probe alone, probe with suppressor, probe alone, and probe with suppressor inverted in phase. First, an average pressure waveform was computed by summing together recordings split into two buffers. The recordings from odd and even buffers were subtracted to get the noise floor waveform. The average waveform was then split so that the probe only blocks and probe plus suppressor blocks were separated. The SFOAE residual was then computed by subtracting the probe plus suppressor waveform from the probe only waveform.

Models of probe and suppressor were created separately in a least-square-fit (LSF) based analysis using custom phase functions. The analysis window (t_{win}) was fixed at 3000 samples or 31 ms to provide a reasonable estimate of high frequency emissions while preserving fine structure at lower frequencies[321]. Magnitude and phase of emission, probe, and suppressor were determined as the estimates with the least RMS error across analysis windows. SFOAE level and phase from the LSF analysis were then used in the wavelet analysis according to the methods described

in Chapters 2 and 3. SFOAE phase gradient delays and tuning estimates were also computed according to the methods described in Chapters 2 and 4.

5.2.5. SFOAE Bandwidth Analysis

Following wavelet filtering, the long-latency SFOAE levels were plotted as a function of frequency for both probe levels. To ensure data quality, only SFOAEs with noise floors below 0 dB SPL and SNR > 3 dB were included in the corner frequency determination. The SFOAE bandwidth determination was performed in MATLAB using a custom program as described herein. The spectra were first down sampled to a frequency resolution of 100 Hz to match the interpolated frequency resolution of behavioral thresholds. The spectra were then smoothed using a robust loess method in MATLAB with a constant smoothing span of 150 points across spectra to match the number of observations in the behavioral threshold corner frequency analysis.

Following the smoothing, median emission and noise floor levels were computed. If the median LL SFOAE level was greater than or equal to 0 dB EPL and the median noise floor levels were less than or equal to -10 dB EPL, the following bandwidth metrics were extracted: 1) first, the end frequency (F_{end}) of the SFOAE spectrum was determined as the highest frequency where the smoothed LL SFOAE levels were at least 9 dB above the smoothed noise floor; 2) the corner frequency (F_c) was manually picked by a rater as the frequency at which LL SFOAE levels drop precipitously.

If the median LL SFOAE level was below 0 dB EPL or the median total noise floor was greater than -10 dB EPL, the programmed determined that the quality of the data were too poor to pick a corner frequency. Unfortunately, only 4 spectra met the quality criteria established based on the LL SFOAE level and total noise floor, therefore, F_c could not be determined for 64 participants and was assigned a 0. Only F_{end} was computed in these cases. If the smoothed LL SFOAE and smoothed noise floor did not show at least 9 dB SNR (n = 11 out of 64), the F_{end} was also assigned a 0.

5.2.6. Statistical Analysis

Correlations between measures were investigated using cor.test function and effects of individual predictors on outcome variables were investigated using generalized linear regressions (glm) and analysis of variance (aov) in the {stats} package in RStudio (version 1.2.5033). A principal component analysis was also performed using the {stats} package and results of the PCA were extracted using the {factoExtra} package. A secondary analysis using logistic regression was performed using the glm function. Statistical significance was established at alpha levels of $p < 0.05$.

5.3. Results

Behavioral thresholds and SFOAEs at fixed probe levels of 30 and 36 dB FPL were collected from 68 participants between the age of 9 and 45 years. Participant demographics are shown in Figure 5.1, which shows that the majority of the participants were white females within the 18-35 age range. As seen in Figure 5.1, there was roughly equal male/female distribution for ages 35 and older, slightly more females in the 18-35 years age group and slightly fewer females in the 9-12 years age group.

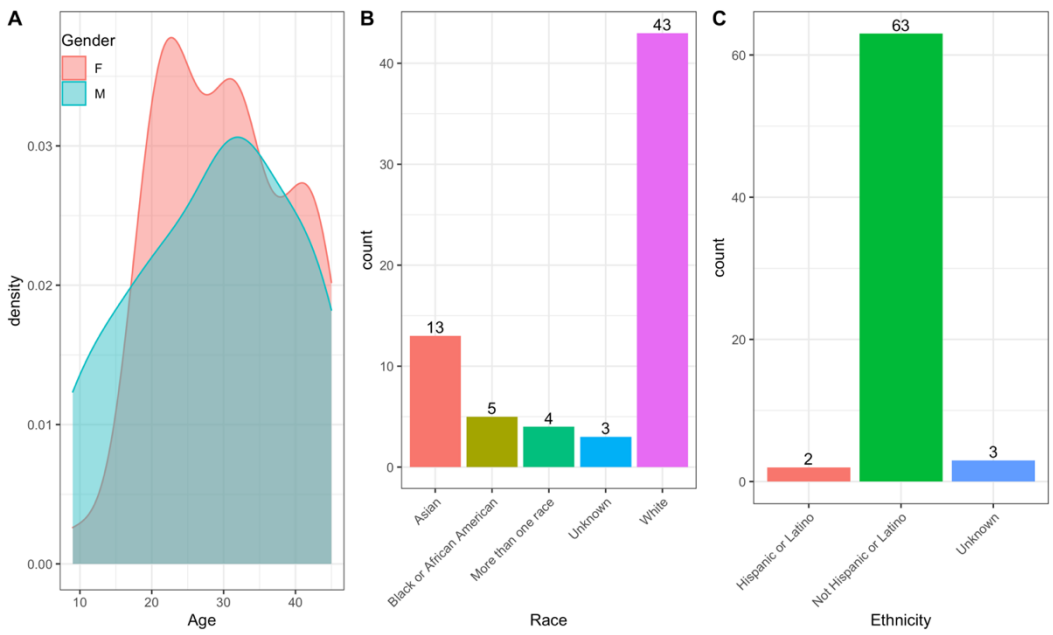

Figure 5.1. Participant demographics for all 68 individuals including gender, age, race, and ethnicity. Panel A shows the gender distributions as a function of age (years). Panel B plots the number of individuals who selected the given responses for race, whereas Panel C plots the number of individuals with given responses for ethnicity.

5.3.1. Behavioral Thresholds Across Age Groups

Figure 5.2 shows the mean behavioral thresholds and 95% confidence intervals as a function of frequency for all age groups. Average thresholds were similar across all groups up to 6 kHz. Compared to the youngest group, the oldest group displayed poorer thresholds by 8.0 dB at 8 kHz, 29.8 dB at 10 kHz, 50.2 dB at 12.5 kHz, 75.9 dB at 14 kHz, and 59.6 dB at 16 kHz. The youngest group (9-12 y.o.) displayed the greatest sensitivity (best thresholds) up to 20 kHz; however, the variability in thresholds was also the largest due to the small number of ears tested compared to the other three age groups. Above 6 kHz, the oldest group displayed thresholds poorer than the 18-25 y.o. group by 9.2 dB at 8 kHz, 12.6 dB at 10 kHz, 25.7 dB at 12.5 kHz, 44.1 dB at 14 kHz, and 44.4 dB at 16 kHz. The data also demonstrate that average thresholds declined as a function of frequency above 6 kHz for the oldest group and above 12.5 kHz for the youngest three groups. However, the corner frequency, i.e., the frequency at which high-frequency thresholds increased dramatically, was variable across individuals within and across groups.

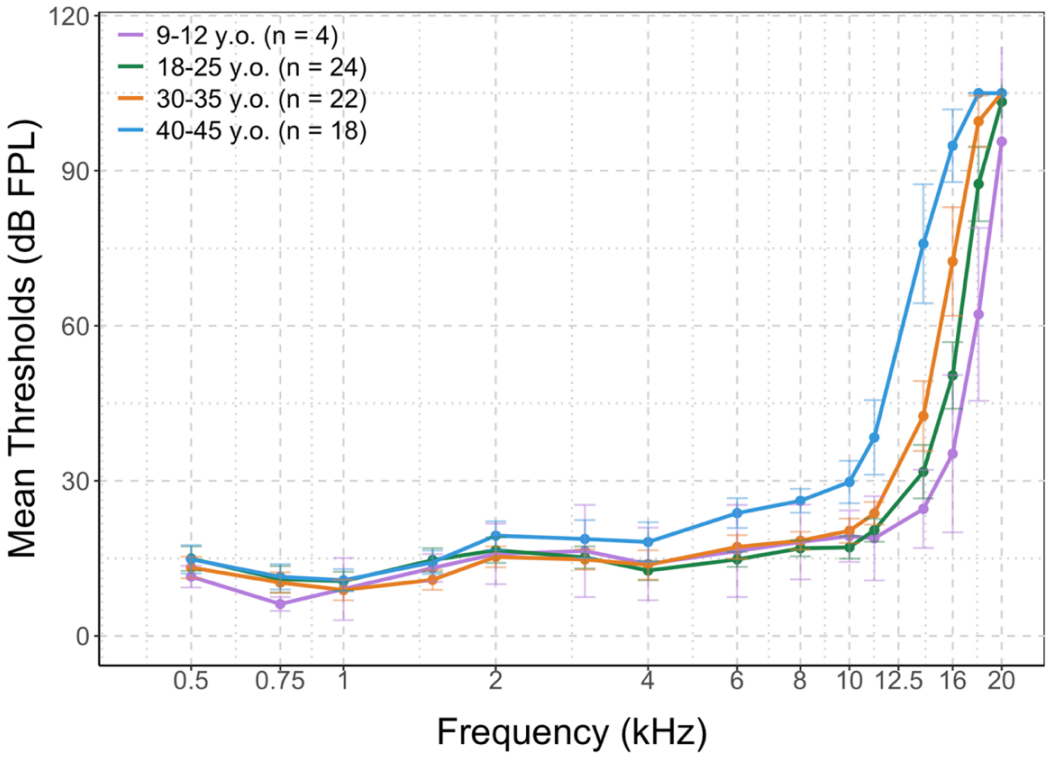

Figure 5.2. Behavioral Thresholds as a function of frequency averaged across all participants in each age group. Individual symbols represent the means, whereas error bars indicate 95% confidence interval for each age group represented by color (key in legend).

5.3.2. SFOAE Levels Across Age Groups

Even though behavioral thresholds were similar up to 4 kHz across groups (Figure 5.2), total SFOAE levels for both probe levels were different across groups, with the highest levels in the youngest age group at 1-4 kHz. (Figure 5.3). This difference was even more pronounced for the filtered long-latency SFOAEs (Figure 5.4). Despite these group differences, there was a large amount of variability noted in the filtered SFOAE levels across all age groups (Figure 5.5). Figure 5.5 shows the trend for lower long-latency SFOAE levels in the oldest group from 2 to 8 kHz and a trend for higher levels below 2 kHz. The effect of age on SFOAE levels was

statistically tested using multiple linear regression models with and without age as the continuous predictor variable, while controlling for repeated measures variables – frequency and probe level. The analysis of variance of the two models showed a significant effect of age group ($X^2(1, 2) = 57.133$, $p < 0.001$). Finally, Figure 5.6 shows the short-latency SFOAE levels as a function of frequency and age group, which did not show significant differences between age groups, except at ~1.5 kHz at 36 dB FPL for the youngest age-group. In this study, short-latency components were defined similar to Mertes & Goodman (2013) as SFOAEs with shorter than predicted latencies[326], although Sisto et al (2013) have also defined short-latency and long-latency components within the main reflection component[261].

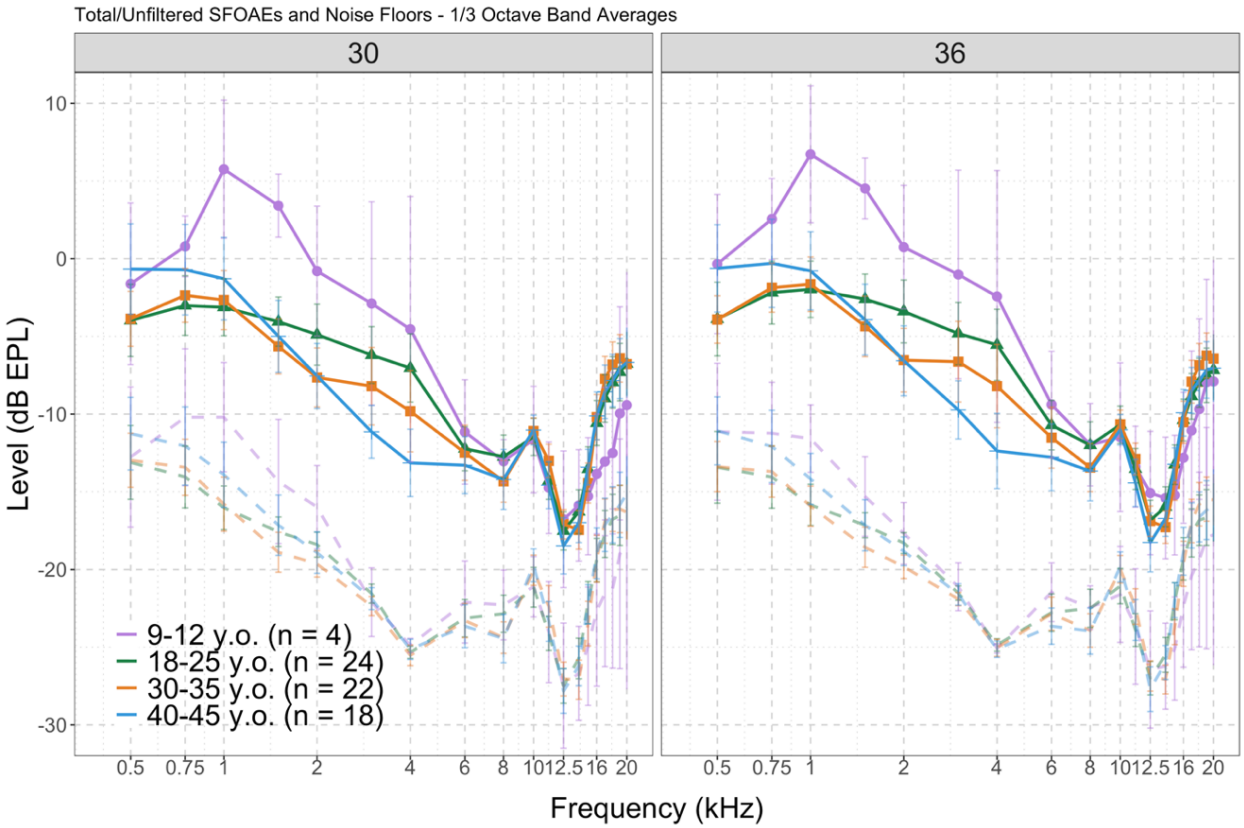

Figure 5.3. Total/Unfiltered SFOAEs as a function of frequency plotted by age group for both 30 and 36 dB FPL probe levels. Filled symbols connected by solid lines indicate the mean 1/3-octave band SFOAE levels in dB EPL for each frequency and each age group as indicated by color for 30 dB FPL (left) and 36 dB FPL (right). Dashed lines represent the average 1/3-octave band noise floor. Error bars represent the 95% confidence interval.

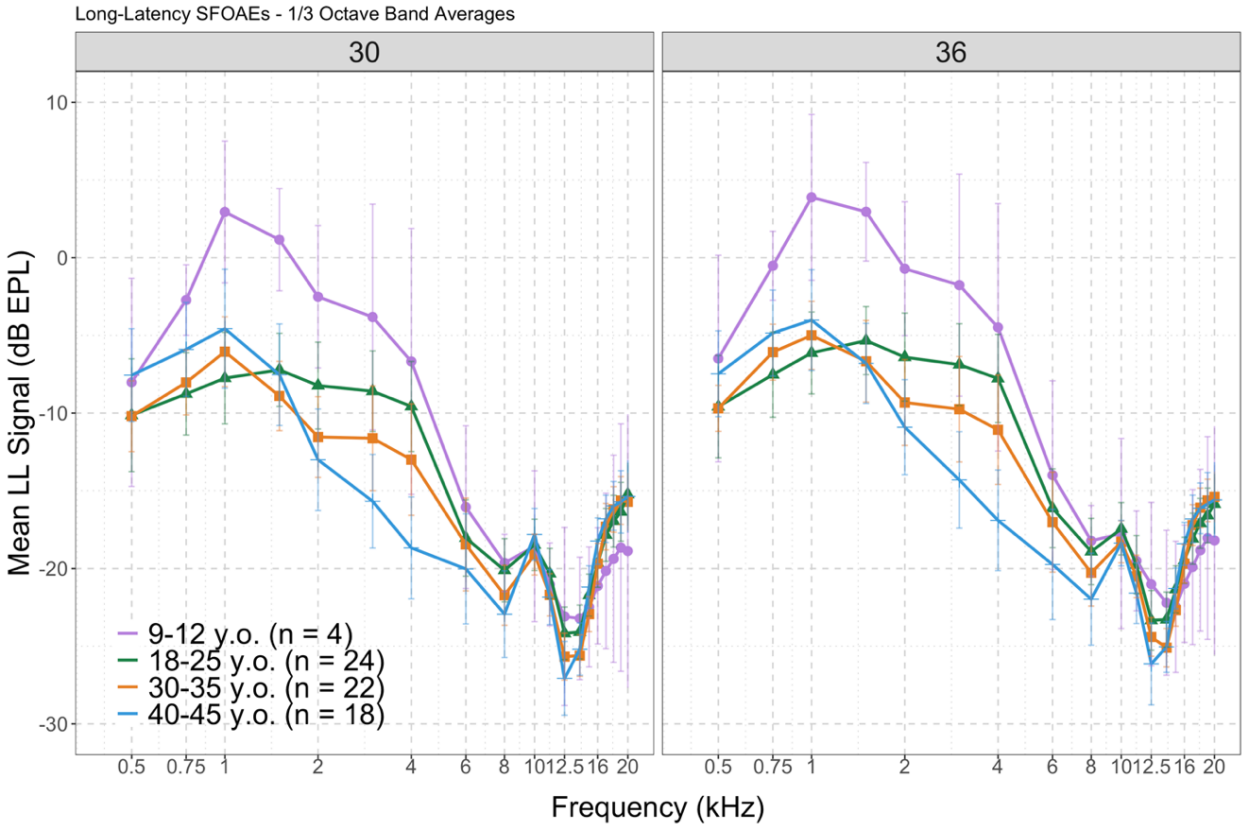

Figure 5.4. Filtered Long-Latency SFOAEs as a function of frequency for all four age groups and both probe levels. Filled symbols connected with lines indicate the mean filtered SFOAE levels for 30 dB FPL (left) and 36 dB FPL (right), whereas error bars indicate 95% confidence interval of the mean.

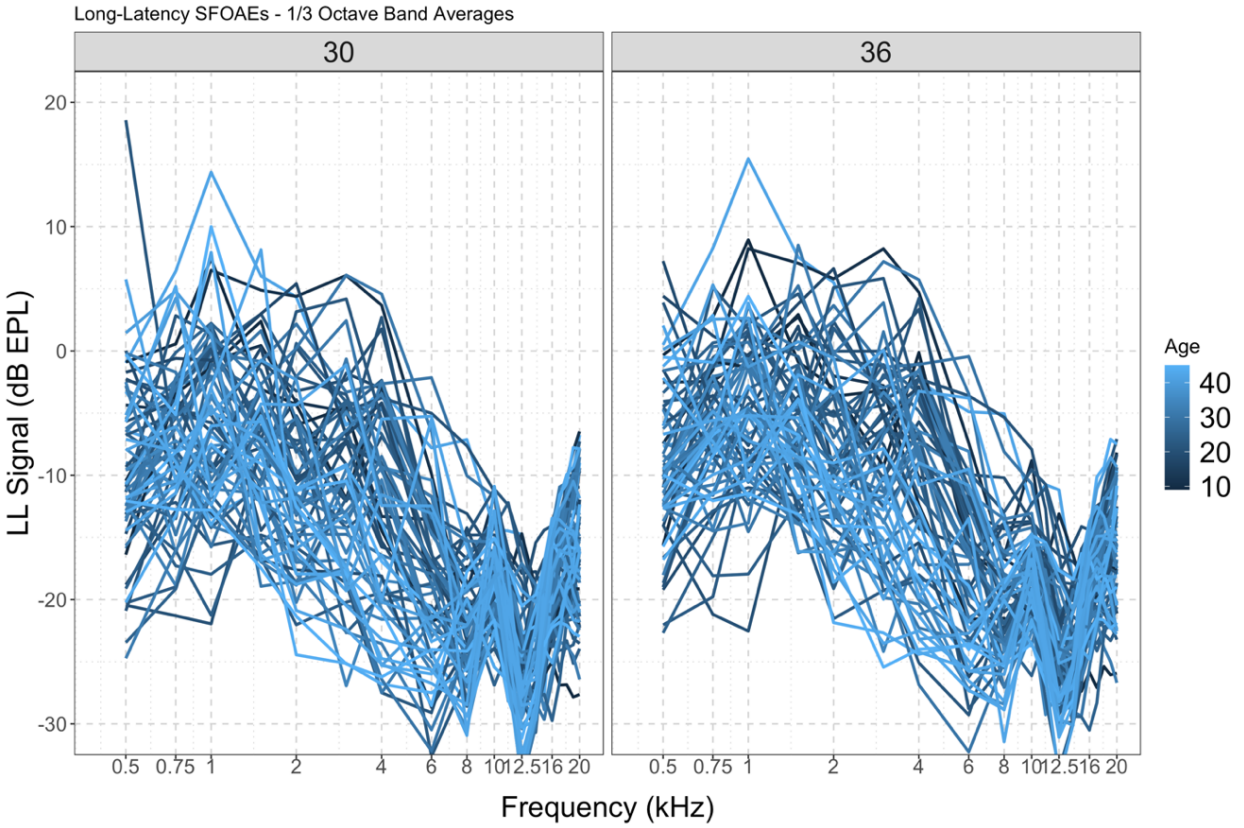

Figure 5.5. Filtered Long-Latency SFOAE levels plotted as a function of frequency and age in years for both probe levels. As indicated by the legend, dark lines represent younger participants which gradually lightened as a function of increasing age in years. Data from 30 dB FPL probe are presented in the left panel, whereas data from 36 dB FPL probe are in the right panel.

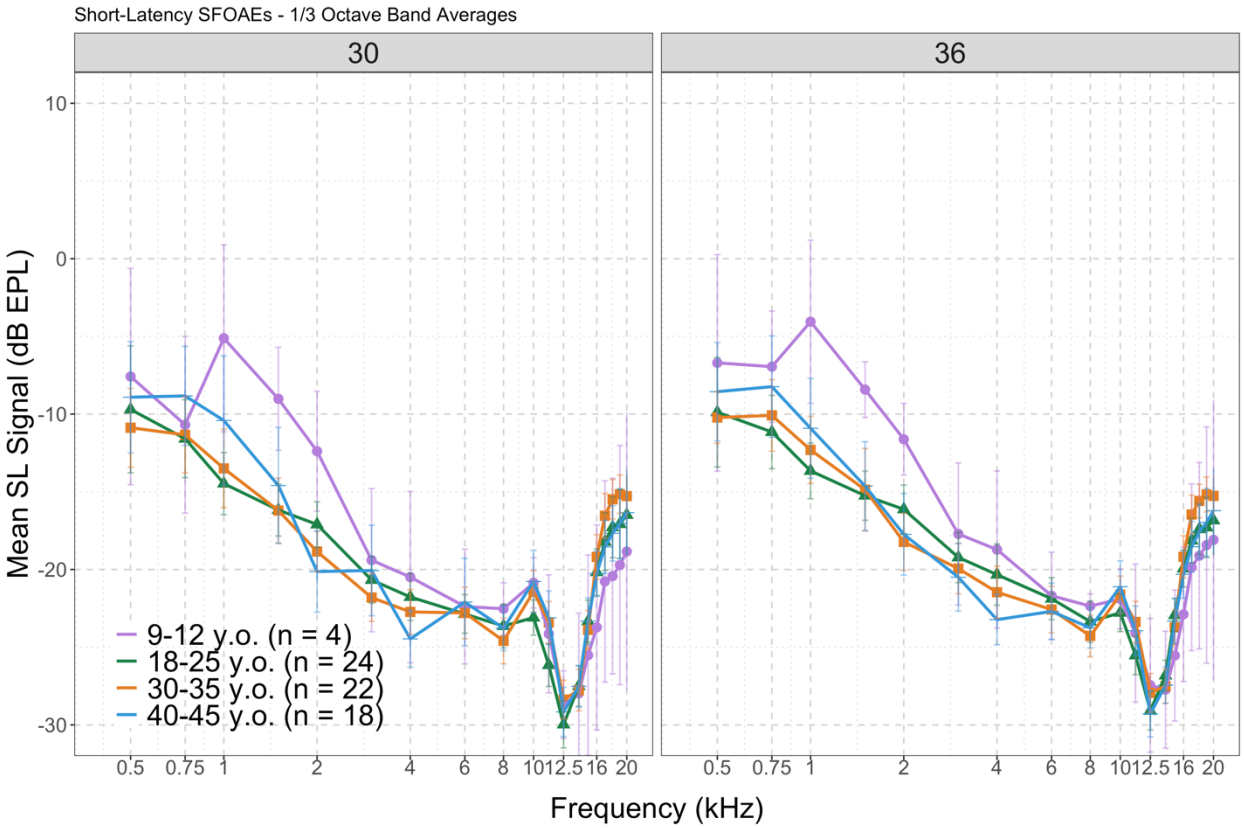

Figure 5.6. Filtered Short-Latency SFOAE levels plotted as a function of frequency for all age groups. Filled symbols connected with lines indicate the mean filtered SFOAE levels for 30 dB FPL (left) and 36 dB FPL (right), whereas error bars indicate 95% confidence interval of the mean.

5.3.3. SFOAE Delays and Tuning Across Age Groups

Next, the delays of the long-latency component of SFOAEs as a function of frequency were investigated, which showed that delays were not different across age groups except at 0.5 kHz at 36 dB FPL for the youngest age group (Figure 5.7). This was also true when delays were plotted in dimensionless units N_{sfoae} (Figure 5.8). There was a trend for slightly longer delays with increasing stimulus levels up to 8 kHz. Across all age groups, there is an abrupt change in the delays around ~1

kHz; however, regression models with and without age groups were not significantly different from each other for delays (Figure 5.7 and 5.8) or for tuning estimates computed from the delays (Figure 5.9). Although delays and tuning estimates were not significantly different between groups, the tuning estimates demonstrate a slight trend for sharper tuning in the youngest age group only. As seen with previous delay-based estimates, tuning increased from 1-8 kHz but declined and plateaued at frequencies > 8 kHz. For all measures, variability was greatest for the youngest group, likely due to the very small number of ears tested (n=4).

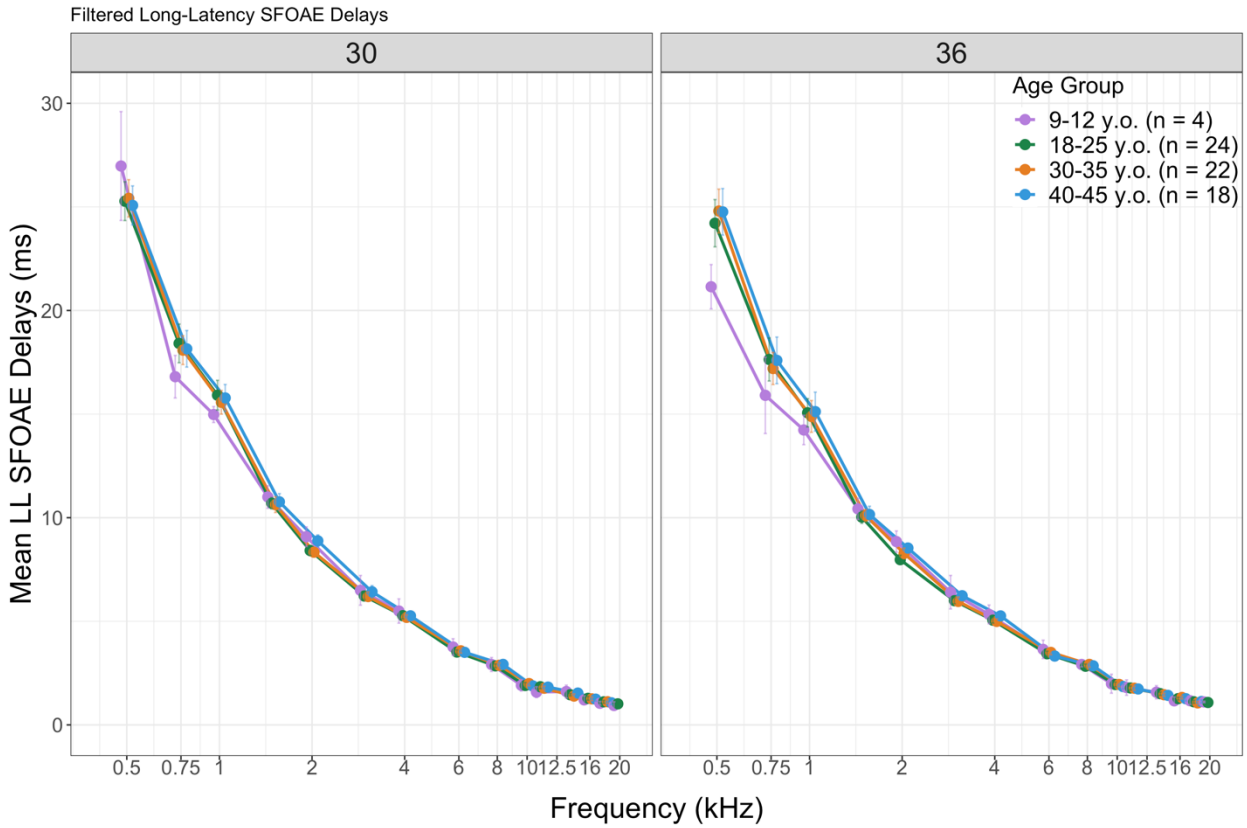

Figure 5.7. Delays computed from the inverse FFT of the long-latency component for all age groups and both probe levels. Symbols connected by lines represent the mean delays (ms) for each age group (color key in legend) for probe levels of 30 dB FPL (left) and 36 dB FPL (right). Error bars indicate the 95% confidence interval of the mean. Points slightly jittered for better visualization.

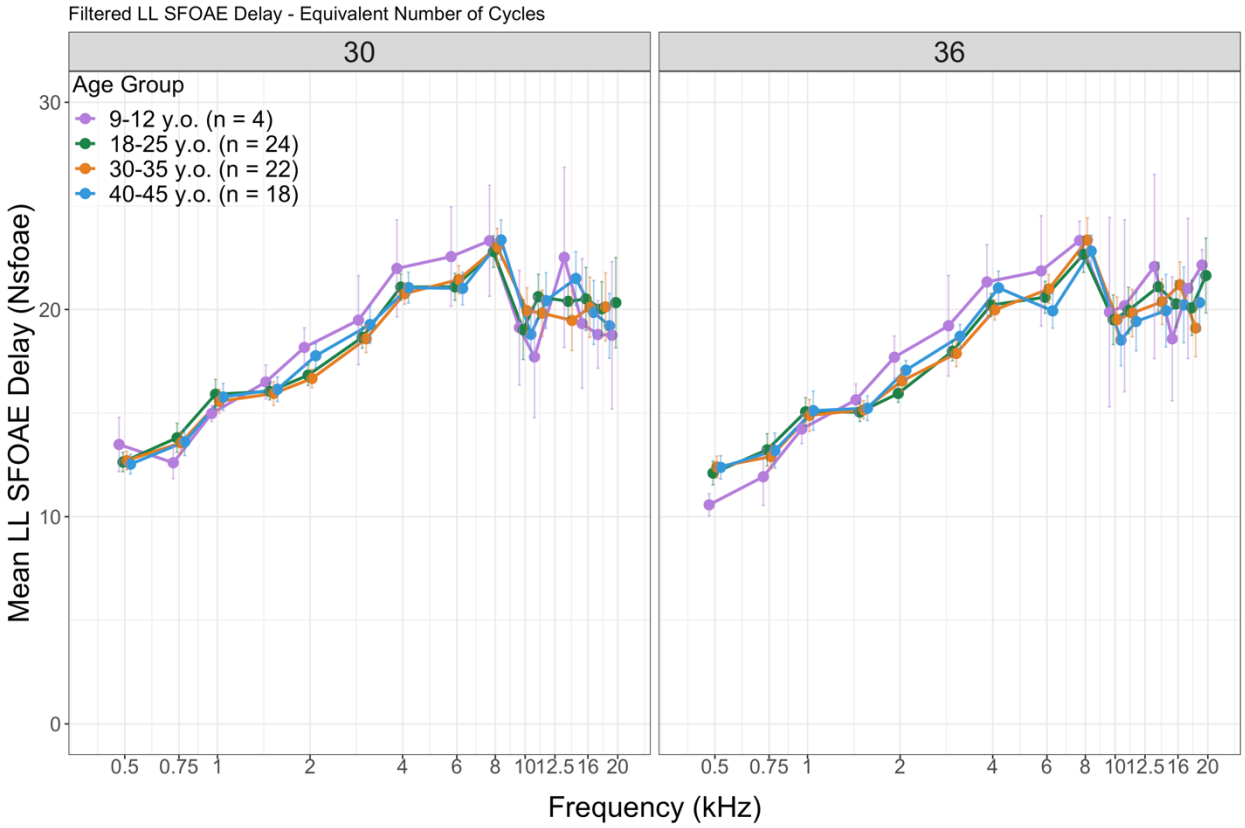

Figure 5.8. Delays expressed in equivalent number of cycles by frequency (N_{sfoae}) across all age groups and both probe levels. Filled circles connected by lines represent the mean delays (N_{sfoae}) for each age group (color key in legend) for probe levels of 30 dB FPL (left) and 36 dB FPL (right). Error bars indicate the 95% confidence interval of the mean. Points slightly jittered for better visualization.

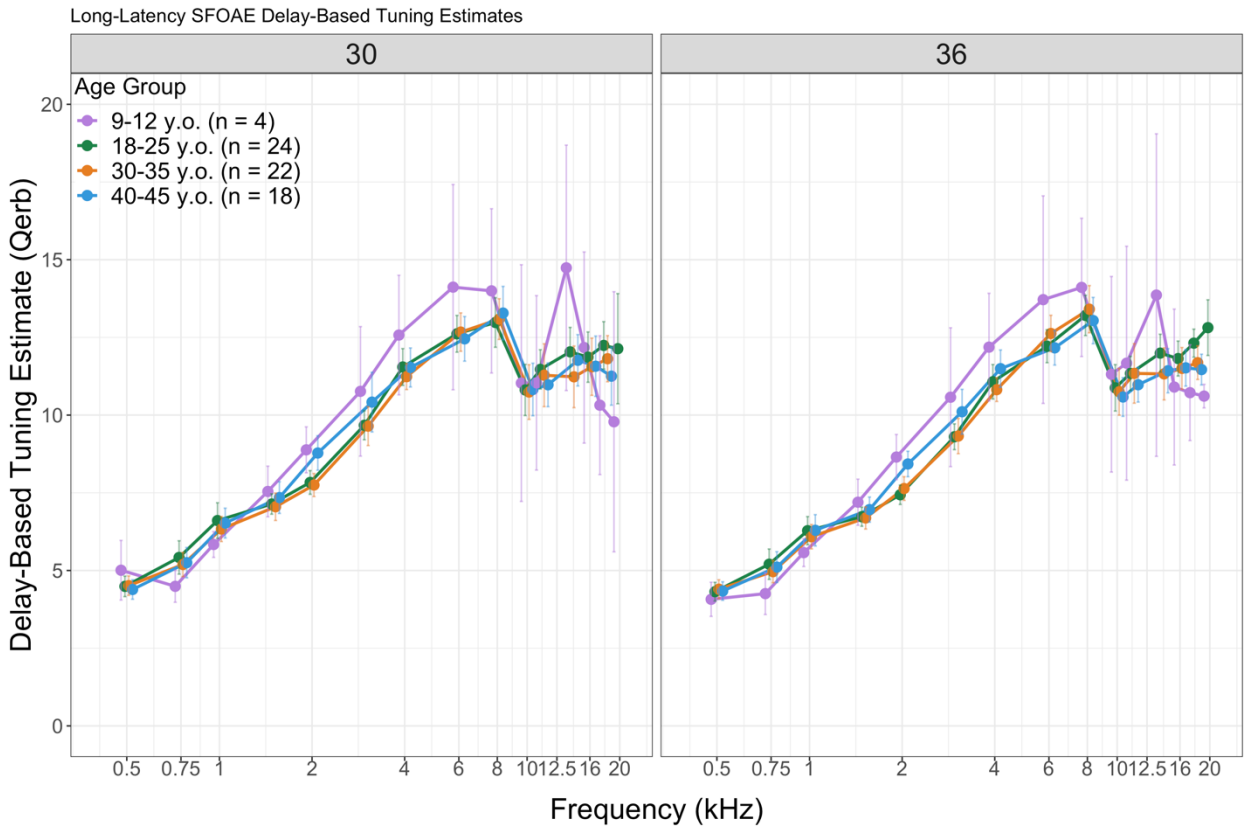

Figure 5.9. Delay-based tuning estimates from the long-latency SFOAE component as a function of frequency for all four age groups and both probe levels. Points slightly jittered for better visualization.

5.3.4. Threshold & SFOAE Bandwidth Across Age Groups

An analysis of the high frequency extent of behavioral thresholds and SFOAE levels was conducted to assess whether changes in cochlear function are concomitant with changes in behavioral thresholds as a function of age. Only the 36 dB FPL corner was chosen for the comparison to behavioral corner frequency; the values will be compared in the Discussion section to Dewey & Dhar (2017b) who also used the 36 dB FPL probe levels in their study[197]. Figure 5.10 demonstrates an example of the SFOAE corner frequency analysis, showing that the smoothed and

original LL SFOAE levels decline around ~7 kHz and fall into the noise floor completely around 10 kHz. Of the 4 spectra analyzed for the SFOAE corner frequency, three showed a corner frequency between 6 and 7 kHz, whereas the fourth showed a much higher corner frequency ~12 kHz.

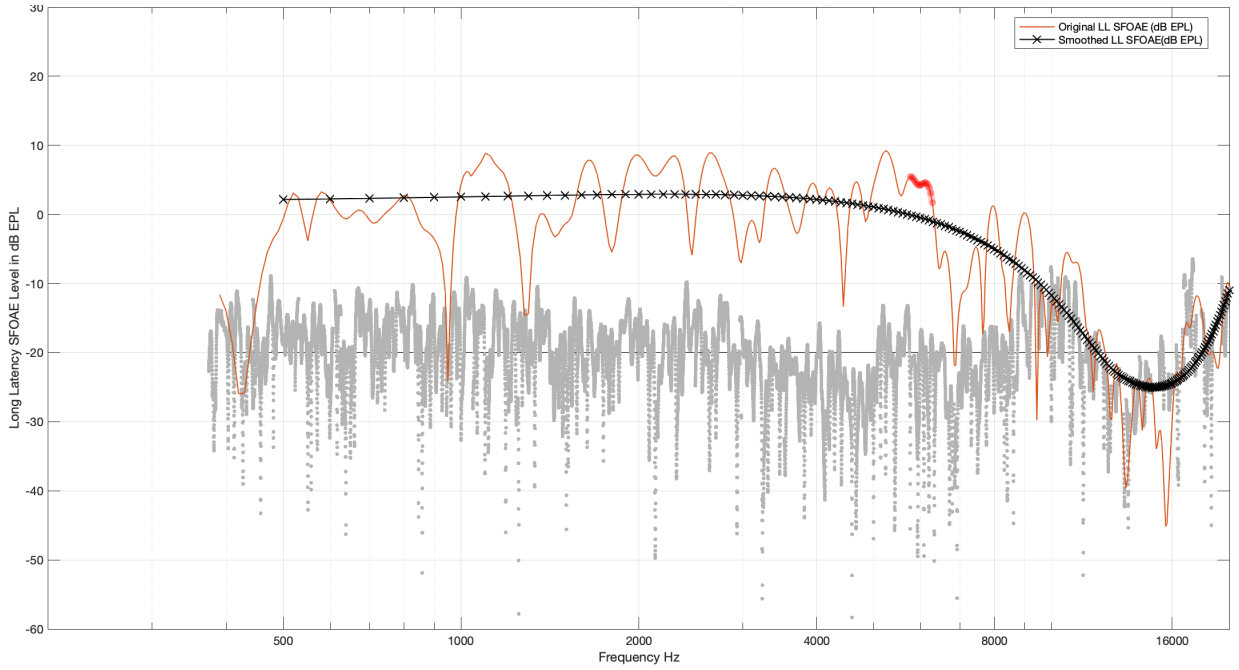

Figure 5.10. Example of SFOAE corner frequency analysis for participant UWSF017CL. Red curve represents the original long-latency SFOAE levels (dB EPL) plotted as a function of frequency (Hz). The black symbols connected with a line represent the smoothed SFOAE over 150 points in 100 Hz steps. The red symbols indicate the frequencies selected as the corner frequencies where both the original and smoothed responses begin to decline. Gray symbols indicate the total SFOAE noise floor in dB EPL.

In addition to the corner frequency, another bandwidth metric was extracted from SFOAEs. The end frequency of SFOAEs (F_{end}), defined as the highest frequency with a 9 dB SNR, was compared to the behavioral corner frequency (Figure 5.11). In contrast to the corner frequency which could only be determined in

4 participants, F_{end} was computed for 57 out of 68 individuals (the remaining 11 participants did not have 9 dB SNR at any frequency). On the other hand, behavioral threshold corner frequencies were measurable in all 68 participants. The behavioral threshold corner frequencies established the behavioral bandwidth of hearing as referred to hereafter.

As shown in Figure 5.11, behavioral bandwidth was highest in the youngest group (~13 kHz) which declined with each age group with the lowest ~9.5 kHz in the oldest age group. Post-hoc comparisons performed using generalized linear regression and contrast coding showed that groups A, B, and C were not significantly different from each other, but group D was significantly different ($t(116) = -2.948$, $p = 0.004$). The mean slope of the behavioral corner frequencies was 91.57 dB/octave in the youngest group and 79.07 dB/octave in the oldest age group.

Analysis of variance showed that there was a main effect of measure (SFOAE vs. behavioral: $F(1,106) = 148.251$, $p < 0.001$)) and age groups ($F(3,106) = 6.472$, $p < 0.001$) on this bandwidth metric, but no significant interaction between measure and group ($F(3,106) = 0.239$, $p = 0.869$). Additional comparisons of the SFOAE bandwidth frequency to various behavioral landmarks are shown in Figure 5.12. As can be gleaned from Figure 5.12, SFOAE F_{end} was only weakly correlated with the behavioral corner frequency ($r(55) = 0.294$, $p = 0.026$), but SFOAE end frequency was much more strongly correlated with the 18 dB FPL-intercept ($r(36)= 0.515$, $p < 0.001$) and the 36 dB FPL-intercept of behavioral thresholds ($r(55) = 0.375$, $p =$

0.004). However, there were fewer behavioral thresholds that could be interpolated to the 18 dB FPL threshold (n = 38) compared to 36 dB FPL (n = 57).

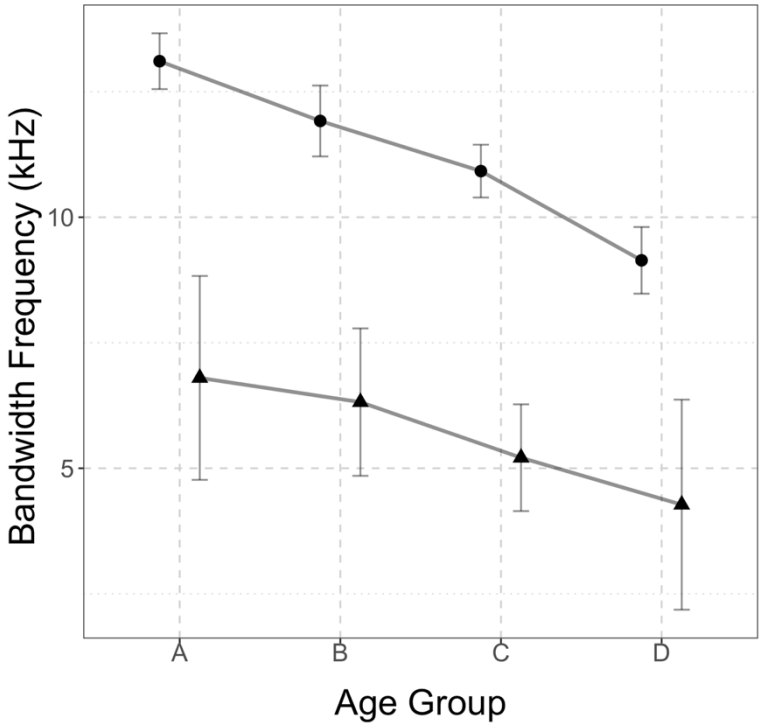

Figure 5.11. Bandwidth of SFOAEs and Behavioral Thresholds by Age Group. SFOAE bandwidth was defined as the highest frequency where SNR is 9 dB. Behavioral bandwidth was defined as the corner frequency of the high-resolution behavioral audiogram. Average SFOAE bandwidth frequency (filled triangles) and average behavioral bandwidth (filled circles) are plotted for each age group. Error bars indicate the 95% confidence intervals.

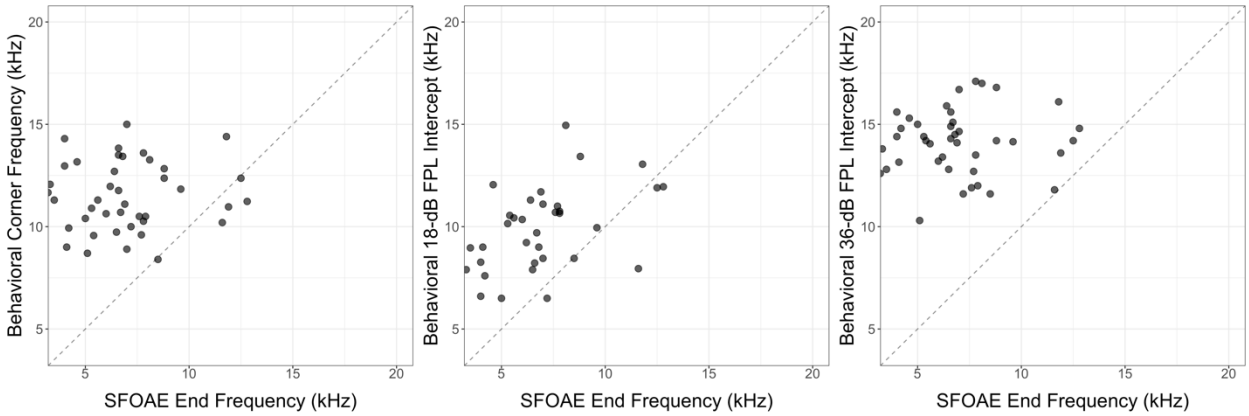

Figure 5.12. Scatterplots of Behavioral Threshold Corner Frequency, 18- and 36- dB FPL Intercepts Plotted against SFOAE End Frequency for All Participants. Scatterplots show the relationship between SFOAE end frequency (kHz) to behavioral threshold corner frequency (left), behavioral 18-dB FPL intercept frequency (middle), and behavioral 36-dB FPL intercept (right). Filled circles represent data from one individual. Note that due to increasing hearing thresholds as a function of frequency and age, the 18 dB FPL intercepts could only be computed for 38 participants. Corner frequency and 36-dB FPL intercepts for 57 participants for whom SFOAE F_{end} could be computed are shown. In all panels, the dashed line represents unity.

5.3.5. Principal Component Analysis (PCA)

In order to better understand the relationship between behavioral thresholds and SFOAE levels, tuning, and bandwidth across different age groups, a principal component analysis was performed using the following variables: frequency, age, behavioral thresholds, SFOAE levels, SFOAE-based Q_{erb}, and SFOAE F_{end}. The results of this analysis showed that Q_{erb}, thresholds, and frequency clustered together, and the first two components explained a total of 74.6% of the variance in the data. When SFOAE-based tuning variable was removed from the PCA model, the variance explained by the first two components improved to 79.5%. Because this model explained more variance and tuning was not significantly different across age

groups, the PCA model with the fewer variables was retained. The variable correlation plot for this analysis (Figure 5.13) shows that the first component explains 47.5% of the variance in the data, whereas the second component explains an additional 32% of the variance.

The figure also shows that SFOAE levels were negatively correlated with frequency and behavioral thresholds, where the latter two were positively correlated. Age was also a significant factor in the second component, which was negatively correlated with the SFOAE end frequency (F_{end}). The outputs of the PCA are shown in Table 5.1 which shows the eigenvalues and variances for each component and in Table 5.2 which shows the contribution of each variable in each component of the PCA expressed in percentage. As seen from these outputs, frequency, SFOAE levels, and behavioral thresholds were the main factors contributing to the first component, whereas age and SFOAE F_{end} were the significant contributors in the second component.

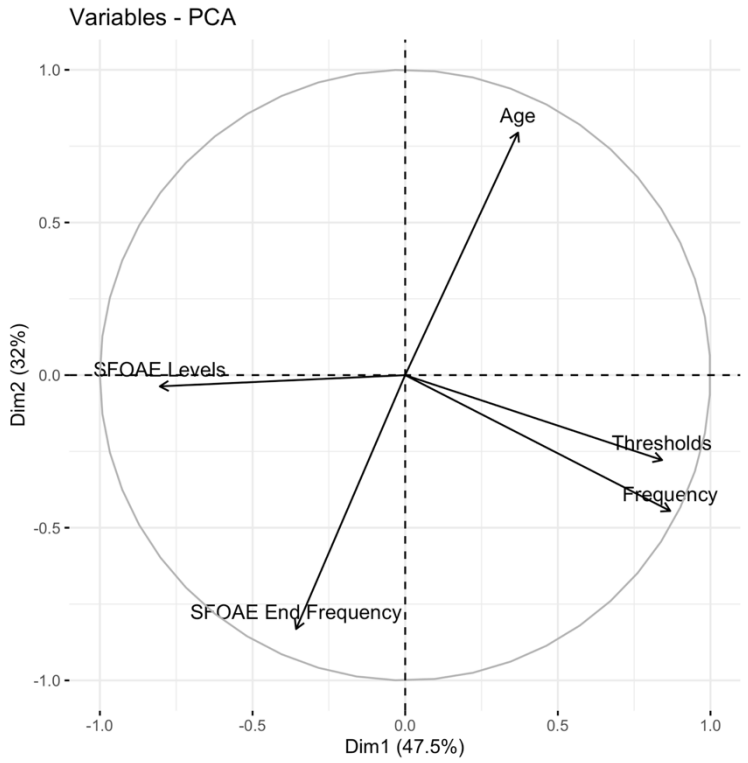

Figure 5.13. Variable Correlation Plot for PCA. Component 1 labeled as Dim1 and its variance are represented on the x-axis and Component 2 labeled as Dim 2 and its variance are shown on the y-axis. The vector length or distance between each variable and the origin represents the relative weight of each variable in that component, where further away from the origin is interpreted as greater influence on the component loadings.

Table 5.1. Eigenvalues, Individual Variance, and Cumulative Variances of the PCA Components

	Eigenvalue	Variance Explained (%)	Cumulative Variance Explained (%)
Component 1	2.373	47.456	47.456
Component 2	1.600	32.997	79.453
Component 3	0.598	11.965	91.419
Component 4	0.345	6.906	98.324
Component 5	0.084	1.676	100.00

Table 5.2. Contributions (%) of Variables Loaded in Each PCA Component

	Comp 1	Comp 2	Comp 3	Comp 4	Comp 5
Frequency	31.778	12.376	0.217	0.023	55.606
Age	5.760	39.456	18.009	35.764	1.011
SFOAE Levels	27.232	0.085	51.347	10.488	10.849
Thresholds	29.847	4.841	27.417	7.097	30.798
SFOAE F_{end}	5.383	43.242	3.010	46.628	1.737

5.3.6. SFOAE Levels & Phase Across Hearing Groups

Because age did not load in the first component and behavioral thresholds did, a secondary analysis splitting the data into better hearing and worse hearing groups based on median split of behavioral threshold averages for frequencies up to 4 kHz (frequencies that did not show significantly different thresholds across age groups). SFOAE levels, $Q_{erb,}$ and F_{end} were examined after splitting the data by hearing group (Figure 5.14), which showed higher SFOAE levels, similar Q_{erb}, and higher SFOAE F_{end} in the better hearing group compared to worse hearing as determined by the pure-tone average (PTA). The worse hearing group based on PTA consisted of 29 participants with a PTA range of 12.8 to 23.0 dB FPL, whereas the better hearing group consisted of 28 participants, with a PTA range of 5.8 to 12.5 dB FPL. A logistic regression was conducted with hearing group as the outcome variable and SFOAE levels, Q_{erb}, and F_{end} as the predictor variables. Based on this analysis, only SFOAE F_{end} was able to predict hearing threshold group (β =0.064, p = 0.008), while SFOAE level (β = -0.003, p = 0.766) and SFOAE Q_{erb} did not (β = -0.00007, p = 0.998). The odds ratio (e^{β}) for SFOAE F_{end} was 1.066 and the 95%

confidence interval for the odds ratio was [1.017 1.118]. In other words, holding SFOAE levels and Q_{erb} constant, for every unit increase in SFOAE F_{end}, the odds of being in the Better PTA group increased by 1.066 times. However, a univariate logistic regression model with just SFOAE F_{end} as the predictor showed that the modeled probabilities of hearing group were not significantly different from each other ($\beta = 0.073$, $p = 0.396$), likely due to the small number of observations included in the model ($n = 57$) compared to the multivariate model ($n = 818$).

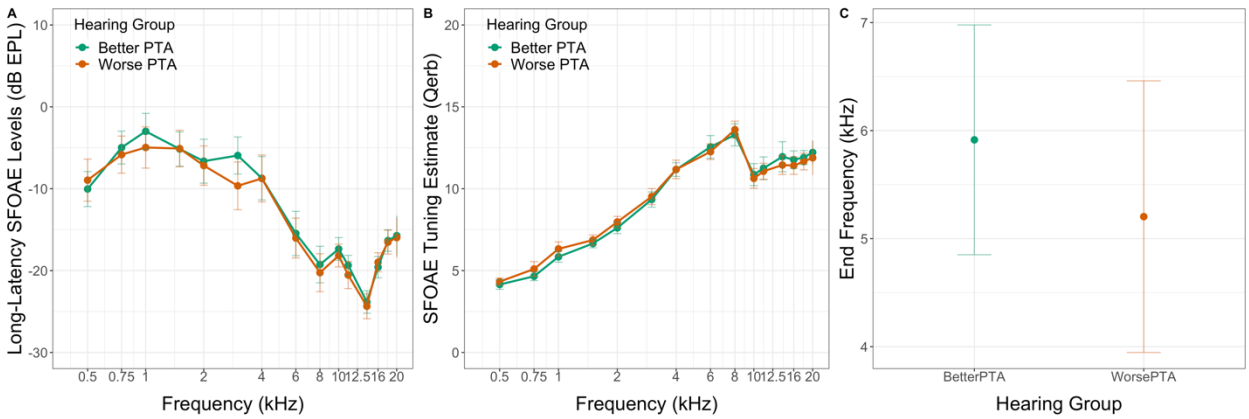

Figure 5.14. SFOAE Levels and Tuning Estimates as a function of Frequency and SFOAE End Frequency for Better PTA and Worse PTA Hearing Groups. Panel A shows the mean long-latency SFOAE levels for both better PTA ($n = 28$) and worse PTA ($n = 29$) groups as represented by color. Panel B shows the mean SFOAE tuning estimates as a function of frequency for both groups. Panel C shows the mean SFOAE end frequency for both groups. The error bars in all panels represent the 95% confidence interval of the means.

5.4. Discussion

The purpose of this study was to examine the influence of age on stimulus frequency otoacoustic emissions (SFOAEs) in individuals between the age of 9 and 45 years. The findings show that LL SFOAE levels measured using fixed probe levels were different at 1- 4 kHz between age groups, despite similar behavioral thresholds up to 6 kHz. At frequencies above 4 kHz, the LL SFOAE levels across age groups were indistinguishable. Tuning estimates derived from SFOAE delays were not significantly different across age groups at any frequencies. On the other hand, the high-frequency extent of measurable SFOAEs, as referred to as the SFOAE bandwidth and measured as the F_{end}, herein was significantly different across age groups and related to various high-frequency behavioral threshold metrics.

A principal component analysis showed that although age was a significant factor in predicting this SFOAE bandwidth metric, age was not loaded in the first component. Instead, among the top contributors to the first component of the PCA, behavioral thresholds contributions were almost 30%. Consequently, a secondary analysis was performed on the various SFOAE metric after splitting participants into better hearing and worse hearing group based on their behavioral pure-tone average (PTA) from 0.5 to 4 kHz. This secondary grouping analysis showed that SFOAE levels and Q_{erb} could not predict hearing group, but high-frequency extent of measurable SFOAEs could. The findings suggest that SFOAE F_{end} is sensitive to both aging and hearing status. The relationship between the various SFOAE

metrics and behavioral thresholds, their respective sensitivities to aging and hearing status, and potential clinical implications will be discussed hereafter.

5.4.1. Characteristics of SFOAE Levels and Delays across Age Groups

The current findings show that behavioral thresholds worsened as a function of frequency and with age. Similarly, SFOAE levels declined as a function of frequency and age, albeit with significant variability across participants. There was a trend for higher levels in the oldest age group at frequencies 0.5 to 1 kHz compared to the other two adult age groups. This could be an indication of changes in the apical OHC status that might be explained as a re-emergence of SFOAEs consistent with the increased irregularity with aging hypothesis. Wu et al., (2021) recently showed that OHC loss in the apex can be as high as 50% even in normal aging adults up to 49 years of age without a history of noise exposure (Figure 3 of reference)[93]. If this apical OHC loss generates additional irregularities along the cochlear spiral, which serve as contributors to the reflection mechanism of SFOAEs, could this elevation in the oldest age group at 1 kHz be an indication of the apical OHC loss?

Only one other study has examined SFOAEs across different age groups up to 20 kHz[23]. Similar to Stiepan et al., (2020), SFOAE levels were highest in the youngest age group and decreased with each increasing age group[23]. Although the age groups between the two studies are different and a direct comparison of levels across age groups is not possible, the overall levels in the current study were

slightly lower than Stiepan et al., (2020), likely due to differences in calibration (correcting for the emission pressure level in the current study)[23,260]. The declines in SFOAE levels with age group were more noticeable, when the total SFOAEs were filtered to examine the long-latency (LL) component only. The LL SFOAE were filtered using time-frequency analysis based on the frequency-delay relationship of adult ears[244,304]. This filtering resulted in a larger difference between unfiltered and filtered SFOAEs in the oldest age group than the youngest three groups. Sisto & Moleti (2002) previously showed that in ears with hearing loss, the delays of TEOAEs were slightly longer than normal hearing ears[304]. This was true for both adults [304] and in neonates who failed the TEOAE screening protocol[327]. If hearing loss affects latencies of OAEs, it is possible that the filtered SFOAE long-latency components, separated based on average delay cut-off parameters of normal-hearing individuals, are outside of the expected delay window for that component.

Alternatively, the significantly lower levels of LL SFOAEs in the oldest group compared to the total SFOAEs could be a result of significant contributions from non-CF places that would result in higher total SFOAE in the ear canal in the oldest group compared to the youngest three age groups. Abdala, Ortmann & Shera (2018) showed that DPOAEs and SFOAEs are affected differently with age, consistent with an increased irregularity hypothesis that preserves SFOAE levels in older participants with hearing loss but diminishes DPOAEs[14]. If true, contributions of other sources to the total ear canal SFOAE levels would be great and filtering of these other sources would reduce the long-latency response in the

oldest group far more than for the younger groups. How does adjusting the different cut-off parameters affect the filtered SFOAE across age groups was not the primary goal of this study. Nonetheless, future studies could examine the optimization parameters depending on the desired application.

At frequencies above 6 kHz, the age groups did not show any differences in SFOAE levels. Because SFOAEs and corresponding noise floors were corrected for ear canal acoustics using emission pressure level, signal to noise ratio was maintained between SFOAE and the noise floor; however, the noise floor mirrors the SFOAE at these frequencies, suggesting that the two may be correlated. This could be related to Compared to the current study's noise floors, the SFOAE noise floors reported by Stiepan et al., (2020) decreased from -10 dB SPL to -20 dB SPL from 0.5 to 3 kHz, which was similar to the current study[23]. However, the noise floors in the Stiepan et al., (2020) measurements increased from -20 dB SPL to -10 dB SPL from 4 to 8 kHz, whereas the current noise floors stayed around -25 dB EPL at those frequencies[23].

Interestingly, the noise floors in the current study matched the DPOAE noise floors of Stiepan et al., (2020) from 0.5 to 10 kHz and not their SFOAE noise floors[23]. Above 10 kHz, the noise floors of the current study follow the contour of the microphone noise as specified by the manufacturer of the ER10x probe used in this study. The noise floors were not significantly different across age groups, although noise floors were highly variable for the youngest group, likely due to the small number of ears tested (n = 4) and potential contributions from noisier participants

in this age group. Dewey & Dhar (2017b) also measured SFOAEs up to 20 kHz in a group of young adults (ages 18-25 years); however, their reported SFOAE levels and noise floors are normalized to the average SFOAE levels at 1 kHz and thus direct comparisons cannot be made between the two studies[197].

In contrast to LL SFOAE levels, the delay estimates across age groups were not significantly different. Abdala, Ortmann & Shera (2018) reported sharper tuning in the older adult group; however, the smoothed delay curves for each of their age groups were overlapping[14]. At similar probe levels of 40 dB SPL/36 dB FPL, the values of N_{sfoae} in the current study increased from ~10 cycles to ~23 cycles from 0.5 – 8 kHz, whereas Abdala, Ortmann & Shera (2018) reported N_{sfoae} values of 8 to ~25 from 0.6 – 8 kHz[14]. The slightly longer delays in the current study compared to Abdala, Ortmann & Shera (2018) may be due to the filtering of the LL component delays in the current study which Abdala, Ortmann & Shera (2018) did not consider[14]. Nonetheless, the general agreement between the two studies suggests that aging without substantial hearing loss is not likely to affect cochlear tuning as reflected in the SFOAE phase-gradient delays.

The delay estimates from the LL component showed a decrease with increasing frequency in terms of physical delay in milliseconds but an increase in delay in terms of equivalent number of cycles accumulated as a function of frequency. Although delays were slightly longer with increasing probe levels from 30 to 36 dB FPL, the difference was only significant at frequencies below 2 kHz. Moleti et al., (2017) showed a decrease in SFOAE latency with increasing stimulus

levels for probes of 25 and 35 dB SPL from 1 to 5 kHz[295]. In another study, Abdala, Guardia & Shera showed a level dependence of delays in N_{sfoae} between stimulus levels of 30 and 40 dB SPL but not between 20 and 30 dB SPL for 0.6 – 8 kHz[214]. These differences in the three studies could be related to the methodological differences in latency computation with and without separating the LL component.

There was an abrupt break in the smooth delay curve around 1 kHz, which has been observed previously in the phase delays of both distortion and reflection OAEs and likely relates to the break in scaling symmetry of the cochlea around 1-2 kHz[220,244,249,295]. In the most recent investigation using similar time-frequency analyses as the current study, Moleti et al., (2017) measured the apical-basal transition frequency in the SFOAEs, TEOAEs, and the reflection component of DPOAEs[295]. They found that all three OAE types had similar delay-frequency functions with a sharp transition around 1 kHz[295]. This apical-basal transition was not as easily observable in delays normalized to frequency or corresponding tuning estimates[295]. The delays at and below this apical-basal transition frequency were lower in the youngest age group compared to the oldest age group, which may be related to developmental differences in the apex of the youngest age group in the current study[220].

5.4.2. SFOAE Bandwidth Metrics in Relation to Behavioral Corner Frequency

The term “corner frequency of the audiogram” has been previously used to describe the sudden roll-off in thresholds. Shaffer & Long (2004) examined the

corner frequency of DPOAEs to determine the low-frequency roll-off in kangaroo rat and its relation to auditory sensitivity[328]. They found that DPOAE levels declined around the same frequency as the increase in hearing thresholds, suggesting that the two are related[328]. Dewey & Dhar (2017b) recently compared the corner frequency of the audiogram to the corner frequency of SFOAEs and found that the latter was always lower than the audiometric corner frequency, suggesting two possible explanations: 1) SFOAE levels at high frequencies may be limited by the reverse transmission characteristics of the middle ear or 2) SFOAEs may be more sensitive to basal cochlear dysfunction than audiometric thresholds[197].

Supporting evidence for the first hypothesis comes from measurements of middle ear vibrations and intracochlear pressures, which suggest that transmission in both the forward- and reverse-directions are affected at frequencies 5 kHz and above[267,329,330]. Cheng et al., (2021) measured the level- and frequency-dependence of the middle ear in human cadavers for frequencies up to 20 kHz and showed that stapes displacements decreased as a function of increasing frequency above 1 kHz to 10 kHz and became even smaller at frequencies above 10 kHz[329]. In differential intracochlear pressure measurements, similar drop at 10 kHz in the pressure magnitude of scale vestibuli has been reported[330]. Furthermore, at frequencies as low as 5 kHz, there is a phase variation hypothesized to be a result of the rocking motion of the stapes at high frequencies rather than a piston-type motion at low frequencies[329,330].

A comparison of forward transmission from the ear canal to the middle ear and reverse transmission from the inner ear to the middle ear has only been reported by Puria, 2003[266]. These measurements have shown large inter-subject variability of the reverse transmission at frequencies below 0.5 kHz and above ~7 kHz[266], which may explain the variability of high-frequency SFOAE levels[197]. Another finding from Cheng et al., (2021) that relates to the variability of SFOAE levels and behavioral thresholds seen in even the relatively young ears, is that umbo and stapes displacements across the entire frequency range can be highly variable across temporal bones from different ears[329], albeit the temporal bones in the Cheng et al., (2021) study are from much older ears (ages 53-65 years).

Dewey & Dhar (2017b) proposed an alternative explanation for the discrepancy between audiometric and SFOAE corner frequencies, one that supposes that SFOAE generation requires a healthy cochlea, hence weak high-frequency SFOAEs could be a result of cochlear dysfunction in the base that is not yet evident in audiometric measurements[197]. In order to test this hypothesis, the current study examined the SFOAE corner frequencies and their relation to audiometric frequencies across participants of different ages and increasing degree of high-frequency hearing loss above ~6-8 kHz. If the explanation proposed by Dewey & Dhar (2017b) were true, both the SFOAE and audiometric corner frequencies would be higher in more pristine ears, i.e., young ears that have not been exposed to noise- or chemico-toxicity. Furthermore, the discrepancy between SFOAE and audiometric

corner frequency would become smaller for younger ears and larger for older ears with more cumulative cochlear dysfunction.

In the current study, the corner frequency of the audiogram followed this trend – the corner frequency was highest in the youngest age group and lowest in the oldest age group. Lee et al., (2012) have previously reported this similar result in a wider age (10-65 years) range of 352 individuals[22]. Although Lee et al., (2012) used a slightly different yet equivalent calibration method to account for standing waves at high frequencies[331] and the age groups were slightly different than the current study, the youngest groups in both studies showed a corner frequency between 12.5-13 kHz, which decreased to ~9.5 kHz in the oldest age group of the current study (40-45 y.o.) and the middle age group of Lee et al., (2012) (i.e 36-45 y.o.)[22].

SFOAE corner frequencies in the current study could not be obtained in any but four participants due to the reduction in SFOAE levels with filtering resulting in poor SNR at high frequencies. Dewey & Dhar (2017b) used an objective criterion based on the roll-off slope of high-frequency SFOAEs to compute corner frequencies but did not find a relationship between the SFOAE corner frequency and audiometric landmarks[197]. This discordance may be due to the idiosyncratic behavior of SFOAE levels and of reflection emissions in general, such that bigger is not always better. For example, studies of reflection emissions in mutant mice have shown enhanced spontaneous emissions and SFOAEs in various anomalies of the tectorial membrane[191,212,213]. Additionally, studies of punctate lesions in other

animals have seen spontaneous emissions around the histologically confirmed regions of damage[201] and at frequencies concomitant with a sharp decline in ABR thresholds[200].

A fixed criterion like Dewey & Dhar (2017b) could not be employed in the current study due to the variable morphologies of SFOAE spectra observed across age groups[197]. Although the exemplar spectra (as shown in Figure 5.10) with robust emissions and a distinct roll-off was observed in a handful of participants, a majority of participants showed a gradual decline of emission levels with frequency without any distinct corner frequencies, yet others showed flat and weak emissions close to the noise floor across the entire frequency range. These variable patterns made it difficult to establish a uniform criterion for all participants.

In contrast to the SFOAE corner frequency, another bandwidth property of SFOAEs was both related to the audiometric corner frequency, 18- and 36- dB FPL threshold intercept frequencies and sensitive to aging. The end frequency of SFOAEs (F_{end}), as defined as the highest frequency with 9 dB SNR was most closely related to the frequency where thresholds crossed 36 dB FPL. This is likely due to the matched stimulus levels between the two measures.

F_{end} was also related to the behavioral corner frequency. Although F_{end} was always lower than the behavioral corner frequencies in all four age groups, the objective criterion of this metric ensured that there would be adequate SNR at frequency regions that reflect functioning OHC status. On the other hand, behavioral corner frequency was a subjective determination of the frequency

demarcating transition from stable hearing thresholds to precipitously poorer hearing.

The stringent treatment of SFOAE F_{end} eliminated some observations, as the SNR criterion was not met for this iso-input metric in some ears, whereas the behavioral threshold corner frequencies as an iso-response metric could be measured for all 68 participants. Future studies could employ measurement of SFOAEs at multiple levels in order to extract an iso-response metric of F_{end}, even in ears with poor SFOAEs at a fixed low level. SFOAE F_{end} was also correlated with the behavioral threshold intercepts for 18-dB FPL. Similar to the current study, Dewey & Dhar (2017) also found a significant correlation between SFOAE F_{end} and the 18-dB FPL behavioral threshold intercept frequency[197]; however, their end frequency was much higher than the current study (~12 kHz vs. ~6.3 kHz) for the same age comparison, which may be related to the filtering of SFOAEs in the current study.

5.4.3. Sensitivity of SFOAEs to Aging and Hearing Status

A principal component analysis showed that age was not loaded in the first component, instead behavioral thresholds and SFOAE levels at each frequency were. This prompted the analysis of SFOAE levels, delays, and bandwidth for two split groups based on pure-tone average hearing thresholds from 0.5-4 kHz. Although this analysis did reveal a slight difference in level and in SFOAE F_{end}, with better hearing group outperforming than the worse hearing group, the effect of

hearing threshold group was not nearly as dramatic as the differences observed across each age group. This suggested that although the PCA correctly identified SFOAE levels and thresholds as inversely related, the effect may be driven by the repeated measures nature of the many frequencies measured for SFOAE levels. On the other hand, the effect of age group was not loaded in the first component because of the much fewer observations (n = 57 vs. n = 818 for frequencies tested for SFOAE levels).

SFOAE delays were not sensitive to different age groups or hearing groups, likely due to the clinically-normal hearing ears in the current study, whereas SFOAE levels and SFOAE F_{end} were. Using a different type of reflection emission, Fultz et al., (2020) examined the cochlear reflectance (CR) in 60 adults from 20-79 years of age[332]. They found that although CR magnitude (CRM) were poorer with increasing age, the effects were mostly driven by hearing sensitivity[332]. They concluded that adults with better pure-tone thresholds had significantly larger CRM than those with poorer CRM thresholds, and therefore, changes in OHC function due to aging also affect pure-tone thresholds[332]. One important consideration for these findings is that Fultz et al., (2020) examined age effects over a wide age range (20-79 years) and varying degrees of hearing thresholds from normal to unmeasurable responses at the limit of the equipment[332]. However, age-related changes in CR can be observed in their dataset as early as 30-39 year olds (see Figure 3 of reference)[332], which is in agreement to the findings of this study.

In contrast to the Fultz et al., (2020) study, the current findings suggest that hearing loss is not required to explain the inter-subject variability of SFOAE levels. SFOAE levels and tuning were not significantly different between better PTA and worse PTA hearing groups, but the high-frequency extent of SFOAEs in these individuals was somewhat different. Together these findings suggest that the clinical definition of normal hearing, relative to other ears within the same age group, may not be appropriate for the purpose of monitoring cochlear changes. However, the current findings are limited to ears with relatively good hearing at standard clinical frequencies. Future studies focusing on longitudinal measurement of SFOAEs could provide insight into the origins of this heterogeneity of SFOAEs, the functional relevance of this heterogeneity, and the clinical implications for assessment of the cochlear status.

5.5. Conclusions

SFOAE levels decreased across age groups even at frequencies where hearing thresholds were within a clinical normal range. SFOAE based tuning estimates on the other hand were not significantly different. Lastly, SFOAE F_{end} determined the high-frequency extent of cochlear function across age groups and across two different groups of normal- and hyper-normal hearing. Furthermore, SFOAE F_{end} was associated with various behavioral threshold metrics, suggesting it could predict the frequencies where normal hearing transitions into regions of cochlear dysfunction. However, this particular SFOAE metric needs further investigation

particularly in ears with known cochlear pathologies towards its implementation in clinical assessment.

CHAPTER 6

Summary

6.1. Overview

Despite advances in SFOAE recording and analysis techniques, the use of SFOAEs in clinical settings is lacking. A comprehensive examination of human SFOAEs, including phase and bandwidth properties, was conducted as a first step towards evaluating the sensitivity and specificity of SFOAEs in detecting cochlear dysfunction due to aging. Insights on SFOAE generation mechanism and source, their relationship to other measures of hearing sensitivity and tuning, and their performance in detecting age-related cochlear dysfunction were obtained.

6.2. Summary of Findings

In the first study, the relationship between SFOAEs and behavioral thresholds was examined for frequencies up to 14 kHz. The findings showed that SFOAEs can predict behavioral thresholds within 5 dB on average. These findings are the first to show that SFOAE predicted thresholds are related to behavioral thresholds up to 14 kHz. Although many previous studies have shown that SFOAEs and behavioral microstructure are related, the nuances of SFOAE measurement paradigms and contributions from various intracochlear sources and mechanisms may have blurred this relationship. As a result, SFOAEs have been disregarded as the ugly duckling of OAEs in their clinical potential and utilization. In the current

study, contributions from other sources impacted the degree of the relationship between SFOAEs and behavioral thresholds, whereas the mitigation of these extraneous contributions to SFOAEs strengthened this relationship. The observation that total SFOAEs measured in the ear canal were greater than the filtered long-latency component, presumably from the characteristic place based on their delay, further provide support for the nonlinearity seen in basilar membrane vibrations[231,278], which is even more enhanced in the reticular lamina vibrations[149]. However, contributions of these nonlinear responses away from the characteristic place are not dominant in the total emission recorded in the ear canal[333].

In the second study, delays of SFOAEs were used to derive a tuning estimate for frequencies up to 14 kHz, and the findings showed a global relationship between the two measures; however, the predictability of tuning estimates at individual frequencies appears to be limited due to the large variability in behavioral tuning at high frequencies (at and above 4 kHz) that is inherent to the paradigm and the heterogeneity of thresholds at those frequencies across ears. SFOAE tuning estimates were also highly variable at high frequencies (at and above 4 kHz), requiring a relatively high SNR. This finding seems to suggest that the phase of SFOAEs might only be informative in cases where OHC function is intact. Although this finding initially presents itself as a limitation of using phase for the purpose of assessing the cochlea, there may be value in obtaining SFOAE phase-based delays to aid in the differential diagnosis of outer vs inner hair cell loss. The exact ratios of

these losses due to various pathologies combined with genetic and environmental susceptibilities are yet to be fully understood.

In the third study, SFOAE levels, tuning, and bandwidth were examined across four age groups. The findings showed that SFOAE levels and tuning did not show a significant difference across age groups, but the high-frequency extent of SFOAEs, i.e., the bandwidth, became more limited with increasing age. Furthermore, within each age group, better and worse hearing threshold averages predicted larger or smaller bandwidth of SFOAEs, respectively. These findings suggest that 1) the variability of SFOAE levels may mirror the variability in thresholds, even when hearing is clinically normal; 2) tuning of the delay-based tuning may be intact with ARHL despite declines in hearing sensitivity starting in the base; and 3) cochlear bandwidth may be an appropriate measure to quantify degree of OHC dysfunction or loss that appears sooner than in behavioral measures; and 4) in addition to tracking the progressive loss of bandwidth with aging, the bandwidth metric could inform the distinction of normal and hyper-normal hearing. How these normal variants of hearing thresholds and SFOAEs exhibit in everyday perceptual abilities remains to be investigated.

6.3. Clinical Implications

SFOAEs, and OAEs in general, are not currently utilized in clinical practice to assess cochlear OHC status. Historically the presence or absence of OAEs did not inform the clinical decision making of the hearing care provider or treatment for the patient in the majority of clinical cases. However, a few exceptions exist. Many clinical ototoxicity monitoring protocols include OAE measurements and conditions such as auditory neuropathy already rely on the combined use of OAEs and ABR. However, the introduction of molecular therapeutics for restoring hearing function into clinical practice requires precision diagnostics that differentiate outer hair cell vs inner hair cell loss.

A new gene therapy drug DB-OTO (https://www.decibeltx.com/pipeline/) is being used to target otoferlin deficiency in children who display the clinical and functional signs of auditory neuropathy. Using OAEs that are frequency-specific, i.e., SFOAEs, could better inform the regions that may be affected in conditions like auditory neuropathy. The same biotechnology company is also evaluating the efficacy of an otoprotective drug DB-020 (https://www.decibeltx.com/pipeline/) that aims to prevent cisplatin-induced hearing loss. A different startup is already in Phase 2 clinical trials to evaluate the use of FX-322 (https://www.frequencytx.com/pipeline-programs/pipeline/) for regenerating cochlear hair cells in patients with noise-induced or sudden sensorineural hearing loss.

These advanced therapeutics require significant modifications to current clinical protocols to ensure a sensitive, accurate, and precise assessment of auditory

function. OAEs are a clinical tool already for evaluating OHC status but different aspects of OAEs could inform a more comprehensive assessment of cochlear sensitivity, tuning, bandwidth, and compression, without subjecting patients to length behavioral paradigms. The findings of the current dissertation provide a suitable protocol for using SFOAEs for assessing cochlear function in a more sensitive and efficient manner.

6.4 Limitations & Future Studies

Several limitations of the current work present opportunities for future studies. These limitations could be categorized into two broad categories: 1) methodological choices made for the purpose of demonstrating feasibility and ensuring efficiency, and 2) issues of generalizability based on the study sample. The specific issues and potential impacts of these limitations are presented below.

6.4.1. Methodological Limitations

A main methodological limitation of this study is that although age-related co cochlear dysfunction was referenced to the youngest age group (9-12 y.o.), only four participants could be included in the study due to the difficulties in recruiting and including this age group during a global pandemic. Although the findings across age groups are still valid, more data from the youngest age group could have helped characterize variants of normal hearing and associated otoacoustic signatures.

As with all research, the availability of time and resources restricted the addition of more levels to the input-output functions in order to better characterize the compressive behavior of SFOAEs measured in dB SL. This important function of the cochlea must be characterized to a greater degree across different age groups using SFOAEs to better understand the physiological bases and the functional effects of compression loss with aging. Furthermore, combining different types of reflection emissions (SOAEs and TEOAEs) to the current findings in SFOAEs could have served as validation measures. On the other hand, combining DPOAEs with SFOAEs in future studies could further solidify the understanding of the joint profile of OAEs in differentiating various pathologies. Lastly, combining OAE and neural measures such as the cochlear microphonic or auditory nerve action potentials, to the current study would have served to better phenotype ARHL. Future studies could be directed at identifying various electrophysiological and OAE biomarkers in known genetic hearing losses.

6.4.2. Generalizability

The generalizability of the current study remains limited to white women as most of the data comes from that demographic. Future studies could focus efforts on recruitment to improve the gender distribution of the sample to equal numbers of both men and women and more equal representation of different races and ethnicities. Furthermore, the current study only included individuals with clinically normal hearing who would otherwise not seek audiological assessment. However, in

order to understand the clinical application of the current study, it may be worthwhile to perform these studies in patients with auditory neuropathy, those undergoing ototoxic monitoring, or individuals who seek regenerative therapies to monitor restored function.

6.5. Conclusions

The findings from the current study suggest that when stimulus levels are equivalent and only contributions from the characteristic place are considered, SFOAEs can provide an assessment of cochlear regions evaluated by behavioral measures, as evidenced by the strong relationship between SFOAE predicted and behaviorally measured thresholds and tuning estimates. Furthermore, SFOAEs are sensitive to age-related cochlear dysfunction, particularly in the bandwidth of recordable SFOAEs. The current dissertation supports the continued investigation of SFOAEs and their sensitivity and specificity for detecting cochlear dysfunction, differentially diagnosing types of cochlear dysfunction, and monitoring cochlear status over time, with insult, and with treatment.

REFERENCES

1 Kemp, D. T. Stimulated acoustic emissions from within the human auditory system. *J Acoust Soc Am* **64**, 1386-1391, doi:10.1121/1.382104 (1978).

2 Davis, B., Qiu, W. & Hamernik, R. P. The use of distortion product otoacoustic emissions in the estimation of hearing and sensory cell loss in noise-damaged cochleas. *Hear Res* **187**, 12-24, doi:10.1016/s0378-5955(03)00339-3 (2004).

3 Lonsbury-Martin, B. L. & Martin, G. K. The clinical utility of distortion-product otoacoustic emissions. *Ear Hear* **11**, 144-154, doi:10.1097/00003446-199004000-00009 (1990).

4 Ryan, A. & Dallos, P. Effect of absence of cochlear outer hair cells on behavioural auditory threshold. *Nature* **253**, 44-46, doi:10.1038/253044a0 (1975).

5 Dallos, P. & Harris, D. Properties of auditory nerve responses in absence of outer hair cells. *J Neurophysiol* **41**, 365-383, doi:10.1152/jn.1978.41.2.365 (1978).

6 Lasak, J. M., Allen, P., McVay, T. & Lewis, D. Hearing loss: diagnosis and management. *Prim Care* **41**, 19-31, doi:10.1016/j.pop.2013.10.003 (2014).

7 Wroblewska-Seniuk, K. E., Dabrowski, P., Szyfter, W. & Mazela, J. Universal newborn hearing screening: methods and results, obstacles, and benefits. *Pediatr Res* **81**, 415-422, doi:10.1038/pr.2016.250 (2017).

8 Konrad-Martin, D. *et al.* Serial Monitoring of Otoacoustic Emissions in Clinical Trials. *Otol Neurotol* **37**, e286-294, doi:10.1097/MAO.0000000000001134 (2016).

9 Balatsouras, D. G. *et al.* Detection of pseudohypacusis: a prospective, randomized study of the use of otoacoustic emissions. *Ear Hear* **24**, 518-827, doi:10.1097/01.AUD.0000100206.96363.05 (2003).

10 Zhou, X., Henin, S., Long, G. R. & Parra, L. C. Impaired cochlear function correlates with the presence of tinnitus and its estimated spectral profile. *Hear Res* **277**, 107-116, doi:10.1016/j.heares.2011.02.006 (2011).

11 van Huffelen, W. M., Mateijsen, N. J. & Wit, H. P. Classification of patients with Meniere's disease using otoacoustic emissions. *Audiol Neurootol* **3**, 419-430, doi:10.1159/000013810 (1998).

12 Ferri, G. G., Modugno, G. C., Calbucci, F., Ceroni, A. R. & Pirodda, A. Hearing loss in vestibular schwannomas: analysis of cochlear function by means of distortion-product otoacoustic emissions. *Auris Nasus Larynx* **36**, 644-648, doi:10.1016/j.anl.2009.02.006 (2009).

13 Abdala, C. & Kalluri, R. Towards a joint reflection-distortion otoacoustic emission profile: Results in normal and impaired ears. *J Acoust Soc Am* **142**, 812, doi:10.1121/1.4996859 (2017).

14 Abdala, C., Ortmann, A. J. & Shera, C. A. Reflection- and Distortion-Source Otoacoustic Emissions: Evidence for Increased Irregularity in the Human

Cochlea During Aging. *J Assoc Res Otolaryngol* **19**, 493-510, doi:10.1007/s10162-018-0680-x (2018).

15 Prieve, B. A. *et al.* Analysis of transient-evoked otoacoustic emissions in normal-hearing and hearing-impaired ears. *J Acoust Soc Am* **93**, 3308-3319, doi:10.1121/1.405715 (1993).

16 Le Prell, C. G., Hammill, T. L. & Murphy, W. J. Noise-induced hearing loss: Translating risk from animal models to real-world environments. *J Acoust Soc Am* **146**, 3646, doi:10.1121/1.5133385 (2019).

17 Schacht, J., Talaska, A. E. & Rybak, L. P. Cisplatin and aminoglycoside antibiotics: hearing loss and its prevention. *Anat Rec (Hoboken)* **295**, 1837-1850, doi:10.1002/ar.22578 (2012).

18 Nieman, C. L. & McMahon, C. M. The World Health Organization's World Report on Hearing: a call to action for hearing care providers. *J Laryngol Otol* **134**, 377-378, doi:10.1017/S0022215120000663 (2020).

19 Blackwell, D. L., Lucas, J. W. & Clarke, T. C. Summary health statistics for U.S. adults: national health interview survey, 2012. *Vital Health Stat 10*, 1-161 (2014).

20 Cruickshanks, K. J. *et al.* Prevalence of hearing loss in older adults in Beaver Dam, Wisconsin. The Epidemiology of Hearing Loss Study. *Am J Epidemiol* **148**, 879-886, doi:10.1093/oxfordjournals.aje.a009713 (1998).

21 Pearson, J. D. *et al.* Gender differences in a longitudinal study of age-associated hearing loss. *J Acoust Soc Am* **97**, 1196-1205, doi:10.1121/1.412231 (1995).

22 Lee, J. *et al.* Behavioral hearing thresholds between 0.125 and 20 kHz using depth-compensated ear simulator calibration. *Ear Hear* **33**, 315-329, doi:10.1097/AUD.0b013e31823d7917 (2012).

23 Stiepan, S., Siegel, J., Lee, J., Souza, P. & Dhar, S. The Association Between Physiological Noise Levels and Speech Understanding in Noise. *Ear Hear* **41**, 461-464, doi:10.1097/AUD.0000000000000753 (2020).

24 Goman, A. M. & Lin, F. R. Prevalence of Hearing Loss by Severity in the United States. *Am J Public Health* **106**, 1820-1822, doi:10.2105/AJPH.2016.303299 (2016).

25 Goman, A. M., Reed, N. S. & Lin, F. R. Addressing Estimated Hearing Loss in Adults in 2060. *JAMA Otolaryngol Head Neck Surg* **143**, 733-734, doi:10.1001/jamaoto.2016.4642 (2017).

26 Humes, L. E. *et al.* Factors associated with individual differences in clinical measures of speech recognition among the elderly. *J Speech Hear Res* **37**, 465-474, doi:10.1044/jshr.3702.465 (1994).

27 Gieseler, A. *et al.* Auditory and Non-Auditory Contributions for Unaided Speech Recognition in Noise as a Function of Hearing Aid Use. *Front Psychol* **8**, 219, doi:10.3389/fpsyg.2017.00219 (2017).

28 Pichora-Fuller, M. K. How Social Psychological Factors May Modulate Auditory and Cognitive Functioning During Listening. *Ear Hear* **37 Suppl 1**, 92S-100S, doi:10.1097/AUD.0000000000000323 (2016).

29 Dalton, D. S. *et al.* The impact of hearing loss on quality of life in older adults. *Gerontologist* **43**, 661-668, doi:10.1093/geront/43.5.661 (2003).

30 Vas, V., Akeroyd, M. A. & Hall, D. A. A Data-Driven Synthesis of Research Evidence for Domains of Hearing Loss, as Reported by Adults With Hearing Loss and Their Communication Partners. *Trends Hear* **21**, 2331216517734088, doi:10.1177/2331216517734088 (2017).

31 Lin, F. R. *et al.* Hearing loss and cognition in the Baltimore Longitudinal Study of Aging. *Neuropsychology* **25**, 763-770, doi:10.1037/a0024238 (2011).

32 Peelle, J. E. & Wingfield, A. The Neural Consequences of Age-Related Hearing Loss. *Trends Neurosci* **39**, 486-497, doi:10.1016/j.tins.2016.05.001 (2016).

33 Downs, D. W. Effects of hearing and use on speech discrimination and listening effort. *J Speech Hear Disord* **47**, 189-193, doi:10.1044/jshd.4702.189 (1982).

34 Picou, E. M., Ricketts, T. A. & Hornsby, B. W. How hearing aids, background noise, and visual cues influence objective listening effort. *Ear Hear* **34**, e52-64, doi:10.1097/AUD.0b013e31827f0431 (2013).

35 Beechey, T., Buchholz, J. M. & Keidser, G. Hearing Aid Amplification Reduces Communication Effort of People With Hearing Impairment and

Their Conversation Partners. *J Speech Lang Hear Res* **63**, 1299-1311, doi:10.1044/2020_JSLHR-19-00350 (2020).

36 Simpson, A. N., Matthews, L. J., Cassarly, C. & Dubno, J. R. Time From Hearing Aid Candidacy to Hearing Aid Adoption: A Longitudinal Cohort Study. *Ear Hear* **40**, 468-476, doi:10.1097/AUD.0000000000000641 (2019).

37 Maharani, A. *et al.* Longitudinal Relationship Between Hearing Aid Use and Cognitive Function in Older Americans. *J Am Geriatr Soc* **66**, 1130-1136, doi:10.1111/jgs.15363 (2018).

38 Reed, N. S. *et al.* Trends in Health Care Costs and Utilization Associated With Untreated Hearing Loss Over 10 Years. *JAMA Otolaryngol Head Neck Surg* **145**, 27-34, doi:10.1001/jamaoto.2018.2875 (2019).

39 Cohen, J. M. *et al.* Studies of Physician-Patient Communication with Older Patients: How Often is Hearing Loss Considered? A Systematic Literature Review. *J Am Geriatr Soc* **65**, 1642-1649, doi:10.1111/jgs.14860 (2017).

40 Christensen, K., Frederiksen, H. & Hoffman, H. J. Genetic and environmental influences on self-reported reduced hearing in the old and oldest old. *J Am Geriatr Soc* **49**, 1512-1517, doi:10.1046/j.1532-5415.2001.4911245.x (2001).

41 Someya, S. & Kim, M. J. Cochlear detoxification: Role of alpha class glutathione transferases in protection against oxidative lipid damage, ototoxicity, and cochlear aging. *Hear Res* **402**, 108002, doi:10.1016/j.heares.2020.108002 (2021).

42 Wang, J. & Puel, J. L. Presbycusis: An Update on Cochlear Mechanisms and Therapies. *J Clin Med* **9**, doi:10.3390/jcm9010218 (2020).

43 Gates, G. A., Couropmitree, N. N. & Myers, R. H. Genetic associations in age-related hearing thresholds. *Arch Otolaryngol Head Neck Surg* **125**, 654-659, doi:10.1001/archotol.125.6.654 (1999).

44 Cunningham, L. L. & Tucci, D. L. Hearing Loss in Adults. *N Engl J Med* **377**, 2465-2473, doi:10.1056/NEJMra1616601 (2017).

45 Bergman, M. Hearing in the Mabaans. A critical review of related literature. *Arch Otolaryngol* **84**, 411-415, doi:10.1001/archotol.1966.00760030413007 (1966).

46 Liberman, M. C. Noise-induced and age-related hearing loss: new perspectives and potential therapies. *F1000Res* **6**, 927, doi:10.12688/f1000research.11310.1 (2017).

47 Muller, U. & Barr-Gillespie, P. G. New treatment options for hearing loss. *Nat Rev Drug Discov* **14**, 346-365, doi:10.1038/nrd4533 (2015).

48 Crowson, M. G., Hertzano, R. & Tucci, D. L. Emerging Therapies for Sensorineural Hearing Loss. *Otol Neurotol* **38**, 792-803, doi:10.1097/MAO.0000000000001427 (2017).

49 Livingston, G. *et al.* Dementia prevention, intervention, and care. *Lancet* **390**, 2673-2734, doi:10.1016/S0140-6736(17)31363-6 (2017).

50 Golub, J. S., Brickman, A. M., Ciarleglio, A. J., Schupf, N. & Luchsinger, J. A. Association of Subclinical Hearing Loss With Cognitive Performance. *JAMA*

Otolaryngol Head Neck Surg **146**, 57-67, doi:10.1001/jamaoto.2019.3375 (2020).

51 Smits, C., Kapteyn, T. S. & Houtgast, T. Development and validation of an automatic speech-in-noise screening test by telephone. *Int J Audiol* **43**, 15-28, doi:10.1080/14992020400050004 (2004).

52 Folmer, R. L. *et al.* Validation of a Computer-Administered Version of the Digits-in-Noise Test for Hearing Screening in the United States. *J Am Acad Audiol* **28**, 161-169, doi:10.3766/jaaa.16038 (2017).

53 De Sousa, K. C., Swanepoel, W., Moore, D. R. & Smits, C. A Smartphone National Hearing Test: Performance and Characteristics of Users. *Am J Audiol* **27**, 448-454, doi:10.1044/2018_AJA-IMIA3-18-0016 (2018).

54 Beck, D. L., Danhauer, J. L., Abrams, H. B., Atcherson, S. R. & al., e. Vol. 25 (The Hearing Review, 2018).

55 Kochkin, S. MarkeTrak VII: Obstacles to adult non-user adoption of hearing aids. *The Hearing Journal.* **60**, 24-51 (2007).

56 Tremblay, K. L. *et al.* Self-Reported Hearing Difficulties Among Adults With Normal Audiograms: The Beaver Dam Offspring Study. *Ear Hear* **36**, e290-299, doi:10.1097/AUD.0000000000000195 (2015).

57 Edwards, B. Emerging Technologies, Market Segments, and MarkeTrak 10 Insights in Hearing Health Technology. *Semin Hear* **41**, 37-54, doi:10.1055/s-0040-1701244 (2020).

58 Spankovich, C., Gonzalez, V. B., Su, D. & Bishop, C. E. Self reported hearing difficulty, tinnitus, and normal audiometric thresholds, the National Health and Nutrition Examination Survey 1999-2002. *Hear Res* **358**, 30-36, doi:10.1016/j.heares.2017.12.001 (2018).

59 Feltner, C., Wallace, I. F., Kistler, C. E., Coker-Schwimmer, M. & Jonas, D. E. Screening for Hearing Loss in Older Adults: Updated Evidence Report and Systematic Review for the US Preventive Services Task Force. *JAMA* **325**, 1202-1215, doi:10.1001/jama.2020.24855 (2021).

60 Reed, N. S. & McCreery, R. Vol. 2022 (American Academy of Audiology, 2020).

61 American National Standards Institute. in *ANSI S3.21-1978; [R92]* (Author, New York, 1978).

62 Rodriguez Valiente, A., Trinidad, A., Garcia Berrocal, J. R., Gorriz, C. & Ramirez Camacho, R. Extended high-frequency (9-20 kHz) audiometry reference thresholds in 645 healthy subjects. *Int J Audiol* **53**, 531-545, doi:10.3109/14992027.2014.893375 (2014).

63 Hunter, L. L. *et al.* Extended high frequency hearing and speech perception implications in adults and children. *Hear Res* **397**, 107922, doi:10.1016/j.heares.2020.107922 (2020).

64 Monson, B. B. & Buss, E. in *The Hearing Journal.* Vol. 72 30-32 (2019).

65 Moore, B. C. & Tan, C. T. Perceived naturalness of spectrally distorted speech and music. *J Acoust Soc Am* **114**, 408-419, doi:10.1121/1.1577552 (2003).

66 Best, V., Carlile, S., Jin, C. & van Schaik, A. The role of high frequencies in speech localization. *J Acoust Soc Am* **118**, 353-363, doi:10.1121/1.1926107 (2005).

67 Vitela, A. D., Monson, B. B. & Lotto, A. J. Phoneme categorization relying solely on high-frequency energy. *J Acoust Soc Am* **137**, EL65-70, doi:10.1121/1.4903917 (2015).

68 Berlin, C. in *The Volta Review*. (1982).

69 Berlin, C. I., Wexler, K. F., Jerger, J. F., Halperin, H. R. & Smith, S. Superior ultra-audiometric hearing: a new type of hearing loss which correlates highly with unusually good speech in the "profoundly deaf". *Otolaryngology* **86**, ORL-111-116, doi:10.1177/019459987808600125 (1978).

70 Kochkin, S. MarkeTrak VIII: Consumer satisfaction with hearing aids is slowly increasing. *The Hearing Journal.* **63**, 19-20. (2010.).

71 Gatehouse, S., Naylor, G. & Elberling, C. Linear and nonlinear hearing aid fittings--1. Patterns of benefit. *Int J Audiol* **45**, 130-152, doi:10.1080/14992020500429518 (2006).

72 Baer, T., Moore, B. C. & Gatehouse, S. Spectral contrast enhancement of speech in noise for listeners with sensorineural hearing impairment: effects on intelligibility, quality, and response times. *J Rehabil Res Dev* **30**, 49-72 (1993).

73 Moore, B. C. *Pitch Perception and Frequency Discrimination.*, (Whurr Publishers Ltd., 1998.).

74 Fullgrabe, C., Moore, B. C. & Stone, M. A. Age-group differences in speech identification despite matched audiometrically normal hearing: contributions from auditory temporal processing and cognition. *Front Aging Neurosci* **6**, 347, doi:10.3389/fnagi.2014.00347 (2014).

75 Ruggles, D., Bharadwaj, H. & Shinn-Cunningham, B. G. Why middle-aged listeners have trouble hearing in everyday settings. *Curr Biol* **22**, 1417-1422, doi:10.1016/j.cub.2012.05.025 (2012).

76 Badri, R., Siegel, J. H. & Wright, B. A. Auditory filter shapes and high-frequency hearing in adults who have impaired speech in noise performance despite clinically normal audiograms. *J Acoust Soc Am* **129**, 852-863, doi:10.1121/1.3523476 (2011).

77 Harris, K. C. & Dubno, J. R. Age-related deficits in auditory temporal processing: unique contributions of neural dyssynchrony and slowed neuronal processing. *Neurobiol Aging* **53**, 150-158, doi:10.1016/j.neurobiolaging.2017.01.008 (2017).

78 Gatlin, A. E. & Dhar, S. History and Lingering Impact of the Arbitrary 25-dB Cutoff for Normal Hearing. *Am J Audiol* **30**, 231-234, doi:10.1044/2020_AJA-20-00181 (2021).

79 Landegger, L. D., Psaltis, D. & Stankovic, K. M. Human audiometric thresholds do not predict specific cellular damage in the inner ear. *Hear Res* **335**, 83-93, doi:10.1016/j.heares.2016.02.018 (2016).

80 Wu, P. Z., O'Malley, J. T., de Gruttola, V. & Liberman, M. C. Age-Related Hearing Loss Is Dominated by Damage to Inner Ear Sensory Cells, Not the Cellular Battery That Powers Them. *J Neurosci* **40**, 6357-6366, doi:10.1523/JNEUROSCI.0937-20.2020 (2020).

81 Wu, P. Z., Wen, W. P., O'Malley, J. T. & Liberman, M. C. Assessing fractional hair cell survival in archival human temporal bones. *Laryngoscope* **130**, 487-495, doi:10.1002/lary.27991 (2020).

82 Hall, J. W. Crosscheck Principle in Pediatric Audiology Today: A 40-Year Perspective. *Journal of Audiology and Otology* **20**, 59-67, doi:10.7874/jao.2016.20.2.59 (2016).

83 Auerbach, B. D., Rodrigues, P. V. & Salvi, R. J. Central gain control in tinnitus and hyperacusis. *Front Neurol* **5**, 206, doi:10.3389/fneur.2014.00206 (2014).

84 Wong, A. C. & Ryan, A. F. Mechanisms of sensorineural cell damage, death and survival in the cochlea. *Front Aging Neurosci* **7**, 58, doi:10.3389/fnagi.2015.00058 (2015).

85 Gates, G. A. & Mills, J. H. Presbycusis. *Lancet* **366**, 1111-1120, doi:10.1016/S0140-6736(05)67423-5 (2005).

86 Ouda, L., Profant, O. & Syka, J. Age-related changes in the central auditory system. *Cell Tissue Res* **361**, 337-358, doi:10.1007/s00441-014-2107-2 (2015).

87 Schuknecht, H. F. Presbycusis. *Laryngoscope* **65**, 402-419, doi:10.1288/00005537-195506000-00002 (1955).

88 Schuknecht, H. F. Further Observations on the Pathology of Presbycusis. *Arch Otolaryngol* **80**, 369-382, doi:10.1001/archotol.1964.00750040381003 (1964).

89 Schuknecht, H. F. & Gacek, M. R. Cochlear pathology in presbycusis. *Ann Otol Rhinol Laryngol* **102**, 1-16, doi:10.1177/00034894931020S101 (1993).

90 Dubno, J. R., Eckert, M. A., Lee, F. S., Matthews, L. J. & Schmiedt, R. A. Classifying human audiometric phenotypes of age-related hearing loss from animal models. *J Assoc Res Otolaryngol* **14**, 687-701, doi:10.1007/s10162-013-0396-x (2013).

91 Wu, P. Z. *et al.* Primary Neural Degeneration in the Human Cochlea: Evidence for Hidden Hearing Loss in the Aging Ear. *Neuroscience* **407**, 8-20, doi:10.1016/j.neuroscience.2018.07.053 (2019).

92 Kujawa, S. G. & Liberman, M. C. Translating animal models to human therapeutics in noise-induced and age-related hearing loss. *Hear Res* **377**, 44-52, doi:10.1016/j.heares.2019.03.003 (2019).

93 Wu, P. Z., O'Malley, J. T., de Gruttola, V. & Liberman, M. C. Primary Neural Degeneration in Noise-Exposed Human Cochleas: Correlations with Outer Hair Cell Loss and Word-Discrimination Scores. *J Neurosci* **41**, 4439-4447, doi:10.1523/JNEUROSCI.3238-20.2021 (2021).

94 Mills, J. H., Schmiedt, R. A. & Kulish, L. F. Age-related changes in auditory potentials of Mongolian gerbil. *Hear Res* **46**, 201-210, doi:10.1016/0378-5955(90)90002-7 (1990).

95 Schmiedt, R. A., Lang, H., Okamura, H. O. & Schulte, B. A. Effects of furosemide applied chronically to the round window: a model of metabolic presbyacusis. *J Neurosci* **22**, 9643-9650 (2002).

96 Mills, D. M. Determining the cause of hearing loss: differential diagnosis using a comparison of audiometric and otoacoustic emission responses. *Ear Hear* **27**, 508-525, doi:10.1097/01.aud.0000233885.02706.ad (2006).

97 Burton, J. A., Mackey, C. A., MacDonald, K. S., Hackett, T. A. & Ramachandran, R. Changes in audiometric threshold and frequency selectivity correlate with cochlear histopathology in macaque monkeys with permanent noise-induced hearing loss. *Hear Res* **398**, 108082, doi:10.1016/j.heares.2020.108082 (2020).

98 Eckert, M. A., Vaden, K. I., Jr. & Dubno, J. R. Age-Related Hearing Loss Associations With Changes in Brain Morphology. *Trends Hear* **23**, 2331216519857267, doi:10.1177/2331216519857267 (2019).

99 Peelle, J. E., Troiani, V., Grossman, M. & Wingfield, A. Hearing loss in older adults affects neural systems supporting speech comprehension. *J Neurosci* **31**, 12638-12643, doi:10.1523/JNEUROSCI.2559-11.2011 (2011).

100 Caspary, D. M., Ling, L., Turner, J. G. & Hughes, L. F. Inhibitory neurotransmission, plasticity and aging in the mammalian central auditory system. *J Exp Biol* **211**, 1781-1791, doi:10.1242/jeb.013581 (2008).

101 Schmiedt, R. A. Effects of aging on potassium homeostasis and the endocochlear potential in the gerbil cochlea. *Hear Res* **102**, 125-132, doi:10.1016/s0378-5955(96)00154-2 (1996).

102 Konrad-Martin, D. *et al.* Age-related changes in the auditory brainstem response. *J Am Acad Audiol* **23**, 18-35; quiz 74-15, doi:10.3766/jaaa.23.1.3 (2012).

103 Bramhall, N. F., Konrad-Martin, D. & McMillan, G. P. Tinnitus and Auditory Perception After a History of Noise Exposure: Relationship to Auditory Brainstem Response Measures. *Ear Hear* **39**, 881-894, doi:10.1097/AUD.0000000000000544 (2018).

104 McClaskey, C. M., Dias, J. W., Dubno, J. R. & Harris, K. C. Reliability of Measures of N1 Peak Amplitude of the Compound Action Potential in Younger and Older Adults. *J Speech Lang Hear Res* **61**, 2422-2430, doi:10.1044/2018_JSLHR-H-18-0097 (2018).

105 Caspary, D. M., Milbrandt, J. C. & Helfert, R. H. Central auditory aging: GABA changes in the inferior colliculus. *Exp Gerontol* **30**, 349-360, doi:10.1016/0531-5565(94)00052-5 (1995).

106 Chen, X. *et al.* Age-associated reduction of asymmetry in human central auditory function: a 1H-magnetic resonance spectroscopy study. *Neural Plast* **2013**, 735290, doi:10.1155/2013/735290 (2013).

107 Brecht, E. J., Barsz, K., Gross, B. & Walton, J. P. Increasing GABA reverses age-related alterations in excitatory receptive fields and intensity coding of

auditory midbrain neurons in aged mice. *Neurobiol Aging* **56**, 87-99, doi:10.1016/j.neurobiolaging.2017.04.003 (2017).

108 Rigters, S. C. *et al.* Hearing Impairment Is Associated with Smaller Brain Volume in Aging. *Front Aging Neurosci* **9**, 2, doi:10.3389/fnagi.2017.00002 (2017).

109 Lin, F. R. *et al.* Association of hearing impairment with brain volume changes in older adults. *Neuroimage* **90**, 84-92, doi:10.1016/j.neuroimage.2013.12.059 (2014).

110 Giroud, N. *et al.* Neuroanatomical and resting state EEG power correlates of central hearing loss in older adults. *Brain Struct Funct* **223**, 145-163, doi:10.1007/s00429-017-1477-0 (2018).

111 Profant, O. *et al.* Diffusion tensor imaging and MR morphometry of the central auditory pathway and auditory cortex in aging. *Neuroscience* **260**, 87-97, doi:10.1016/j.neuroscience.2013.12.010 (2014).

112 Gratton, M. A., Schmiedt, R. A. & Schulte, B. A. Age-related decreases in endocochlear potential are associated with vascular abnormalities in the stria vascularis. *Hear Res* **94**, 116-124, doi:10.1016/0378-5955(96)00011-1 (1996).

113 Cheatham, M. A., Naik, K. & Dallos, P. Using the cochlear microphonic as a tool to evaluate cochlear function in mouse models of hearing. *J Assoc Res Otolaryngol* **12**, 113-125, doi:10.1007/s10162-010-0240-5 (2011).

114 Kamerer, A. M., Diaz, F. J., Peppi, M. & Chertoff, M. E. The potential use of low-frequency tones to locate regions of outer hair cell loss. *Hear Res* **342**, 39-47, doi:10.1016/j.heares.2016.09.006 (2016).

115 Eckert, M. A. *et al.* Translational and interdisciplinary insights into presbyacusis: A multidimensional disease. *Hear Res* **402**, 108109, doi:10.1016/j.heares.2020.108109 (2021).

116 Sewell, W. F. The effects of furosemide on the endocochlear potential and auditory-nerve fiber tuning curves in cats. *Hear Res* **14**, 305-314, doi:10.1016/0378-5955(84)90057-1 (1984).

117 Gates, G. A., Cooper, J. C., Jr., Kannel, W. B. & Miller, N. J. Hearing in the elderly: the Framingham cohort, 1983-1985. Part I. Basic audiometric test results. *Ear Hear* **11**, 247-256 (1990).

118 Moscicki, E. K., Elkins, E. F., Baum, H. M. & McNamara, P. M. Hearing loss in the elderly: an epidemiologic study of the Framingham Heart Study Cohort. *Ear Hear* **6**, 184-190 (1985).

119 Brant, L. J. & Fozard, J. L. Age changes in pure-tone hearing thresholds in a longitudinal study of normal human aging. *J Acoust Soc Am* **88**, 813-820, doi:10.1121/1.399731 (1990).

120 Lin, F. R. *et al.* Hearing loss and incident dementia. *Arch Neurol* **68**, 214-220, doi:10.1001/archneurol.2010.362 (2011).

121 Cruickshanks, K. J. *et al.* Smoking, central adiposity, and poor glycemic control increase risk of hearing impairment. *J Am Geriatr Soc* **63**, 918-924, doi:10.1111/jgs.13401 (2015).

122 Cruickshanks, K. J. *et al.* The 5-year incidence and progression of hearing loss: the epidemiology of hearing loss study. *Arch Otolaryngol Head Neck Surg* **129**, 1041-1046, doi:10.1001/archotol.129.10.1041 (2003).

123 Agrawal, Y., Platz, E. A. & Niparko, J. K. Prevalence of hearing loss and differences by demographic characteristics among US adults: data from the National Health and Nutrition Examination Survey, 1999-2004. *Arch Intern Med* **168**, 1522-1530, doi:10.1001/archinte.168.14.1522 (2008).

124 Gopinath, B. *et al.* Prevalence of age-related hearing loss in older adults: Blue Mountains Study. *Arch Intern Med* **169**, 415-416, doi:10.1001/archinternmed.2008.597 (2009).

125 Reed, N. S. *et al.* Association of Midlife Hypertension with Late-Life Hearing Loss. *Otolaryngol Head Neck Surg* **161**, 996-1003, doi:10.1177/0194599819868145 (2019).

126 Joo, Y. *et al.* The Contribution of Ototoxic Medications to Hearing Loss Among Older Adults. *J Gerontol A Biol Sci Med Sci* **75**, 561-566, doi:10.1093/gerona/glz166 (2020).

127 Ferguson, M. A. & Henshaw, H. Auditory training can improve working memory, attention, and communication in adverse conditions for adults with hearing loss. *Front Psychol* **6**, 556, doi:10.3389/fpsyg.2015.00556 (2015).

128 McLean, W. J. *et al.* Improved Speech Intelligibility in Subjects With Stable Sensorineural Hearing Loss Following Intratympanic Dosing of FX-322 in a Phase 1b Study. *Otol Neurotol* **42**, e849-e857, doi:10.1097/MAO.0000000000003120 (2021).

129 McLean, W. J. *et al.* Clonal Expansion of Lgr5-Positive Cells from Mammalian Cochlea and High-Purity Generation of Sensory Hair Cells. *Cell Rep* **18**, 1917-1929, doi:10.1016/j.celrep.2017.01.066 (2017).

130 Scott, S. K. & Johnsrude, I. S. The neuroanatomical and functional organization of speech perception. *Trends Neurosci* **26**, 100-107, doi:10.1016/S0166-2236(02)00037-1 (2003).

131 Yeend, I., Beach, E. F. & Sharma, M. Working Memory and Extended High-Frequency Hearing in Adults: Diagnostic Predictors of Speech-in-Noise Perception. *Ear Hear* **40**, 458-467, doi:10.1097/AUD.0000000000000640 (2019).

132 Charaziak, K. K., Shera, C. A. & Siegel, J. H. Using Cochlear Microphonic Potentials to Localize Peripheral Hearing Loss. *Front Neurosci* **11**, 169, doi:10.3389/fnins.2017.00169 (2017).

133 Muller, J. & Janssen, T. Impact of occupational noise on pure-tone threshold and distortion product otoacoustic emissions after one workday. *Hear Res* **246**, 9-22, doi:10.1016/j.heares.2008.09.005 (2008).

134 Ren, Y., Landegger, L. D. & Stankovic, K. M. Gene Therapy for Human Sensorineural Hearing Loss. *Front Cell Neurosci* **13**, 323, doi:10.3389/fncel.2019.00323 (2019).

135 Parker, A., Parham, K. & Skoe, E. Reliability of Serological Prestin Levels in Humans and its Relation to Otoacoustic Emissions, a Functional Measure of Outer Hair Cells. *Ear Hear* **42**, 1151-1162, doi:10.1097/AUD.0000000000001026 (2021).

136 Bergevin, C., Verhulst, S. & van Dijk, P. in *Understanding the Cochlea.* Vol. 62 (eds G.A. Manley, A.W. Gummer, A.N. Popper, & R.R. Fay) 287-318. (Springer International Publishing., 2017).

137 Chertoff, M. E., Earl, B. R., Diaz, F. J. & Sorensen, J. L. Analysis of the cochlear microphonic to a low-frequency tone embedded in filtered noise. *J Acoust Soc Am* **132**, 3351-3362, doi:10.1121/1.4757746 (2012).

138 Chertoff, M. E. *et al.* Predicting the location of missing outer hair cells using the electrical signal recorded at the round window. *J Acoust Soc Am* **136**, 1212, doi:10.1121/1.4890641 (2014).

139 Patuzzi, R. B., Yates, G. K. & Johnstone, B. M. Changes in cochlear microphonic and neural sensitivity produced by acoustic trauma. *Hear Res* **39**, 189-202, doi:10.1016/0378-5955(89)90090-7 (1989).

140 Elberling, C. Action potentirals along the cochlear partition recorded from the ear canal in man. *Scandinavian Audiology.* **3**, 13-19. (1974.).

141 Ferraro, J. A. Electrocochleography: a review of recording approaches, clinical applications, and new findings in adults and children. *J Am Acad Audiol* **21**, 145-152, doi:10.3766/jaaa.21.3.2 (2010).

142 Lichtenhan, J. T., Cooper, N. P. & Guinan, J. J., Jr. A new auditory threshold estimation technique for low frequencies: proof of concept. *Ear Hear* **34**, 42-51, doi:10.1097/AUD.0b013e31825f9bd3 (2013).

143 Zhang, M. Using a concha electrode to measure response patterns based on the amplitudes of cochlear microphonic waveforms across acoustic frequencies in normal-hearing subjects. *Ear Hear* **36**, 53-60, doi:10.1097/AUD.0000000000000071 (2015).

144 Dreisbach, L. E. & Siegel, J. H. Distortion-product otoacoustic emissions measured at high frequencies in humans. *J Acoust Soc Am* **110**, 2456-2469, doi:10.1121/1.1406497 (2001).

145 Poling, G. L., Siegel, J. H., Lee, J., Lee, J. & Dhar, S. Characteristics of the 2f(1)-f(2) distortion product otoacoustic emission in a normal hearing population. *J Acoust Soc Am* **135**, 287-299, doi:10.1121/1.4845415 (2014).

146 Charaziak, K. K. & Siegel, J. H. Tuning of SFOAEs Evoked by Low-Frequency Tones Is Not Compatible with Localized Emission Generation. *J Assoc Res Otolaryngol* **16**, 317-329, doi:10.1007/s10162-015-0513-0 (2015).

147 Martin, G. K., Stagner, B. B., Chung, Y. S. & Lonsbury-Martin, B. L. Characterizing distortion-product otoacoustic emission components across four species. *J Acoust Soc Am* **129**, 3090-3103, doi:10.1121/1.3560123 (2011).

148 Lee, H. Y. *et al.* Two-Dimensional Cochlear Micromechanics Measured In Vivo Demonstrate Radial Tuning within the Mouse Organ of Corti. *J Neurosci* **36**, 8160-8173, doi:10.1523/JNEUROSCI.1157-16.2016 (2016).

149 Dewey, J. B., Applegate, B. E. & Oghalai, J. S. Amplification and Suppression of Traveling Waves along the Mouse Organ of Corti: Evidence for Spatial Variation in the Longitudinal Coupling of Outer Hair Cell-Generated Forces. *J Neurosci* **39**, 1805-1816, doi:10.1523/JNEUROSCI.2608-18.2019 (2019).

150 Withnell, R. H. Brief report: the cochlear microphonic as an indication of outer hair cell function. *Ear Hear* **22**, 75-77, doi:10.1097/00003446-200102000-00008 (2001).

151 Liberman, M. C., Zuo, J. & Guinan, J. J., Jr. Otoacoustic emissions without somatic motility: can stereocilia mechanics drive the mammalian cochlea? *J Acoust Soc Am* **116**, 1649-1655, doi:10.1121/1.1775275 (2004).

152 Hood, L. J. Auditory Neuropathy/Auditory Synaptopathy. *Otolaryngol Clin North Am* **54**, 1093-1100, doi:10.1016/j.otc.2021.07.004 (2021).

153 Poling, G. L., Vlosich, B. & Dreisbach, L. E. Emerging distortion product otoacoustic emission techniques to identify preclinical warning signs of basal cochlear dysfunction due to ototoxicity. *Applied Sciences.* **9**, 3132. (2019).

154 Reavis, K. M. *et al.* Distortion-product otoacoustic emission test performance for ototoxicity monitoring. *Ear Hear* **32**, 61-74, doi:10.1097/AUD.0b013e3181e8b6a7 (2011).

155 Reavis, K. M. *et al.* Factors affecting sensitivity of distortion-product otoacoustic emissions to ototoxic hearing loss. *Ear Hear* **29**, 875-893, doi:10.1097/AUD.0b013e318181ad99 (2008).

156 Gibson, W. P. & Sanli, H. Auditory neuropathy: an update. *Ear Hear* **28**, 102S-106S, doi:10.1097/AUD.0b013e3180315392 (2007).

157 Gates, G. A., Mills, D., Nam, B. H., D'Agostino, R. & Rubel, E. W. Effects of age on the distortion product otoacoustic emission growth functions. *Hear Res* **163**, 53-60, doi:10.1016/s0378-5955(01)00377-x (2002).

158 Lapsley Miller, J. A., Marshall, L. & Heller, L. M. A longitudinal study of changes in evoked otoacoustic emissions and pure-tone thresholds as measured in a hearing conservation program. *Int J Audiol* **43**, 307-322, doi:10.1080/14992020400050040 (2004).

159 Verpy, E. *et al.* Stereocilin-deficient mice reveal the origin of cochlear waveform distortions. *Nature* **456**, 255-258, doi:10.1038/nature07380 (2008).

160 Cheatham, M. A., Katz, E. D., Charaziak, K. K., Dallos, P. & Siegel, J. in *What Fire Is In Mine Ears: Progress in Auditory Biomechanics.* 383-388 (American Institute of Physics.).

161 Dallos, P. *et al.* Prestin-based outer hair cell motility is necessary for mammalian cochlear amplification. *Neuron* **58**, 333-339, doi:10.1016/j.neuron.2008.02.028 (2008).

162 Pickles, J. O. in *The Human Auditory System*. Vol. 129 (eds G.G. Celesia & G. Hickok) Ch. 1, 3-25 (Elsevier, B.V., 2015).

163 Voss, S. E., Rosowski, J. J. & Peake, W. T. Is the pressure difference between the oval and round windows the effective acoustic stimulus for the cochlea? *J Acoust Soc Am* **100**, 1602-1616, doi:10.1121/1.416062 (1996).

164 Dallos, P. Cochlear amplification, outer hair cells and prestin. *Curr Opin Neurobiol* **18**, 370-376, doi:10.1016/j.conb.2008.08.016 (2008).

165 Békésy, G. V. The Variation of Phase Along the Basilar Membrane with Sinusoidal Vibrations. *J Acoust Soc Am* **19**, 452-460 (1947).

166 Goodyear, R. J. & Richardson, G. P. Structure, Function, and Development of the Tectorial Membrane: An Extracellular Matrix Essential for Hearing. *Curr Top Dev Biol* **130**, 217-244, doi:10.1016/bs.ctdb.2018.02.006 (2018).

167 Hakizimana, P. & Fridberger, A. Inner hair cell stereocilia are embedded in the tectorial membrane. *Nat Commun* **12**, 2604, doi:10.1038/s41467-021-22870-1 (2021).

168 Slepecky, N. B. in *The Cochlea.* Vol. 8 (eds P. Dallos, A.N. Popper, & R.R. Fay) Ch. 2, 44-129. (Springer., 1996).

169 Chien, W. *et al.* Measurements of stapes velocity in live human ears. *Hear Res* **249**, 54-61, doi:10.1016/j.heares.2008.11.011 (2009).

170 Reichenbach, T. & Hudspeth, A. J. The physics of hearing: fluid mechanics and the active process of the inner ear. *Rep Prog Phys* **77**, 076601, doi:10.1088/0034-4885/77/7/076601 (2014).

171 Johnstone, B. M. & Boyle, A. J. Basilar membrane vibration examined with the Mossbauer technique. *Science* **158**, 389-390, doi:10.1126/science.158.3799.389 (1967).

172 Rhode, W. S. in *Basic Mechanisms in Hearing* (ed A. Moller) 49-68. (Academic, 1973).

173 Sellick, P. M., Patuzzi, R. & Johnstone, B. M. Measurement of basilar membrane motion in the guinea pig using the Mossbauer technique. *J Acoust Soc Am* **72**, 131-141, doi:10.1121/1.387996 (1982).

174 Ruggero, M. A. & Rich, N. C. Furosemide alters organ of corti mechanics: evidence for feedback of outer hair cells upon the basilar membrane. *J Neurosci* **11**, 1057-1067 (1991).

175 Ashmore, J. *et al.* The remarkable cochlear amplifier. *Hear Res* **266**, 1-17, doi:10.1016/j.heares.2010.05.001 (2010).

176 Fettiplace, R. Hair Cell Transduction, Tuning, and Synaptic Transmission in the Mammalian Cochlea. *Compr Physiol* **7**, 1197-1227, doi:10.1002/cphy.c160049 (2017).

177 Dewey, J. B., Altoe, A., Shera, C. A., Applegate, B. E. & Oghalai, J. S. Cochlear outer hair cell electromotility enhances organ of Corti motion on a cycle-by-cycle basis at high frequencies in vivo. *Proc Natl Acad Sci U S A* **118**, doi:10.1073/pnas.2025206118 (2021).

178 Ren, T., He, W. & Kemp, D. Reticular lamina and basilar membrane vibrations in living mouse cochleae. *Proc Natl Acad Sci U S A* **113**, 9910-9915, doi:10.1073/pnas.1607428113 (2016).

179 Ruggero, M. A. Responses to sound of the basilar membrane of the mammalian cochlea. *Curr Opin Neurobiol* **2**, 449-456, doi:10.1016/0959-4388(92)90179-o (1992).

180 Ren, T. Reverse propagation of sound in the gerbil cochlea. *Nat Neurosci* **7**, 333-334, doi:10.1038/nn1216 (2004).

181 Kemp, D. T. Evidence of mechanical nonlinearity and frequency selective wave amplification in the cochlea. *Arch Otorhinolaryngol* **224**, 37-45, doi:10.1007/BF00455222 (1979).

182 Probst, R., Coats, A. C., Martin, G. K. & Lonsbury-Martin, B. L. Spontaneous, click-, and toneburst-evoked otoacoustic emissions from normal ears. *Hear Res* **21**, 261-275, doi:10.1016/0378-5955(86)90224-8 (1986).

183 Hubbard, A. E. & Mountain, D. C. Alternating current delivered into the scala media alters sound pressure at the eardrum. *Science* **222**, 510-512, doi:10.1126/science.6623090 (1983).

184 Nuttall, A. L. & Ren, T. Electromotile hearing: evidence from basilar membrane motion and otoacoustic emissions. *Hear Res* **92**, 170-177, doi:10.1016/0378-5955(95)00216-2 (1995).

185 Henry, K. S., Snyder, S. F. & Heinz, M. in *International Congrees on Acoustics* (Acoustical Society of America.).

186 Alam, S. A. *et al.* Cisplatin-induced apoptotic cell death in Mongolian gerbil cochlea. *Hear Res* **141**, 28-38, doi:10.1016/s0378-5955(99)00211-7 (2000).

187 Breglio, A. M. *et al.* Cisplatin is retained in the cochlea indefinitely following chemotherapy. *Nat Commun* **8**, 1654, doi:10.1038/s41467-017-01837-1 (2017).

188 Helleman, H. W., Eising, H., Limpens, J. & Dreschler, W. A. Otoacoustic emissions versus audiometry in monitoring hearing loss after long-term noise exposure - a systematic review. *Scand J Work Environ Health* **44**, 585-600, doi:10.5271/sjweh.3725 (2018).

189 Vasilyeva, O. N., Frisina, S. T., Zhu, X., Walton, J. P. & Frisina, R. D. Interactions of hearing loss and diabetes mellitus in the middle age CBA/CaJ mouse model of presbycusis. *Hear Res* **249**, 44-53, doi:10.1016/j.heares.2009.01.007 (2009).

190 Voss, S. E. *et al.* Posture systematically alters ear-canal reflectance and DPOAE properties. *Hear Res* **263**, 43-51, doi:10.1016/j.heares.2010.03.003 (2010).

191 Cheatham, M. A. *et al.* Loss of the tectorial membrane protein CEACAM16 enhances spontaneous, stimulus-frequency, and transiently evoked otoacoustic emissions. *J Neurosci* **34**, 10325-10338, doi:10.1523/JNEUROSCI.1256-14.2014 (2014).

192 Lonsbury-Martin, B. L., Stagner, B. B. & Martin, G. K. in *Acoustics Today* Vol. 13 44-51. (2017).

193 Liberman, M. C., Epstein, M. J., Cleveland, S. S., Wang, H. & Maison, S. F. Toward a Differential Diagnosis of Hidden Hearing Loss in Humans. *PLoS One* **11**, e0162726, doi:10.1371/journal.pone.0162726 (2016).

194 Goodman, S. S., Lee, C., Guinan, J. J., Jr. & Lichtenhan, J. T. The Spatial Origins of Cochlear Amplification Assessed by Stimulus-Frequency Otoacoustic Emissions. *Biophys J* **118**, 1183-1195, doi:10.1016/j.bpj.2019.12.031 (2020).

195 Shera, C. A. & Guinan, J. J., Jr. Evoked otoacoustic emissions arise by two fundamentally different mechanisms: a taxonomy for mammalian OAEs. *J Acoust Soc Am* **105**, 782-798, doi:10.1121/1.426948 (1999).

196 Gorga, M. P. *et al.* From laboratory to clinic: a large scale study of distortion product otoacoustic emissions in ears with normal hearing and ears with hearing loss. *Ear Hear* **18**, 440-455, doi:10.1097/00003446-199712000-00003 (1997).

197 Dewey, J. B. & Dhar, S. Profiles of Stimulus-Frequency Otoacoustic Emissions from 0.5 to 20 kHz in Humans. *J Assoc Res Otolaryngol* **18**, 89-110, doi:10.1007/s10162-016-0588-2 (2017).

198 Zweig, G. & Shera, C. A. The origin of periodicity in the spectrum of evoked otoacoustic emissions. *J Acoust Soc Am* **98**, 2018-2047, doi:10.1121/1.413320 (1995).

199 Lonsbury-Martin, B. L., Martin, G. K., Probst, R. & Coats, A. C. Spontaneous otoacoustic emissions in a nonhuman primate. II. Cochlear anatomy. *Hear Res* **33**, 69-93, doi:10.1016/0378-5955(88)90021-4 (1988).

200 Ruggero, M. A., Kramek, B. & Rich, N. C. Spontaneous otoacoustic emissions in a dog. *Hear Res* **13**, 293-296, doi:10.1016/0378-5955(84)90083-2 (1984).

201 Clark, W. W., Kim, D. O., Zurek, P. M. & Bohne, B. A. Spontaneous otoacoustic emissions in chinchilla ear canals: correlation with histopathology and suppression by external tones. *Hear Res* **16**, 299-314, doi:10.1016/0378-5955(84)90119-9 (1984).

202 Elliott, E. A ripple effect in the audiogram. *Nature* **181**, 1076, doi:10.1038/1811076a0 (1958).

203 Kemp, D. T. The evoked cochlear mechanical response and the auditory microstructure - evidence for a new element in cochlear mechanics. *Scand Audiol Suppl*, 35-47 (1979).

204 Shera, C. A. & Zweig, G. Noninvasive measurement of the cochlear traveling-wave ratio. *J Acoust Soc Am* **93**, 3333-3352, doi:10.1121/1.405717 (1993).

205 Talmadge, C. L., Tubis, A., Long, G. R. & Piskorski, P. Modeling otoacoustic emission and hearing threshold fine structures. *J Acoust Soc Am* **104**, 1517-1543, doi:10.1121/1.424364 (1998).

206 Long, G. R. & Tubis, A. Investigations into the nature of the association between threshold microstructure and otoacoustic emissions. *Hear Res* **36**, 125-138, doi:10.1016/0378-5955(88)90055-x (1988).

207 Dewey, J. B. & Dhar, S. A common microstructure in behavioral hearing thresholds and stimulus-frequency otoacoustic emissions. *J Acoust Soc Am* **142**, 3069, doi:10.1121/1.5009562 (2017).

208 Baiduc, R. R., Lee, J. & Dhar, S. Spontaneous otoacoustic emissions, threshold microstructure, and psychophysical tuning over a wide frequency range in humans. *J Acoust Soc Am* **135**, 300-314, doi:10.1121/1.4840775 (2014).

209 Bergevin, C., Freeman, D. M., Saunders, J. C. & Shera, C. A. Otoacoustic emissions in humans, birds, lizards, and frogs: evidence for multiple generation mechanisms. *J Comp Physiol A Neuroethol Sens Neural Behav Physiol* **194**, 665-683, doi:10.1007/s00359-008-0338-y (2008).

210 Bergevin, C. Comparison of otoacoustic emissions within gecko subfamilies: morphological implications for auditory function in lizards. *J Assoc Res Otolaryngol* **12**, 203-217, doi:10.1007/s10162-010-0253-0 (2011).

211 Goodyear, R. J. *et al.* Accelerated Age-Related Degradation of the Tectorial Membrane in the Ceacam16(betagal/betagal) Null Mutant Mouse, a Model for Late-Onset Human Hereditary Deafness DFNB113. *Front Mol Neurosci* **12**, 147, doi:10.3389/fnmol.2019.00147 (2019).

212 Cheatham, M. A. *et al.* Increased Spontaneous Otoacoustic Emissions in Mice with a Detached Tectorial Membrane. *J Assoc Res Otolaryngol* **17**, 81-88, doi:10.1007/s10162-015-0551-7 (2016).

213 Cheatham, M. A., Zhou, Y., Goodyear, R. J., Dallos, P. & Richardson, G. P. Spontaneous Otoacoustic Emissions in Tecta(Y1870C/+) Mice Reflect Changes in Cochlear Amplification and How It Is Controlled by the Tectorial Membrane. *eNeuro* **5**, doi:10.1523/ENEURO.0314-18.2018 (2018).

214 Abdala, C., Guardia, Y. C. & Shera, C. A. Swept-tone stimulus-frequency otoacoustic emissions: Normative data and methodological considerations. *J Acoust Soc Am* **143**, 181, doi:10.1121/1.5020275 (2018).

215 Abdala, C., Luo, P. & Guardia, Y. Swept-Tone Stimulus-Frequency Otoacoustic Emissions in Human Newborns. *Trends Hear* **23**, 2331216519889226, doi:10.1177/2331216519889226 (2019).

216 Kalluri, R. & Abdala, C. Stimulus-frequency otoacoustic emissions in human newborns. *J Acoust Soc Am* **137**, EL78-84, doi:10.1121/1.4903915 (2015).

217 Wright, A., Davis, A., Bredberg, G., Ulehlova, L. & Spencer, H. Hair cell distributions in the normal human cochlea. *Acta Otolaryngol Suppl* **444**, 1-48 (1987).

218 Rao, A. & Long, G. R. Effects of aspirin on distortion product fine structure: interpreted by the two-source model for distortion product otoacoustic emissions generation. *J Acoust Soc Am* **129**, 792-800, doi:10.1121/1.3523308 (2011).

219 Henin, S., Thompson, S., Abdelrazeq, S. & Long, G. R. Changes in amplitude and phase of distortion-product otoacoustic emission fine-structure and

separated components during efferent activation. *J Acoust Soc Am* **129**, 2068-2079, doi:10.1121/1.3543945 (2011).

220 Abdala, C. & Dhar, S. Maturation and aging of the human cochlea: a view through the DPOAE looking glass. *J Assoc Res Otolaryngol* **13**, 403-421, doi:10.1007/s10162-012-0319-2 (2012).

221 Burns, E. M. Even-longer-term stability of spontaneous otoacoustic emissions. *J Acoust Soc Am* **142**, 1828, doi:10.1121/1.5005607 (2017).

222 Siegel, J. H. *et al.* Delays of stimulus-frequency otoacoustic emissions and cochlear vibrations contradict the theory of coherent reflection filtering. *J Acoust Soc Am* **118**, 2434-2443, doi:10.1121/1.2005867 (2005).

223 Schairer, K. S., Ellison, J. C., Fitzpatrick, D. & Keefe, D. H. Use of stimulus-frequency otoacoustic emission latency and level to investigate cochlear mechanics in human ears. *J Acoust Soc Am* **120**, 901-914, doi:10.1121/1.2214147 (2006).

224 Wilson, U. S. *et al.* Relationship Between Behavioral and Stimulus Frequency Otoacoustic Emissions Delay-Based Tuning Estimates. *J Speech Lang Hear Res* **63**, 1958-1968, doi:10.1044/2020_JSLHR-19-00386 (2020).

225 Charaziak, K. K., Souza, P. E. & Siegel, J. H. Exploration of stimulus-frequency otoacoustic emission suppression tuning in hearing-impaired listeners. *Int J Audiol* **54**, 96-105, doi:10.3109/14992027.2014.941074 (2015).

226 Margolis, R. H. & Heller, J. W. Screening tympanometry: criteria for medical referral. *Audiology* **26**, 197-208, doi:10.3109/00206098709081549 (1987).

227 Groon, K. A., Rasetshwane, D. M., Kopun, J. G., Gorga, M. P. & Neely, S. T. Air-leak effects on ear-canal acoustic absorbance. *Ear Hear* **36**, 155-163, doi:10.1097/AUD.0000000000000077 (2015).

228 Keefe, D. H., Bulen, J. C., Arehart, K. H. & Burns, E. M. Ear-canal impedance and reflection coefficient in human infants and adults. *J Acoust Soc Am* **94**, 2617-2638, doi:10.1121/1.407347 (1993).

229 Abdala, C., Luo, P. & Shera, C. A. Characterizing spontaneous otoacoustic emissions across the human lifespan. *J Acoust Soc Am* **141**, 1874, doi:10.1121/1.4977192 (2017).

230 Long, G. R. & Talmadge, C. L. Spontaneous otoacoustic emission frequency is modulated by heartbeat. *J Acoust Soc Am* **102**, 2831-2848, doi:10.1121/1.420339 (1997).

231 Robles, L. & Ruggero, M. A. Mechanics of the mammalian cochlea. *Physiol Rev* **81**, 1305-1352, doi:10.1152/physrev.2001.81.3.1305 (2001).

232 Zwicker, E. & Schloth, E. Interrelation of different oto-acoustic emissions. *J Acoust Soc Am* **75**, 1148-1154, doi:10.1121/1.390763 (1984).

233 Gorga, M. P. *et al.* Otoacoustic emissions from normal-hearing and hearing-impaired subjects: distortion product responses. *J Acoust Soc Am* **93**, 2050-2060, doi:10.1121/1.406691 (1993).

234 Gorga, M. P., Neely, S. T. & Dorn, P. A. Distortion product otoacoustic emission test performance for a priori criteria and for multifrequency

audiometric standards. *Ear Hear* **20**, 345-362, doi:10.1097/00003446-199908000-00007 (1999).

235 Kemp, D. T., Ryan, S. & Bray, P. A guide to the effective use of otoacoustic emissions. *Ear Hear* **11**, 93-105, doi:10.1097/00003446-199004000-00004 (1990).

236 Gorga, M. P., Neely, S. T., Dorn, P. A. & Hoover, B. M. Further efforts to predict pure-tone thresholds from distortion product otoacoustic emission input/output functions. *J Acoust Soc Am* **113**, 3275-3284, doi:10.1121/1.1570433 (2003).

237 Zelle, D., Lorenz, L., Thiericke, J. P., Gummer, A. W. & Dalhoff, E. Input-output functions of the nonlinear-distortion component of distortion-product otoacoustic emissions in normal and hearing-impaired human ears. *J Acoust Soc Am* **141**, 3203, doi:10.1121/1.4982923 (2017).

238 Gorga, M. P., Neely, S. T., Kopun, J. & Tan, H. Distortion-product otoacoustic emission suppression tuning curves in humans. *J Acoust Soc Am* **129**, 817-827, doi:10.1121/1.3531864 (2011).

239 Abdala, C., Sininger, Y. S., Ekelid, M. & Zeng, F. G. Distortion product otoacoustic emission suppression tuning curves in human adults and neonates. *Hear Res* **98**, 38-53, doi:10.1016/0378-5955(96)00056-1 (1996).

240 Avan, P., Bonfils, P., Loth, D., Narcy, P. & Trotoux, J. Quantitative assessment of human cochlear function by evoked otoacoustic emissions. *Hear Res* **52**, 99-112, doi:10.1016/0378-5955(91)90191-b (1991).

241 Ellison, J. C. & Keefe, D. H. Audiometric predictions using stimulus-frequency otoacoustic emissions and middle ear measurements. *Ear Hear* **26**, 487-503, doi:10.1097/01.aud.0000179692.81851.3b (2005).

242 Goodman, S. S., Fitzpatrick, D. F., Ellison, J. C., Jesteadt, W. & Keefe, D. H. High-frequency click-evoked otoacoustic emissions and behavioral thresholds in humans. *J Acoust Soc Am* **125**, 1014-1032, doi:10.1121/1.3056566 (2009).

243 Shera, C. A., Tubis, A. & Talmadge, C. L. Testing coherent reflection in chinchilla: Auditory-nerve responses predict stimulus-frequency emissions. *J Acoust Soc Am* **124**, 381-395, doi:10.1121/1.2917805 (2008).

244 Moleti, A., Longo, F. & Sisto, R. Time-frequency domain filtering of evoked otoacoustic emissions. *J Acoust Soc Am* **132**, 2455-2467, doi:10.1121/1.4751537 (2012).

245 Joris, P. X. *et al.* Frequency selectivity in Old-World monkeys corroborates sharp cochlear tuning in humans. *Proc Natl Acad Sci U S A* **108**, 17516-17520, doi:10.1073/pnas.1105867108 (2011).

246 Shera, C. A., Guinan, J. J., Jr. & Oxenham, A. J. Revised estimates of human cochlear tuning from otoacoustic and behavioral measurements. *Proc Natl Acad Sci U S A* **99**, 3318-3323, doi:10.1073/pnas.032675099 (2002).

247 Sumner, C. J. *et al.* Mammalian behavior and physiology converge to confirm sharper cochlear tuning in humans. *Proc Natl Acad Sci U S A* **115**, 11322-11326, doi:10.1073/pnas.1810766115 (2018).

248 Levitt, H. Transformed up-down methods in psychoacoustics. *J Acoust Soc Am* **49**, Suppl 2:467+ (1971).

249 Dhar, S., Rogers, A. & Abdala, C. Breaking away: violation of distortion emission phase-frequency invariance at low frequencies. *J Acoust Soc Am* **129**, 3115-3122, doi:10.1121/1.3569732 (2011).

250 Boege, P. & Janssen, T. Pure-tone threshold estimation from extrapolated distortion product otoacoustic emission I/O-functions in normal and cochlear hearing loss ears. *J Acoust Soc Am* **111**, 1810-1818, doi:10.1121/1.1460923 (2002).

251 Verhulst, S., Jagadeesh, A., Mauermann, M. & Ernst, F. Individual Differences in Auditory Brainstem Response Wave Characteristics: Relations to Different Aspects of Peripheral Hearing Loss. *Trends Hear* **20**, doi:10.1177/2331216516672186 (2016).

252 Ortmann, A. J. & Abdala, C. Changes in the Compressive Nonlinearity of the Cochlea During Early Aging: Estimates From Distortion OAE Input/Output Functions. *Ear Hear* **37**, 603-614, doi:10.1097/AUD.0000000000000319 (2016).

253 Schairer, K. S., Fitzpatrick, D. & Keefe, D. H. Input-output functions for stimulus-frequency otoacoustic emissions in normal-hearing adult ears. *J Acoust Soc Am* **114**, 944-966, doi:10.1121/1.1592799 (2003).

254 Gong, Q., Liu, Y. & Peng, Z. Estimating Hearing Thresholds From Stimulus-Frequency Otoacoustic Emissions. *Trends Hear* **24**, 2331216520960053, doi:10.1177/2331216520960053 (2020).

255 Musiek, F. E. & Baran, J. A. Distortion product otoacoustic emissions: hit and false-positive rates in normal-hearing and hearing-impaired subjects. *Am J Otol* **18**, 454-461 (1997).

256 Bakdash, J. Z. & Marusich, L. R. Repeated Measures Correlation. *Front Psychol* **8**, 456, doi:10.3389/fpsyg.2017.00456 (2017).

257 Stelmachowicz, P. G., Beauchaine, K. A., Kalberer, A. & Jesteadt, W. Normative thresholds in the 8- to 20-kHz range as a function of age. *J Acoust Soc Am* **86**, 1384-1391, doi:10.1121/1.398698 (1989).

258 Charaziak, K. K., Souza, P. & Siegel, J. H. Stimulus-frequency otoacoustic emission suppression tuning in humans: comparison to behavioral tuning. *J Assoc Res Otolaryngol* **14**, 843-862, doi:10.1007/s10162-013-0412-1 (2013).

259 Dhar, S., Talmadge, C. L., Long, G. R. & Tubis, A. Multiple internal reflections in the cochlea and their effect on DPOAE fine structure. *J Acoust Soc Am* **112**, 2882-2897, doi:10.1121/1.1516757 (2002).

260 Charaziak, K. K. & Shera, C. A. Compensating for ear-canal acoustics when measuring otoacoustic emissions. *J Acoust Soc Am* **141**, 515, doi:10.1121/1.4973618 (2017).

261 Sisto, R., Sanjust, F. & Moleti, A. Input/output functions of different-latency components of transient-evoked and stimulus-frequency otoacoustic emissions. *J Acoust Soc Am* **133**, 2240-2253, doi:10.1121/1.4794382 (2013).

262 Boothalingam, S. & Goodman, S. S. Click evoked middle ear muscle reflex: Spectral and temporal aspects. *J Acoust Soc Am* **149**, 2628, doi:10.1121/10.0004217 (2021).

263 Robles, L., Ruggero, M. A. & Rich, N. C. Basilar membrane mechanics at the base of the chinchilla cochlea. I. Input-output functions, tuning curves, and response phases. *J Acoust Soc Am* **80**, 1364-1374, doi:10.1121/1.394389 (1986).

264 Ruggero, M. A., Rich, N. C., Recio, A., Narayan, S. S. & Robles, L. Basilar-membrane responses to tones at the base of the chinchilla cochlea. *J Acoust Soc Am* **101**, 2151-2163, doi:10.1121/1.418265 (1997).

265 Konrad-Martin, D. *et al.* Sources of DPOAEs revealed by suppression experiments, inverse fast Fourier transforms, and SFOAEs in impaired ears. *J Acoust Soc Am* **111**, 1800-1809, doi:10.1121/1.1455024 (2002).

266 Puria, S. Measurements of human middle ear forward and reverse acoustics: implications for otoacoustic emissions. *J Acoust Soc Am* **113**, 2773-2789, doi:10.1121/1.1564018 (2003).

267 Stieger, C., Rosowski, J. J. & Nakajima, H. H. Comparison of forward (ear-canal) and reverse (round-window) sound stimulation of the cochlea. *Hear Res* **301**, 105-114, doi:10.1016/j.heares.2012.11.005 (2013).

268 Oxenham, A. J. How We Hear: The Perception and Neural Coding of Sound. *Annu Rev Psychol* **69**, 27-50, doi:10.1146/annurev-psych-122216-011635 (2018).

269 Moore, B. C. Dead regions in the cochlea: diagnosis, perceptual consequences, and implications for the fitting of hearing AIDS. *Trends Amplif* **5**, 1-34, doi:10.1177/108471380100500102 (2001).

270 Chistovich, L. A. Frequency characteristics of the masking effect. *Biophys J* **2**, 714-725 (1957).

271 Small, A. M. Pure-tone masking. *J Acoust Soc Am* **31**, 1619-1625 (1959).

272 Zwicker, E. in *Facts and models in hearing* 132-141 (Springer, 1974).

273 Moore, B. C. Psychophysical tuning curves measured in simultaneous and forward masking. *J Acoust Soc Am* **63**, 524-532, doi:10.1121/1.381752 (1978).

274 Sek, A., Alcantara, J., Moore, B. C., Kluk, K. & Wicher, A. Development of a fast method for determining psychophysical tuning curves. *Int J Audiol* **44**, 408-420, doi:10.1080/14992020500060800 (2005).

275 Sek, A. & Moore, B. C. Implementation of a fast method for measuring psychophysical tuning curves. *Int J Audiol* **50**, 237-242, doi:10.3109/14992027.2010.550636 (2011).

276 Malicka, A. N., Munro, K. J., Baer, T., Baker, R. J. & Moore, B. C. The effect of low-pass filtering on identification of nonsense syllables in quiet by school-age children with and without cochlear dead regions. *Ear Hear* **34**, 458-469, doi:10.1097/AUD.0b013e3182775982 (2013).

277 Malicka, A. N., Munro, K. J. & Baker, R. J. Fast method for psychophysical tuning curve measurement in school-age children. *Int J Audiol* **48**, 546-553, doi:10.1080/14992020902845899 (2009).

278 Narayan, S. S., Temchin, A. N., Recio, A. & Ruggero, M. A. Frequency tuning of basilar membrane and auditory nerve fibers in the same cochleae. *Science* **282**, 1882-1884, doi:10.1126/science.282.5395.1882 (1998).

279 de Boer, E. & Viergever, M. A. Wave propagation and dispersion in the cochlea. *Hear Res* **13**, 101-112, doi:10.1016/0378-5955(84)90101-1 (1984).

280 Patuzzi, R. in *The Cochlea* (ed P. Dallos) 186-257 (Springer, 1996).

281 Carney, A. E. & Nelson, D. A. An analysis of psychophysical tuning curves in normal and pathological ears. *J Acoust Soc Am* **73**, 268-278, doi:10.1121/1.388860 (1983).

282 Charaziak, K. K., Souza, P. & Siegel, J. H. Time-efficient measures of auditory frequency selectivity. *Int J Audiol* **51**, 317-325, doi:10.3109/14992027.2011.625982 (2012).

283 Buus, S. R., Florentine, M. & Mason, C. R. in *Auditory Frequency Selectivity* 341-350 (Springer, 1986).

284 Moleti, A. & Sisto, R. Estimating cochlear tuning dependence on stimulus level and frequency from the delay of otoacoustic emissions. *J Acoust Soc Am* **140**, 945, doi:10.1121/1.4960588 (2016).

285 Shera, C. A. & Guinan, J. J., Jr. Stimulus-frequency-emission group delay: a test of coherent reflection filtering and a window on cochlear tuning. *J Acoust Soc Am* **113**, 2762-2772, doi:10.1121/1.1557211 (2003).

286 Yasin, I. & Plack, C. J. Psychophysical tuning curves at very high frequencies. *J Acoust Soc Am* **118**, 2498-2506, doi:10.1121/1.2035594 (2005).

287 Liberman, M. C. & Dodds, L. W. Single-neuron labeling and chronic cochlear pathology. III. Stereocilia damage and alterations of threshold tuning curves. *Hear Res* **16**, 55-74, doi:10.1016/0378-5955(84)90025-x (1984).

288 Ryan, A., Dallos, P. & McGee, T. Psychophysical tuning curves and auditory thresholds after hair cell damage in the chinchilla. *J Acoust Soc Am* **66**, 370-378, doi:10.1121/1.383194 (1979).

289 Liberman, M. C. & Kiang, N. Y. Acoustic trauma in cats. Cochlear pathology and auditory-nerve activity. *Acta Otolaryngol Suppl* **358**, 1-63 (1978).

290 Talmadge, C. L., Tubis, A., Long, G. R. & Tong, C. Modeling the combined effects of basilar membrane nonlinearity and roughness on stimulus frequency otoacoustic emission fine structure. *J Acoust Soc Am* **108**, 2911-2932, doi:10.1121/1.1321012 (2000).

291 Zhao, W., Dewey, J. B., Boothalingam, S. & Dhar, S. Efferent Modulation of Stimulus Frequency Otoacoustic Emission Fine Structure. *Front Syst Neurosci* **9**, 168, doi:10.3389/fnsys.2015.00168 (2015).

292 Shera, C. A. & Bergevin, C. Obtaining reliable phase-gradient delays from otoacoustic emission data. *J Acoust Soc Am* **132**, 927-943, doi:10.1121/1.4730916 (2012).

293 Lineton, B. & Wildgoose, C. M. Comparing two proposed measures of cochlear mechanical filter bandwidth based on stimulus frequency otoacoustic emissions. *J Acoust Soc Am* **125**, 1558-1566, doi:10.1121/1.3068452 (2009).

294 Francis, N. A. & Guinan, J. J., Jr. Acoustic stimulation of human medial olivocochlear efferents reduces stimulus-frequency and click-evoked otoacoustic emission delays: Implications for cochlear filter bandwidths. *Hear Res* **267**, 36-45, doi:10.1016/j.heares.2010.04.009 (2010).

295 Moleti, A., Pistilli, D. & Sisto, R. Evidence for apical-basal transition in the delay of the reflection components of otoacoustic emissions. *J Acoust Soc Am* **141**, 116, doi:10.1121/1.4973866 (2017).

296 Goodman, S. S., Withnell, R. H. & Shera, C. A. The origin of SFOAE microstructure in the guinea pig. *Hear Res* **183**, 7-17, doi:10.1016/s0378-5955(03)00193-x (2003).

297 Choi, Y. S., Lee, S. Y., Parham, K., Neely, S. T. & Kim, D. O. Stimulus-frequency otoacoustic emission: measurements in humans and simulations with an active cochlear model. *J Acoust Soc Am* **123**, 2651-2669, doi:10.1121/1.2902184 (2008).

298 Shera, C. A. & Charaziak, K. K. Cochlear Frequency Tuning and Otoacoustic Emissions. *Cold Spring Harb Perspect Med* **9**, doi:10.1101/cshperspect.a033498 (2019).

299 Olson, E. S. Direct measurement of intra-cochlear pressure waves. *Nature* **402**, 526-529, doi:10.1038/990092 (1999).

300 Shera, C. A. in *Biophysics of the Cochlea* 439-453 (2003).

301 Ruggero, M. A. & Temchin, A. N. Unexceptional sharpness of frequency tuning in the human cochlea. *Proc Natl Acad Sci U S A* **102**, 18614-18619, doi:10.1073/pnas.0509323102 (2005).

302 Sisto, R., Moleti, A. & Altoe, A. Decoupling the level dependence of the basilar membrane gain and phase in nonlinear cochlea models. *J Acoust Soc Am* **138**, EL155-160, doi:10.1121/1.4928291 (2015).

303 Sisto, R., Moleti, A. & Shera, C. A. On the spatial distribution of the reflection sources of different latency components of otoacoustic emissions. *J Acoust Soc Am* **137**, 768-776, doi:10.1121/1.4906583 (2015).

304 Sisto, R. & Moleti, A. On the frequency dependence of the otoacoustic emission latency in hypoacoustic and normal ears. *J Acoust Soc Am* **111**, 297-308, doi:10.1121/1.1428547 (2002).

305 Keefe, D. H., Ellison, J. C., Fitzpatrick, D. F. & Gorga, M. P. Two-tone suppression of stimulus frequency otoacoustic emissions. *J Acoust Soc Am* **123**, 1479-1494, doi:10.1121/1.2828209 (2008).

306 Moleti, A. & Sisto, R. Localization of the Reflection Sources of Stimulus-Frequency Otoacoustic Emissions. *J Assoc Res Otolaryngol* **17**, 393-401, doi:10.1007/s10162-016-0580-x (2016).

307 Wilson, U. S. *et al.* Cochlear tuning estimates from level ratio functions of distortion product otoacoustic emissions. *Int J Audiol* **60**, 890-899, doi:10.1080/14992027.2021.1886352 (2021).

308 Lasky, R. E., Snodgrass, E. B., Laughlin, N. K. & Hecox, K. E. Distortion product otoacoustic emissions in Macaca mulatta and humans. *Hear Res* **89**, 35-51, doi:10.1016/0378-5955(95)00120-1 (1995).

309 Valero, M. D., Pasanen, E. G., McFadden, D. & Ratnam, R. Distortion-product otoacoustic emissions in the common marmoset (Callithrix jacchus): parameter optimization. *Hear Res* **243**, 57-68, doi:10.1016/j.heares.2008.05.006 (2008).

310 Moore, B. C. & Alcantara, J. I. The use of psychophysical tuning curves to explore dead regions in the cochlea. *Ear Hear* **22**, 268-278, doi:10.1097/00003446-200108000-00002 (2001).

311 Glasberg, B. R. & Moore, B. C. Derivation of auditory filter shapes from notched-noise data. *Hear Res* **47**, 103-138, doi:10.1016/0378-5955(90)90170-t (1990).

312 Bentsen, T., Harte, J. M. & Dau, T. Human cochlear tuning estimates from stimulus-frequency otoacoustic emissions. *J Acoust Soc Am* **129**, 3797-3807, doi:10.1121/1.3575596 (2011).

313 Marshall, L., Lapsley Miller, J. A. & Heller, L. M. Distortion-Product Otoacoustic Emissions as a Screening Tool for Noise-Induced Hearing Loss. *Noise Health* **3**, 43-60 (2001).

314 Helleman, H. W., Jansen, E. J. & Dreschler, W. A. Otoacoustic emissions in a hearing conservation program: general applicability in longitudinal monitoring and the relation to changes in pure-tone thresholds. *Int J Audiol* **49**, 410-419, doi:10.3109/14992020903527616 (2010).

315 Hussain, D. M., Gorga, M. P., Neely, S. T., Keefe, D. H. & Peters, J. Transient evoked otoacoustic emissions in patients with normal hearing and in patients with hearing loss. *Ear Hear* **19**, 434-449, doi:10.1097/00003446-199812000-00005 (1998).

316 Vaden, K. I., Jr., Matthews, L. J. & Dubno, J. R. Transient-Evoked Otoacoustic Emissions Reflect Audiometric Patterns of Age-Related Hearing Loss. *Trends Hear* **22**, 2331216518797848, doi:10.1177/2331216518797848 (2018).

317 Kalluri, R. & Shera, C. A. Near equivalence of human click-evoked and stimulus-frequency otoacoustic emissions. *J Acoust Soc Am* **121**, 2097-2110, doi:10.1121/1.2435981 (2007).

318 Brass, D. & Kemp, D. T. The objective assessment of transient evoked otoacoustic emissions in neonates. *Ear Hear* **15**, 371-377, doi:10.1097/00003446-199410000-00004 (1994).

319 Keefe, D. H. *et al.* High frequency transient-evoked otoacoustic emission measurements using chirp and click stimuli. *Hear Res* **371**, 117-139, doi:10.1016/j.heares.2018.09.010 (2019).

320 Knight, R. D. & Kemp, D. T. Indications of different distortion product otoacoustic emission mechanisms from a detailed f1,f2 area study. *J Acoust Soc Am* **107**, 457-473, doi:10.1121/1.428351 (2000).

321 Kalluri, R. & Shera, C. A. Measuring stimulus-frequency otoacoustic emissions using swept tones. *J Acoust Soc Am* **134**, 356-368, doi:10.1121/1.4807505 (2013).

322 Mishra, S. K. & Talmadge, C. L. Sweep-tone evoked stimulus frequency otoacoustic emissions in humans: Development of a noise-rejection algorithm and normative features. *Hear Res* **358**, 42-49, doi:10.1016/j.heares.2017.11.006 (2018).

323 Shera, C. A., Guinan, J. J., Jr. & Oxenham, A. J. Otoacoustic estimation of cochlear tuning: validation in the chinchilla. *J Assoc Res Otolaryngol* **11**, 343-365, doi:10.1007/s10162-010-0217-4 (2010).

324 Mishra, S. K. & Biswal, M. Time-frequency decomposition of click evoked otoacoustic emissions in children. *Hear Res* **335**, 161-178, doi:10.1016/j.heares.2016.03.003 (2016).

325 American National Standards Institute. in *ANSI S3.1-1999; [R2018]* (Author, New York, 1999).

326 Mertes, I. B. & Goodman, S. S. Short-latency transient-evoked otoacoustic emissions as predictors of hearing status and thresholds. *J Acoust Soc Am* **134**, 2127-2135, doi:10.1121/1.4817831 (2013).

327 Moleti, A. *et al.* Otoacoustic emission latency, cochlear tuning, and hearing functionality in neonates. *J Acoust Soc Am* **118**, 1576-1584, doi:10.1121/1.2000769 (2005).

328 Shaffer, L. A. & Long, G. R. Low-frequency distortion product otoacoustic emissions in two species of kangaroo rats: implications for auditory sensitivity. *J Comp Physiol A Neuroethol Sens Neural Behav Physiol* **190**, 55-60, doi:10.1007/s00359-003-0471-6 (2004).

329 Cheng, J. T., Ghanad, I., Remenschneider, A. & Rosowski, J. The onset of nonlinear growth of middle-ear responses to high intensity sounds. *Hear Res* **405**, 108242, doi:10.1016/j.heares.2021.108242 (2021).

330 Nakajima, H. H., Merchant, S. N. & Rosowski, J. J. Performance considerations of prosthetic actuators for round-window stimulation. *Hear Res* **263**, 114-119, doi:10.1016/j.heares.2009.11.009 (2010).

331 Souza, N. N., Dhar, S., Neely, S. T. & Siegel, J. H. Comparison of nine methods to estimate ear-canal stimulus levels. *J Acoust Soc Am* **136**, 1768-1787, doi:10.1121/1.4894787 (2014).

332 Fultz, S. E. *et al.* Age Effects on Cochlear Reflectance in Adults. *Ear Hear* **41**, 451-460, doi:10.1097/AUD.0000000000000772 (2020).

333 Bowling, T., Wen, H., Meenderink, S. W. F., Dong, W. & Meaud, J. Intracochlear distortion products are broadly generated by outer hair cells but their contributions to otoacoustic emissions are spatially restricted. *Sci Rep* **11**, 13651, doi:10.1038/s41598-021-93099-7 (2021).